Mapping Freshwater Resilience

across the Conterminous U.S.

Mark Anderson, Arlene Olivero,
Analie Barnett, Mary Khoury,
& Erik Martin

Center for Resilient Conservation Science

The Nature Conservancy

March 2024

Please cite as:

Anderson, M.G., Olivero, A.P., Barnett, A.R., Khoury, M.L., and Martin, E.H. 2024. Mapping Freshwater Resilience across the Conterminous U.S. The Nature Conservancy, Center for Resilient Conservation Science. Newburyport, MA.

For more information on CRCS and to access the report and data, visit: http://crcs.tnc.org

Funding for this project was provided by The Volgenau Foundation, The Kohler Foundation, and an Anonymous Donor.

About the Cover

Photo credits, top to bottom and left to right:
© Tim Lumley, Yellowstone River. This view of the Yellowstone River is about 1,000 yards downstream from Tower Fall. Tower Creek can be seen emptying into the river in the lower left corner. The storm clouds rolling in over the horizon had enough snow in them to close the Grand Loop Road near Mt. Washburn and block our planned route back to the Lodge. *Flickr*, 2015. https://flic.kr/p/ApyZWo
© James Loesch, Wing Dam on Delaware River. Lambertville New Jersey on the left and New Hope Pennsylvania on the right. *Flickr*, 2019. https://flic.kr/p/2hPXeLL
© dtroyka, Black Creek National Scenic River, MS. *Flickr*, 2010. https://flic.kr/p/8nkPrF
© Thomas Elliot, Drone on South Platte River, CO. *Flickr*, 2019. https://flic.kr/p/2i2GUx5
© orientalizing, Sandhill Cranes, Platte River, NE. Every March, more than half a million Sandhill cranes congregate along a stretch of the Platte river during their migration north. *Flickr*, 2016. https://flic.kr/p/QwEE8E

3/20/2024

Dedication

Our colleague, Jonathan Higgins (1958-2022), contributed in so many ways to this work that we wanted to take this opportunity to acknowledge him and dedicate this work to him. From the beginning, he was a champion of mapping freshwater resilience, giving us sage advice to keep the model simple and grounded in the key attributes of freshwater ecosystems. While we are sure his blunt appraisal of our analysis would have improved it, we hope this work reflects his efforts to sharpen our critical thinking.

Acknowledgments

This work would not have been possible without the contributions of colleagues across The Nature Conservancy (TNC) and beyond. From champions to challengers, we are grateful for everyone's input. At the risk of leaving someone out, below are listed the colleagues who advocated for and participated in mapping freshwater resilience for the conterminous U.S. We also acknowledge the generous funding of an anonymous donor in the Great Lakes as well as the funding support of TNC's North America Region Divisions.

Michael Reuter, Midwest Division Director
Michael Lipford, former Southern Division Director
Terry Sullivan, former Northeast Division Director

Freshwater Advisory Committee
Allison Aldous, TNC Global Provide
Roshni Arora, TNC India
Alison Bowden, TNC Massachusetts
Jonathan Higgins, formerly TNC Global Protect
Jeanette Howard, TNC California
Nathan Karres, TNC Global Provide
Patrick McCarthy, formerly TNC Colorado River Program
Paulo Petry, TNC Latin America Region
Meg White, formerly TNC North America Region

Mississippi and Great Plains Steering Committee
Danna Baxley, TNC Kentucky
Kristen Blann, TNC Minnesota/Dakotas
Rob Bullard, TNC Tennessee
Darren Crabtree, formerly TNC New York Division
Jeff Fore, TNC Arkansas
Cassie Hauswald, formerly TNC Indiana
Matt Herbert, TNC Michigan

Mississippi and Great Plains Steering Committee (continued)
Steve Herrington, TNC Minnesota/Dakotas
Suzanne Hickey, formerly TNC Iowa
Amy Holtshouse, TNC Ohio
Nathan Korb, formerly TNC Montana
Courtney Larson, TNC Wyoming
Maria Lemke, TNC Illinois
Scott Lemmons, TNC Mississippi
Heidi Mehl, TNC Kansas
Chris Pague, TNC Colorado
Bryan Piazza, TNC Louisiana
Terri Schulz, TNC Colorado*
Ryan Smith, TNC Texas*
Scott Sowa, TNC Great Lakes Program
Rip Sparks, TNC Illinois Science Advisory Committee
Josh Spies, TNC Iowa
John Wagner, TNC Wisconsin
Rick Walters, TNC Nebraska

*also served on Western U.S. Steering Committee

Eastern U.S. Steering Committee
Braven Beaty, TNC Virginia
Dirk Bryant, TNC New York Division
Mark Bryer, TNC Northeast Division Director
Barbara Charry, TNC Massachusetts
Chuck DeCurtis, TNC New Hampshire
Julie DeMeester, TNC North Carolina
Holly Drinkuth, TNC Connecticut
Su Fanok, TNC Pennsylvania
Sara Gottlieb, TNC Southern Appalachians Program, formerly TNC Georgia
Katie Kennedy, TNC North America Region
Eric Krueger, TNC South Carolina
Beth Lewis, TNC Florida
Josh Royte, TNC Maine
Danica Schaffer – Smith, formerly TNC North Carolina
George Shuler, formerly TNC New York Division
Sarah Whateley, formerly TNC New York Division

Western U.S. Steering Committee
Martha Cooper, TNC New Mexico
Emily Howe, TNC Washington
Aaron Jones, TNC New Mexico
Jessie Pearl, TNC Arizona
Louis Provencher, TNC Nevada (also represented Utah)
Holly Richter, formerly TNC Arizona
Corinna Riginos, TNC Wyoming

Western U.S. Steering Committee (continued)
Claire Ruffing, TNC Oregon
Laurel Saito, TNC Nevada
Melissa Stamp, Utah Reclamation Mitigation and Conservation Commission
Joe Trungale, TNC Colorado River Program
Nathan Welch, formerly TNC Idaho

Table of Contents

List of Tables

List of Figures

CHAPTER

Introduction 1

Streams and rivers in the U.S. were once connected into large free-flowing networks supporting the most diverse freshwater biota in the temperate world. What were once 6,000 free-flowing river networks are now fragmented into over 54,000 segments by dams and other barriers (Cooper et al. 2017). As a result of this and other river degradation, fish, crayfish, and mussels are the nation's most endangered species groups. Freshwater ecosystems are even more vulnerable to climate change as changes in temperature and precipitation necessitate movement by aquatic species to access suitable habitats, but such movement is curtailed by barriers. We urgently need to reconnect our streams and rebuild the resilience of our freshwater networks so they will sustain diversity into the future. This study of freshwater resilience, and detailed mapping of characteristics that influence resilience, is intended to provide conservationists with the information needed to restore and sustain our freshwater systems.

Background

Rivers, streams, lakes, ponds, wetlands, and springs are essential features of our landscape and history. Collectively, these freshwater ecosystems are critical to most life on earth and provide goods and services that support the livelihoods of billions of people (Russi et al. 2013). Fundamental services provided by freshwater biodiversity have been cataloged as material (food, health resources, goods), nonmaterial (educational and cultural values), and regulating (catchment integrity, water purification, and nutrient cycling) (Lynch et al. 2023). Covering less than one percent of the Earth's surface, rivers and lakes harbor at least 12 percent of the world's known animal species (Abramovitz 1996). In North America, freshwater ecosystems support 1,200 fish species that contribute to biodiversity, ecosystem productivity, human well-being, livelihoods, and prosperity (Burkhead 2012). Inland recreational fisheries, for example, generate more than $31 billion annually in the United States and Canada (DFO 2010; USFWS & USCB 2011).

The United States ranks first in fish diversity among all temperate countries (801 species), and first among the globe for diversity of crayfish (322), freshwater mussels (300), freshwater snails (600), stoneflies (600), and mayflies (590) (Master et al. 1998). However, freshwater species are also the country's most threatened species group. Three decades ago, The Nature Conservancy (TNC), in cooperation with the state Natural Heritage Network released a species "report card" for the United States (Stein & Flack 1997) which found that:

- *"67 percent of U.S. freshwater mussels are vulnerable to extinction or are already extinct;*
- *More than 1 in 10 mussels may have become extinct during this century alone.*
- *303 fish species—37 percent of the U.S. freshwater fish fauna—are at risk of extinction;*
- *17 fish species have already gone extinct, mostly in this century.*
- *51 percent of U.S. crayfishes are imperiled or vulnerable.*
- *40 percent of amphibians are imperiled or vulnerable.*
- *At least 106 major populations of salmon and steelhead trout have been extirpated."*

Recent studies suggest that the situation has only worsened. A quarter of the world's 14,898 species of freshwater fish are now at risk of extinction according to the most recent International Union for Conservation of Nature assessment (IUCN 2023b). The IUCN study found that pollution from

fertilizers and pesticides, sediment clogging up streams, and human sewage and industrial waste were the biggest threats, affecting 57% of the imperiled species. Dams and water extraction came in second, affecting 45% of threatened freshwater fish. Climate change compounds these threats. In drought-prone regions, water extractions reduce the absolute amount of freshwater available for other species, and dams and barriers hamper the ability of species to move to adjust to new climatic conditions (IUCN 2023a).

Freshwater fish are uniquely vulnerable to changes in climate because they are confined to aquatic habitats, and movement to alternative habitats is often more restricted than in terrestrial systems (Lynch et al. 2016). Movement is further restricted when stream networks are fragmented by dams and barriers, but adaptive movement is a necessary behavior when aquatic species encounter changing climatic conditions. A nationwide study in France comparing electrofishing results from over 3,000 sites across four decades found systematic shifts in species distributions upstream and towards higher elevations (0.6 km upstream and 13.6 m in elevation per decade, Comte & Grenouillet 2013). Similarly, a 30-year survey of 1,500 lakes in Ontario Canada found sportfish range boundaries had shifted northward significantly at a rate of approximately 13-18 km per decade while baitfish had shifted southward (Alofs et al. 2014). In marine environments, climate driven changes in species distributions and commercial fish stocks are well documented, and adjustments are being made in fisheries management (Karp et al. 2019).

In the U.S., freshwater fish distributions are affected by contemporary climate change in ways consistent with anticipated responses under future climate scenarios. That is, the ranges of most coldwater species are shifting to higher altitudes or latitudes, whereas the ranges of cool and warmwater species are both expanding and contracting (Comte et al. 2013). Evidence for fish population movements in response to climate change is apparent in connected stream networks with wide temperature gradients such as the Bitterroot and Flathead rivers (Eby et al. 2014; Mulfeld et al. 2016) and the Great Lakes (Johnson & Evans 1990). In these systems, species are moving to track cooler temperatures and find suitable habitats or thermal refugia. Presumably, similar movements are also happening within smaller networks, but with more than 7,000 river dams fragmenting U.S. rivers and over 145,000 small dams preventing access to headwater streams (per this analysis), such movements are increasingly a challenge.

Climate change may have other consequences for aquatic organisms because temperature and precipitation affect most of the physiological and geochemical processes that regulate their life history (Whitney et al. 2016). Evidence is beginning to accrue documenting phenological shifts in the timing of seasonal migrations or spawning, demographic changes in abundance, growth, and recruitment, and even evolutionary responses indicated by genetic change (Lynch et al. 2016). Although aquatic species have dealt with climate changes in the past, fragmented systems and restricted movement may hamper their ability to adjust to changing conditions. As Woodward et al. (2010) stated, “all organisms face the same options as the climate changes: adapt, migrate, or perish. However, an organism’s success in implementing the first two strategies will depend largely on its life history and dispersal traits in relation to habitat fragmentation and the rate at which its environment changes.”

Approach

Freshwater Resilience is the ability of a stream network or other aquatic setting to maintain biologic diversity even as the system changes in composition and structure in response to changes in climate. TNC's Center for Resilient Conservation Science (CRCS) led a project to assess the characteristics of freshwater systems that convey resilience to climate change and identify a representative set of resilient freshwater networks across the conterminous United States that if conserved, could sustain aquatic biodiversity into the future.

Our approach to resilience was based on the idea of Conserving Nature's Stage (Beier et al. 2010). That is, we did not attempt to predict all the possible implications and interactions expected from climate change, but instead, we sought to identify and map the enabling physical conditions that set the stage for aquatic species and assemblages to adapt to a changing climate with flexibility and integrity. We focused on the abiotic components of a freshwater network such as its length and diversity, the condition of its watershed and floodplain, its access to surface water and groundwater, and the availability and alteration of its flow regime. We recognize that in some parts of the country, even a system with all the enabling conditions (i.e., a highly resilient network) may still need management and restoration.

To identify a network of connected rivers and streams likely to sustain biodiversity under a changing climate, we developed a series of spatially explicit datasets targeting key aspects of a climate-smart freshwater conservation network: resilience, connectivity, and recognized biodiversity value. Each dataset covered the conterminous U.S. (hereafter CONUS) and was reviewed by a steering committee of 60 scientists from 44 state and regional TNC programs with expert knowledge of the geographic region they represented. Map products were evaluated and delivered for HUC-12 watersheds, a spatial resolution appropriate for informing local, regional, and national decisions.

Initially, we divided CONUS into three study regions, Mississippi-Great Lakes, Western U.S., and Eastern U.S., and we convened a steering committee of TNC scientists from each included state. We held bimonthly virtual meetings to discuss methods, identify relevant datasets, review draft results, obtain feedback, iterate, and finalize results. We began this study in the Mississippi-Great Lakes region (2020-2021) and then expanded the mapping westward and eastward (2022-2023). As the study progressed, we determined that insufficient data was available to reliably assess the resilience of the South Florida ecoregion which has substantial water diversions and inconsistently mapped hydrography. For this reason, HUC-12 watersheds in the South Florida ecoregion were excluded from our analysis and are grayed out in maps of the results. It took three years to complete the entire CONUS region and by the time we were finished, we had adjusted many details of our original methods to accommodate the wide variety of freshwater systems across the U.S. The methods presented here reflect our final synthesis.

We are deeply appreciative of our steering committee participants who stayed fully engaged in the work throughout the entire time frame, and without whose attention, constructive criticism, and review we would not have been able to accomplish this work (see Acknowledgments). Their understanding of freshwater systems and careful review of our results sent us back to the drawing board multiple times. We are also grateful for a national advisory committee of colleagues who helped us simplify and communicate the study as our model grew increasing complex and detailed.

Mapping Freshwater Resilience

Our approach to mapping terrestrial resilience (Anderson et al. 2023, see https://www.maps.tnc.org/resilientland/) identified areas of high physical diversity and connectedness both locally and regionally, based on enduring features that provide species habitat options and the ability to move as the climate changes. This Conserving Nature's Stage approach (Beier et al. 2010; Anderson et al. 2014) recognizes that while the actors at any given site may change, we can focus conservation efforts on maintaining the diversity and ecological function of the stage. Similarly, this freshwater resilience analysis identified characteristics that confer resilience for freshwater biodiversity in a changing climate. Our hypothesis for mapping freshwater resilience was that the physical setting and its condition, together with water availability and its alteration, drive resilience in freshwater systems by providing habitat options and the conditions to maintain ecological function.

We used the term "functional connectivity" to refer to the contiguous portions of a river network available for a fish or aquatic organism to move through before they encounter a dam or other barrier. The characteristics of this "functionally connected network" - its size, diversity, condition, and available water – determine its ability to support aquatic diversity under changing climates. When there were no dams in CONUS, natural drainage basins formed 6,000 connected networks, and we would have concluded that the Mississippi Basin is the most resilient network due to its huge connected length and diversity. The basin was a primary center of fish diversity with natural barriers and long-term stability of aquatic habitats being the most important factors controlling species density and broad patterns of evolution (Robinson 1986). Today, the natural pattern of connectivity has been severely compromised as large dams have fragmented stream networks into thousands of isolated groups of segments, increasing by 801% the number of separate networks compared to free-flowing streams in the absence of dams (Cooper et al. 2017). Many streams and rivers (79% of stream length) are disconnected from their outlet (i.e., oceans and Great Lakes) which has contributed to the severe decline of many anadromous and potadromous species (Cooper et al. 2017).

Our model of freshwater resilience reflects the hypothesis that the physical setting and its condition, together with water availability and hydrologic alteration, drive freshwater resilience by providing options and the conditions to maintain ecological function. The resulting "resilience score" estimates the relative capacity of a river network to maintain species diversity and ecological function as the climate changes. The building blocks of the resilience score are:

- Physical Score
    - Connectivity
    - Condition
- Water Score
    - Potential Water Availability
    - Flow Alteration

In our analysis, a resilience score is calculated for every HUC-12 watershed by integrating connectivity and condition into a physical score, integrating potential water availability and flow alteration into a water score, and finally integrating these two scores into an overall resilience score. As the factors driving resilience vary in importance with climate region (see Arid/Humid Stratification section), we adjusted the weight of each factor in the integration based on climatic region. See Appendix 1 for summary model diagrams for each climatic region. We expect the climatic regions to

remain relatively stable as they are determined by enduring continental, orographic, and coastal processes.

- In humid regions, more weight was given to the physical score, and the water score was based mostly on flow alteration because water availability is rarely limiting.
- In arid regions, equal weight was given to the physical and water score as both factors could be limiting.
- In xeric regions, more weight was given to the water score, and potential water availability was a large contributing factor as water is often the most limiting factor.

Many of our analyses use the arid and humid distinction without breaking out the xeric region, but the water scores required the xeric split to make ecological sense. This document explains in detail which variables went into each component and how they were combined into indices and scores.

CHAPTER 2

Base Data & Analysis Units

In this chapter, we describe the foundational data sets, analysis units, and climatic regions that were used in the freshwater resilience analysis.

Hydrography

To assess streams, rivers, and waterbodies for CONUS, we used the medium resolution 1:100,000 National Hydrography Dataset Plus version 2.1 (NHDPlusV2.1, USGS 2016). This dataset includes natural and constructed waterbodies (lakes, ponds, and reservoirs), paths through which water flows (streams and rivers, canals, ditches), and related point features such as springs, wells, and stream gages. Each stream reach has a unique identification code (COMID) that relates to multiple federal and state databases containing reach attributes used for reporting here and in other regional and national assessments.

To work with the NHDPlus, we converted it into a dendrite (continuous branching network) using the following standard query:

FLOWDIR = 'With Digitized' AND Divergence in (0,1) AND StreamCalc <>0

This query creates a dendritic network with a single downstream arc for every node and simplifies stream braiding and multiple downstream divergent paths into a single main path.

Stream size is indicative of major ecosystem changes along the stream-river continuum, such as transitions in the state and source of energy and ecosystem metabolism (Vannote et al. 1980). We defined stream size based on total upstream drainage, which is the most stable and geomorphologically comparable measure of size across the country. Size class breaks were based on the National River Fish Habitat Condition Assessment (Wang et al. 2011), which was designed to provide a coarse-level understanding of the diversity of river sizes at a national scale. We made two modifications to the Wang et al. (2011) classification by adding two more size classes for very large rivers and combining the two smallest (and highly correlated) classes into one (Table 2.1, Figure 2.1).

Table 2.1. River reach size classes.

Size Class Number	Size Class Name	Catchment Area (km^2)	Catchment Area (acres)
10,11	Headwaters, Creeks	≤ 100	≤ 25 K
20	Small Rivers	≤ 1000	≤ 247 K
30	Medium Rivers	≤ 10,000	≤ 2.5 M
40	Mainstem Rivers	≤ 25,000	≤ 6.2 M
50	Large Rivers	≤ 100,000	≤ 25 M
60	Great Rivers	≤ 1,000,000	≤ 247 M
70	Mega Rivers	> 1,000,000	> 247 M

Rivers (drainage area over 100 km^2) were combined with a dataset of dams to create Functionally Connected Networks (FCNs) described later in the Functionally Connected Networks section. Headwaters and creeks (drainage area less than or equal to 100 km^2) were assessed separately for headwater fragmentation.

Figure 2.1. Rivers by size class.

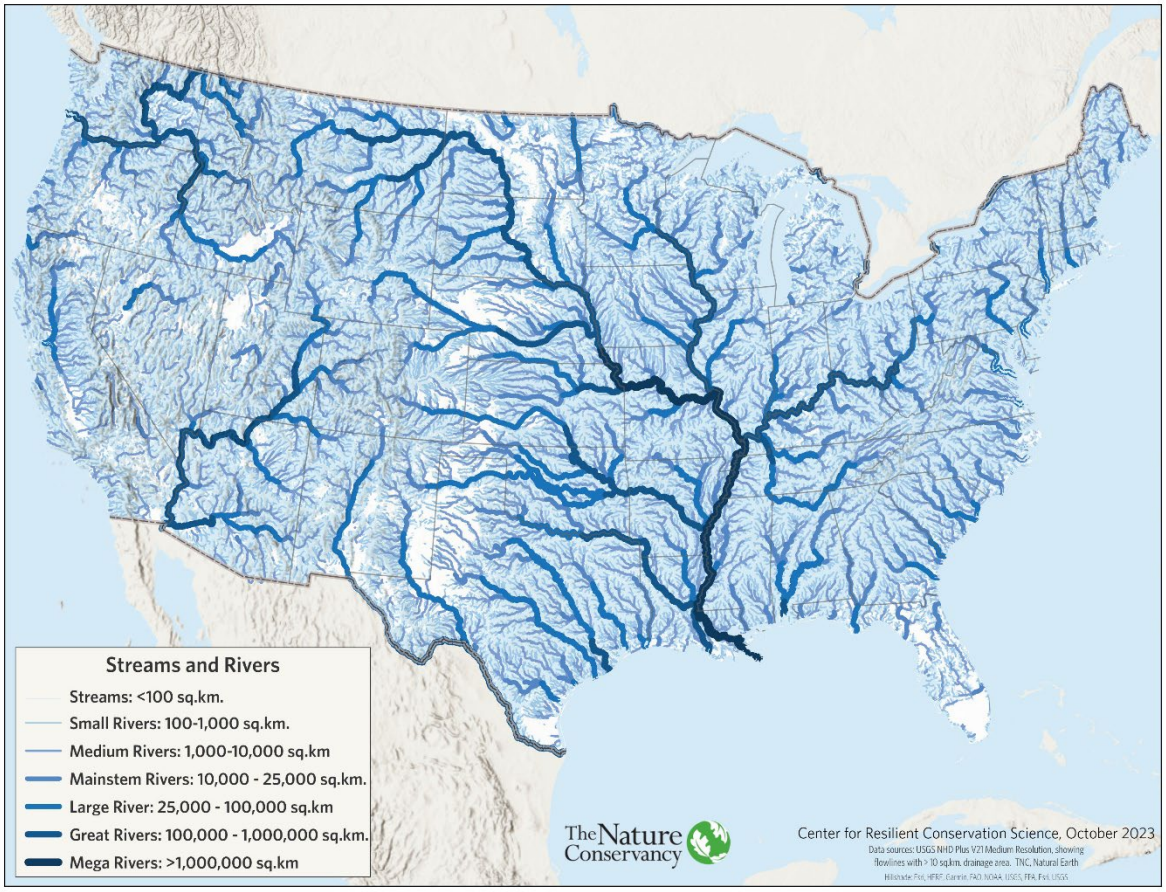

Dams

A central intent of this study was to estimate the effect of dams on species movement by evaluating the location and configuration of multiple dams against the dendritic branches of each stream network. To do this we needed spatially accurate data on dams in CONUS. Compiling, reviewing, correcting, and processing dam information was a major focus of our work at the onset of this study. As our initial step, we compiled dam information from the following four sources:

- **Northeast Connectivity dams** (**NECON**,12/9/20 version) provided by TNC, E. Martin. Included the states of VA, WV, PA, MD/DC, NJ, DE, NY, CT, RI, MA, VT, NH, and ME (Martin & Levine 2017).

- **TNC California Field Office (CAFO)** dam compilation (1/1/22), which included the USGS National Anthropogenic Barrier dataset (USGS 2020), California Passage Assessment Database September 2019 version (CDFW 2019), Oregon's Fish Barrier Dataset 2019 (ODFW 2019), and Lahontan Cutthroat Trout 5-Year Review (USFWS 2009).

- **National Anthropogenic Barrier Dataset (NABD) Version 2 Beta.** Updated as of 6/23/2020 NABDV2 (USGS 2020, A. Cooper personal communication). These data were used in all states except those in the Northeast Connectivity Project and California.

- **Southern Aquatic Resource Partnership (SARP) Comprehensive Southeast Aquatic Barrier Inventory – Dams**. Downloaded: 4/14/22 from http://connectivity.sarpdata.com/. States of AL, AR, AZ, CO, FL, GA, IA, ID, IL, KS, KY, LA, MN, MO, MS, MT, NC, ND, NE, NM, NV, OK, SC, SD, TN, TX, UT, and WY.

We compiled these sources into a single dataset and reviewed it for quality using a multi-step process. We first split the dataset into two parts: 1) dams on headwaters and creeks (drainage area less than or equal to 100 km^2), hereafter "**headwater dams**," and 2) dams on small to large rivers (drainage area greater than 100 km^2), hereafter "**river dams**."

For headwater dams we did not confirm the accuracy of the dam locations or flowlines, both of which had considerable spatial error. Instead, these dams were incorporated into the analysis using an approach that did not rely on their exact location and which is described in the Headwater Fragmentation section.

In contrast to the headwater dams, we manually reviewed the spatial position and attributes of all river dams, and where needed, "snapped" the dams to the NHDPlus flowline dendrites (Figure 2.2). This ensured the dams were located correctly with respect to the flowlines and allowed us to quantify network characteristics including size, diversity, and configuration. We distributed this revised dataset to TNC state-based freshwater staff for review and incorporated their edits into a final dataset.

Figure 2.2. Conceptual illustration of snapping a dam to the river network.

The review process consisted of TNC state representatives and CRCS staff using online web map services to review and edit the river dam dataset during three sets of reviews from 2021-2023. The goals were to: 1) review all dams to ensure they were truly barriers to passage, 2) update key attributes such as dam name, type, height, or passability, and 3) add missing dams and/or move onto rivers any dams erroneously snapped to nearby streams or left unsnapped off channel. During this review, TNC

staff added 173 dams. Dams identified in the American Rivers Removal database (American Rivers 2022) as of Feb. 2022 were removed. Passability was updated as described below.

Dam Passability

Not all dams are a complete barrier to aquatic organism passage. Examples of dams that may allow for the movement of some species under certain conditions include dams with fish passage structures, navigation locks, and very small dams that are submerged at high flows. We refer to dams that allow some degree of aquatic organism passage (AOP) as "partially passable." We identified these using multiple criteria including: the presence of locks, presence of a fish passage facility, those with a height less than two feet, and those identified as partially passable by the steering committee or TNC staff.

Dam height and the presence of locks are attributes generally available in the source dam data. Dams with locks were identified via the U.S. Army Corps' National Inventory of Dams (NID, USACE 2021), which contains attributes for number of locks or the length of locks. Additional dams with locks were identified from a dam's name (e.g., "Lock and Dam"). Dam height was also taken from the source data attributes (NID or other data).

Data on fish passage facilities came primarily from two sources. The first was the USGS Fishway Structure Data (Gressler et al. 2022), which covers portions of the Eastern U.S. The dataset does not include an ID number from the NID nor any other national database, so dams were flagged as having a fish passage facility if they were within 100 m of an identified fish passage dam. The second source was expert knowledge of barriers from the project steering committee members and state chapter staff.

Monitoring and field studies are required to understand the effectiveness of fish passage facilities at any given location. Lacking this information across the board, all dams with some amount of partial passability were assigned a score of 0.5, where 0 represents a complete barrier and 1 indicates no barrier to the movement of aquatic organisms. These passability values were used to calculate the cumulative discounted network length described in Chapter 3.

Results of Dam Review

Compilation and review of the dataset resulted in a core set of 7,399 river dams and another 145,109 headwater dams for a total of 152,508 valid dams[1]. The true number of headwater dams is most certainly higher given small dams are inconsistently inventoried from state to state.

We used the full set of 7,399 river dams to define the Functionally Connected Networks described below. For the headwater fragmentation analysis, we only used headwater dams that intersected streams with drainage areas over 2.6 km2 (643 acres) to ensure the analysis focused on streams more consistently mapped across the country. The latter is a common hydrography stream size threshold used in other regional stream connectivity analyses for consistency in dam inventory and stream length calculations when using the NHDPlus medium resolution hydrography (Martin & Levine 2017). This

[1] 80,073 from Southern Aquatic Resource Partnership (SARP); 40,241 from National Anthropogenic Barrier Dataset (NABD); 28,048 from Northeast Connectivity Project (NECON); 1973 from California TNC Field Office (CAFO); 173 from steering committee additions.

resulted in 65,282 dams used in the analysis (Figure 2.3). The remaining 94,675 dams consisted of numerous farm ponds, off channel retention ponds, and dams on extremely small streams. These were excluded from the analysis because they limited access to only a small amount of upstream habitat.

Figure 2.3. Results of dam review. The map shows the location of the 65,282 dams used in this analysis.

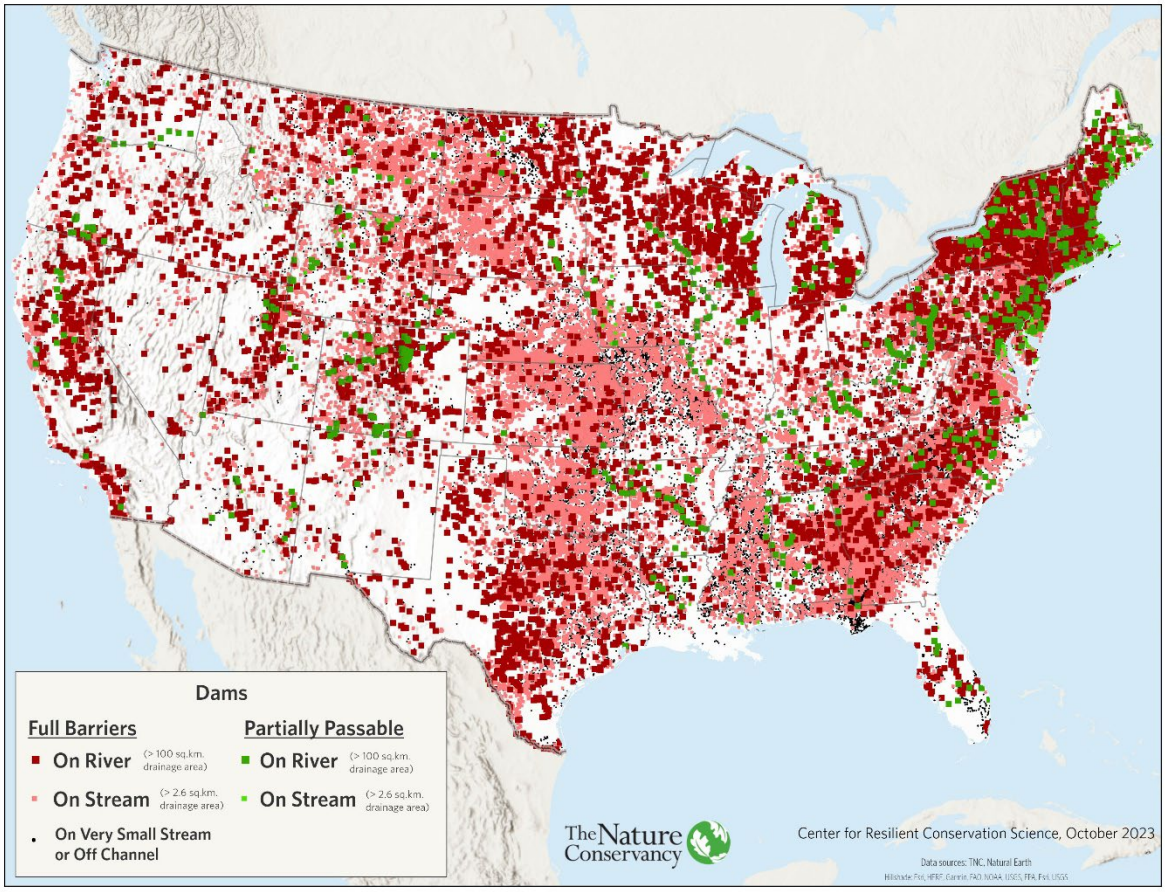

Analysis Units

The resilience of freshwater ecosystems plays out at multiple spatial scales. To account for this, we used two primary units of analysis: the Functionally Connected Network (FCN) and the HUC-12 watershed. Data at finer reach catchment or other scales were summarized for these two units. Final resilience scores were assigned to the intersection of the two units. Most HUC-12 watersheds nested perfectly within an FCN (75%), but 25% of the HUCs were split by an FCN boundary or vice versa. In all cases, the information was used to address multiple scales. For example, HUC-12 values for connectivity were derived from the size of the FCN in which they occurred, whereas their condition values were derived primarily from local elements and could vary within the FCN. The scale at which specific metrics in this analysis were summarized is available in Appendix 2, Table A2-1.

Functionally Connected Networks

A Functionally Connected Network (FCN) was defined as the amount of locally connected freshwater habitat available for the movement and life history needs of aquatic species. Spatially, we defined an FCN as the set of connected rivers, streams, and headwaters bounded on all sides by dams, by the upper extent of headwaters, or by the confluence with an ocean or the Great Lakes. A free-flowing river in FCN terminology is bounded only by its headwaters and mouth, whereas most FCNs are bounded on all sides by dams or by a combination of dams and headwaters, or all three (Figure 2.4).

Figure 2.4. A Functionally Connected Network (FCN). This FCN is bounded by two dams on the river portion and by the headwaters of the two tributaries. The network includes a diversity of bedrocks, slopes, stream temperatures, waterbodies, wetlands, seeps, and floodplain forest.

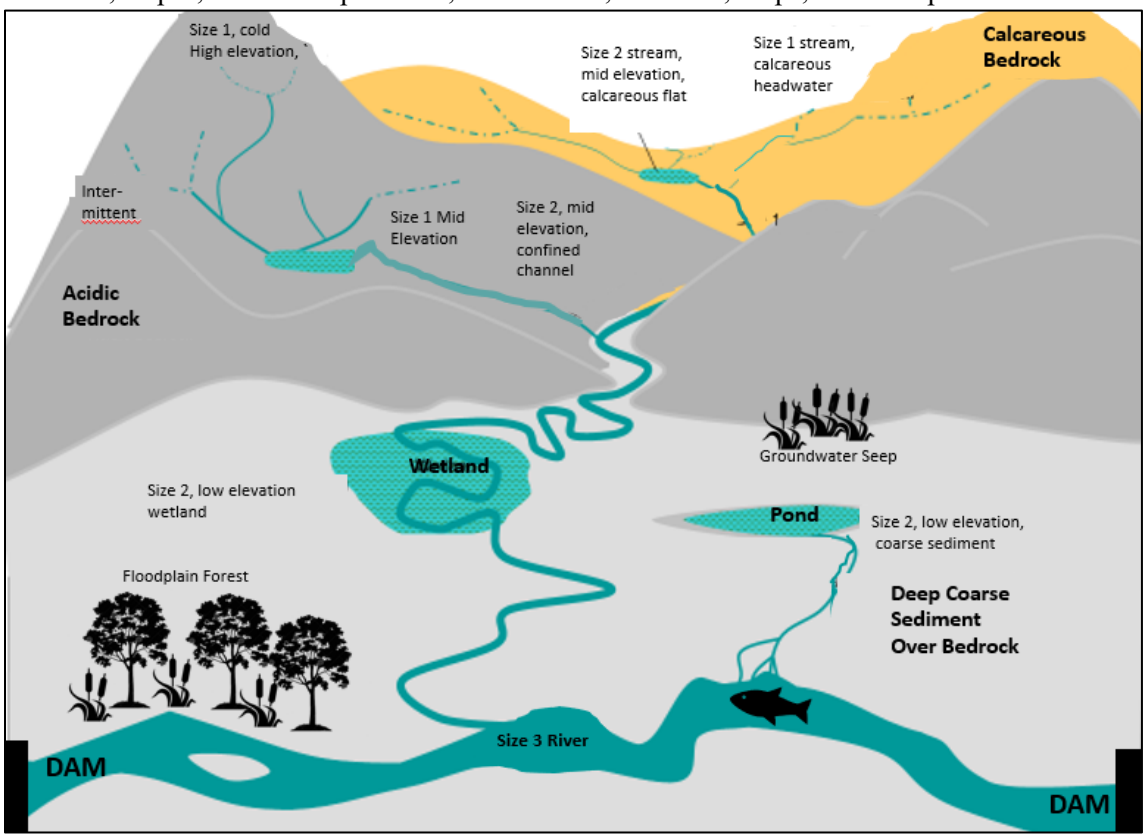

We created FCNs by intersecting the river dams with the NHDPlus hydrography, the approach used by Cooper et al. (2017) to define stream network catchments. The land area draining to the connected set of streams and rivers of each FCN was delineated using the NHDPlus flow direction grid derived from a 30-m Digital Elevation Model (DEM) and distributed with the NHDPlus dataset. We characterized each FCN by its watershed area (Figure 2.5) rather than the length of its rivers because we found the FCN drainage area to be more closely correlated with the total length of all streams in the network (including headwaters and creeks).

Figure 2.5. The Lower Wisconsin River FCN. The map depicts a single FCN based on dam locations (icon) and local watershed area.

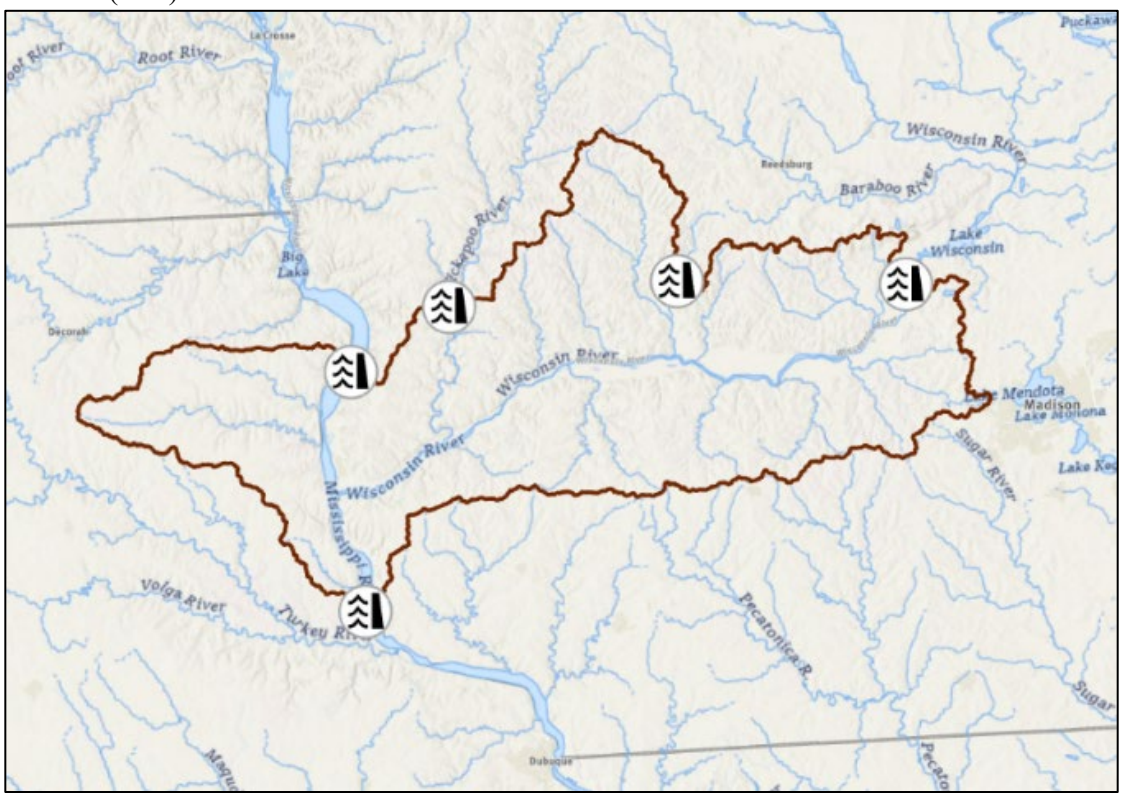

HUC-12 Watersheds and Finer Units

A Hydrologic Unit (HU) watershed represents the area of the landscape that drains to a portion of a stream network (Figure 2.6). The United States is divided and sub-divided into successively smaller hydrologic units which are nested within each other, from the largest geographic area (HUC-2 "region") to the smallest geographic area (HUC-12 subwatershed). Each hydrologic unit is identified by a unique hydrologic unit code (HUC), a numeric code that corresponds to the level of classification in the hydrologic unit system (Seaber et al. 1987).

In some cases, freshwater resilience metrics were first calculated for the catchment of NHDPlusV2.1 stream reaches before being summarized to the HUC-12 units. Reach catchments are the watersheds delineated for each NHDPlus stream reach and are distributed with the NHDPlus V2.1 database (USGS 2016). Figure 2.7 shows how the HUC-12s and reach catchments might nest within a single FCN.

Figure 2.6. Hydrologic Unit Codes (HUCs). The relative scale of Hydrologic Unit Codes from HUC-2 to HUC-12. Graphic from USGS (public domain)

Figure 2.7. The Lower Wisconsin River FCN divided by HUC-12s. This map shows the analysis units of a single FCN. The FCN (brown) is determined by five dams, three are full barriers (black) and two are partially passable (green). River line color and thickness indicate size class. The HUC-12 boundaries are shown in dark yellow and reach catchments in light gray. This FCN contains 93 HUC-12s and 3,730 reach catchments.

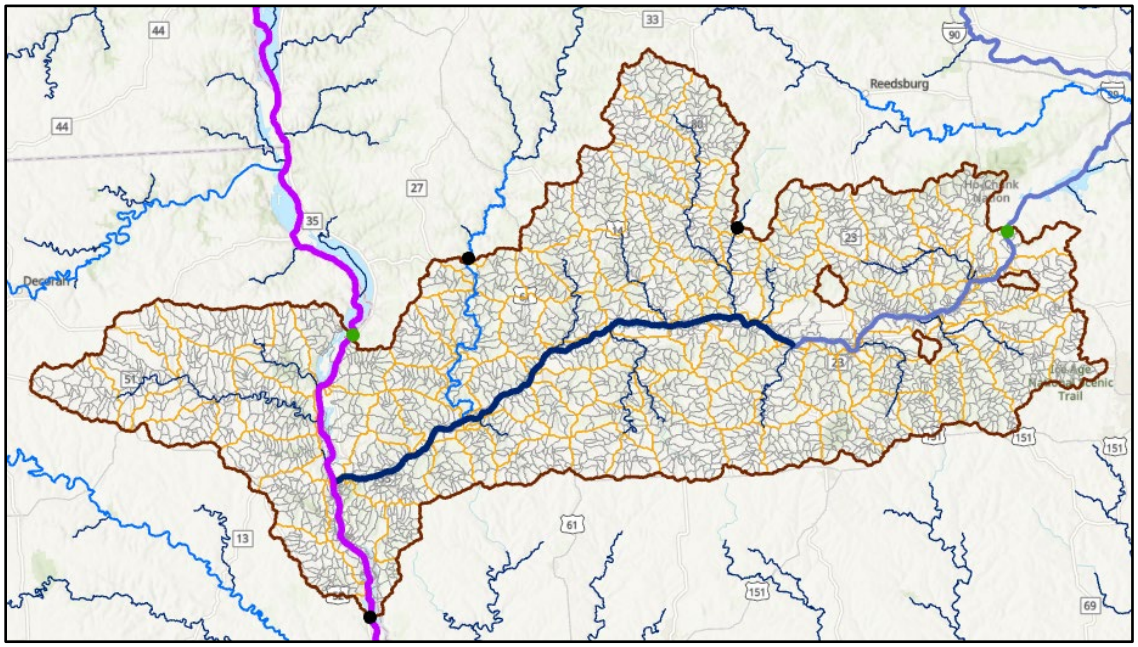

Scoring of the FCN and HUC-12 Units

Throughout this analysis, we scored the FCN and HUC-12 units based on the component datasets and often combined scores into an index. Statistical analyses and data management were performed using R Statistical Software (R Core Team 2022). Before combining FCN and HUC-12 variables, we transformed all scores to standard normal units (z-scores). A z-score describes the number of standard deviations a value is from the mean of a distribution. Thus, a z-score of "0" equals the mean, a value of "1" is one standard deviation above the mean, and a value of "-1" is one standard deviation below the mean. Z-scores allowed us to combine variables with unequal means and variances and different distribution patterns while retaining equal influence. We capped the z-scores to range from -3 to 3 to avoid giving outliers undue influence, and when necessary, we used the *bestNormalize* R package (Peterson 2021) to transform input data to approximate a normal distribution before calculating z-scores.

One consequence of this approach is that all scores are relative to the population assessed. This allowed us to identify areas that are relatively more resilient or relatively less resilient (Table 2.2) without knowing exactly how the climate will change.

Table 2.2. Scoring scale based on z-score standardization.

Z-Score Class	Standard Deviation Range
Far Above Average	>2
Above Average	>1 - ≤ 2
Slightly Above Average	>0.5 - ≤ 1
Average	> -0.5 - ≤ 0.5
Slightly Below Average	> -1 - ≤ -0.5
Below Average	>-2 - ≤ -1.0
Far Below Average	≤ -2

Arid/Humid Stratification

The climatic regions of CONUS are expected to remain stable into the future because they are determined by continental, orographic, and coastal processes that will continue to endure and operate. Although the factors that determine a river network's resilience may be universal, the relative importance of one factor or another was strongly related to the climatic region in which the network occurred. For example, water availability is essential in the xeric Western U.S. where dams are few and far between, but in the humid Eastern U.S., where water is plentiful and rivers are fragmented by thousands of dams, the size and alteration of the network are more critical factors in determining resilience. Throughout the evaluation of freshwater resilience, we recognized that different components of the model had differing levels of influence depending on climatic zones.

To capture these differences and have a consistent basis to adjust weighting of factors in our model, we created a stratification scheme based on climate information and attributes of the freshwater ecoregions (WWF & TNC 2019). We first divided the country into two zones, arid and humid, based on an aridity index calculated from temperature and rainfall values for CONUS (Zomer et al. 2008), and then classified each freshwater ecoregion as arid or humid based on the dominant zone in the ecoregion (Figure 2.8). For some analyses, we further split the arid region into xeric and non-xeric based on a global aridity index (Trabucco & Zomer 2019). This spatial framework was used for

applying weighting factors when combining components of the model, details of which are provided in Appendix 1.

Figure 2.8. Arid and humid classes of freshwater ecoregions. The map shows freshwater ecoregions grouped by whether their climate regimes are dominantly humid or arid, with arid further split into xeric and non-xeric based on Freshwater Ecoregions of the World (WWF & TNC 2019) and a global aridity index (Trabucco & Zomer 2019).

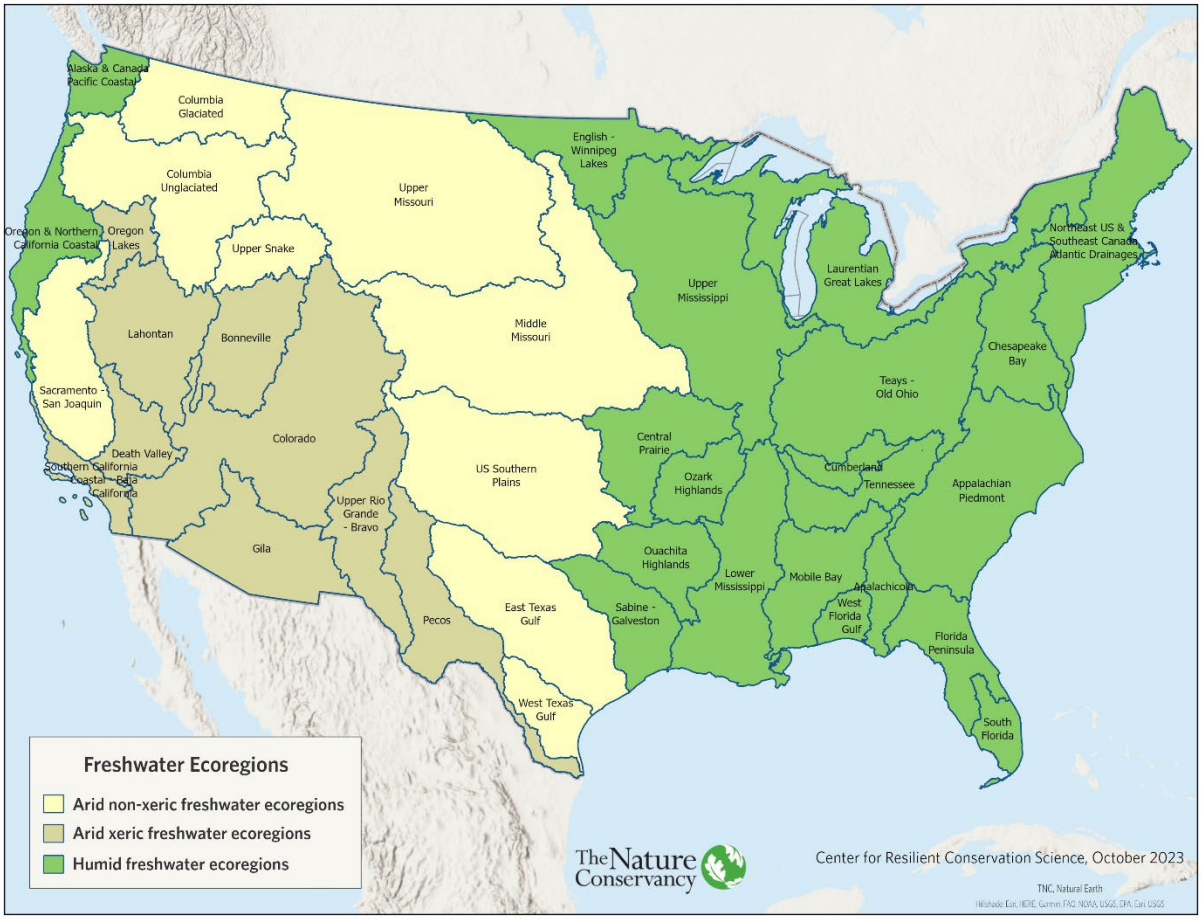

CHAPTER 3

Mapping Freshwater Resilience

In this chapter we present the model for estimating freshwater resilience. For each component, we explain the metrics calculated and how they were integrated to assess the resilience of each HUC-12. Appendix 1 contains detailed diagrams of the freshwater resilience model used for each climatic region (Figure 2.8).

Our model reflects the hypothesis that the physical setting and its condition, together with water availability and alteration, drive freshwater resilience by providing options and the integrity to maintain ecological function (Paukert et al. 2021). The resilience score estimates the relative capacity of a HUC-12 watershed to maintain species diversity and ecological function as the climate changes. The building blocks of the resilience score are connectivity and condition, which were combined to create a physical score; and potential water availability and flow alteration, which were combined to create a water score (Figure 3.1). The physical and water scores were then integrated to calculate freshwater resilience, the details of which are explained in the last section of this chapter and graphically displayed in Appendix 1.

Each of these scores comes from components that represent both the physical freshwater stage and the ability of current conditions to provide ecological functions to sustain resilience in the face of climate change. The physical score describes the extent and complexity of the connected freshwater habitat along with its current condition as affected by land use. Both aspects provide organisms with options to move and adapt to changing climatic conditions (Paukert et al. 2021; Pelletier et al. 2020). The water score expresses the importance of the availability of freshwater to long-term resilience, coupled with existing flow alteration (Kaufman et al. 2022a; McManamay et al. 2022; Pennock et al. 2022). Each of these main components is calculated from multiple metrics as detailed in the following sections.

Figure 3.1. Major components of freshwater resilience.

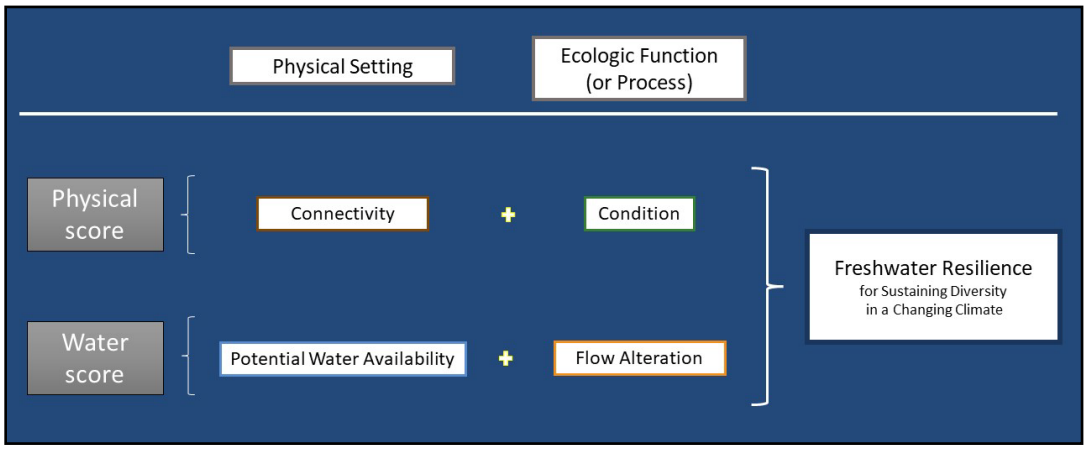

Physical Score

In this section we explain how the physical score was derived. First, we describe the components of connectivity and describe how they were integrated. Next, we explain how the condition score was calculated from its component metrics and integrated into an index. Finally, we describe how the connectivity score was integrated with the condition score to calculate the physical score.

Our basic model was as follows:

Physical Score = Connectivity + Condition

Connectivity = Functional Connectivity + Diversity

Condition = Naturalness + Water Quality + Impervious Surface Override

Connectivity Score

The connectivity score was comprised of two components, functional connectivity and diversity. The following sections detail how we defined, mapped, and assessed these two elements.

Functional Connectivity

In this analysis, functional connectivity refers to the longitudinal connectivity of a river network accounting for the location of barriers, the passability of those barriers, the detrimental influence of reservoirs, and the benefits of connection to the Great Lakes and to oceans. Larger and more complex networks provide greater access to life-stage habitat needs, refugia, and unimpaired riverine processes. Longitudinal connectivity matters to the resilience of riverine ecosystems because it provides access to habitat needs at various life-history stages, refugia, and unimpaired riverine processes (Tickner et al. 2020). Connectivity within a network of streams is essential to support ecosystem processes and recovery from disturbances. It enables water flow, sediment and nutrient regimes to function naturally, allows species to move throughout the network to find feeding and spawning habitat, and, in times of stress, enables individuals to relocate in pursuit of more suitable conditions for survival (Pringle 2001). Likewise, disruptions in hydrologic connectivity have had negative ecological impacts on several aquatic faunal groups including migratory fish and native freshwater mussels (Pringle 2003).

We measured the size of each Functionally Connected Network (FCN) using area to estimate the amount of connected freshwater habitat. We used area instead of river length because tests showed that area better approximated the true size and length of the connected freshwater network, including all rivers, headwaters, creeks, lakes, ponds, and connected wetlands. Specifically, area is highly correlated with the full network length, including all headwaters and intermittent streams. This approach also allowed us to integrate a suite of important soil and land use processes influencing the health of the connected river network and was not affected by issues arising from stream mapping and digitizing. All else being equal, the larger the connected network, the more likely it is to be resilient because large networks are likely to provide more options for species to move in response to changes in temperature and precipitation and stay within their physiological tolerances (Timpane-Padgham et al. 2017). Connected river networks provide species the ability to disperse to avoid negative impacts of climate change (Comte et al. 2014; Paukert et al. 2021).

Delineating FCNs

We used Python scripts developed using Esri's arcpy package, in combination with all verified river dams, to generate FCNs and calculate the total length and area of each FCN (Figure 3.2). The scripts used a barrier dataset (points) to split a river network (polylines) into connected networks with unique ID's. We determined the land area draining directly into each FCN using ArcPro's Watershed Delineation tool and the NHDPlus flow direction grid. The resultant watershed grid provided the drainage area of each unique FCN. The watersheds were then converted to polygons and the area of each FCN was calculated.

Figure 3.2. River dams. This map shows the 7,399 river dams used to define FCN boundaries.

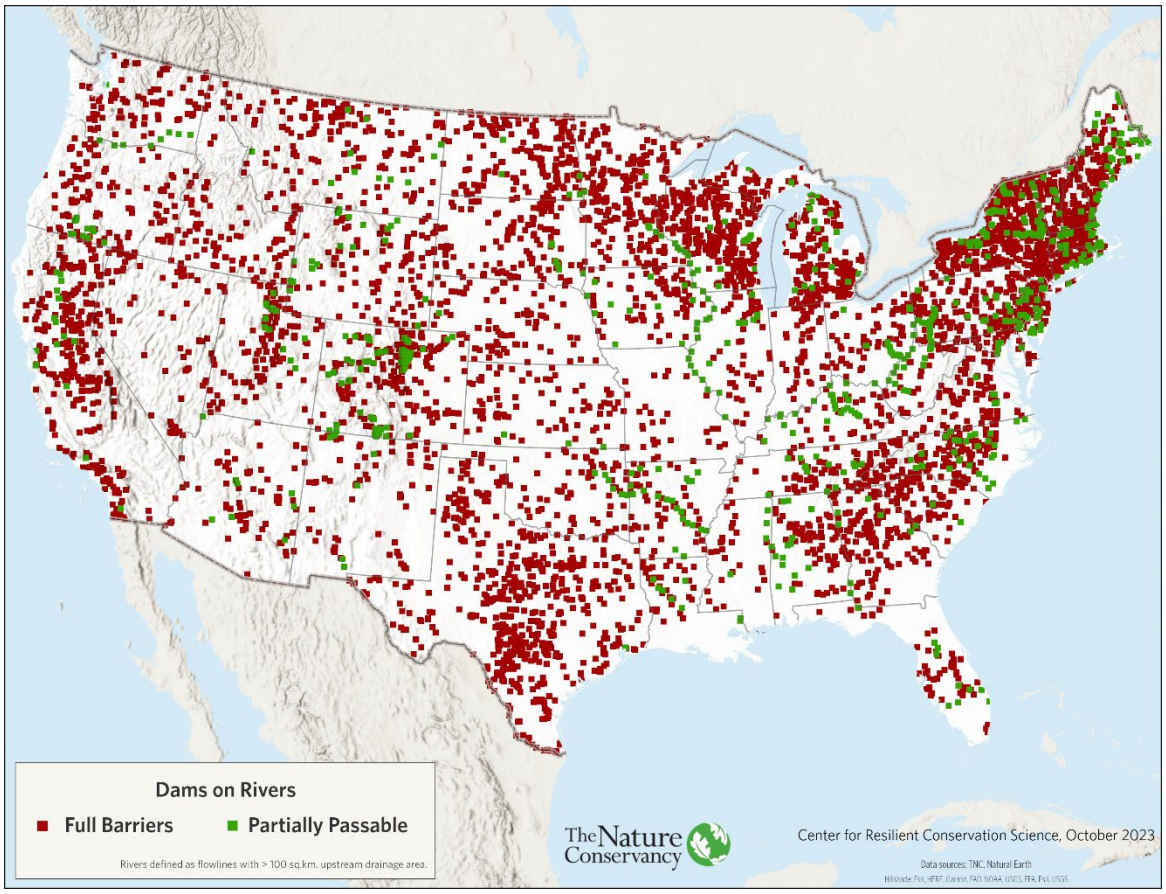

FCN Size Class

The size of the FCNs was highly skewed towards small values, but also contained a few huge outliers. To represent the variation in FCN size, we used natural breaks (Jenks) to guide our classification of each FCN into one of 11 national size classes (Table 3.1, Figure 3.3).

Table 3.1. FCN national size classes.

Size Class	Name	Area (km^2)
1	Enormous	>100,000
2	Huge	>50,000 – 100,000
3	Very large	>25,000 – 50,000
4	Large	>10,000 – 25,000
5	Largish	>5,000 – 10,000
6	Moderate	>2,500 – 5,000
7	Smallish	>1,000 – 2,500
8	Small	>500 – 1,000.
9	Very small	>250 – 500
10	Tiny	<=250
11	Minuscule	< 50

Figure 3.3. Functionally Connected Network original size. Size (km^2) of the local watershed area of each Functionally Connected Network bounded by dams, coast, or upper extent of headwaters draining to these river segments.

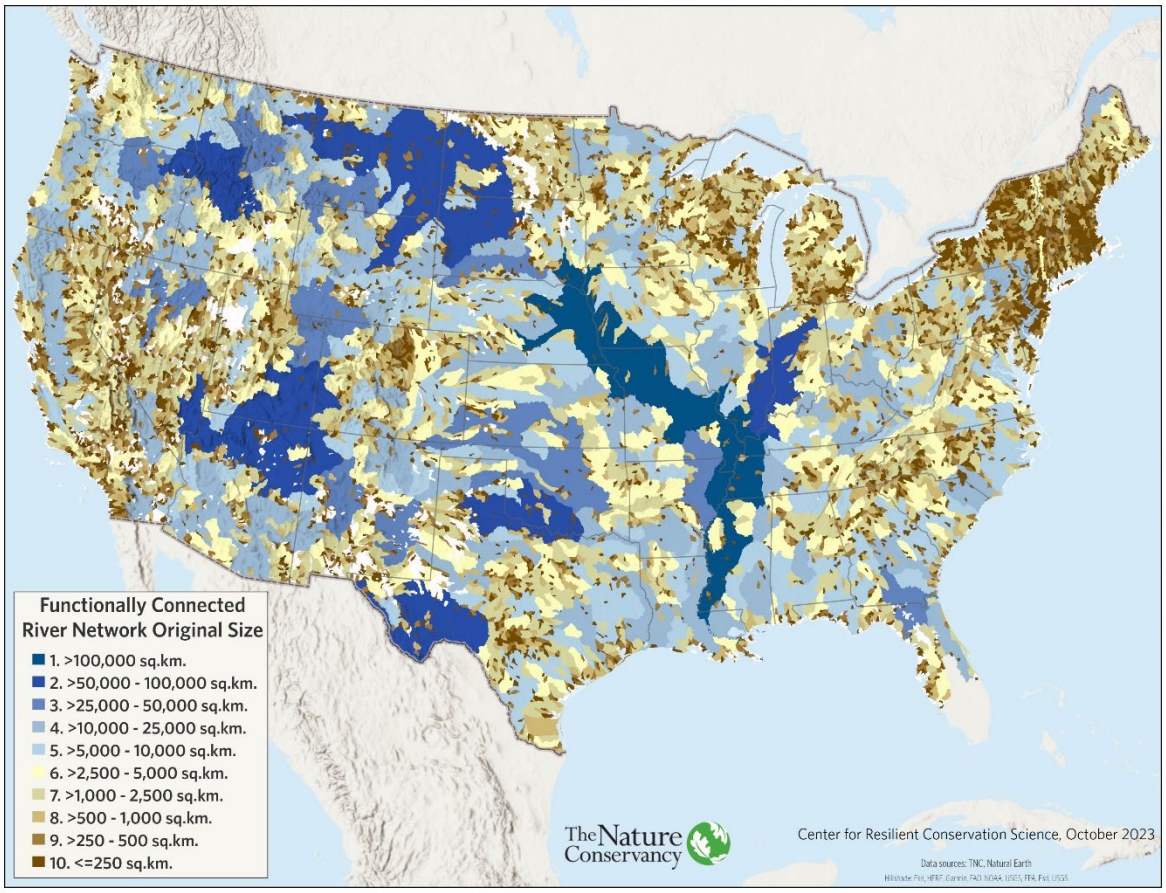

We then adjusted an FCN's size class to account for the following characteristics which altered the realized size of the network, and thus the availability of habitat to aquatic organisms:

- Dam passability (adjusted upward for partially passable dams)
- Great Lakes or ocean connection (adjusted upward for increased area)
- Reservoirs (adjusted downward for decreased traversability)
- Headwater fragmentation (adjusted downward for decreased headwater connection)

Accounting for Partially Passable Dams

Our dataset of river dams included 780 partially passable dams that allow AOP under some conditions. To account for this, we calculated a cumulative discounted length for each FCN bounded by a permeable dam to provide an estimate of the increase in network length. For a given FCN, the cumulative discounted length was calculated by multiplying the permeability of the dam by the length of the FCN on the other side of the dam and continuing in an iterative fashion, multiplying the area of each FCN by the product of all passability scores between it and the given FCN, until a full barrier, coastline, or upper headwater bound is reached (Figure 3.4). Thus, a large FCN immediately adjacent to a given FCN will have more influence on the cumulative discounted value than a large FCN that is accessed via multiple partially passable barriers. The resulting estimated increase is less than if the dam was removed but reflects a proportionally weighted increase in potential access to the networks upstream or downstream.

To estimate the *area* of the network described by the cumulative discounted length, we used the relationship between the FCN watershed area and the length of FCN rivers plus creeks (flowlines > 10 km^2 drainage area) by fitting a regression model to the datasets (adj $R^2 = 0.89$, $p < 0.0001$):

$$Area\ (log\ km) = 1.3 + 0.979\ FCN\ length\ in\ log\ km$$

We then evaluated the size class of the predicted watershed area. In many cases, the small increase in accessible area was not enough to place the FCN into a larger size class, but in some cases the FCN moved up one or two size classes. We capped the increase at two size classes after inspecting the few FCNs that received more than a two-size class increase.

Figure 3.4. Cumulative-discounted FCN length. The left network comprises five FCNs defined by four full-barrier dams. The right network shows how the cumulative discounted length was calculated when three of the dams were partially passable.

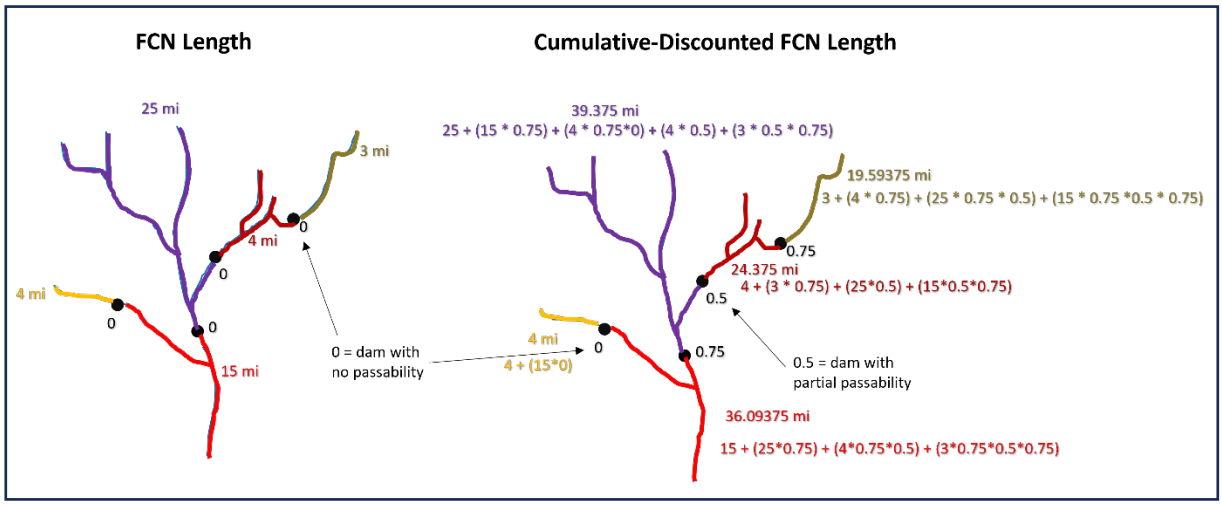

Connectivity to Large Water Bodies

We made further adjustments to the FCN size classes to reflect terminal connections to the Great Lakes or the ocean and the ability of many aquatic organisms to move through these environments.

- Great Lakes: All FCNs connected to the Great Lakes were moved to the largest size class to represent how these networks interact with a larger freshwater system.

- Oceans: We used the following rules, based on the median or mean size of all ocean-connected FCNs, to determine the appropriate size class for ocean-connected FCNs. While we increased the size class of these FCNs, they were not all moved to the largest size class as we did for the Great Lakes-connected FCNs, due to the traversability impediment for freshwater species not adapted to move through saline environments.
    1. If already in size class 3 or larger (>25,000 km^2), no change in size class
    2. If already in size class 4 (>10,000-25,000 km^2), move to size class 3
    3. If greater than the mean size (2,000 km^2) and less than 10,000 km^2, move to size class 4
    4. If greater than the median size (300 km^2) and less than the mean (2,000 km^2), move to size class 5
    5. If less than the median size (300 km^2), move to size class 6

Reservoir Penalty

Reservoirs create challenges for movement, especially in regions without large natural lakes. For freshwater biota adapted to riverine habitats, large reservoirs may present a significant obstacle to the movement of many species or disrupt reproductive strategies that require long, continuous streams for broadcast reproductive strategies (Gido et al. 2010). Additionally, reservoirs are often stocked with predatory invasive species which can have a negative effect on native biota (Juracek 2015), as can the recreational use of motorized boats. However, reservoir habitat is highly variable and sometimes may provide important refugia or connecting tissue especially during times of drought for freshwater biota.

We applied a traversability penalty to the size class of FCNs that contained a large reservoir to account for the increased difficulty freshwater biota could experience moving through large reservoir habitat. We only applied this penalty in ecoregions where large deep lakes do not naturally occur (Figure 3.5), and we limited it to large deep reservoirs over 1,000 acres in size or reservoirs over 30 feet deep and at least 500 acres in size.

In ecoregions with many natural lakes, we assumed that the freshwater biota evolved with the interspersion of large waterbodies. To identify these ecoregions, we selected freshwater and terrestrial ecoregions where no natural large and deep natural lakes occurred using the "origin" attribute for lakes in the National Lake Assessment dataset (EPA 2012).

Figure 3.5. Reservoir penalty. The reservoir penalty was applied in the freshwater ecoregions shown in light brown because they had no natural large and deep lakes.

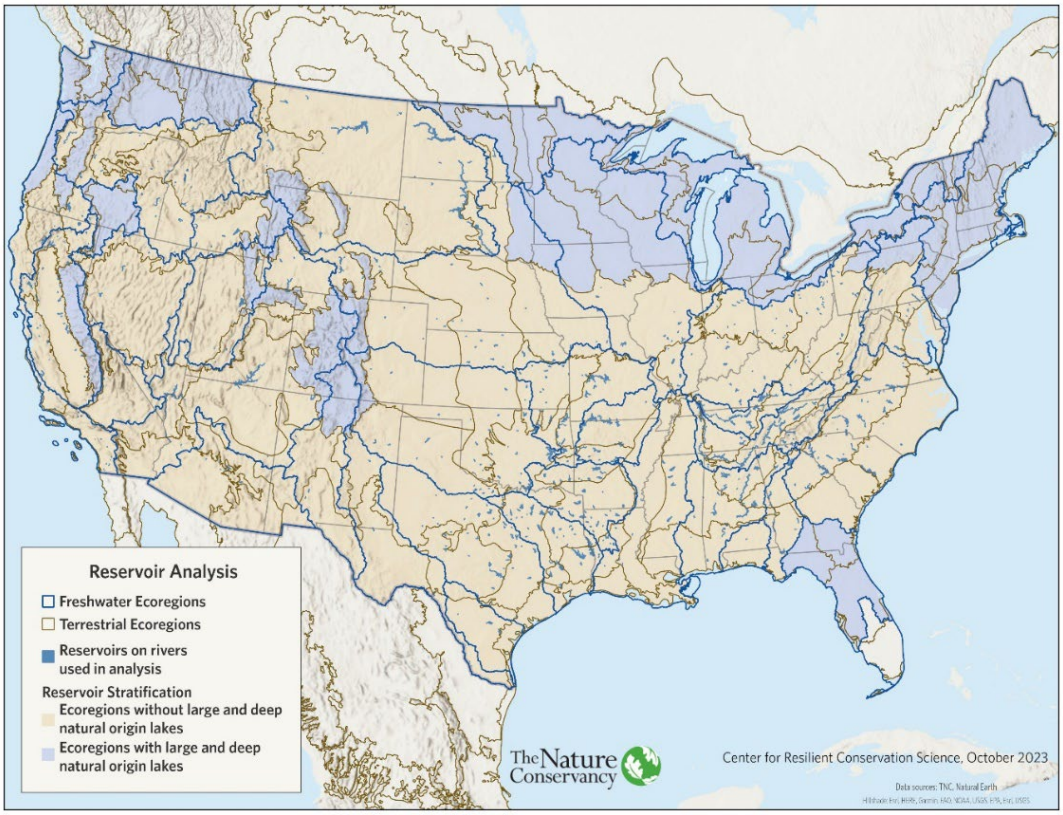

We calculated the reservoir penalty as a function of the reservoir position within the FCN and the orientation of incoming river(s). An example of a reservoir with minimal impact on connectivity would be one located at the base of an FCN where the total length of the longest incoming river above the reservoir was very close to the total length of the FCN (Figure 3.6 example 1). An example of a high impact reservoir would be one where the location of the reservoir and incoming tributaries fragments the total FCN length into many small segments (Figure 3.6 example 2). In the latter case, the longest riverine length above the reservoir would be a small percentage of the total FCN length. For every FCN that contained a reservoir, we calculated the length of the largest lobe above the reservoir and then the percentage of the total FCN length accounted for by the lobe. If the longest reservoir lobe was less than 70% of the total FCN size, we lowered the FCN size class by one class.

Figure 3.6. Reservoir position. In example 1, the reservoir has a minimal impact because the longest river network above the reservoir is 90% of the previously connected riverine FCN length. In example 2, the reservoir has a high impact on connectivity because the longest river lobe above the reservoir is only 50% of the total connected riverine FCN length.

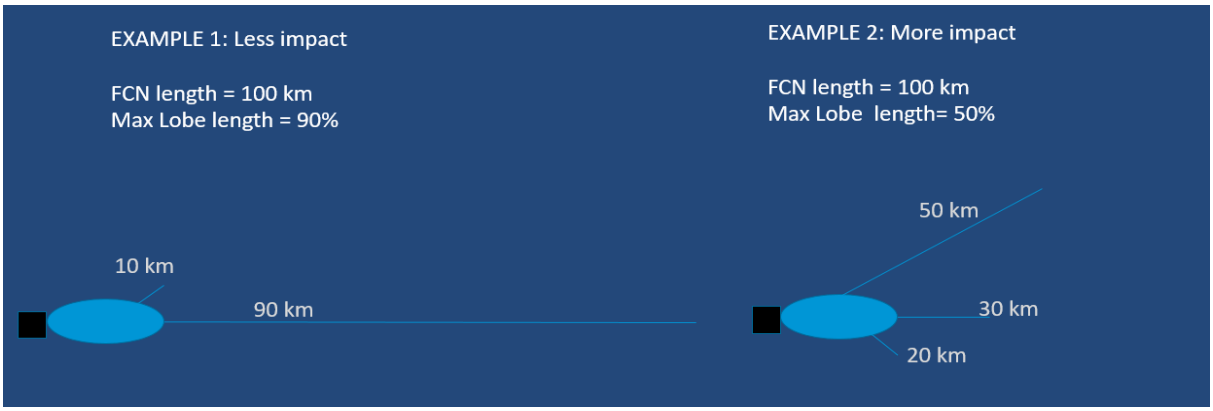

Headwater Fragmentation

The headwater fragmentation metric expresses how much of the headwater area of a HUC-12 and an FCN is likely to be connected to its rivers. Headwater connectivity is critical to protecting and maintaining downstream ecological integrity (Alexander et al. 2018). We used this analysis to adjust the FCN size, lowering the size class by one class if the headwaters were highly fragmented ("Below Average" or "Far Below Average" score). The analysis used the 58,000 dams falling on headwater streams, which we did not review for accuracy or location. We used the number and configuration of small headwater dams to compare the drainage area upstream of the small dams to the total area of the FCN to provide an estimate of the degree to which small dams are likely decreasing overall headwater connectivity within a network.

HUC-12 Headwater Fragmentation

We delineated the upstream drainage area of each dam on headwaters and creeks (draining 100 km^2 or less), excluding any dams that were used to create the FCNs. We then spatially intersected the HUC-12 watersheds with these upstream dam drainages and calculated the total dam drainage area for each HUC-12. To calculate the percent headwater connectivity, we divided the largest drainage area in each HUC-12 by the total HUC-12 area (Figure 3.7).

We calculated z-scores by freshwater ecoregion, climatic zone, and CONUS-wide, and for each we assigned the connectivity values to seven classes using natural breaks (Table 3.2). After reviewing maps of the z-score and natural break classes, we selected the CONUS natural break classes as the most accurate representation of headwater fragmentation (Figure 3.8). We then translated the natural break classes to z-scores (Table 3.2).

Figure 3.7. HUC-12 percent headwater connectivity examples. Watersheds in red are the most fragmented by dams on headwaters and creeks, while watersheds in green have no stream dams or the location of stream dams has a minimal impact on headwater connectivity.

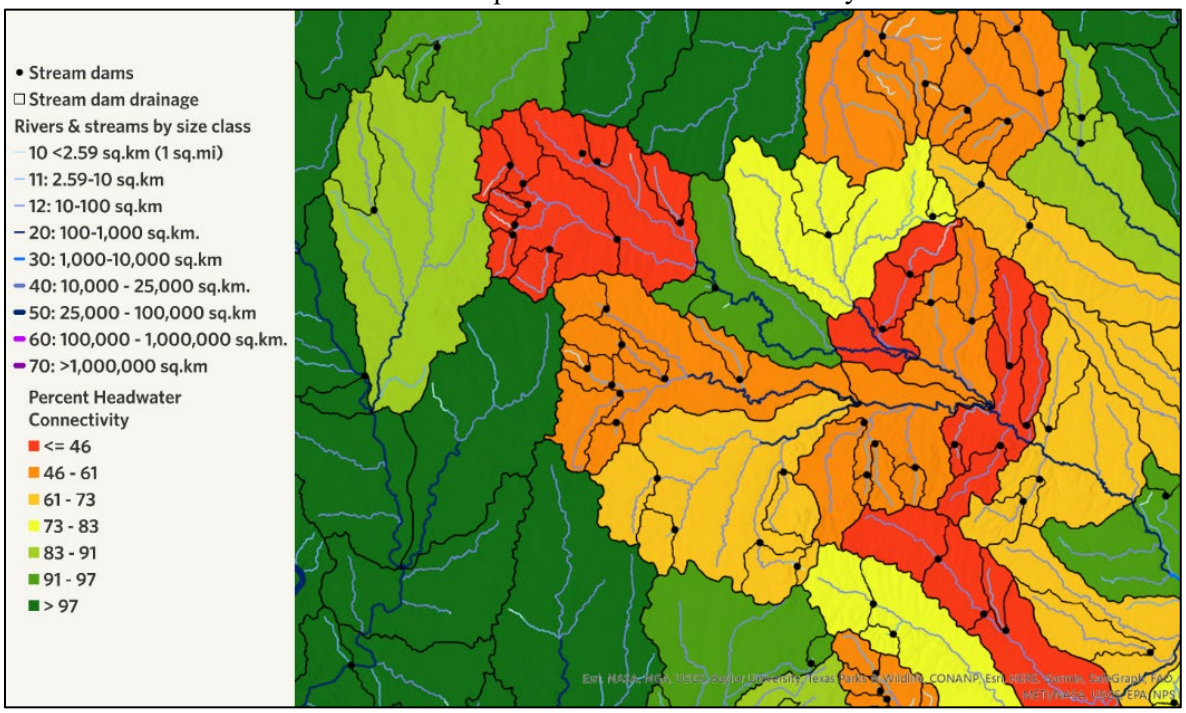

Table 3.2. Assignment of HUC-12 headwater connectivity values to z-scores.

Headwater Connectivity (%)	Natural Break Class	Z-Score Range	Z-Score Class
≤45.53	1	-3 to -2	Far Below Average
> 45.53 & ≤ 60.61	2	-2.1 to -1	Below Average
> 60.61 & ≤ 72.72	3	-1.1 to -0.5	Slightly Below Average
> 72.72 & ≤ 82.64	4	-0.51 to 0.51	Average
> 82.64 & ≤ 90.60	5	0.51 to 1	Slightly Above Average
> 90.60 & ≤ 97.04	6	1.1 to 2	Above Average
> 97.04	7	2.1 to 2	Far Above Average

Figure 3.8. HUC-12 headwater connectivity classes. These natural-break classes were translated to z-scores as shown in Table 3.2. Watersheds in red are the most fragmented by the location and/or number of stream dams while watersheds in green have no stream dams or the location of stream dams has very little impact on headwater connectivity.

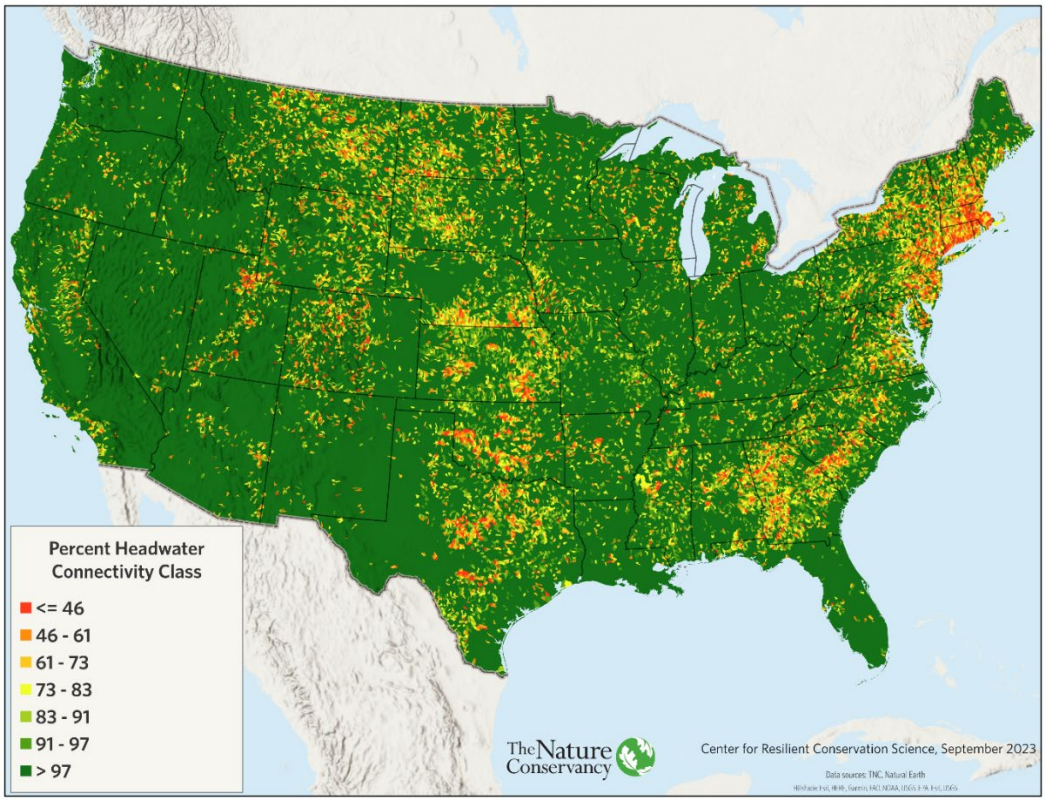

FCN Headwater Fragmentation

We calculated percent headwater connectivity for FCNs using the same approach as described above for HUC-12 watersheds. That is, we spatially intersected the stream dam drainages with the FCN watersheds, calculated the total dam drainage area for each FCN, calculated the FCN area not in an upstream dam drainage, and found the largest drainage area in each FCN.

To calculate the percent headwater connectivity metric, we divided the largest drainage area in each FCN by the total FCN area. As for the HUC-12s, we used the CONUS-wide natural break classes and translated those classes to z-scores (Table 3.3, Figure 3.9). If FCN headwater connectivity was "Below Average" or "Far Below Average," we lowered the size class by one class.

Table 3.3. Assignment of FCN headwater connectivity values to z-scores.

Headwater Connectivity (%)	Natural Break Class	Z-Score Range	Z-Score Class
≤ 40.47	1	-3 to -2	Far Below Average
> 40.47 & ≤ 56.02	2	-2.1 to -1	Below Average
> 56.02 & ≤ 68.30	3	-1.1 to -0.5	Slightly Below Average
> 68.30 & ≤ 79.05	4	-0.51 to 0.51	Average
> 79.05 & ≤ 88.52	5	0.51 to 1	Slightly Above Average
> 88.52 & ≤ 96.34	6	1.1 to 2	Above Average
> 96.34	7	2.1 to 2	Far Above Average

Figure 3.9. FCN headwater connectivity classes. These natural-break classes were translated to z-scores as shown in Table 3.3. FCN watersheds in red are the most fragmented by the location and/or number of stream dams while watersheds in green have no stream dams or the location of stream dams has very little impact on headwater connectivity.

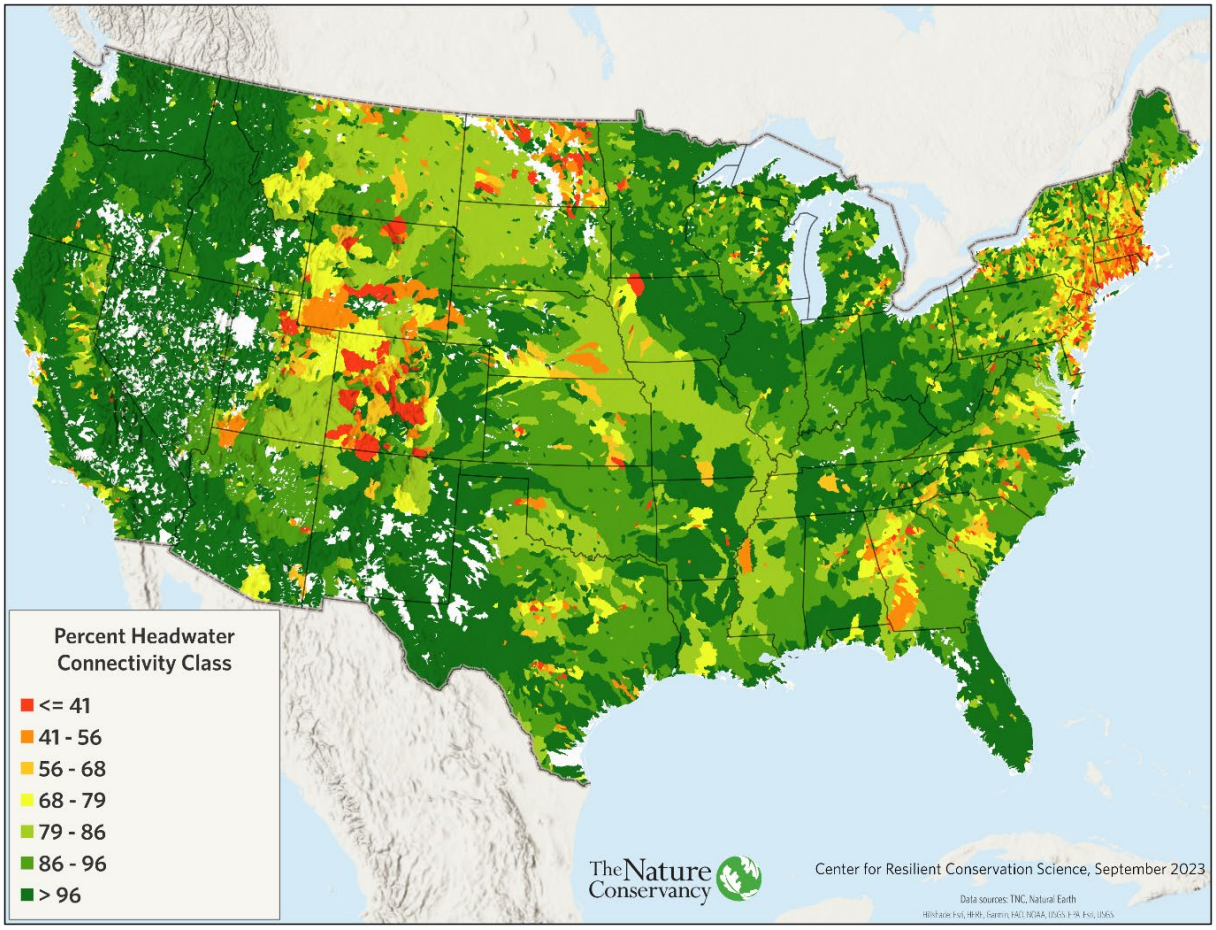

Scoring of HUC-12s not within an FCN

A small number of HUC-12s were not part of any FCN as they did not include a mapped river. Rather than exclude these HUC-12s from our analysis, we chose to assign them to a small to medium size class using the following rules based on their downstream connectivity type and headwater connectivity. High headwater fragmentation refers to HUC-12s that scored "Below Average" or "Far Below Average" for headwater connectivity.

- Ocean connected without high headwater fragmentation = size 7
- Ocean connected with high headwater fragmentation = size 8
- Great Lakes connected without high headwater fragmentation = size 3
- Great Lakes connected with high headwater fragmentation = size 4
- Internal HUCs not connected to a river, without high headwater fragmentation = size 10
- Internal HUCs not connected to a river with high headwater fragmentation = size 11
- Internal HUCs less than 50 km^2 = size 11

Final Functional Connectivity Score

All the foregoing adjustments were used to determine the final functional connectivity score. Figure 3.10 shows which FCN and HUC-12 units were adjusted for their level of functional connectivity and for what reason (dam passability, large water-body connection, reservoirs, and headwater fragmentation). Table 3.4 shows how we translated the final size classes based on natural breaks to z-scores. Figure 3.11 shows the final adjusted functional connectivity z-score for all FCNs.

Figure 3.10. HUC-12 units adjusted for functional connectivity by type of adjustment.

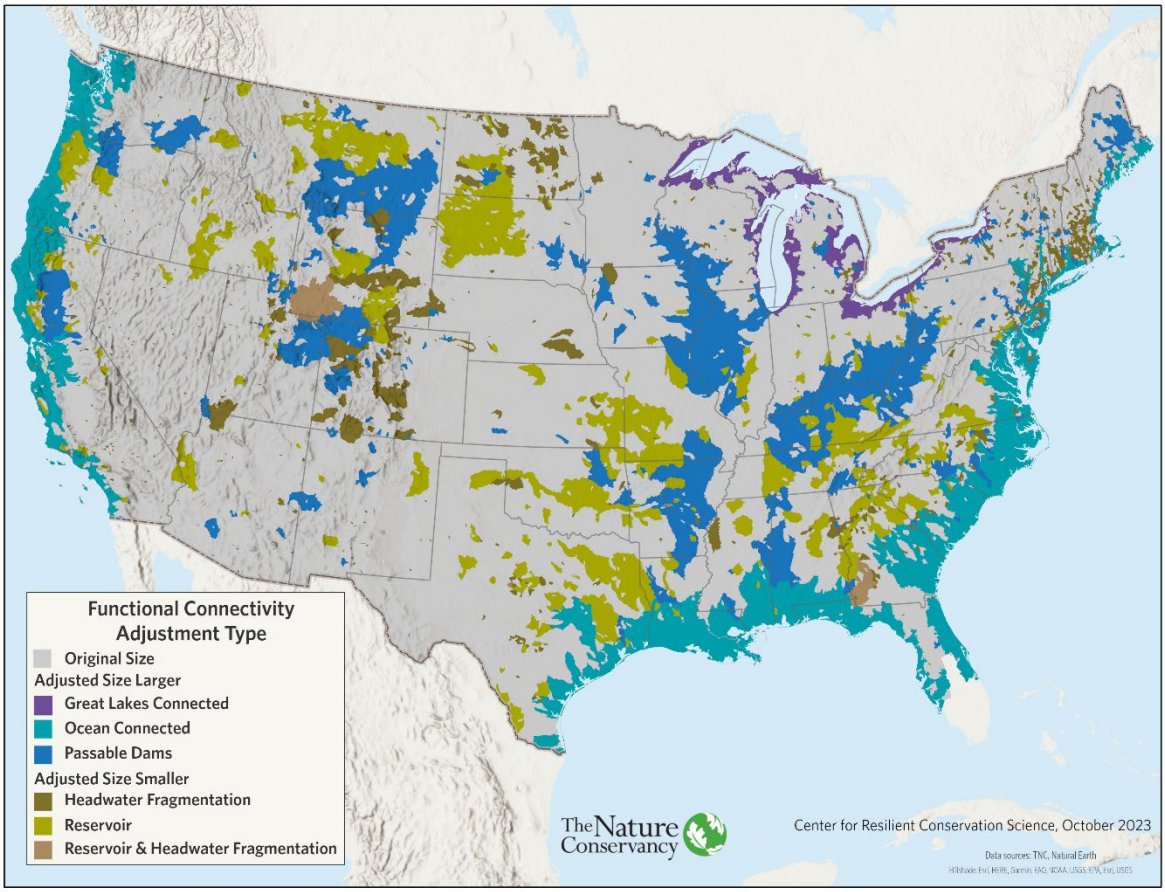

Table 3.4. Final FCN size class z-scores.

Size Class	Area (km^2) Thresholds	Z-Score
1	>100,000	3.0
2	>50,000 - 100,000	3.0
3	>25,000 - 50,000	2.3
4	>10,000 - 25,000	1.7
5	>5,000 - 10,000	.99
6	>2,500 - 5,000	0.5
7	>1,000 - 2,500	-0.51
8	>500 - 1,000	-1.01
9	>250 - 500	-1.7
10	<=250	-2.3
11	< 50	-3.0

Figure 3.11. Final functional connectivity scores. This map shows the functional connectivity score for each FCN based on the original size of the riverine network adjusted for passable dams, connectivity to the ocean or Great Lakes, large reservoirs, headwater fragmentation, and for HUCs not within FCNs.

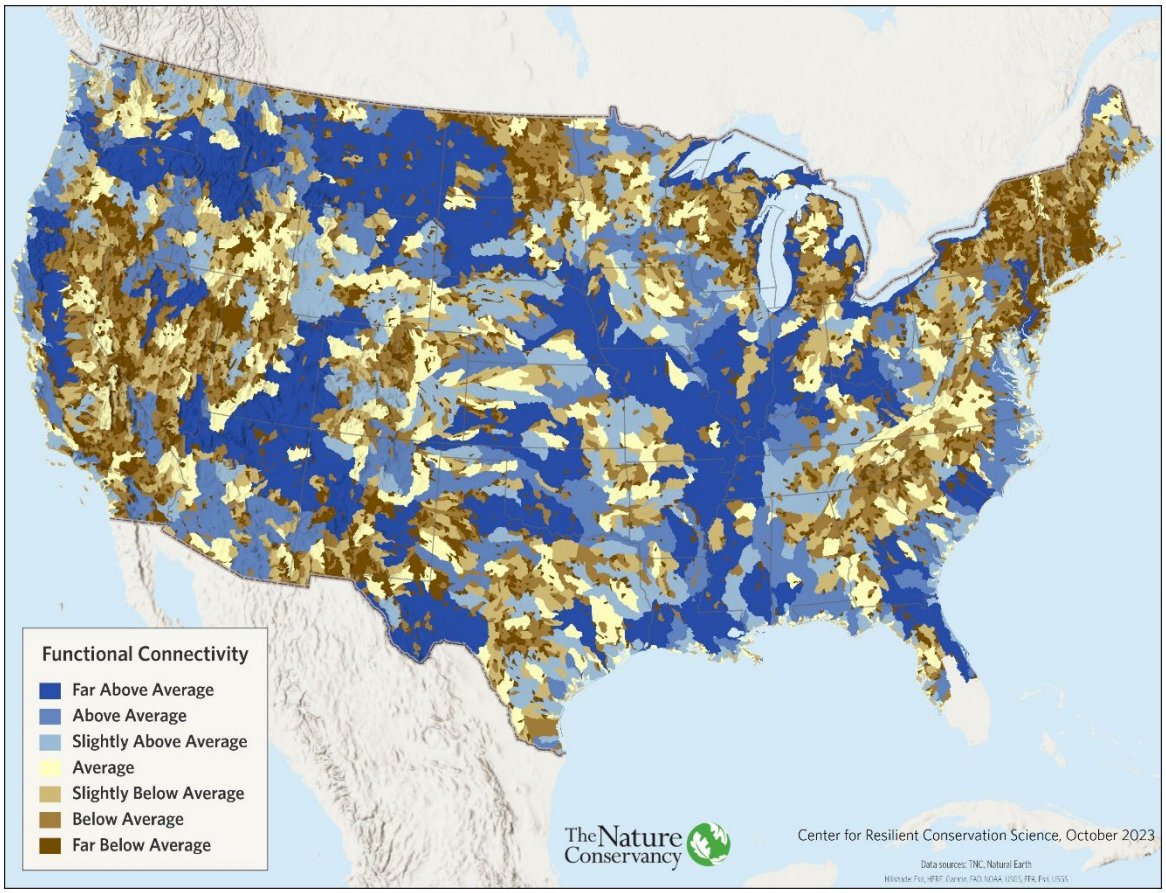

Diversity

The diversity score measures the physical habitat variation in an FCN. Greater connectivity increases the opportunity for dispersal, while variation in connectivity among multiple stream sizes and major habitats increases resilience and metapopulation stability (Pelletier et al. 2020). In other words, the connectivity of a variety of habitats in an FCN gives organisms options to move in response to seasonal and interannual changes in the ambient environment. Not only does this include connectivity across scales, but also the availability of diverse habitats for various life-history stages and to buffer aquatic systems from physical disturbance or invasive species, creating an insurance effect (Pelletier et al. 2020). This is important in a changing climate for species moving north or up in elevation seeking cooler waters (Comte & Grenouillet 2013), but also for species in prairie streams, such as in the Great Plains, as it maintains connectivity to larger order streams with more abundant perennial water (Dodds et al. 2004). When accessible, a diversity of temperatures, gradients, size classes, and habitats creates options for species to find suitable habitat as conditions change. For example, an FCN with a range of temperatures, especially cooler or colder waters, can provide habitat and refugia for species able to access them as temperatures increase.

Temperature Diversity

Stream temperature is fundamental to freshwater resilience because it sets the physiological limits of persistence for many organisms, and temperature extremes may directly preclude certain taxa from inhabiting a water body. Seasonal changes in water temperature often cue development or migration, and temperature can influence growth rates and fecundity. Ideally, a resilient stream network would span a range of current temperatures, offering options for both coldwater and warmwater species and providing connected habitats for species to stay within their thermal preferences in the future (Woodward et al. 2010). For each FCN, we calculated the diversity of temperature classes and gave more weight to areas with persistent cold water.

Mean summer stream water temperature modeled data was available for most reaches from the EPA's Stream-Catchment (StreamCat) dataset (Hill et al. 2016), a national source widely used to study reference temperatures. The StreamCat model is based on stream gage data from 1999-2008 and fits a single, nation-wide predictive model to the data by applying variable selection techniques to potential variables. The final model used six predictors: mean summer air temperature, watershed area, base-flow index, mean stream channel slope, soil bulk density, and elevation ranges within each watershed. The model predicts stream temperature by accounting for differences in the physical environments among streams.

We extracted the mean summer stream temperature variable (MSST 2014) to represent the predicted reference-condition mean summer stream temperatures. The missing data for streams in northern Michigan was filled in using Lyons et al. (2009). Temperature predictions were not available for very large rivers (>100,000 km^2) because they were not represented in the MSST gage dataset.

Temperature Classes

The continuous temperature predictions were lumped into five summer classes following McManamay et al. (2019), except that we lumped the two coldest classes for which there were few reaches (Table 3.5). The temperature class breaks matched closely to those used in other stream and river classifications developed in Michigan (Lyons et al. 2009), the Appalachians (Olivero-Sheldon et al. 2015), and the Eastern U.S (McManamay et al. 2018).

Table 3.5. Temperature classes in Celsius and Fahrenheit.

Temperature Class	Celsius	Fahrenheit
Very Cold	<15	<59
Cold	>15-18	59-64.4
Cool	>18-21	64.4-69.8
Cool-Warm	>21-24	69.8-75.2
Warm	>24C	>75/.2

Weighting for Cold Temperatures

The FCN represents the accessible stream network for populations to use and move within. Given stream temperatures are warming from climate change, our temperature metric incorporated a count of the diversity of temperature classes present in the FCN with more weight given to colder temperature classes. A temperature class was counted if it made up more than 5% of the network, exclusive of very small headwater streams (less than 10 km^2). The classes were weighted as follows to form an index of temperature diversity:

*Temperature Diversity = (5*Very Cold) + (4*Cold) + (3*Cool) + (2*Cool-Warm) + (1*Warm)*

These scores were transformed into z-scores and an additional 0.5 SD increase was added to the score if modeling indicated the lowest temp class was maintained in a future that was 2.2°C warmer. An increase of 2.2°C is the rise in average summer stream temperature predicted for U.S. streams by 2100 (Hill et al. 2014). To calculate this, we added 2.2 degrees C to the reference predicted MSST stream temperatures of each flowline (Figure 3.12) and recalculated the presence and proportions of each class in the FCN in this new scenario (Figure 3.13).

Figure 3.12. Adjustment in mean summer stream temperature. Left map shows the temperature reference condition estimated from the EPA StreamCat model. Right map shows the model results with a 2.2^0 C rise in temperature.

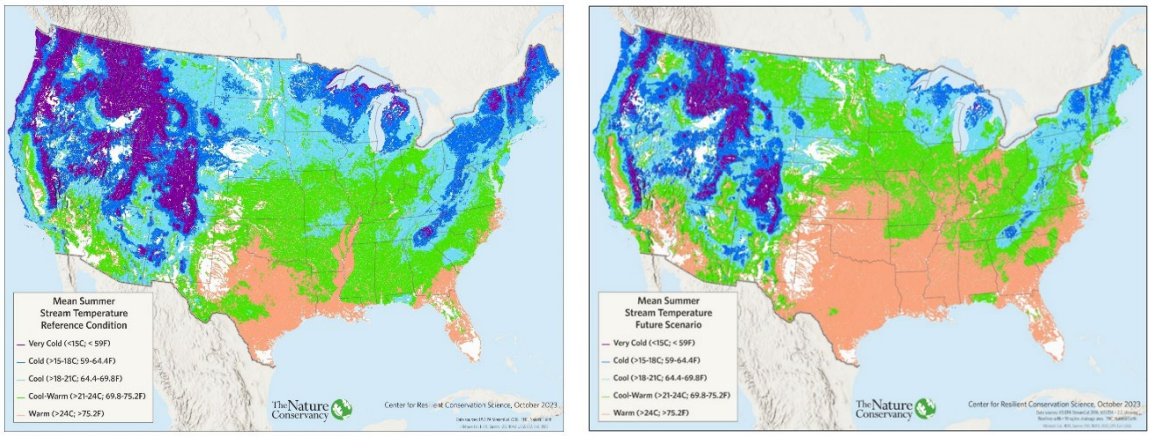

Figure 3.13. Final temperature model. This map shows the z-scores of the cold-weighted temperature index and the 0.5 SD persistent cold bump.

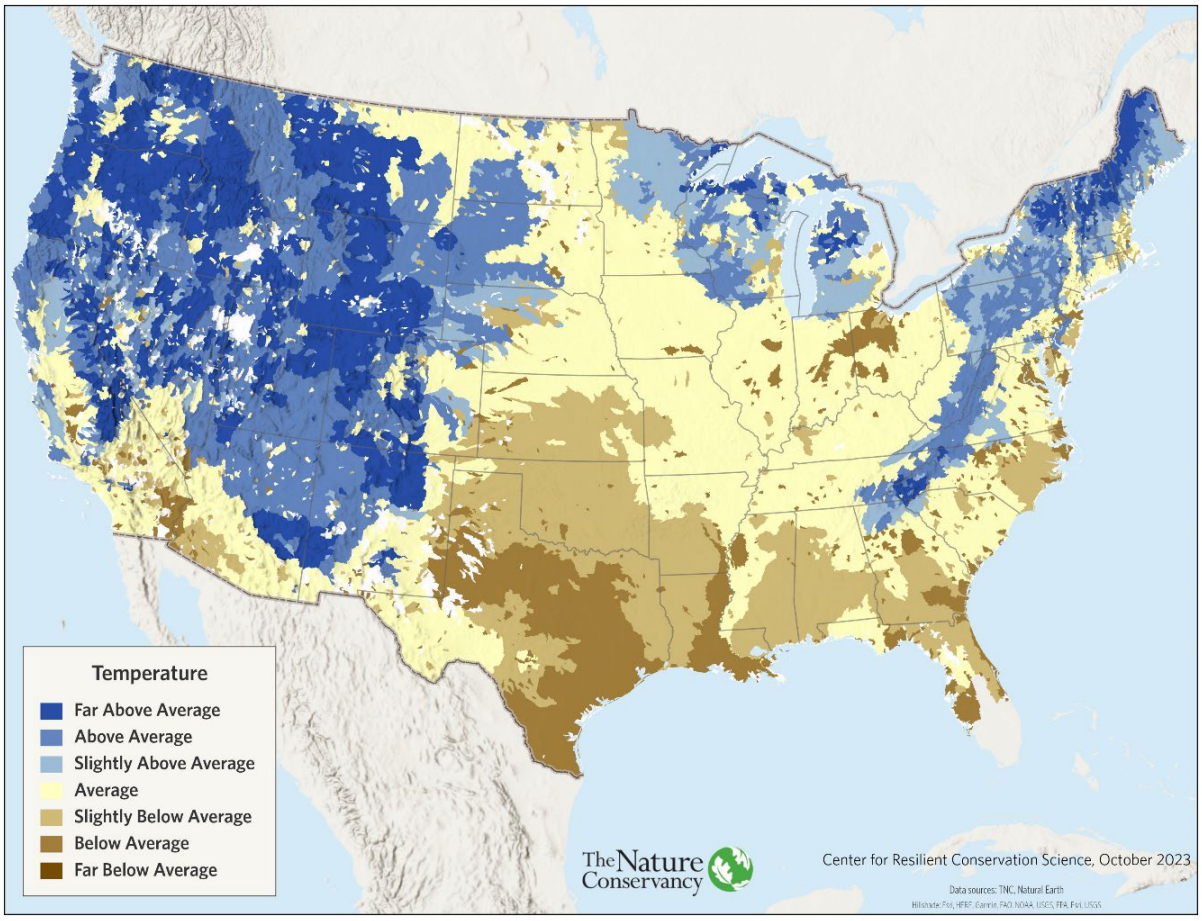

Macrohabitat Diversity

Macrohabitats are the finest scale unit of hierarchical aquatic classification types defined in TNC's freshwater classification approach (Higgins et al. 2005). They define stream reach types or lake types and are based on key abiotic variables known to structure aquatic communities at the reach or lake scale. For this analysis, we created simplified macrohabitat types to represent variation in major aquatic physical habitats at the stream reach or individual lake scale using variables possible to model in GIS. Our hypothesis was that HUC-12 units with more macrohabitats would provide more options for species to adapt to change and thus support resilience.

Development of the macrohabitats was guided by the variables and ecologically relevant classes included in the national stream classification developed by McManamay and DeRolph (2019) and related studies on physical freshwater classification and conservation assessment (McManamay et al. 2018; Higgins et al. 2005). Lotic macrohabitats were calculated at the HUC-12 scale based on unique combinations of stream size (7 classes), gradient (5 classes), temperature (5 classes), and tidal influence (2 classes). Stream size is indicative of major ecosystem changes along the stream-river continuum, such as transitions in the state and source of energy and ecosystem metabolism (Vannote et al. 1980). Stream gradient also highly influences aquatic communities at the reach scale due to its

influence on stream bed morphology, flow velocity, sediment transport/deposition, substrate, and grain size (Rosgen 1994). Local temperature was included to account for physiological limits of persistence for many organisms. Tidal influence and lake types were also counted as providing unique habitat diversity. Lake macrohabitats were based on depth to represent major differences in the probability of the presence of cold water in the summer (Olivero-Sheldon & Anderson 2016). A detailed explanation and maps of each macrohabitat component can be found in Appendix 3.

Scoring Macrohabitat Diversity

The final macrohabitat diversity score for each HUC-12 unit was calculated as the number of macrohabitat types, relative to the average number of macrohabitats expected for the size of the HUC. Because the count of macrohabitats was correlated with HUC size, we used a Poisson regression to establish a relationship between the size of the HUC and the count of macrohabitats, and then calculated the standardized residuals to identify HUCs that had more or less macrohabitat diversity than expected for their size. The standardized residuals were used as the z-score.

We made two adjustments to the scores (Appendix 3, Figure A3-4). First, to account for the larger effect of perennial macrohabitats on the available diversity, we calculated z-scores for all streams and for perennial streams only. We combined the two scores, giving equal weight to each, and thus more weight to perennial streams, which were included in both.

Macrohabitat Diversity = (standard residual all streams + standard residual perennial only)/ 2

Small dams on headwaters and creeks decrease the accessibility of all types of macrohabitats within a HUC-12. In HUCs with "Average" or worse headwater fragmentation, we adjusted the macrohabitat diversity score by taking the average of the combined macrohabitat diversity z-score and the headwater fragmentation z-score. Finally, we integrated all the components and penalties into a single weighted map of macrohabitat diversity for CONUS (Figure 3.14).

Figure 3.14. Macrohabitat diversity score. This map reflects all components and weightings.

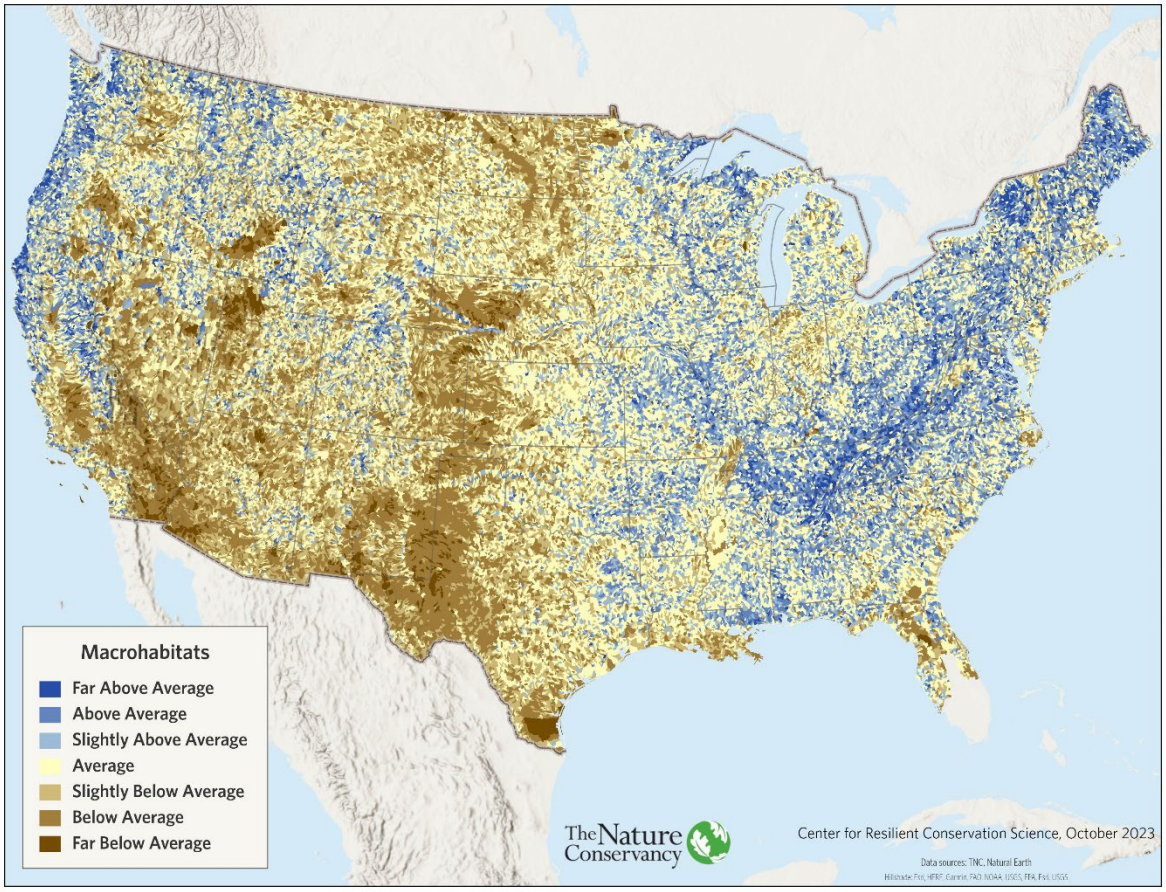

Integrated Diversity Score

Diversity Score = (Temperature score + Macrohabitat Diversity score) / 2

The final diversity score combined the temperature score at the FCN scale and the macrohabitat score at the HUC-12 scale (Figure 3.15). We combined the two scores at the HUC level, giving equal weight to both scores. In the rare cases where HUCS were not within an FCN (e.g., some coastal watersheds or internally draining basins), the diversity score was based only on the macrohabitat diversity score.

Figure 3.15. Diversity score. This map shows the integration of the FCN temperature diversity and the HUC-12 macrohabitat diversity scores.

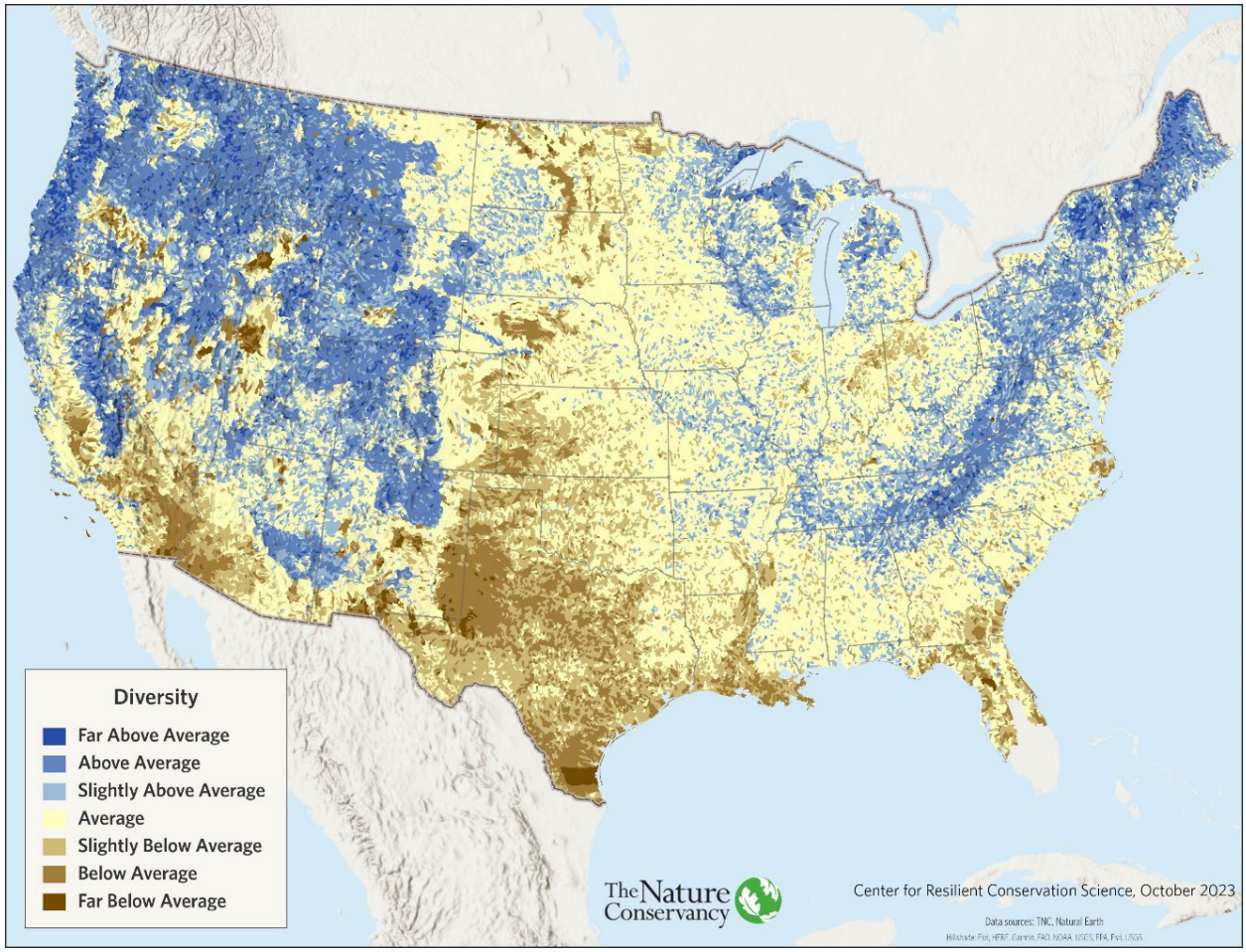

Integrated Connectivity Score

*Connectivity Score = (2*Functional Connectivity + 1*Diversity) / 3*

Our final step was to integrate the functional connectivity score measured at the FCN scale with the diversity score measured at the HUC-12 scale (Figure 3.16). The aim was to be able to assess the size and diversity of a network with a single index that expresses the complexity of the available habitats. While each factor contributes to network resilience, they are not fully independent because functional connectivity is based on size of the network and diversity is also highly correlated with size. To account for this, we assessed macrohabitat diversity based on the departure from expected diversity when compared to that predicted from size alone. However, given the importance of network size to the availability of habitats, we gave functional connectivity twice the weight as diversity in our combined index.

Figure 3.16. Final connectivity score. In this map, the size of the network is given twice the weight as the diversity of the network.

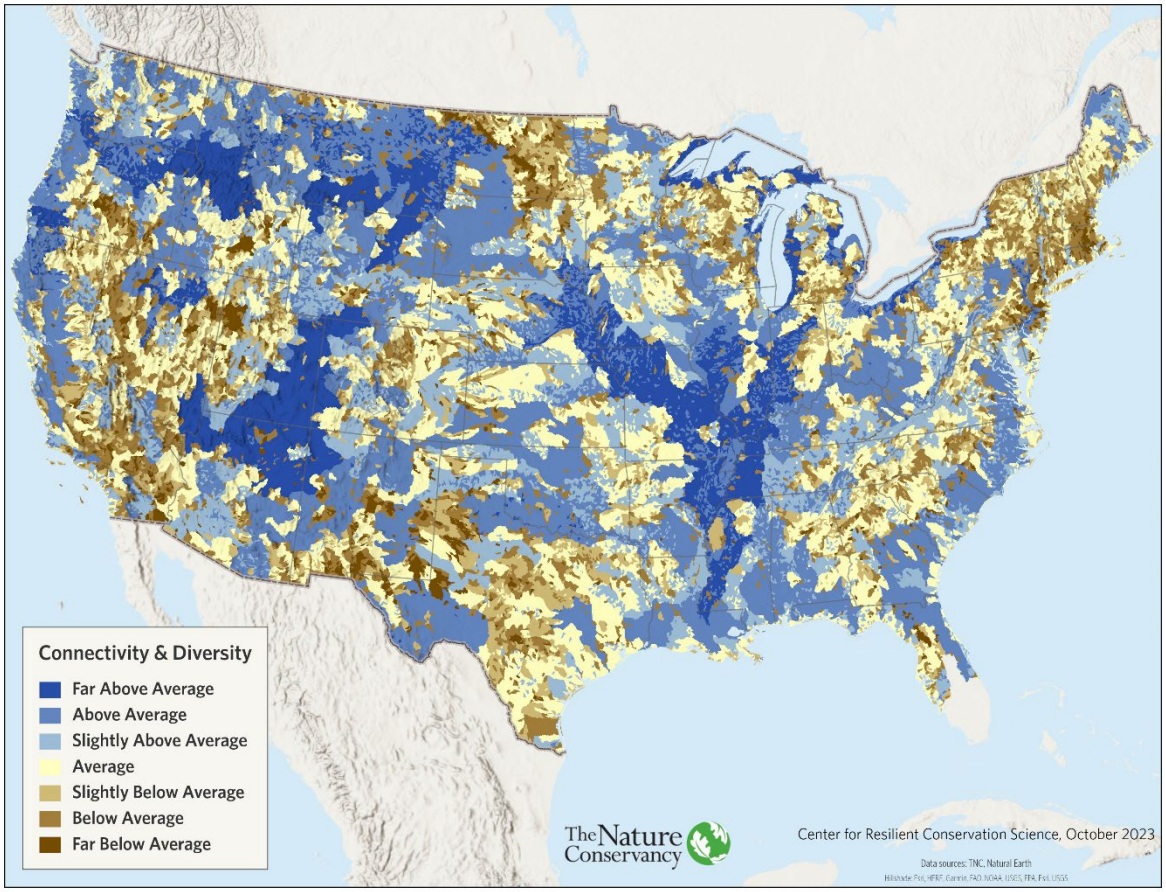

Condition Score

Condition = Naturalness + Water Quality adj. for Surface Mining + Impervious Surface Override

Condition is a measure of current ecological function from landscape influences and accounts for two key ecological attributes of freshwater systems, habitat quality and water quality. This analysis was stratified by arid and humid regions (Figure 2.8).

Naturalness

Naturalness = Floodplain and/or Riparian Naturalness + Watershed Naturalness

In this section, we assess the naturalness of three essential river features, the floodplain, riparian area, and watershed. For each feature, we first developed a map of its extent and then overlaid land cover data to quantify the types and amounts of natural, agricultural, and developed land within the extent.

Floodplains

Connections between a river and its floodplain are essential to the resilience of the system because floodplains allow for water storage, nutrient flushes, and create spatial and temporal feeding and breeding habitat (Pringle 2003). The connection can be interrupted by roads and levees, although this can be difficult to precisely measure because it depends in part on the intensity and depth of each flood event, or the return interval of the flood. We calculated a metric of floodplain naturalness to estimate the relative intactness and availability of the floodplain.

To map floodplains, we compiled all data (10-m GeoTIFFs) representing the 100-year floodplain from the Fathom-U.S. 2.0 dataset (Bates et al. 2021; First Street Foundation 2020) for CONUS. These were merged into a single 10-m raster, taking the maximum value if two grid cells overlapped. We used the "defended" version, meaning that the spatial data accounts for known flood defenses such as levees. We reprojected and resampled the data to a 30-m resolution and snapped it to a base grid to ensure alignment with other grids developed for this analysis. All cells representing modeled water depth values were reclassified to a single value. Permanent water bodies were removed.

To identify watersheds where floodplains were a predominant freshwater feature, we summarized the floodplain area in each HUC-12 and calculated the floodplain percentage in each. We translated the floodplain percentage values to standardized normal scores (z-scores) by arid and humid ecoregions (Figure 3.17). We used this metric to determine how much weight to give the floodplain naturalness score as described below.

Figure 3.17. HUC-12 watershed 100-year floodplain percentage. Watersheds in green have a large area of 100-year floodplain relative to their humid or arid ecoregion (inset map with blue indicating humid ecoregions and lime denoting arid). Watersheds in the Southeastern U.S. coastal plain and parts of the Mississippi River Basin had the highest percentages of floodplain area. There is no floodplain area in the lower Mississippi Alluvial Valley because the data incorporated flood defenses such as levees.

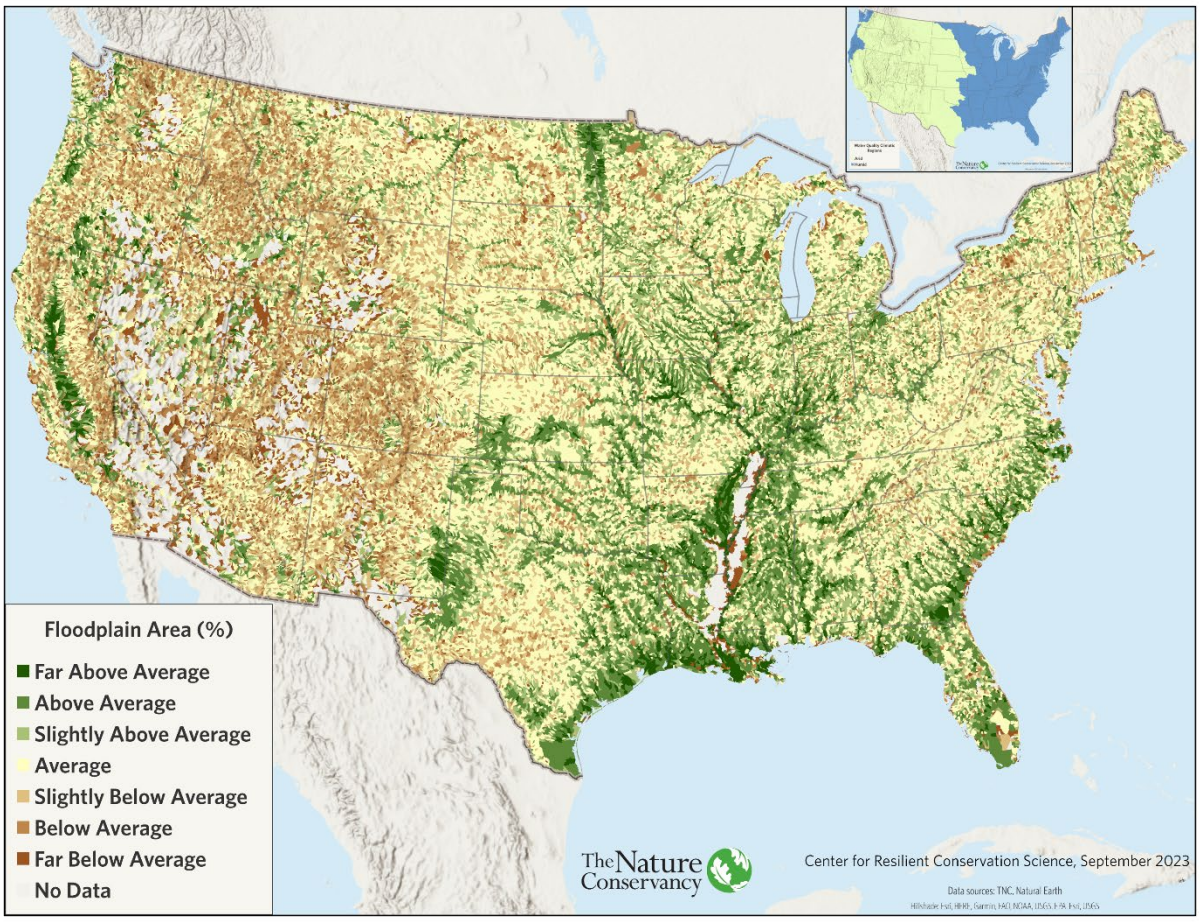

Floodplain Naturalness Index

After removing open water from the 100-year floodplain, we quantified the extent of four land cover categories (Table 3.6) in this zone using data from the National Land Cover Dataset (NLCD, Dewitz & USGS 2019) augmented with surface mining extent (see Surface Mining Penalty section and Appendix 6). Land cover classes were weighted such that wetlands or natural forests had the highest positive influence and roads or permanent development had the highest negative influence, with agricultural lands in between. We did not include pasture and hay lands in the agriculture category as research has shown this land use is not strongly correlated with poor water quality (de Mello et al. 2018). Degree of naturalness was quantified using a weighted index:

$$(1 * \% \text{ High Intensity}) + (0.75 * \% \text{ Agriculture}) + (0.25 * \% \text{ Low Intensity})$$

The index ranged from 0 for a floodplain in completely natural cover to 100 for a completely developed floodplain. We translated the floodplain naturalness index values to standardized normal scores (z-scores) by arid and humid ecoregions (Figure 3.18).

Table 3.6. Land cover class assignment used in the floodplain and riparian naturalness index.

Naturalness Category	NLCD 2019 Class (Value Code)
High Intensity	Low Intensity Developed (22), Medium Intensity Developed (23), High Intensity Developed (24), Mining
Agriculture	Cultivated Crops (82)
Low Intensity	Pasture/Hay (81), Open Space Developed (21), Barren (31)
Natural	Open Water (11), Perennial Ice/Snow (12), Deciduous Forest (41), Evergreen Forest (42), Mixed Forest (43), Shrub/Scrub (52), Herbaceous (71), Woody Wetlands (90), Emergent Herbaceous Wetlands (95)

Figure 3.18. Land cover naturalness index of the 100-year floodplain. Scores were converted to z-scores by humid (blue in inset map) and arid (lime in inset map) ecoregions. Watersheds in green have floodplains in more natural land cover while those in brown are dominated by agricultural and/or developed land uses.

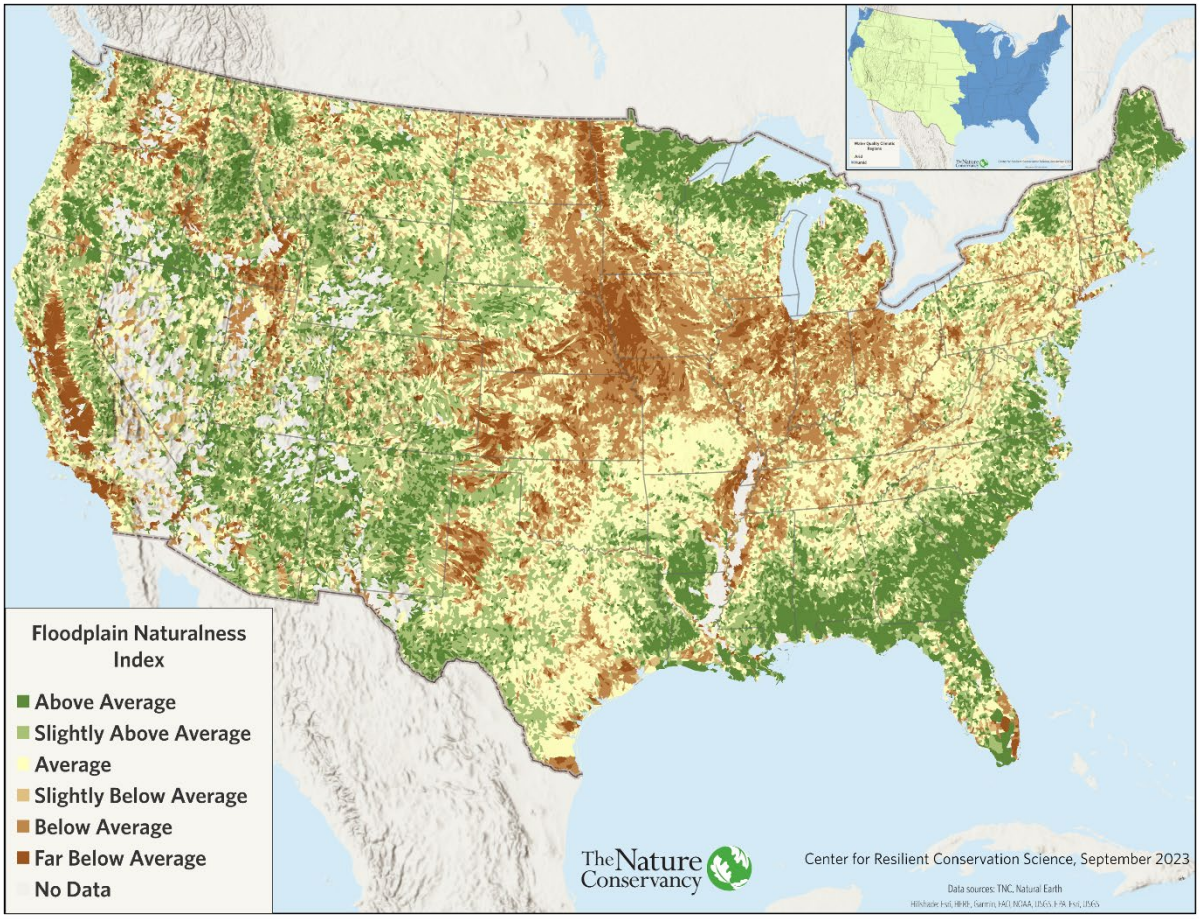

Riparian Areas

Riparian zones contribute to freshwater resilience through their potential to attenuate the effects of precipitation changes (Paukert et al. 2021), dampen temperature rise impacts (Bowler et al. 2012), and for their ability to retain sediments and nutrients that could degrade water quality (Kaufman et al. 2022). To map riparian areas, we compiled the pluvial data (10-m GeoTIFFs) representing the 100-year flood return interval from the Fathom-U.S. 2.0 dataset (Bates et al. 2021; First Street Foundation 2020) and again merged them into a single 10-m raster, taking the maximum value if two grid cells overlapped. "Pluvial" refers to flooding based on the accumulation of rainfall in topographic depressions and accounting for impervious surfaces and land cover. We reprojected and resampled the data to a 30-m resolution and snapped it to a base grid to ensure alignment with other grids developed for this analysis. All cells representing modeled water depth values were reclassified to a single value. Permanent water bodies were removed to avoid inflating natural areas due to the presence of water.

We considered other data sources to map riparian areas including a fixed distance buffer of stream reaches and the U.S. Forest Service national riparian areas (Abood et al. 2022) but found the Fathom pluvial model provided a consistent and comprehensive delineation of areas likely to be riparian based on topography.

Floodplain and Riparian Naturalness

The resampled 30-m grid had unique values to denote if the source was pluvial, fluvial, or both. We classified land cover in the combined fluvial and pluvial area of each HUC-12 into the four categories previously described and shown in Table 3.6. Using those categories, we calculated the land cover naturalness index as described above in the floodplain naturalness section. We again translated HUC-12 index values into z-scores stratified by arid and humid ecoregions (Figure 3.19).

Figure 3.19. Land cover naturalness index of the 100-year floodplain-riparian area. Scores were converted to z-scores by humid (blue in inset map) and arid (lime in inset map) ecoregions. Watersheds in green have floodplain and riparian areas largely in natural land cover while those in brown are dominated by agricultural and/or developed land use.

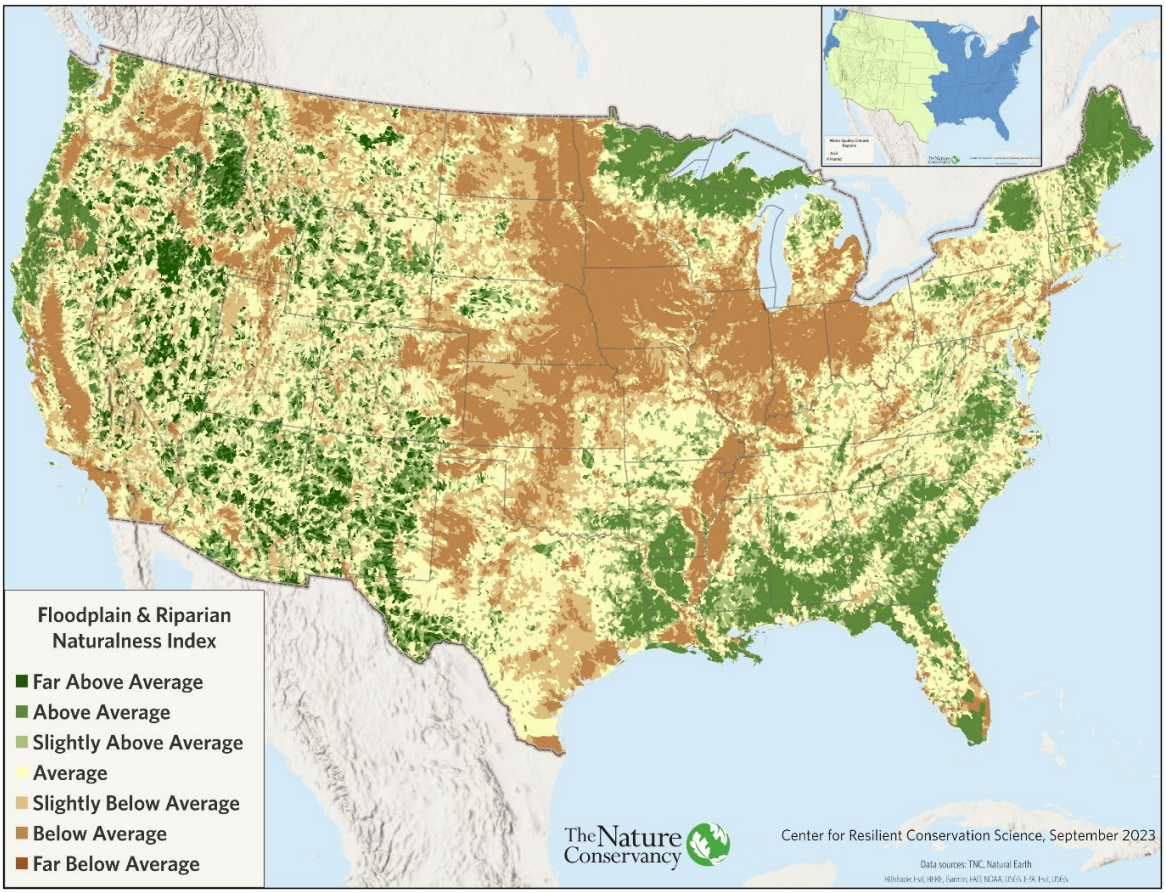

Integrating Floodplain-Riparian and Floodplain-Only Naturalness

After reviewing the land cover naturalness indices for the two different extents (floodplain-only vs. floodplain-riparian), we established a set of rules to guide their use. In arid ecoregions, given the importance of riparian areas and the lack of large floodplains, particularly those with a high number of intermittent or ephemeral streams and rivers, we always used the floodplain-riparian naturalness score. For watersheds in humid ecoregions, we used the floodplain-only score (Figure 3.18) when the percentage of floodplain area was "Above Average" or "Far Above Average." For watersheds in humid ecoregions where floodplains were not a dominant feature (< 1 SD, in the "Slightly Above Average" or lower classes), we used the floodplain and riparian naturalness index score (Figure 3.19).

Relativization of naturalness index values by arid and humid ecoregions led to some unintuitive patterns, particularly in the Western U.S. Because land is less urbanized and there is less water for row crops, land cover in western floodplain and riparian zones is often quite natural. Thus, a western watershed with an "average" naturalness z-score could be completely natural. While this situation also occurred in humid ecoregions, it was less pronounced. To address this issue, we adjusted the z-scores

of HUC-12 watersheds with high floodplain and riparian naturalness scores. Regardless of climatic zone, if the floodplain-only or the floodplain and riparian raw naturalness index score was less than five (highly natural), an increase of 0.5 SD was applied to the respective z-score. If the naturalness index score was greater than or equal to five and less than ten, a smaller increase of 0.25 SD was awarded to the z-scores of those HUC-12s. After making these adjustments, we also adjusted z-scores for humid HUC-12s where floodplains are a critical freshwater component. For humid HUC-12s where the floodplain size was "Far Above Average," we applied a 0.5 SD bump to the adjusted floodplain-only score if the z-score was "Average" or higher. Conversely, if the floodplain land cover was highly altered (less than "Average") but comprised a large proportion of the HUC-12 (floodplain size $\geq$ 2.0 SD, "Far Above Average"), we deducted 0.5 SD from the z-score. For HUC-12 watersheds with an "Above Average" floodplain percentage, we applied a 0.25 SD increase if the naturalness z-score was "Average" or higher and a 0.25 SD penalty if the naturalness z-score was less than "Average." Figure 3.20 shows the results of applying these adjustments, summarized below.

Floodplain-Riparian Score (raw scores)	
Floodplain or Floodplain/Riparian Score < 5	0.50 SD increase
Floodplain or Floodplain/Riparian Score >= 5 & <10	0.25 SD increase

Floodplain-Only Score (z-scores)	Z-score adjustment
Floodplain size >2 SD & Adjusted Naturalness Score >=0.5 SD	0.50 SD increase
Floodplain size >1 SD & Adjusted Naturalness Score >=0.5 SD	0.25 SD increase
Floodplain size >2 SD & Adjusted Naturalness Score < -0.5 SD	-0.50 SD penalty
Floodplain size >1 SD & Adjusted Naturalness Score < -0.5 SD	-0.25 SD penalty

Figure 3.20. Integration of floodplain-only and floodplain-riparian land cover naturalness. Results reflect the integration rules and z-score adjustments described in the text.

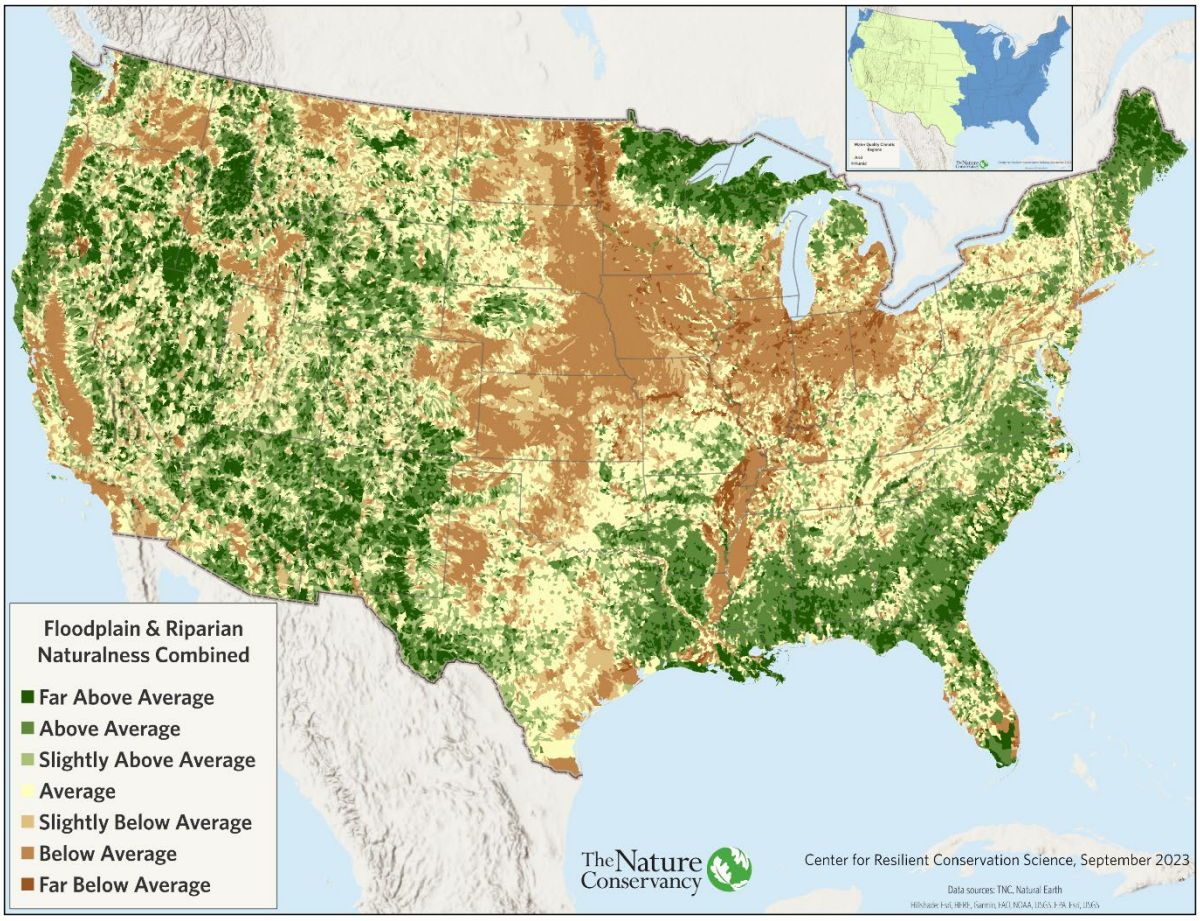

Watershed Naturalness

To put the floodplain and riparian scores in context and assess the degree of degradation within the whole watershed, we calculated a watershed naturalness score for each HUC-12 based on current landcover, adjusted for mining (NLCD 2019, see Surface Mining Penalty section and Appendix 6) and using the same naturalness index methods as described for the floodplain and riparian zones. We translated the watershed naturalness index values to z-scores by arid and humid ecoregions (Figure 3.21).

Figure 3.21. Land cover naturalness index of HUC-12 watersheds. Scores are converted to z-scores by humid (blue in inset map) and arid (lime in inset map) ecoregions. Watersheds in green have more natural and intact land cover while those in brown are dominated by agricultural and/or developed land use.

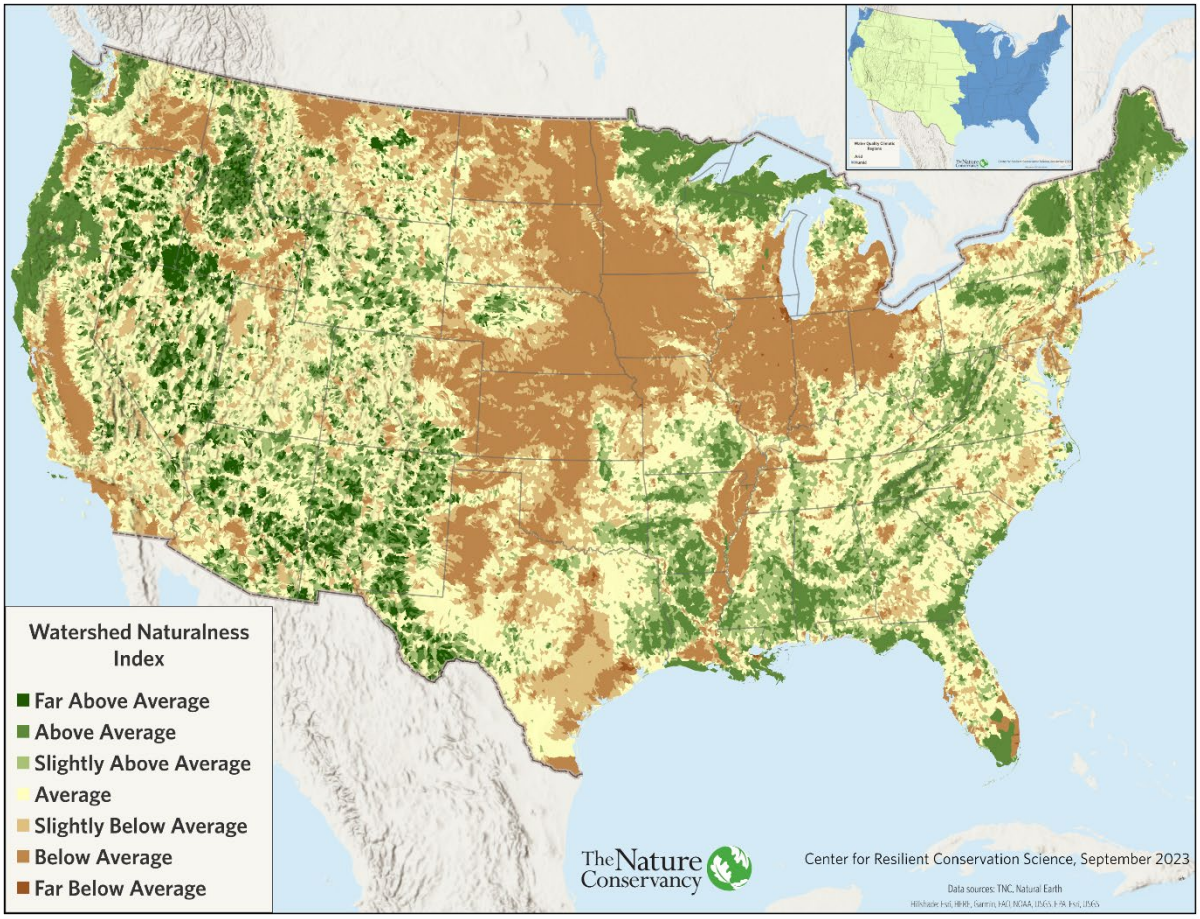

Integrating Floodplain, Riparian, and Watershed Naturalness

A visual comparison of the combined floodplain and riparian land cover naturalness index and the watershed naturalness index shows there are many watersheds where the two metrics are quite similar (e.g., Mississippi River Basin). However, there are also areas where the two metrics paint a different picture such as in North Carolina's coastal plain where riverine floodplains are often large and intact, but their watersheds tend to have altered land cover. We explored several different weighting schemes to address the correlation between these two indices and found that simply averaging the two z-scores seemed to appropriately balance the interplay between these different scales. For example, a watershed with a very natural floodplain but a less natural watershed typically received an "Average" overall naturalness score (dependent on the actual z-scores for the two scales). A watershed primarily in natural cover and with a floodplain in natural cover received a high overall naturalness score. Our final integrated score (Figure 3.22) can be thought of as a watershed naturalness score (Figure 3.21) with more weight given to the floodplain and riparian zone (Figure 3.20) to reflect the importance of direct interaction with streams and rivers in this region.

Figure 3.22. Integrated watershed and floodplain-riparian naturalness scores. The z-scores are the average of the watershed naturalness z-score and the floodplain only or floodplain and riparian naturalness z-score for each HUC-12. The floodplains and land cover of watersheds in green are more natural while the floodplain and land cover of watersheds in brown are characterized by agricultural and/or developed land uses.

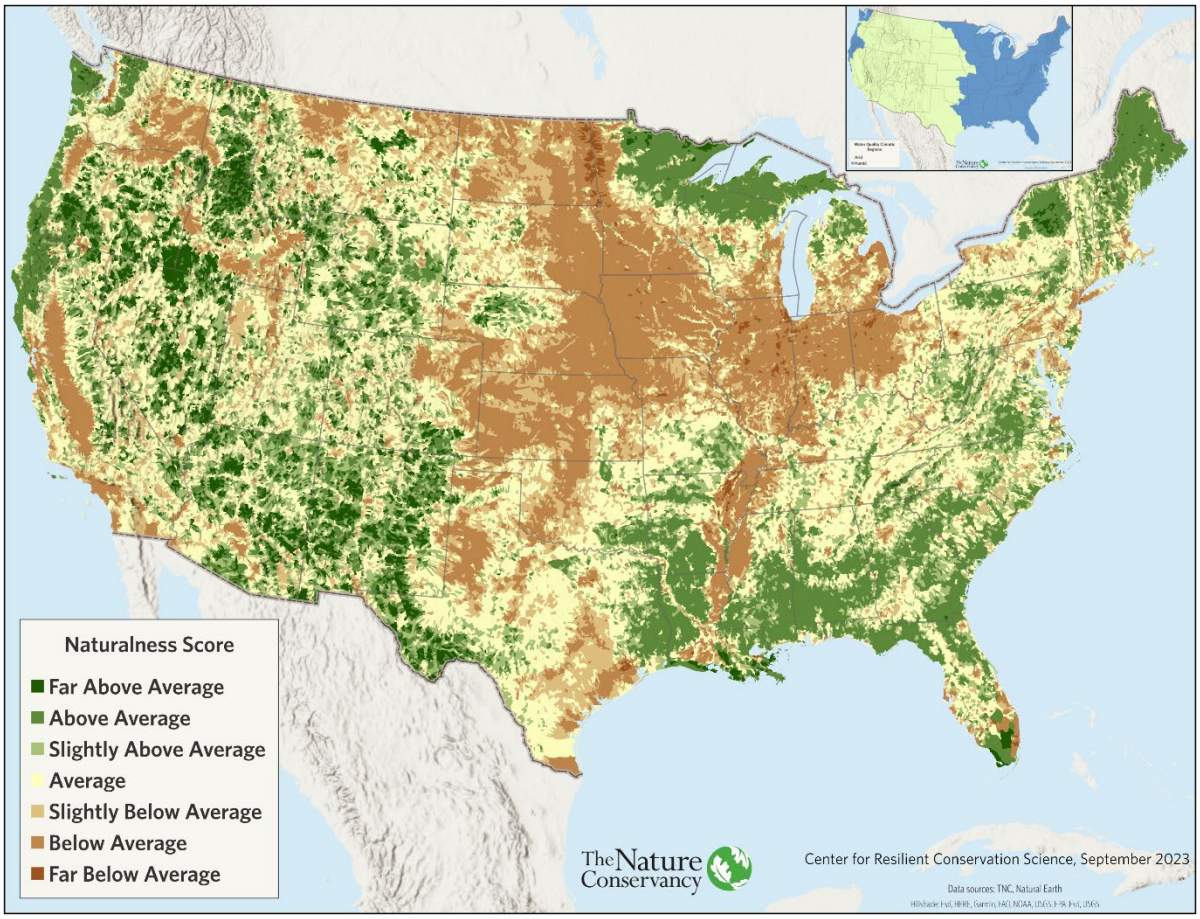

Water Quality

Water Quality = Nutrient and Sediment Index adjusted for Surface Mining

Nutrients and Sediment

Recent studies suggest most U.S. streams and rivers continue to have higher levels of nitrogen and phosphorus than is recommended (Manning et al. 2020). Although these nutrients are a natural part of aquatic ecosystems, human activity has increased their levels beyond what the system can naturally absorb and buffer. At high levels, nutrients can lead to excessive algal growth which can harm water quality, alter food webs and resources, change community composition and diversity, decrease the oxygen that fish and other aquatic life need to survive, and contribute to hypoxia in coastal waters (Frei et al. 2021; Piggott et al. 2015).

Excess sediment is another pollutant persistently found in U.S. streams and rivers (Murphy 2020). In addition to reducing water clarity, excess sediments can bury and suffocate benthic organisms and fish eggs, cover habitat, and disrupt food webs (Robertson & Saad 2019). Sediment can also impact fish by clogging their gills and reducing disease resistance, growth rates, and altering egg and larvae development. Sediment can bind harmful contaminants, and sedimentation of rivers can change stream flow and reduce water depth (MARC 2023). Nutrient and sediment pollution is also impacted by changes in streamflow (Murphy 2020) which can be exacerbated by climate change and dams.

The EPA's most recent national assessment of streams and rivers in CONUS found 58% were rated poor for phosphorus and 43% were rated poor for nitrogen (USEPA 2020). The study found phosphorus, nitrogen, and suspended sediment had the highest attribute risk values of all the stressors assessed. For example, rivers and streams rated poor for nutrients and sediment levels were almost twice as likely to have poor biological condition based on multi-metric scores for benthic macroinvertebrate assemblages (USEPA 2020).

Sources of nutrient and sediment pollution vary but most are correlated with agricultural practices. Nitrogen is most likely to come from crop fertilizers, wastewater, and animal wastes as well as atmospheric deposition from the burning of fossil fuels. Increased phosphorus is more commonly the result of poor agricultural practices, sewage waste, increased soil erosion, and urban runoff. Sediment sources include runoff from agricultural fields, intensive forestry operations, urban areas, and construction activities.

While enforcement of the Clean Water Act has led to the reduction of point source pollutants in American rivers and streams, nonpoint source pollution, especially from agricultural activities, continues to be a regulatory challenge (Stets et al. 2020; Frei et al. 2021). Crop productivity and nitrogen from fertilizer has grown dramatically in the Midwestern U.S. as have concentrated livestock operations (Falcone et al. 2018). Another notable water quality trend, and one that we did not assess due to insufficient national data, is the emergence of salinity as a rapidly growing threat to freshwater systems (Stets et al. 2020). There are a few bright spots. A recent USGS study of 137 U.S. sites found that in some places, efforts to reduce sediment pollution entering waterways appear to be making a difference (Murphy 2020). Similarly, efforts to control nonpoint source pollution in urbanized areas also appear to be reducing nutrient loads to streams and rivers (Stets et al. 2020).

For these reasons, we considered water quality to be an important component of a resilient freshwater network. Fortunately, USGS SPARROW models provide spatially explicit estimates of nutrient loads, concentrations, and yields for all streams in CONUS. SPARROW uses spatially comprehensive geospatial data in a calibrated model to predict water-quality conditions at unmonitored stream locations. The most recent SPARROW models provide estimated nutrient information for each NHDPlus reach catchment, based on source inputs (e.g., land cover) and management practices existing during or near 2012 (USGS 2019). The streamflow component of the SPARROW models is based on the average input precipitation minus actual evapotranspiration from 2000 to 2014.

We obtained the SPARROW Northeast (Ator 2020), Southeast (Roland and Hoos 2020), Midwest (Saad & Robertson 2020), Southwest (Miller et al. 2020), and Pacific (Wise 2020) model outputs to cover CONUS. South Florida watersheds have significant water diversions and fluxes for which there is insufficient data to model in SPARROW. Thus, this region was excluded from the Southeast SPARROW models and is shown in gray to indicate "No Data" for all water quality maps. We used

incremental and accumulated yield values for total nitrogen (TN), total phosphorus (TP), and suspended sediment (SS). Incremental values are the predicted mean annual loads of a stream that are contributed from sources in the immediate drainage area of a stream reach (equal to NHD catchment). Accumulated values are loads contributed by all sources in the total upstream drainage area of the reach outlet and include the effects of in-stream attenuation processes in all upstream reaches. Incremental yield is the incremental load divided by the local catchment area, while accumulated yield is the accumulated load divided by the total upstream drainage area. TN and TP yield units are kilograms per km^2 per year, and SS yield units are metric tons per km^2 per year.

The dataset for the Southwest contained duplicate units where catchments crossed state lines. To address this issue, we took the maximum suspended sediment value for duplicate units. We then combined the selected attributes for all SPARROW regions, assigned "no-data" values to closed catchments with no predicted nutrient loads, and examined patterns in the incremental and accumulated yields for each constituent. To capture the cumulative impact of nutrients and sediments on freshwater systems, we used cumulative yields for each constituent as our measures of nutrients and sediments (Figure 3.23).

Figure 3.23. Cumulative yield maps for SPARROW total nitrogen, total phosphorus, and suspended sediment, and their integration. Maps A-C show classes relative to each SPARROW model region (black lines) of cumulative yields for A) TN total nitrogen, B) TP total phosphorus, and C) SS suspended sediment with higher loads denoted with darker colors. D) The integrated water quality index z-scores stratified by arid/humid zones.

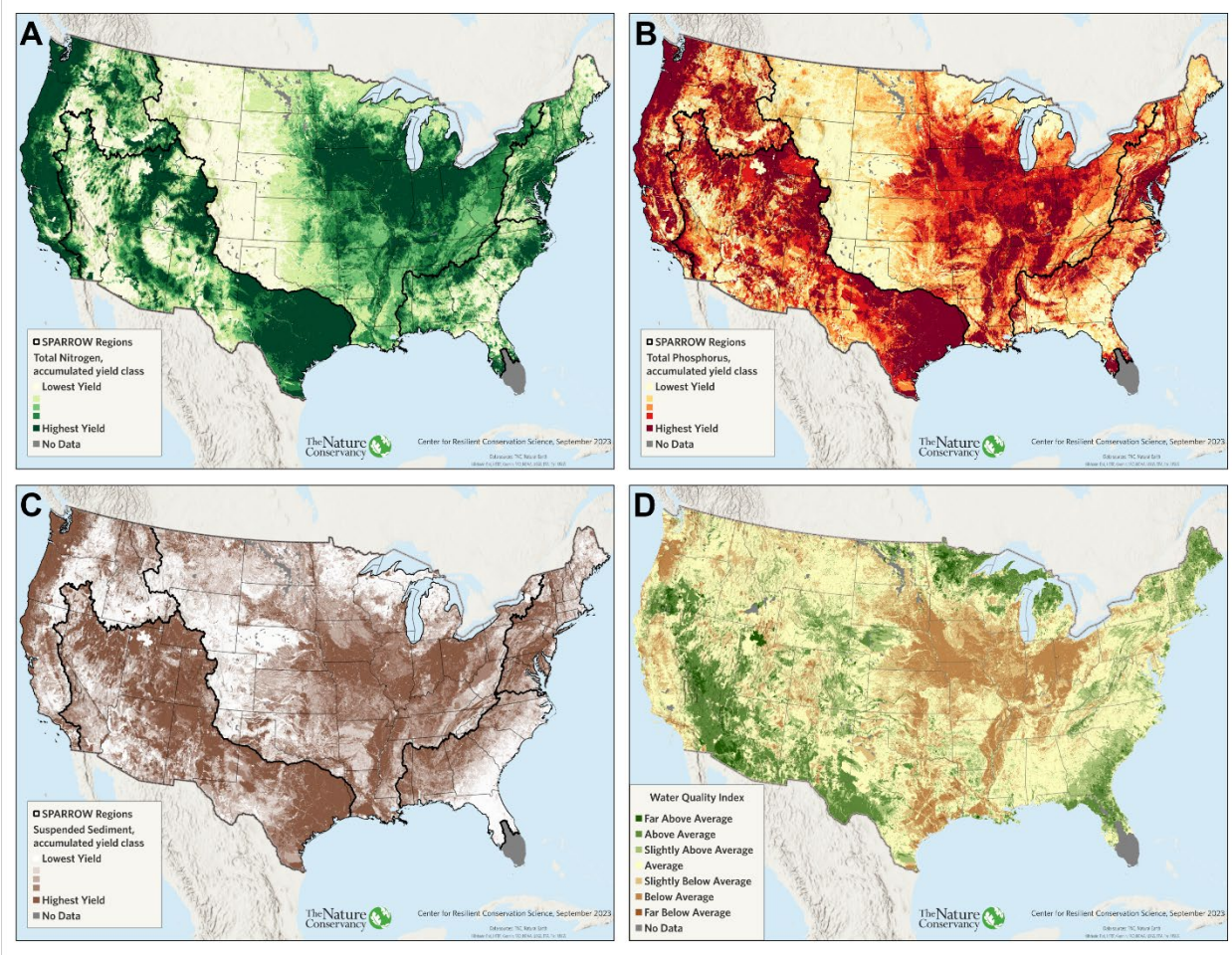

We assigned each catchment to its dominant freshwater ecoregion and converted the TN, TP, and SS accumulated yield values to standard normal scores (z-scores) by arid and humid ecoregions, and CONUS. CONUS level z-scores highlighted western watersheds, which typically have lower nutrient and sediment loads relative to midwestern and eastern watersheds. Relativizing results by arid and humid ecoregions (Figure 2.8) resulted in the most logical and interpretable patterns. Regardless of the stratification used, the TN and TP z-scores were often strongly correlated. Thus, for each catchment, we took an average of the TN and TP z-scores, and then combined that score with the SS z-score to calculate a cumulative water quality index for each catchment (Figure 3.23).

We used an area-weighted approach to translate the cumulative water quality index (Figure 3.23D) to HUC-12 watersheds. Specifically, we calculated the proportion that each catchment contributed to the total HUC-12 watershed area. We then multiplied the cumulative water quality z-score by catchment proportion and summed the values by HUC-12 (Figure 3.24).

Figure 3.24. Cumulative water quality index. Scores are by HUC-12 watersheds. Black lines indicate the arid and humid climatic regions used to stratify the cumulative water quality yields at the catchment scale (Figure 3.23).

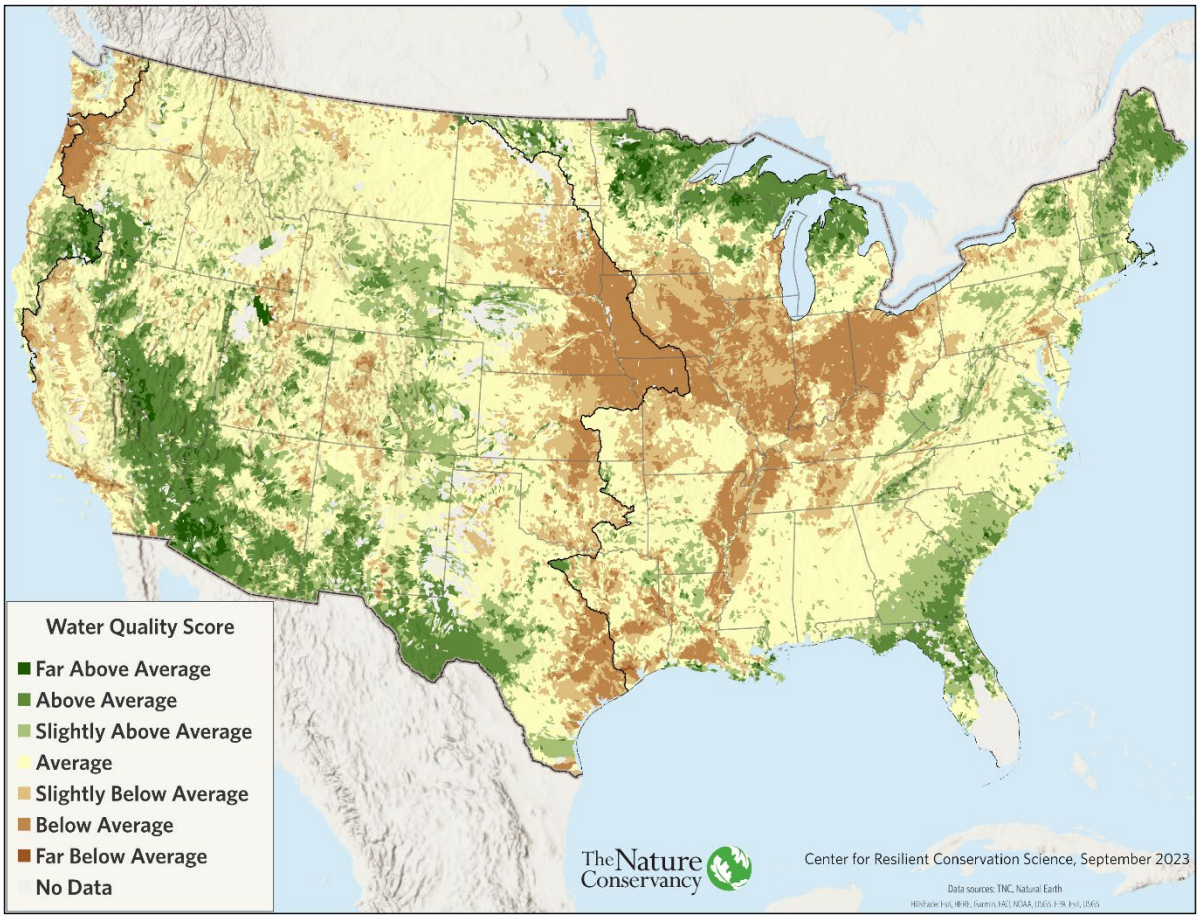

Surface Mining Penalty

Metals, minerals, and rocks are extensively mined in the U.S., with coal, sand and gravel, gold, and copper the top mined commodities. Mining can be detrimental to freshwater systems due to land degradation, depletion of surface and groundwater supplies, stream channel and stream flow alterations, water pollution, alteration of soil and subsurface geologic structure, and disruption of surface and subsurface hydrologic regimes (SDWF 2017; Starnes & Casper 1995). The primary water quality concerns from mining activities are acid mine drainage, heavy metal contamination and leaching, pollution from processing chemicals, and sedimentation and erosion (SDWF 2017).

While there are a range of both national and regional spatial datasets that identify mine footprints in the U.S., many are outdated, inconsistent, and/or have incomplete geographic coverage. To estimate the potential impact of surface mining activities (e.g., mountaintop removal, quarries, strip mines, open pit mines, dredging) on watersheds, we developed a new dataset of mining footprints in CONUS using current land cover with global, national, regional, and state mining datasets (Appendix 6). Here we summarize our approach to identify surface mining areas.

We compiled, compared, and error checked all the data sources and made adjustment until they represented a spatially consistent dataset of mining operations (details in Appendix 6). We converted the selected mining polygons to a 30-m raster and merged all the grids using Cell Statistics in ArcGIS to retain the source datasets for all mapped mining areas. We created a mining area raster where all mining areas were coded as 10 and then we merged this on top of the 2019 NLCD land cover for use in the water quality mining metric and the floodplain, riparian, and watershed land cover naturalness metrics.

Percent Mining Area

We tabulated the area of mine land in each HUC-12 watershed and calculated the percentage of mining area in each watershed. After removing HUC-12s with no mine area, we converted the percent mining area values to z-scores, stratified by the two aridity zones. For watersheds with mining area, the stratified z-scores ranged from -3.00 to 2.78. Watersheds with z-score values greater than zero had low percentages of mining but we didn't want to treat the presence of any mine area, no matter how small, as a positive attribute. Thus, we rescaled the z-scores for watersheds with mining area. We explored three different rescaling scenarios that varied in penalty strength and chose a -2.0 SD penalty as the most appropriate to reflect the detrimental water quality impacts of coal mining in the Appalachian region of the Eastern U.S. and mineral mining in the Western U.S.

In all scenarios, HUC-12 watersheds with the lowest percentage of mining area received the smallest penalty (-0.1 SD) while the largest penalty went to watersheds with the highest mining area percentage (-2.0 SD, Figure 3.25). The mining penalty was then deducted from the HUC-12 cumulative SPARROW water quality index z-scores (Figure 3.26). Although we were unable to find information on the reclamation status of western mines, water quality was ultimately weighted lower in the arid ecoregions than in the humid ecoregions (see Condition Integration) and the role of mining areas should be considered when interpreting water quality values in the Western U.S.

Figure 3.25. Mining penalty deducted from cumulative water quality score. This map groups HUC-12 watersheds into classes based on their mining penalty. Watersheds in yellow had no estimated mining area and thus received no mining penalty. Watersheds in dark brown had the largest percentage of mining area relative to all other watersheds with mine land, and received the largest range of mining penalties, up to 2 SD.

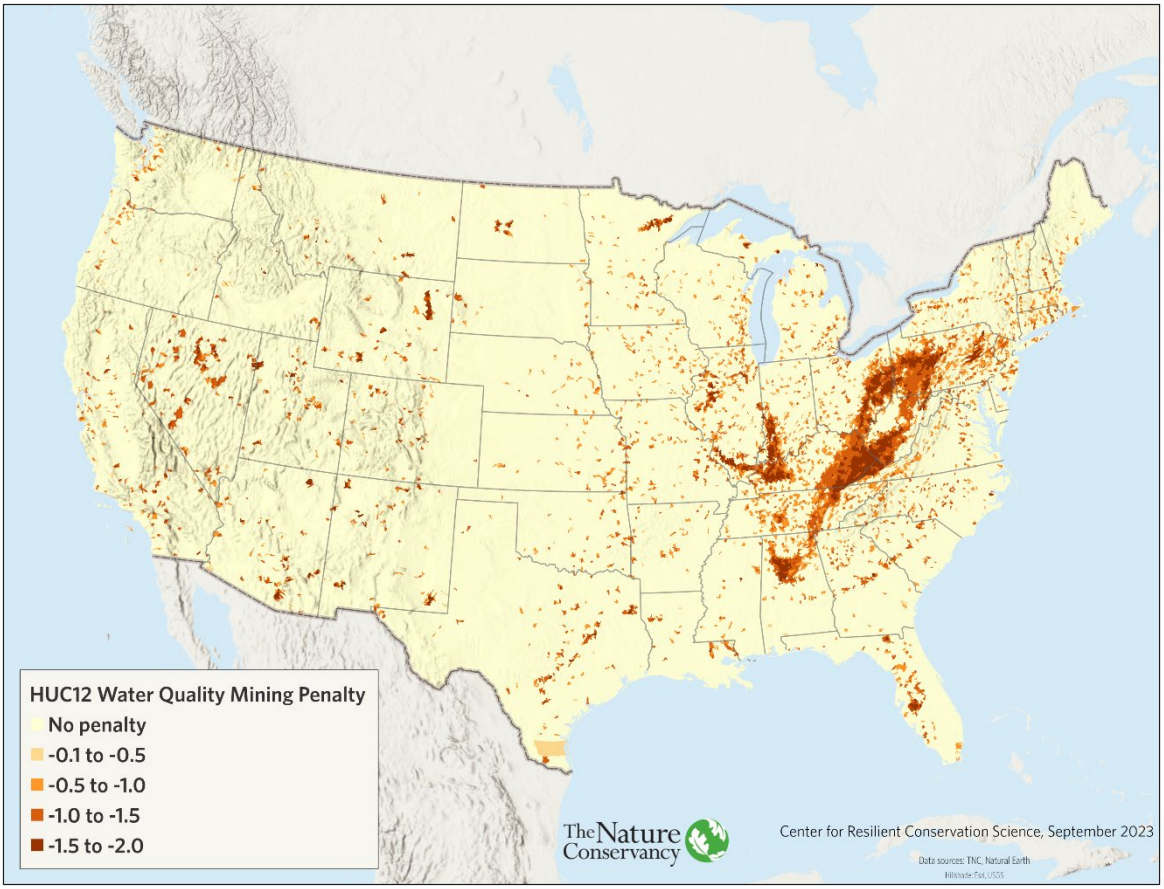

Figure 3.26. Cumulative water quality score with mining penalty. This map reflects the map shown in Figure 3.24 with the mining area penalty shown in Figure 3.25 subtracted from the score.

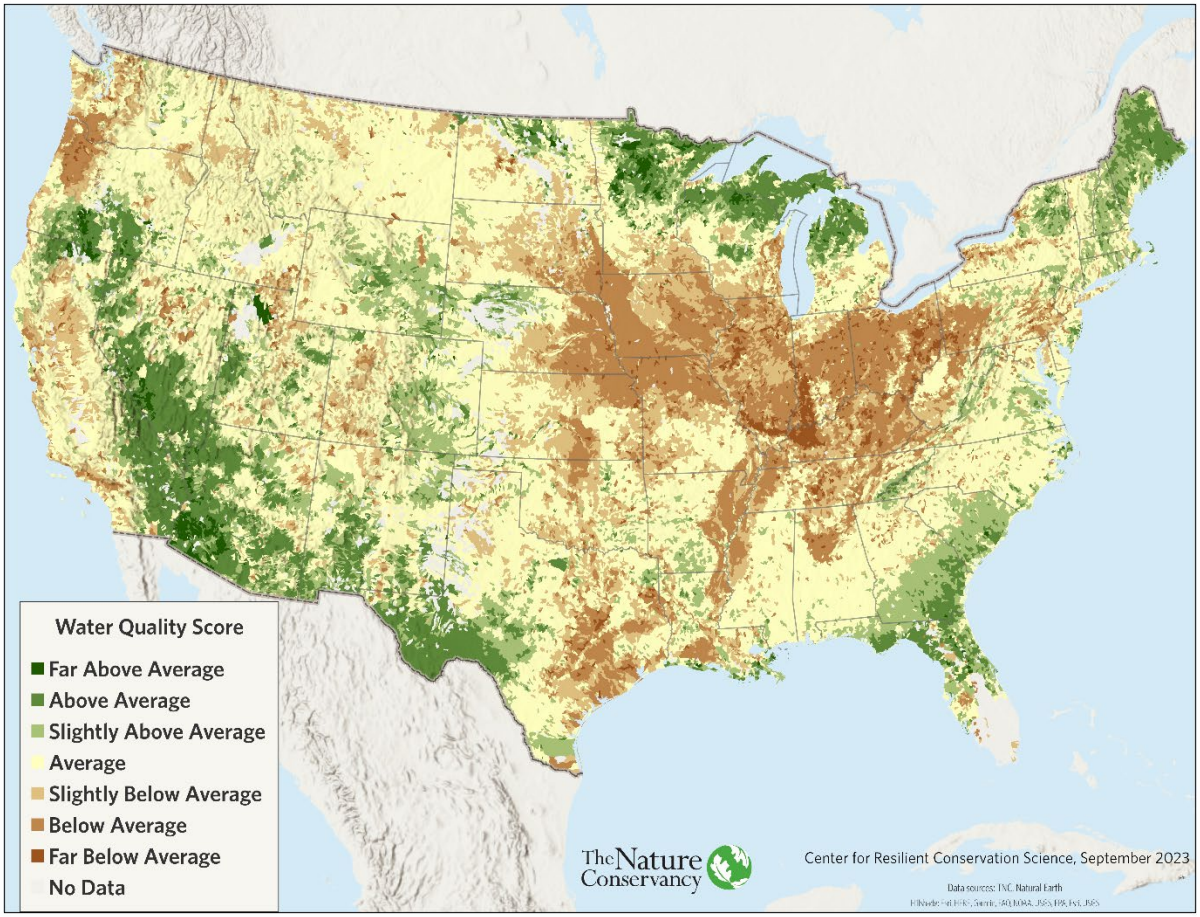

Impervious Surface Override

Impervious surfaces, such as asphalt or concrete, are surfaces incapable of being penetrated by water. These surfaces alter the natural pattern of rainwater soaking into the ground and slowly seeping into streams. Instead, rainwater accumulates and flows rapidly overland, altering streams in important ways (Chithra et al. 2015). Storm drains deliver large volumes of water to streams much faster than would occur naturally, resulting in flooding and bank erosion. Flows peak more rapidly during storms, and peak flows are higher and more frequent. Lack of groundwater recharge during rain events leads to lower daily base flows. Additionally, stream channels become wider, less stable, and less complex. Stream inhabitants are stressed, displaced, or killed by fast moving water and the debris, sediment, and disturbed channel habitat it brings. Pollutants such as gasoline, oil, and fertilizers accumulate on impervious surfaces and are washed into the streams. Finally, during hot weather, rain that falls on impervious surfaces becomes superheated and can stress or kill stream biota.

All indicators of stream quality relative to biotic condition, hydrologic integrity, and water quality decline with increasing watershed imperviousness. Research suggests that aquatic systems become

seriously impacted when watershed impervious cover exceeds 10% (CWP 2003) and show significant declines in many stream taxa at levels of impervious surface as low as 0.5 to 2% of the watershed. Serious (40-45%) declines in invertebrates, fish, amphibians have been found at watershed imperviousness greater than 3% (King & Baker 2010).

While we calculated condition metrics for all HUC-12 watersheds, the impact of impervious surfaces in highly urbanized watersheds can override other condition characteristics. In these situations, we applied an impervious override to account for high levels of impervious surfaces. To identify highly urbanized watersheds, we calculated the average percent impervious surface in each HUC-12 using zonal statistics in a GIS (Figure 3.27). We clipped the HUC-12 watersheds to the CONUS boundary and then calculated the area of each. We evaluated different impervious surface percent thresholds and determined that a threshold greater than 20% identified the most urban watersheds across the country. The small number of HUC-12s that met this threshold (1,487, less than 2%), were automatically assigned a "Far Below Average" condition score (Figure 3.28).

Figure 3.27. HUC-12 watersheds shown by average 2019 NLCD Percent Developed Imperviousness in five impact classes.

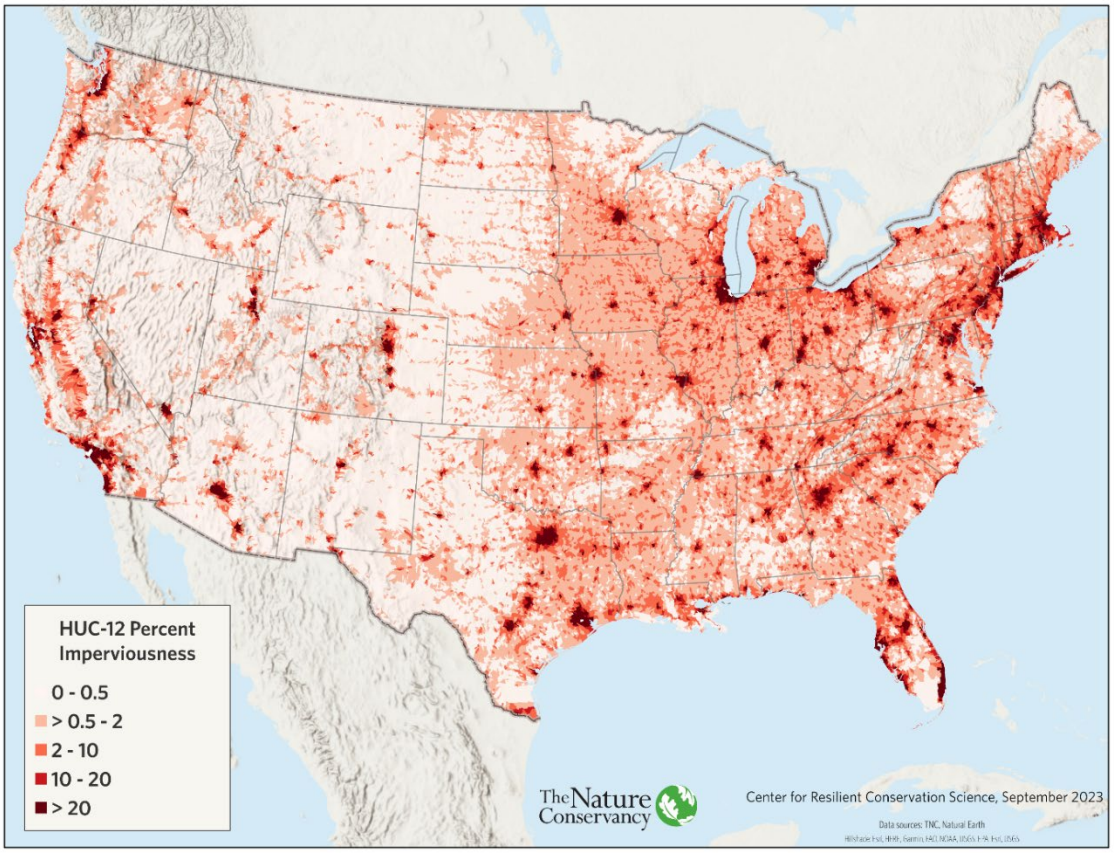

Figure 3.28. HUC-12 watersheds with greater than 20% impervious surface. These watersheds (n=1,487) automatically received an overall condition score of "Far Below Average."

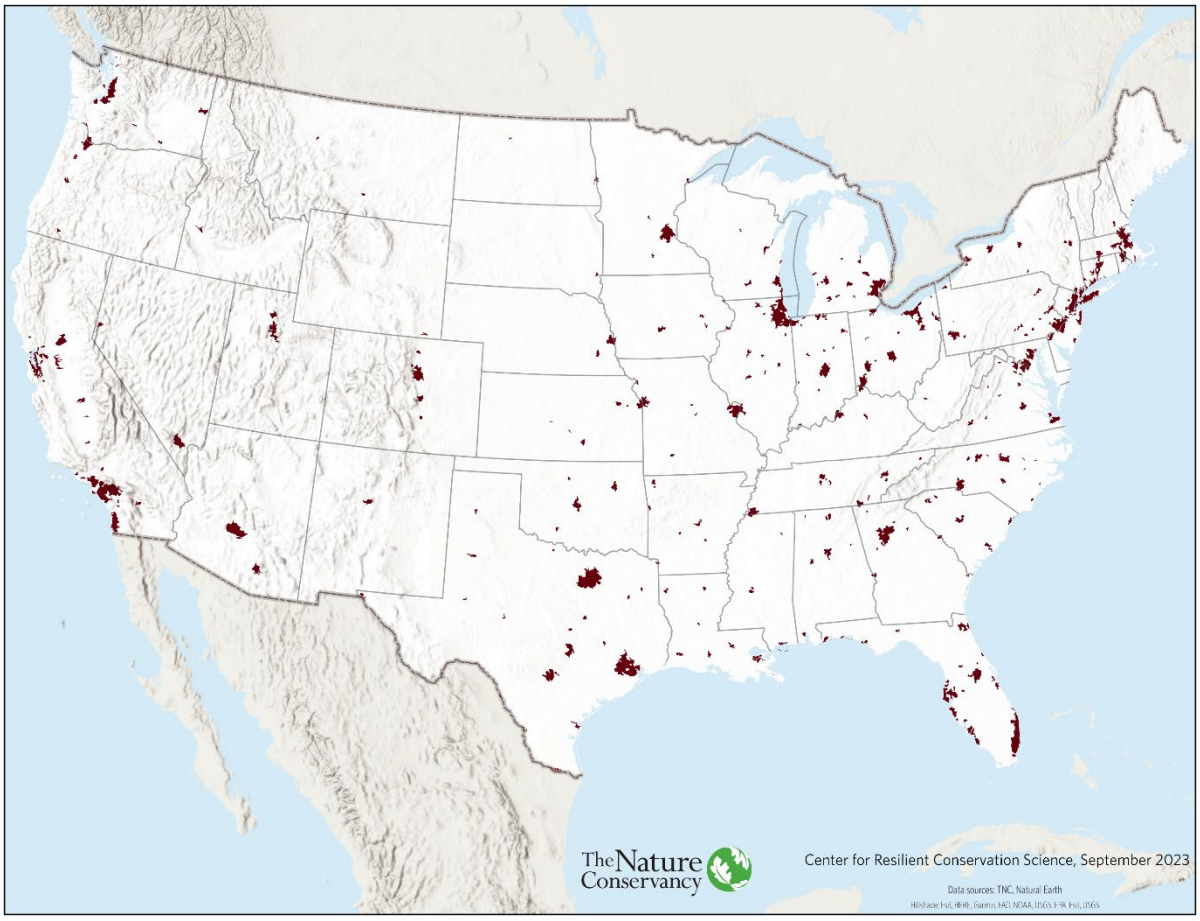

Integration of Condition Metrics

After assigning HUC-12 watersheds that met the impervious surface threshold an overall condition score of "Far Below Average," we explored different approaches and weights to combine the naturalness metric with the water quality metric. In our final integration, we assigned the naturalness metric the highest weight of five, and the water quality with mining penalty a weight of three for humid ecoregions and a weight of two for arid ecoregions. We weighted the water quality metric lower in the arid ecoregions because water availability is a bigger stressor. The impervious surface override was applied equally in both regions.

*Humid Region Condition = (5*Naturalness + 3*Water quality with Mining penalty) / 8*

*Arid Region Condition = (5*Naturalness + 2*Water quality with Mining penalty) / 7*

Lastly, the condition z-score was capped at one rather than allowing it to go as high as three for the arid intermittent HUC-12s, defined as those with more than 75% of their streams and rivers (size 11 and larger) coded as intermittent and less than one km of perennial large river (size 30 and larger) (Figure 3.29). This was done to limit the extreme positive influence of condition in these watersheds where there is little permanent water and minimal amounts of freshwater habitats available for freshwater dependent biota.

Figure 3.29. Final condition score. This map shows the integrated condition score after accounting for arid HUC-12 watersheds characterized by intermittent streams and rivers.

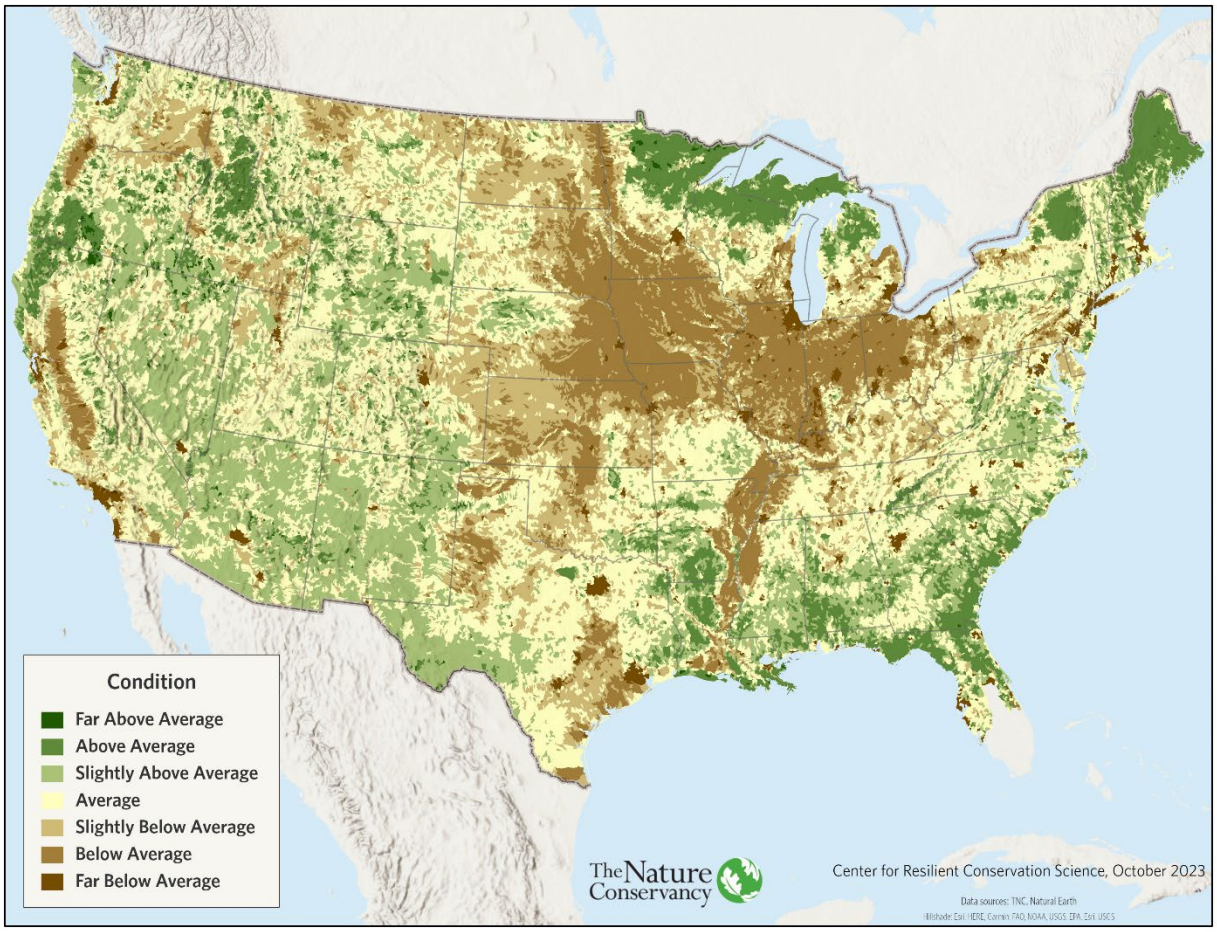

Integrated Physical Score

*Physical Score = (1*Connectivity + 1*Condition) / 2*

Our final physical score was an equally weighted combination of the connectivity score (Figure 3.16) and the condition score (Figure 3.29).

Figure 3.30. Physical score. This map shows the final integration of the connectivity score (Figure 3.16) and the condition score (Figure 3.29) with appropriate weights, overrides, and score caps.

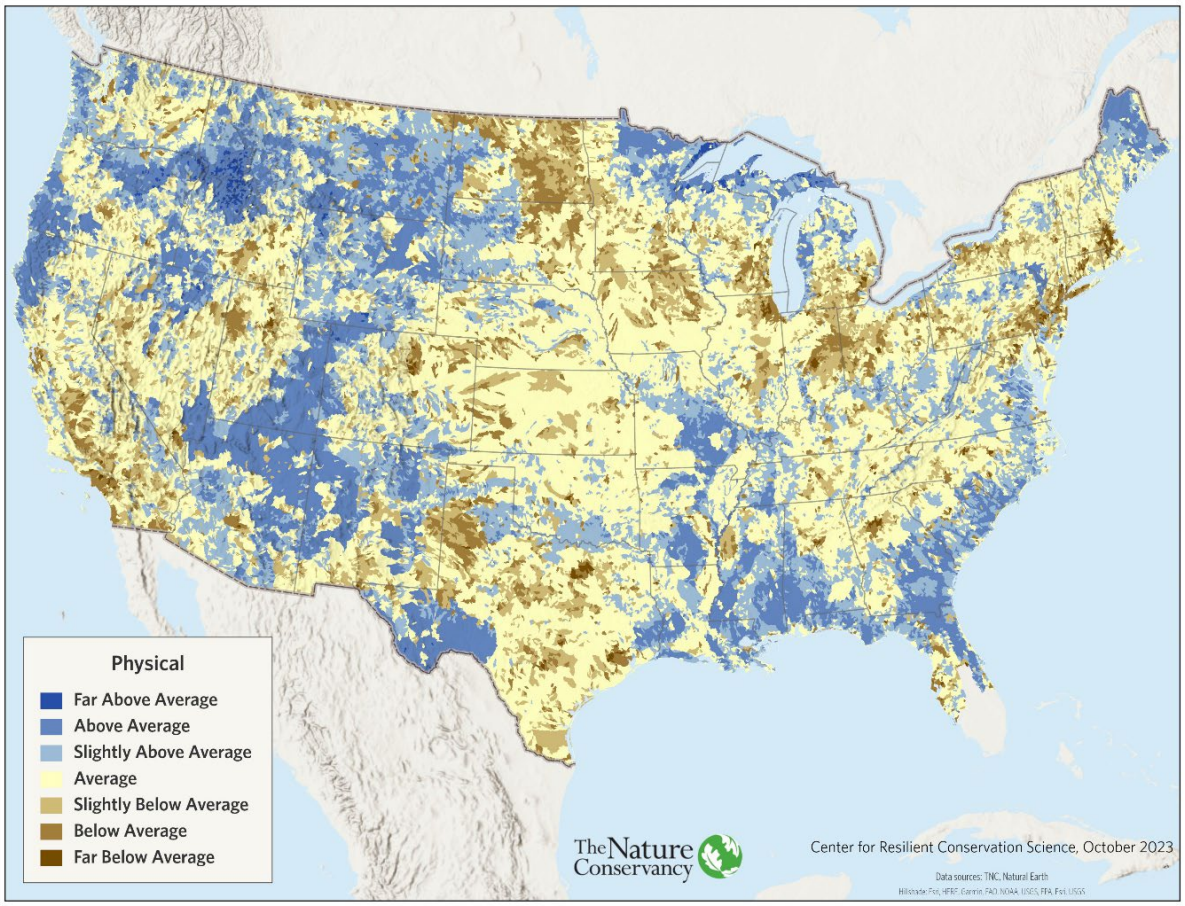

Water Score

Water Score = Potential Water Availability + Hydrologic Alteration

The water score was designed to estimate the availability of ample unaltered water to each river network. As the natural levels of precipitation, surface water, and groundwater differ markedly across the U.S., we often had to stratify the results by climate regions (humid, arid, and xeric, Figure 2.8) to obtain accurate and locally relevant results. The score is a function of potential water availability and hydrologic alteration, which we describe in detail below.

Potential Water Availability

Potential Water Availability = Surface Water Index + Groundwater Adjustments

Potential water availability accounts for the presence of significant surface water and the potential presence of groundwater adjusted for depletion near the surface. We reasoned that areas with greater availability of water will be more resilient to climate change (Wilby 2020), particularly in the arid region of the U.S. where water availability is a key factor in distinguishing resilient systems (Rieman & Isaak 2010).

Surface Water Index

Land surfaces that express or store perennial water support freshwater resilience by providing direct habitat for freshwater biota, and by collecting precipitation and providing gradual release and continual access to water throughout the season and during droughts. Surface water is made available throughout the year through a complex set of hydrologic process integrating precipitation, transpiration, evaporation, overland flow, depressional storage, interflow, and groundwater baseflow (Figure 3.31).

While we anticipate changes in precipitation, evaporation, and transpiration rates as the climate continues to change, local hydrologic processes driven by geophysical processes like topography and soil type will continue to function. Thus, we developed a surface water storage index based on more stable topographic features such as depressions and gullies, runoff waterways, incised channels; areas with predicted persistent snow; as well as verifiable expressions of surface water such as wetlands and perennial streams and rivers.

Figure 3.31. Hydrologic processes (Tarboton 2003).

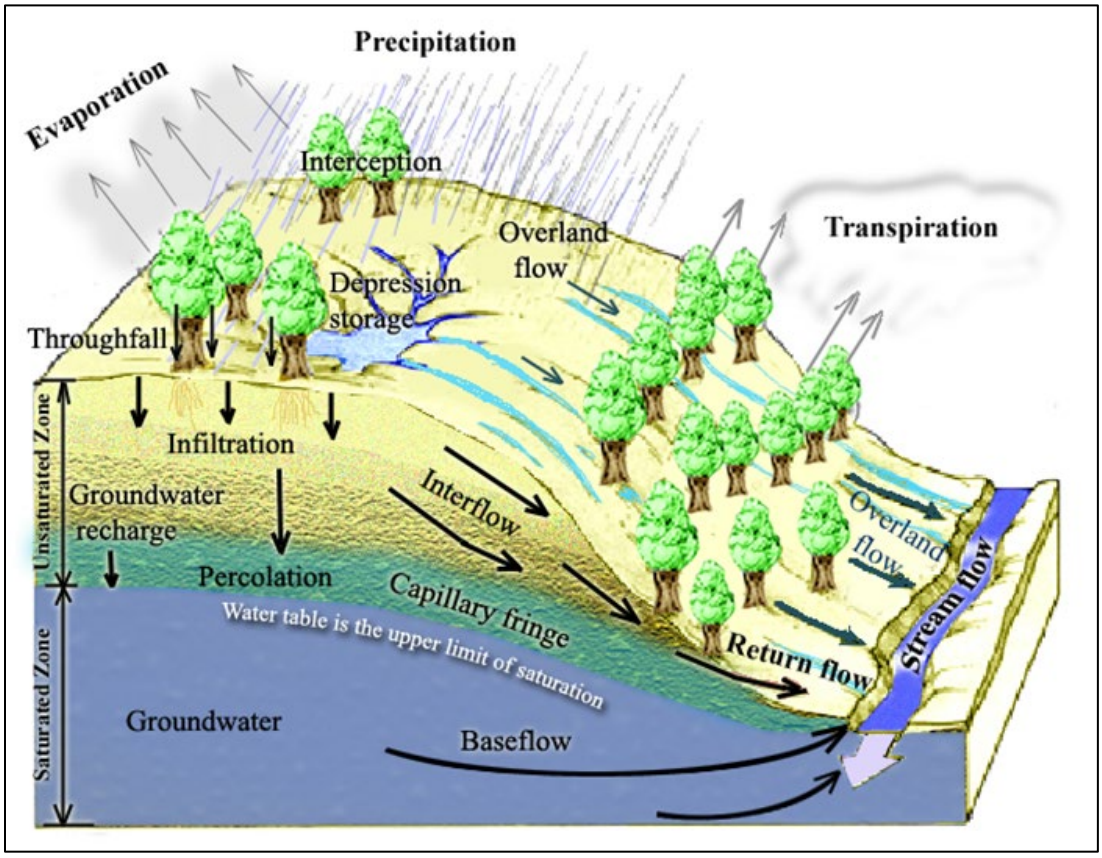

Mapping Surface Water

To create an index of surface water likely to be meaningful under future climate scenarios, we compiled existing data from multiple sources (Table 3.7) on the location of:

- Wetlands, springs, perennial lakes, streams, and rivers, and floodplains
- Pluvial depressions and moisture accumulating flats adjusted for land cover type
- Areas of more persistent snowpack in the western U.S.
- Tile drainage applied in heavily agricultural areas

These inputs were merged into a single dataset reflecting the enduring sources and storage areas for surface water across CONUS (Figure 3.32). As these areas have distinct topographic signatures or are associated with groundwater outlets such as springs or seeps, we expect their locations to remain relatively stable into the future, even though the actual amount of water they collect and store will fluctuate with changes in the climate. We recognized the massive influence of tile drainage in parts of the country where agriculture is dominant and is likely to remain dominant into the future by incorporating a recent dataset showing areas of tile drainage (Valayamkunnath et al. 2020)

Table 3.7. Data sources for surface water features and modifiers in the surface water index.

Feature	Data Source
Wetlands	NLCD, USGS 2019
Perennial Rivers	NHDPlusV21, USGS 2016
Perennial Headwaters	NHDPlusV21, USGS 2016
Perennial Waterbodies	NHDPlusV21, USGS 2016
Springs and Seeps	NHDPlusV21, USGS 2016
Wet Flat Landforms	TNC 2020a
Pluvial Moist Flat Landform	TNC 2020a
Tile Drained Agriculture	Valayamkunnath et al. (2020)
Persistent Snowpack	Developed for this analysis

Figure 3.32. Inputs to the surface water index.

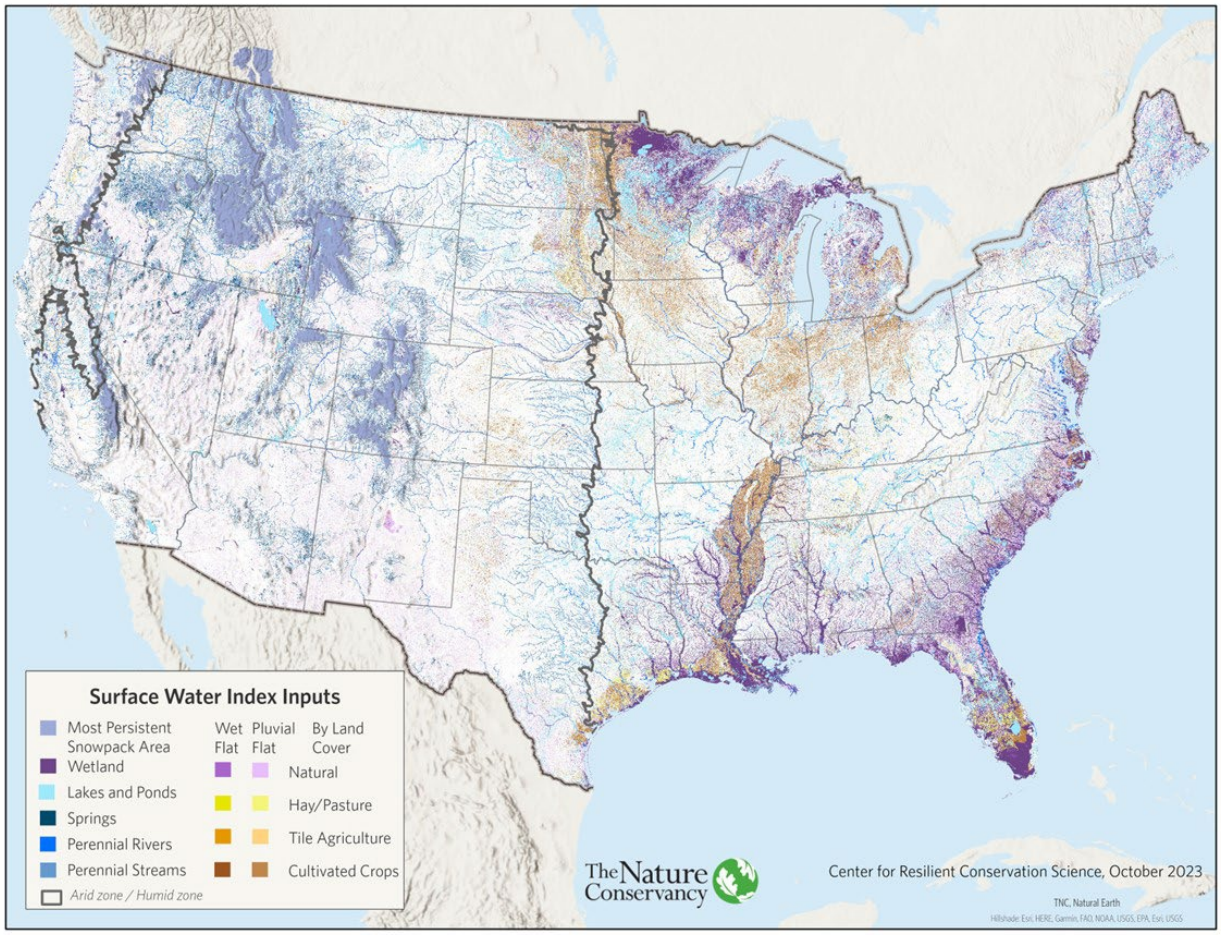

Persistent Snowpack

In the western U.S., many freshwater ecosystems are dependent on snow as a high percentage of their total water balance (Mayer & Naman 2011; Barnhart et al. 2016). As the climate changes, areas with persistent snowpack are likely to provide some freshwater systems with a more continuous supply of freshwater, increasing their resilience. To identify these areas, we developed a snowpack persistence map based on elevation and topographic influence on local temperature, climate, and solar radiation.

First, we used datasets from TNC (Anderson et al. 2019) and LANDFIRE (2022) to identify upper montane and higher elevation zones as they are expected to maintain colder temperatures into the future, facilitating the persistence of deep snow accumulations and later snowmelt (Jones et al. 2021; Provencher et al. 2021). Upper montane elevation thresholds differed by ecoregion and ranged from 800 meters in the Pacific Northwest to 2,422 m in the Sierra Nevada. Elevation thresholds for the Rocky Mountain and Desert Southwest ecoregions were from Anderson et al. (2019). For other western ecoregions, we defined the lowest elevation as the mean elevation (0.5 SD) of biophysical settings that only occurred in the upper montane zone of each ecoregion (Comer 2022; LANDFIRE 2022). To identify the cells most hydrologically dependent on snowpack, we removed areas where snow comprised less than 50% of water in a NHDPlus catchment water balance model (Wolock & McCabe 2017).

Lastly, we used the Continuous Heat-Insolation Load Index (CHILI, Theobald et al. 2015; Theobald 2022) to assign surface water index scores for the cells identified above. The CHILI model uses topographic slope and latitude to predict potential direct radiation. We considered areas with less incident radiation and a lower heat load, such as north-facing slopes, to be more persistent as they retain snow longer. We z-scored the CHILI data within the upper montane and higher-elevation zones to distinguish areas receiving the least solar radiation (e.g., most persistent snowpack) from those experiencing the most solar radiation (less persistent and/or faster melting snow). We classified the continuous CHILI z-scores into three classes for inclusion in the surface water index which had values that ranged from 0 to 500, with 500 indicating the most water storage and 0 the least. Cells with the least solar radiation, those that scored greater than "Average" in the CHILI z-scores, were assigned a surface water index value of 500. Areas with an "Average" CHILI z-score received a value of 400 while cells receiving the most solar radiation, those with z-scores less than "Average," were assigned a value of 300 (Figure 3.33).

Figure 3.33. Areas of persistent snowpack.

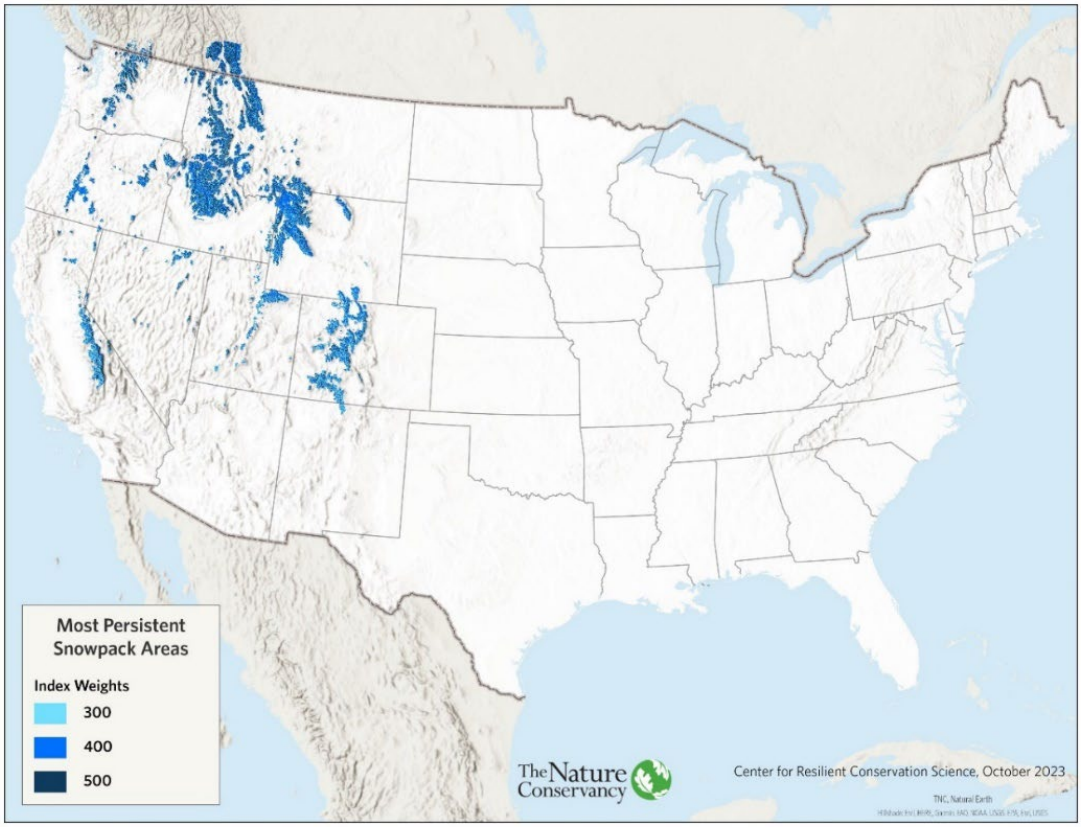

Integrated Surface Water Index

To create a continuous surface water index, the compiled inputs were weighted from 0 to 500 based on their expression and storage of surface water and their relative importance to river networks (Table 3.8). The input weights for certain features were adjusted by climatic zone to reflect the greater importance of perennial water in the arid zone where these features are rare and often the only wet habitats. Wetlands and snowpack areas were given the highest value (500), reflecting their ability to collect and store water, and slowly release it over the season to feed flows in adjacent streams and rivers. Wetlands also directly provide aquatic habitat for many freshwater dependent species throughout the year. Perennial streams, rivers, lakes, and springs/seeps were given moderate values in the humid zone (50-100) where they are relatively common, but higher values in the arid zone (150-300), where they are often the only source of available water and aquatic habitat. Fluvial wet flats and pluvial moist flats are topographic depressions and channels that accumulate overland flows during precipitation events or overbank flooding but are not continuously wet, and thus were given lower values (5-100). In the agricultural regions of the country, the weights on pluvial landforms were decreased slightly where there was tile drainage to reflect the negative effect of tile drainage on water storage.

We then calculated the mean of the surface water index grid cells for each HUC-12 and transformed the values to z-scores relative to CONUS (Figure 3.34). The results highlight areas where we expect surface water to be more persistent, given enduring topographic water storage and surface expression.

This analysis does not consider precipitation patterns and as the humid and arid regions differ markedly in overall precipitation, a less than "Average" score in the humid region may have more absolute surface water than a greater than "Average" score in the arid region.

Table 3.8. Surface water inputs and relative weighting scheme.

	Land Cover						
	Natural Land						
Feature	**Arid**	**Humid**	**Hay**	**Tile Ag. & Hay**	**Row Crops**	**Tile Ag. &Row Crops**	**Developed**
Wetlands	500	500					
Persistent Snowpack	300-500						
Waterbodies: Natural	300	300					
Springs & Seeps	300	100					
Perennial Rivers	150	50					
Perennial Headwaters	300	100					
Waterbodies: non-natural	50	50					
Wet Flat	50	100	50-60	30	20	10	0
Pluvial or Moist Flat	25	25	20	15	10	5	0

Figure 3.34. Surface water index. This map shows the integrated surface water score.

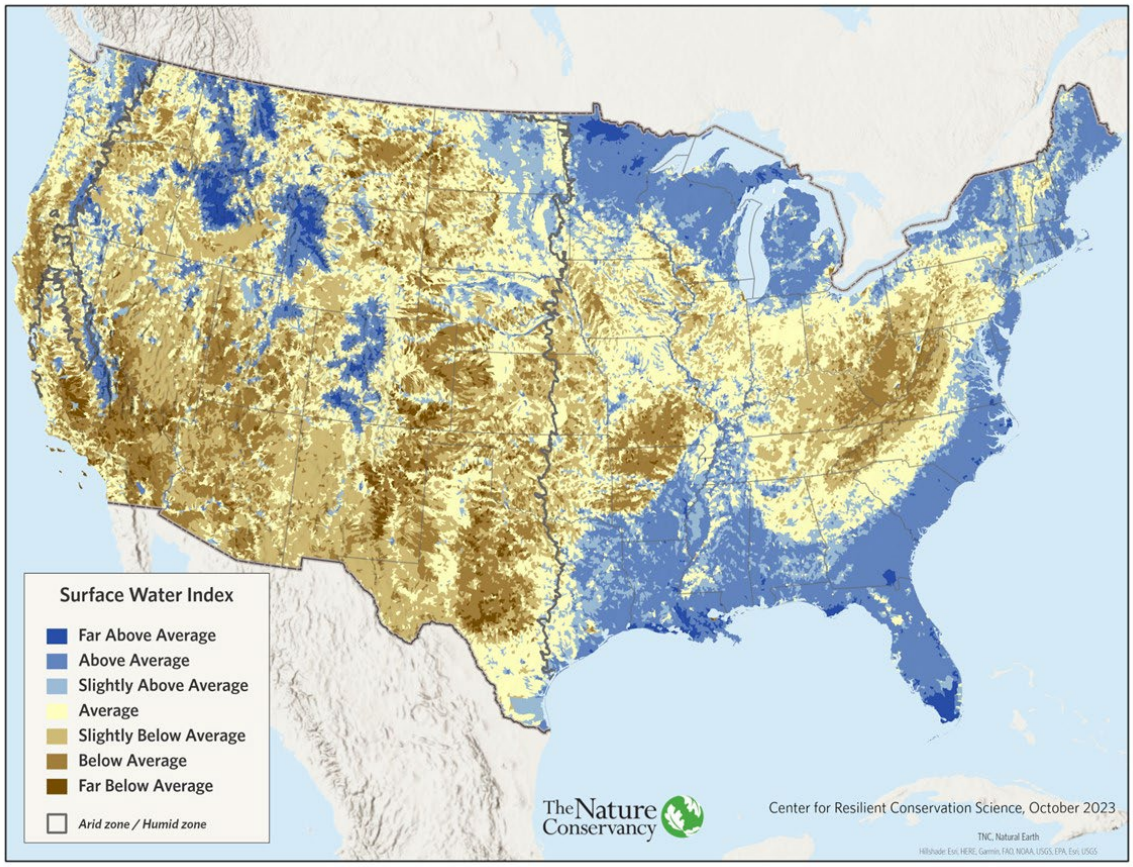

Groundwater Adjustments

Groundwater inputs support freshwater resilience by providing baseflow in times of low precipitation, colder water under moderate temperatures, and maintaining a stable hydrograph. In arid regions, groundwater supply is often critical to maintaining perennial rivers and local water sources such as seeps and springs. In some cases, karst underground freshwater rivers or springs provide important habitat and refuges for freshwater biodiversity (Hare et al. 2021). We accounted for the groundwater influence on available water by developing hydrologic landscapes derived from soils, geology, and aquifer maps, and we also incorporated the location of springs, seeps, and perennial rivers. To adjust for groundwater depletion, we used remotely sensed measures of near-surface groundwater change over the last 18 years.

Hydrologic Landscape Regions

Groundwater is notoriously difficult to map at a national scale, as its expression is often subject to recharge levels and underground flow hydrology that is poorly understood. Multiple attempts have been made to interpolate baseflow from gauge data with limited success (Wolock 2003; Santhi 2008; USFS 2023), but an approach developed by Wolock et al. (2004) for identifying and mapping hydrologic landscape regions (HLRs) proved to be useful for our purposes. HLRs delineate groundwater potential based on dominant soil, bedrock, and aquifer characteristics. The landscape is

divided into categories based on similarities in landforms and geologic texture, and these groups are assigned weights that reflect their potential to support and store groundwater. We created an HLR map for CONUS following Wolock et al. (2004), using their suggested weightings for the individual geophysical components but with more recent soil (TNC 2020c), geology (TNC 2020c), and landform data (TNC 2020a) to map those components (Figure 3.35). See Appendix 4 for a full description of the process and data sources.

Figure 3.35. Hydrologic landscape regions (HLRs). This map of groundwater potential is revised from Wolock et al. (2004) using recent data on soil texture, bedrock geology, and landforms.

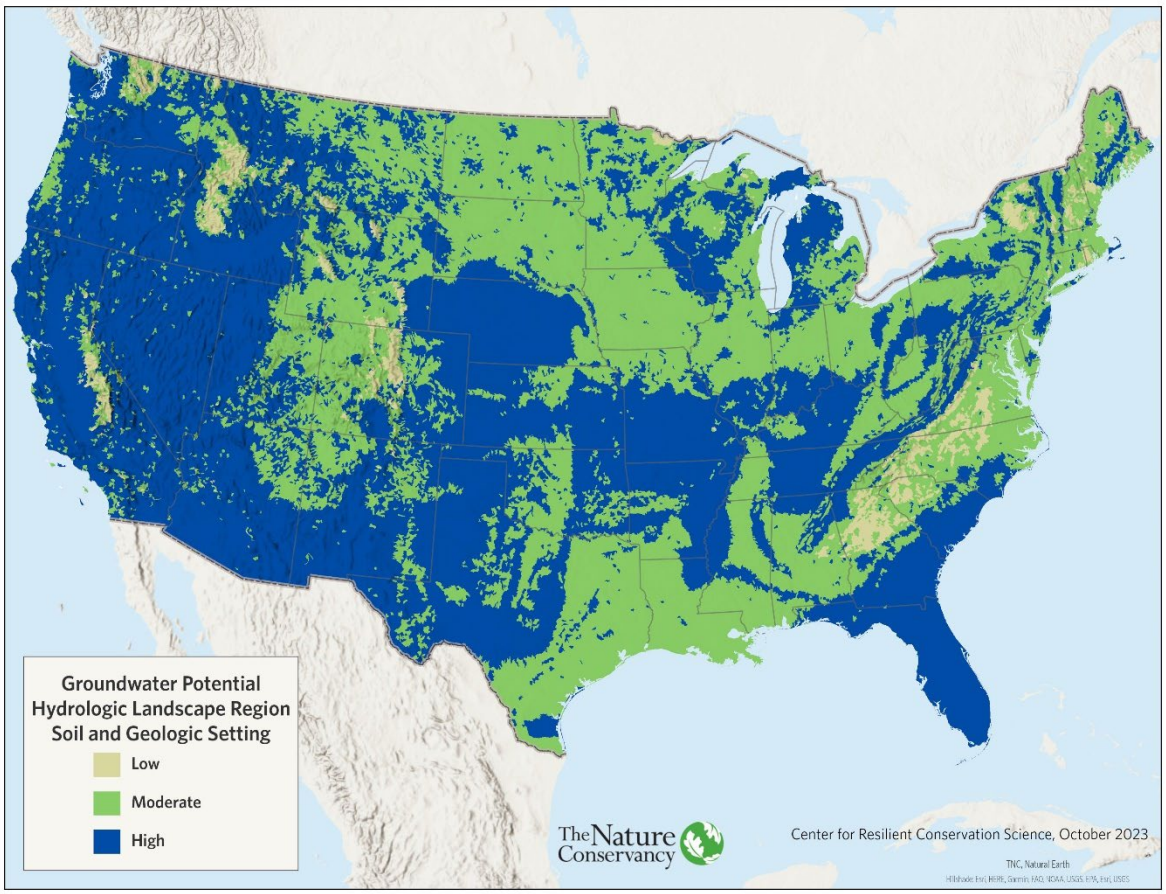

Following suggestions from TNC's global groundwater group, we used the HLRs as a framework to map expected groundwater influence, and to apply increases or penalties to the water availability score based on the mapped locations of confirmed springs and seeps, and in the arid zone, perennial rivers and areas of groundwater depletion. For example, a confirmed spring in an area of high groundwater potential received a larger *increase* than a spring in an area of low groundwater potential because it is likely to represent an area of more available groundwater. In contrast, groundwater depletion was penalized in areas with high groundwater potential as depletion is likely to represent a greater hardship to groundwater dependent species and ecosystems.

Springs and Seeps Adjustment

As groundwater availability is complex, we wanted to confirm groundwater areas with other sources of data. The NHDPlus springs/seep point dataset (USGS 2016) provides information on the locations where spring water emerges and thus is available at the surface for freshwater biota. A spring is a water resource formed when a landform (often a hillslope or valley bottom) intersects groundwater at or below the local water table. Springs may be formed in any sort of rock at bedrock fractures, although they are common in limestone and dolomite geology because these geologies fracture relatively easily when weak carbonic acid from percolating rainwater enters and dissolves the bedrock. Factors such as fracture size, aquifer water pressure, size of the spring basin, and rainfall influence the amount of water flowing from a spring. Although the spring dataset did not contain information on the amount of water emerging, we treated high spring density as an indicator of confirmed groundwater availability.

We calculated a spring density map based on the density of spring points in each HUC-12. We converted the results to z-scores and selected all areas that scored greater than average (z-score > 0) and rescaled them to be between 0 and 1 (Figure 3.36). The rescaled z-score was used to increase the potential water availability score with weighting in proportion to the HLR where the spring occurred. The highest increases were given to high spring densities in high groundwater HLRs, which accounted for 95% of the springs. Moderate and low increases were given to spring densities in moderate or low groundwater HLRs, with the lowest increases given to low spring densities in low groundwater HLRs.

Figure 3.36. Spring density increase. Areas where spring density is greater than average, with scores reflecting relative density per HUC-12.

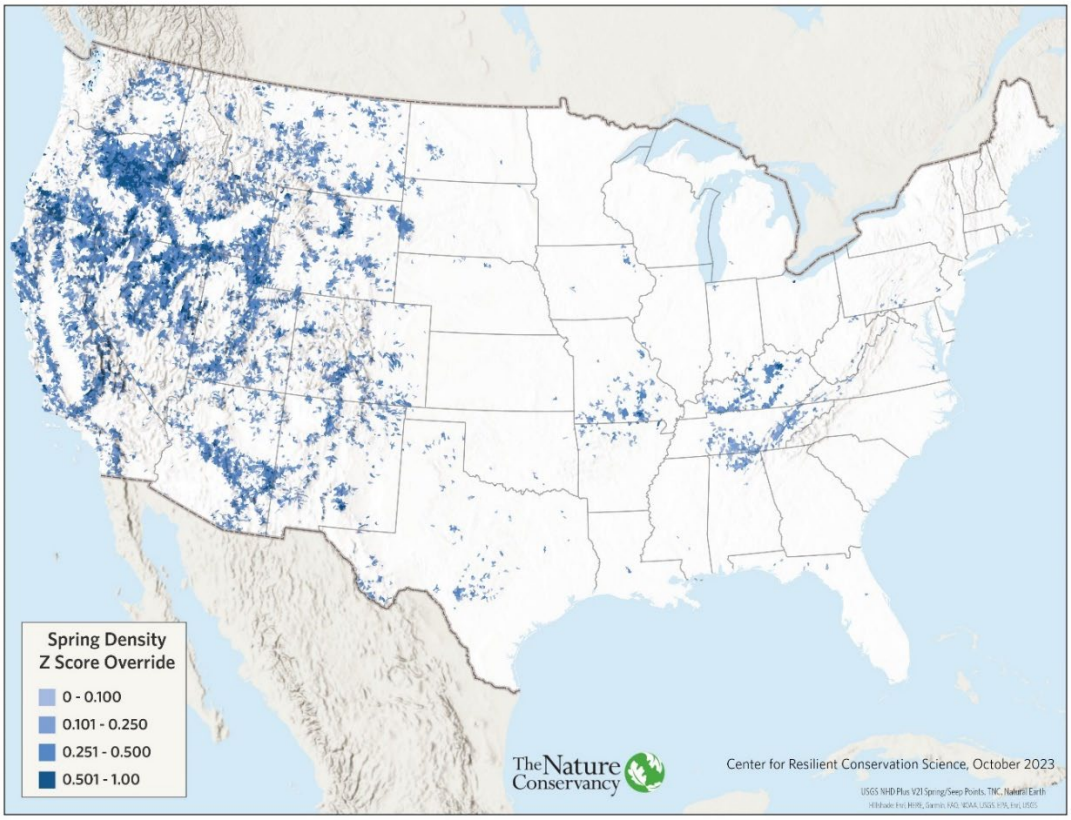

Perennial Streams & Rivers Adjustment

In arid ecoregions, perennial streams and rivers are essential for maintaining freshwater biodiversity and resilience as they represent the only places where water is reliably found throughout the year. For example, 56% of the streamflow in the Upper Colorado River Basin originates as baseflow, with precipitation being the dominant driver of spatial variability in baseflow (Miller et al. 2016). Because arid region rivers are so dependent on groundwater and snowmelt, we used the occurrence of perennial rivers in this region as an indicator of groundwater at or near the surface.

To account for their importance in the arid region, we used an override to increase the potential water availability score of HUC-12s that had perennial rivers and streams. For each qualifying HUC-12, we increased the water score from 0.10 to 1.0 SD based on the percentage of perennial streams in the HUC, ranging from 10% to 100%. Additionally, we increased the water score of a HUC to a minimum of "Above Average" (1 SD) if it had a perennial river greater than 1,000 km^2 in drainage area, regardless of the HUC perennial river percentage (Figure 3.37). This increase was only applied if the score was not already greater than 1 SD based on the surface water index and spring density. We did not adjust the increases by HLRs because rivers crossed multiple HLRs.

Figure 3.37. Perennial streams and rivers adjustment. This map shows where the perennial streams and rivers increase from 0.1-1.0 SD was applied.

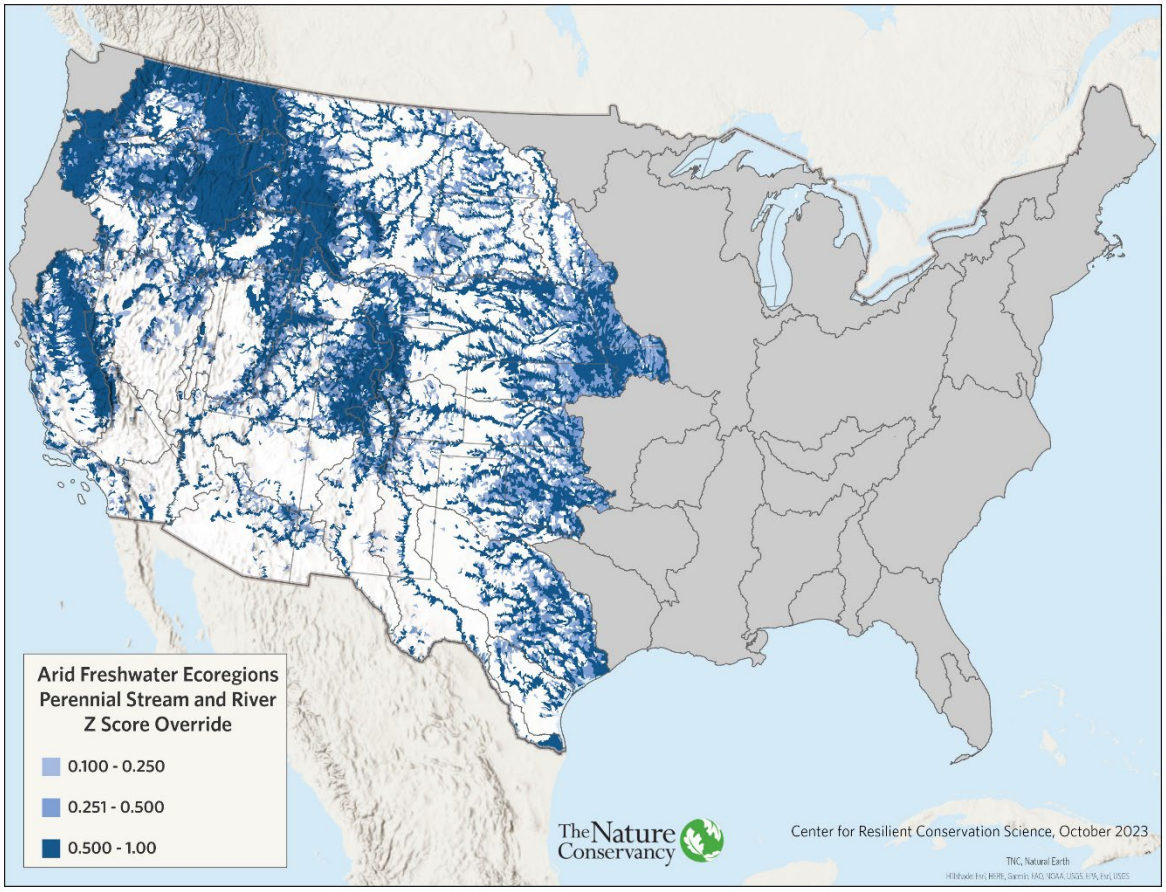

Groundwater Depletion Adjustment

Our final groundwater adjustment to the water availability score was a penalty imposed for groundwater depletion in the arid region, usually due to excessive pumping from underground aquifers. Following the advice of TNC's global groundwater group, we imposed a larger penalty for groundwater depletion in high groundwater HLRs as these are the most likely areas to support groundwater dependent ecosystems. Areas in low groundwater HLRs were given a small penalty as these areas are likely to be more surface water dependent and groundwater depletion has less of an impact. We benefited from a new remotely sensed dataset of shallow groundwater depletion that allowed us to identify areas showing groundwater losses when compared to historical conditions.

The dataset we used for evaluating groundwater alteration was NASA's GRACE Shallow Groundwater Drought Indicator: Wetness Percentile relative to 1948-2012 (Houborg et al. 2012; Getirana et al. 2020). The GRACE data measures how altered the groundwater volume is compared to historic levels. It integrates multiple ground and space based observing systems, including NASA's Gravity Recovery and Climate Experiment (GRACE) satellite mission and provides weekly data at 12.5-km resolution grid cells across CONUS from 2003-2022. The GRACE satellite pair detects small changes in the Earth's gravity field caused by the redistribution of water on and beneath the land surface. The resulting maps of North America depict the "Groundwater Wetness Percentile," which compares the amount of groundwater storage at a given date with the historic period of 1948-2012. Negative changes are primarily a result of groundwater withdrawals, while positive changes appear to result from irrigation, but they may also reflect climatic changes in precipitation.

Groundwater Depletion Metric

We focused our analysis on the months of February and March, the period of most complete groundwater recharge. We compiled the data for an 18-year period (2003-2021) relative to a 64-yr. average (1948-2012). We categorized the results into classes representing the depletion level most common over the 18-year period. We assigned each grid cell the most frequent percentile class (0-20%, 20-50%, 50-80%, 80-100%) relative to the historic period (Figure 3.38). For example, a result of 0-20% indicates that in February and March for the 2003-2021 time period, the shallow groundwater was most frequently at 0-20% of its historic (64-year) level.

The GRACE data focuses on relative change and does not consider the total groundwater storage present or available. After review of the data, we limited our groundwater penalty to the most severely altered class in the arid region, where we were most confident that shallow groundwater declines would directly affect water availability and resilience. We defined this as areas of 0-20% historic groundwater levels in the arid freshwater ecoregions (Figure 3.39). We weighted the penalty by HLRs, giving the greatest penalty to regions most dependent on groundwater, and the least to regions primarily dependent on surface water. Thus, HUCs in the 0-20% high depletion class received a penalty of -0.25 SD to -0.50 SD depending on the proportion of the HUC covered (10%-100%). HUCs in moderate groundwater HLRs received a penalty of -0.05 to -0.25 SD, and those in the low groundwater HLR class received no penalty.

Figure 3.38. Shallow groundwater depletion categories. The map shows the most frequent percentile class (0-20%, 20-50%, 50-80%, 80-100%) found in Feb. and March during an 18-year period. A result of 0-20% indicates that over the period from 2003-2021, the shallow groundwater was most frequently at 0-20% of its historic level.

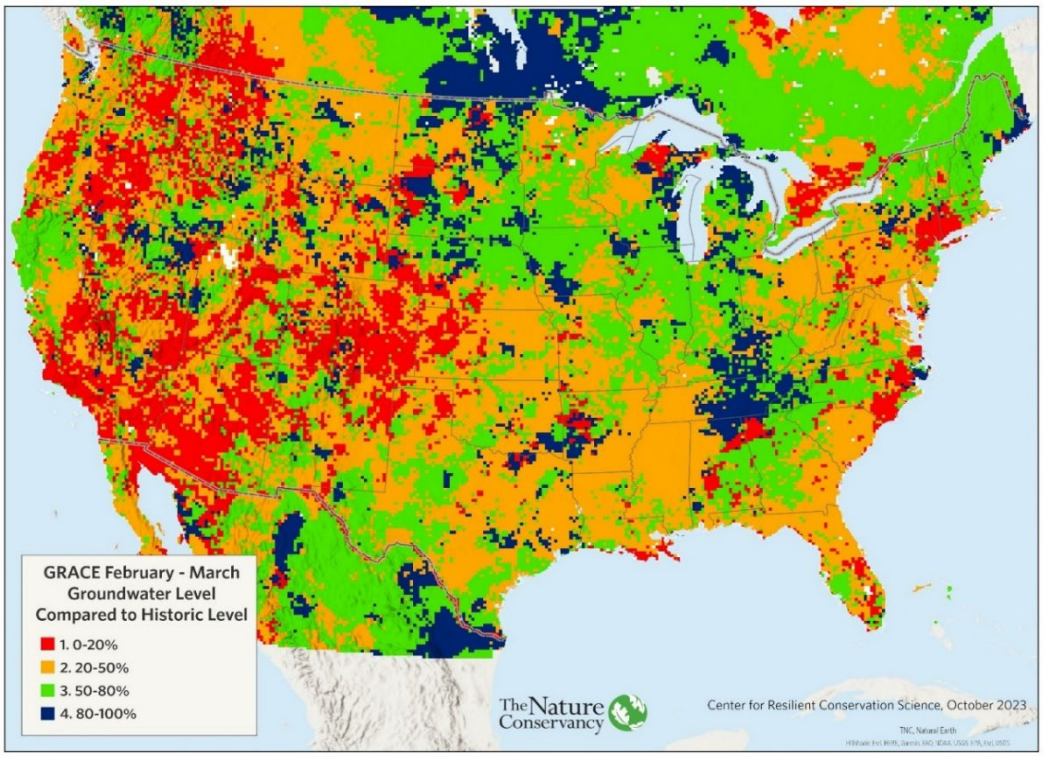

Figure 3.39. Areas receiving the shallow groundwater depletion penalty.

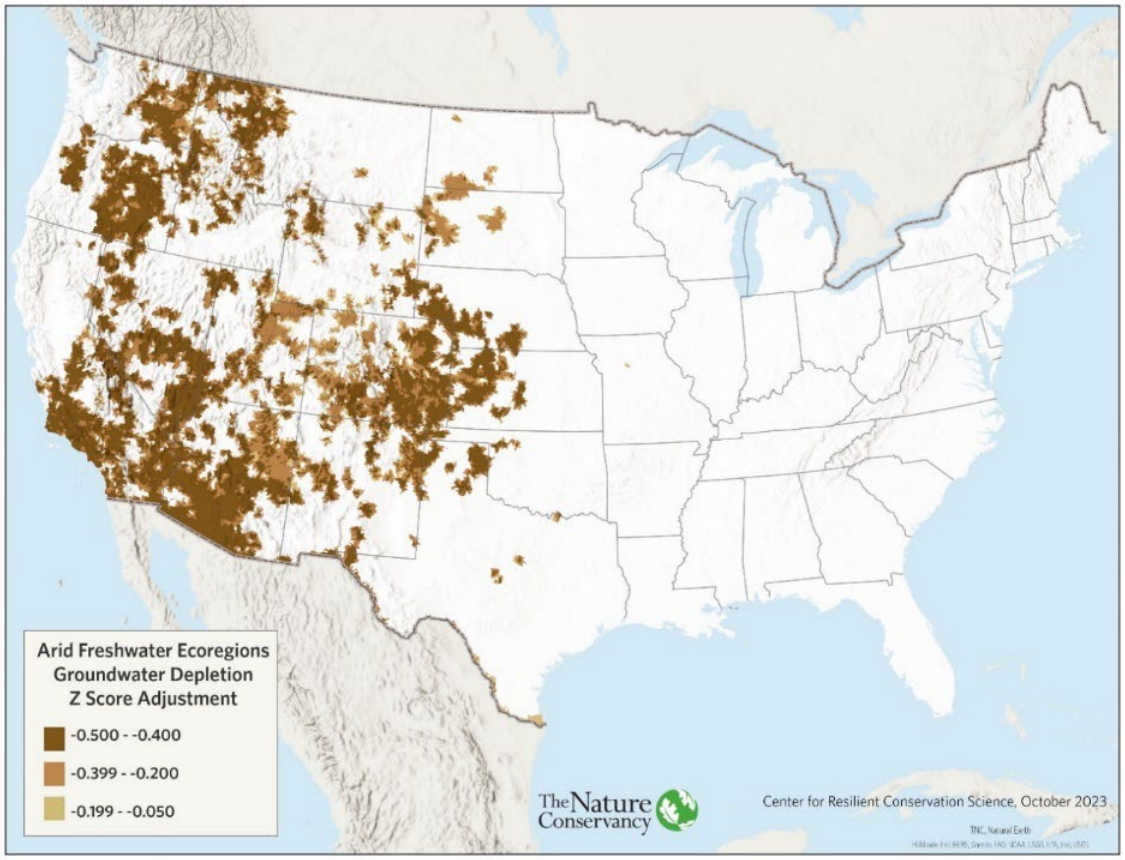

Integrated Map of Potential Water Availability

Our final potential water availability score was calculated differently for arid and humid regions. In both, we began with the surface water score and applied the HLR-weighted increases and penalties for groundwater springs, seeps, perennial rivers, and shallow groundwater depletion. In the humid region, the final score is dominated by surface water availability, driven by wetlands and topographic storage, with adjustment for springs and seeps. In the arid region, the score reflects a more combined surface-groundwater score reflecting wetland features, snowpack areas, springs and seeps, perennial rivers, and groundwater depletion (Figure 3.40):

- *Humid Region: PWA = Surface Water Index + Spring Density weighted by HLRs*
- *Arid Region: PWA = Surface Water Index + Spring Density weighted by HLRs + Perennial Rivers - Groundwater Depletion weighted by HLRs*

Figure 3.40. Potential water availability. The map is stratified by the arid and humid regions (black line) and includes all the appropriate surface water weights and groundwater adjustments.

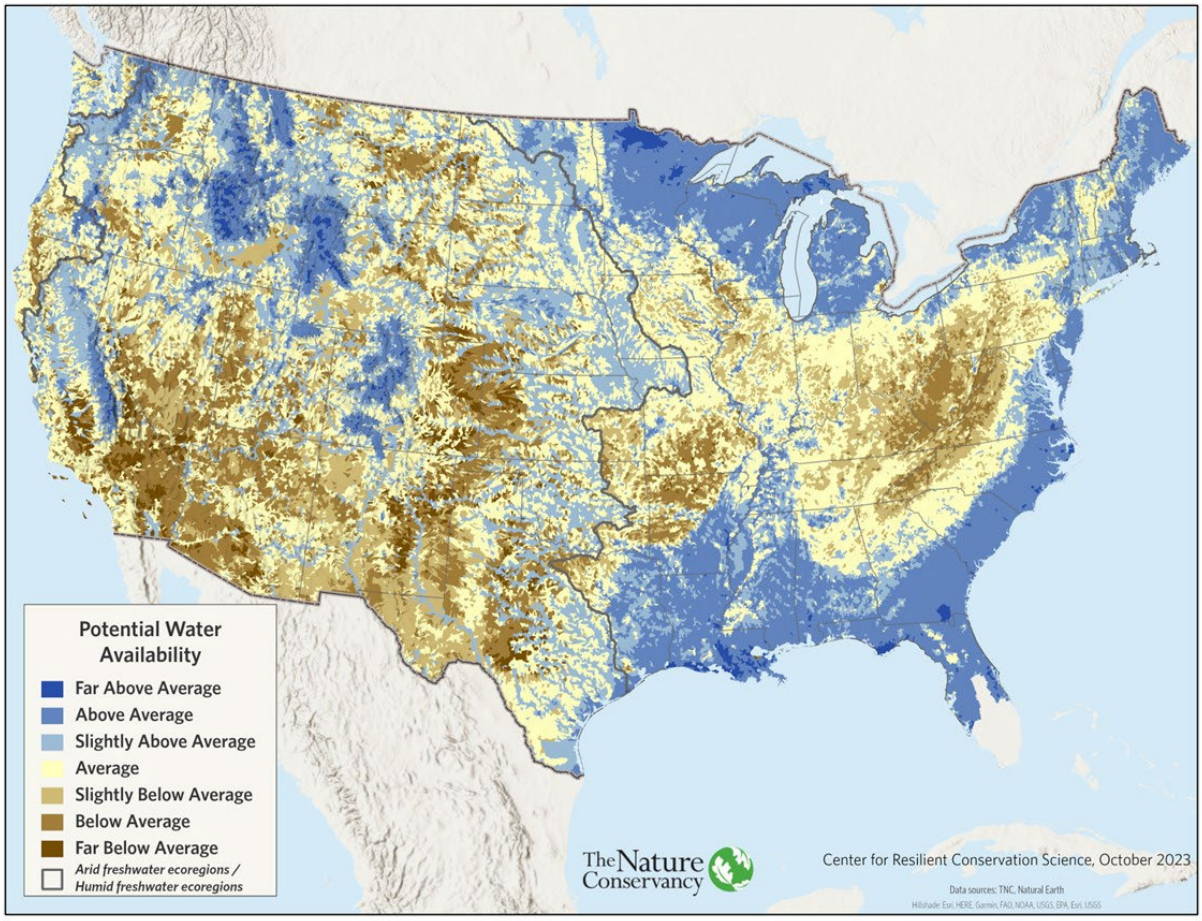

Flow Alteration

Protecting and restoring natural flow regimes, hydrologic integrity, and environmental flows are consistently pointed to as climate change adaptation and biodiversity conservation strategies for inland rivers (Paukert et al. 2021; Wilby 2020; Tickner et al. 2020). Flow is considered the master variable to sustain ecological integrity (Poff et al. 1987). We accounted for flow alteration using the Hydrologic Alteration Index (HAI) from McManamay et al. (2022). This index compares stream flows to reference conditions at a set of gages, then uses random forest models to assign a degree of flow alteration to each NHDPlus stream reach. We summarized the HAI for river reaches (drainage area greater than 100 km^2) at the HUC-12 scale using a length-weighted average that accounted for whether a reach was intermittent or perennial. For HUC-12s with no river length, we summarized the HAI for stream and headwater reaches based on the proportion of perennial and intermittent length.

HUCs were then z-scored across CONUS to derive a final hydrologic alteration score where 3 SD equaled no alteration, -3 SD equaled highly altered, and 0 was the average degree of alteration. We capped the flow alteration score at 1 for HUCs dominated by intermittent streams in the arid ecoregion (criteria = greater than 75% intermittent and/or less than 25% perennial). We did this because alteration was not independent of the amount of available water, and intermittent systems usually did

not have enough surface water to experience flow alteration. This allowed us to distinguish flow alteration from little water (Figure 3.41).

Figure 3.41. Flow alteration score. Hydrologic Alteration Index (HAI) scores from McManamay et al. (2022) were summarized for rivers by HUC-12 watersheds, transformed to z-scores relative to CONUS, and capped for high scores in the intermittent systems of the arid west.

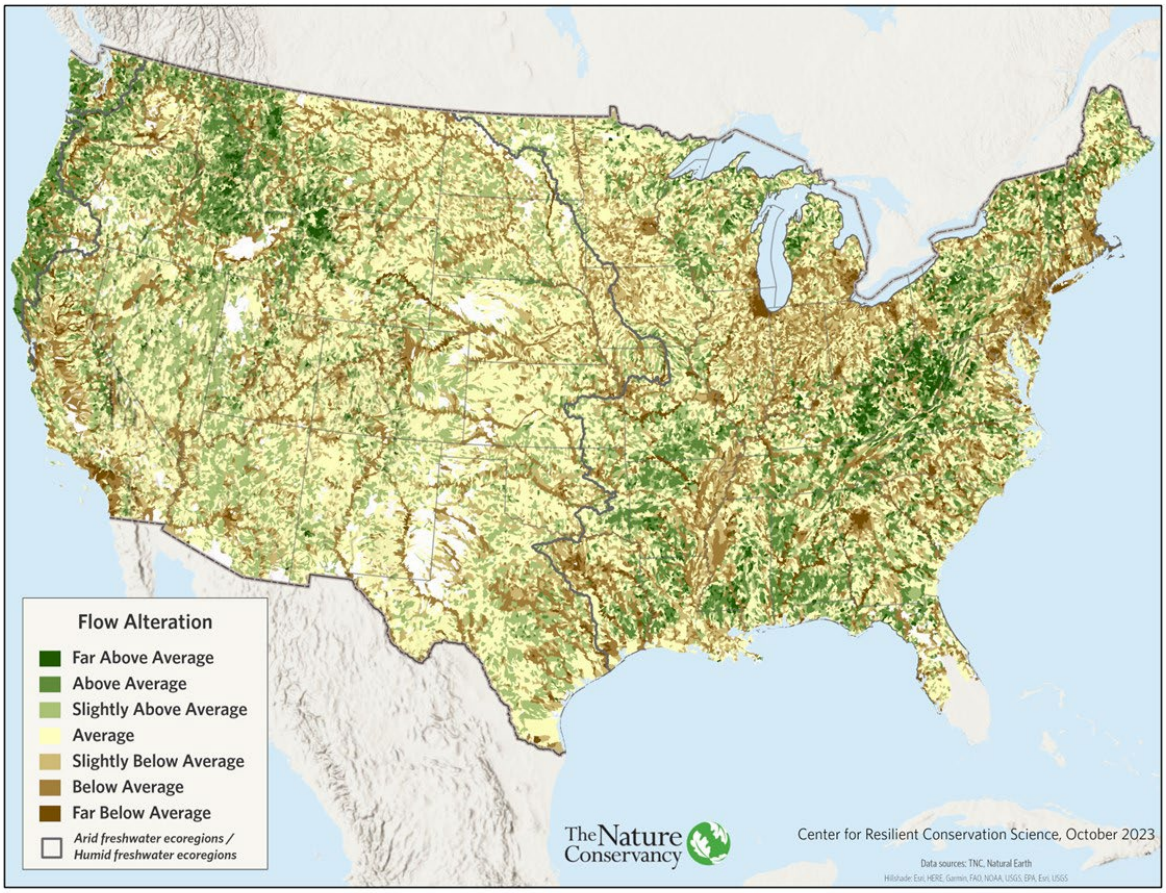

Integrated Water Score

Potential Water Availability + Flow Alteration

For each HUC-12, we integrated potential water availability and flow alteration into a water score by taking a weighted average of the two scores, with the weights differing substantially as the climatic regions became more arid (Figure 3.42). In the humid region where water is readily available, the score was based primarily on flow alteration (three times the weight). In arid regions dominated by perennial rivers, the score was an equal combination of water availability and alteration. In arid regions characterized by intermittent streams, the score was based primarily on water availability (three times the weight) as water is the more limiting factor in these extremely dry landscapes.

The final water score map (Figure 3.43) is stratified by these regions, and the scores are relative to each.

- *Humid = (3*Flow Alteration+ 1*Potential Water Availability / 4*
- *Arid-Perennial = (1*Flow Alteration + 1*Potential Water Availability)/ 2*
- *Arid-Intermittent = (1*Flow Alteration + 3*Potential Water Availability / 4*

Figure 3.42. Stratification regions for the water score.

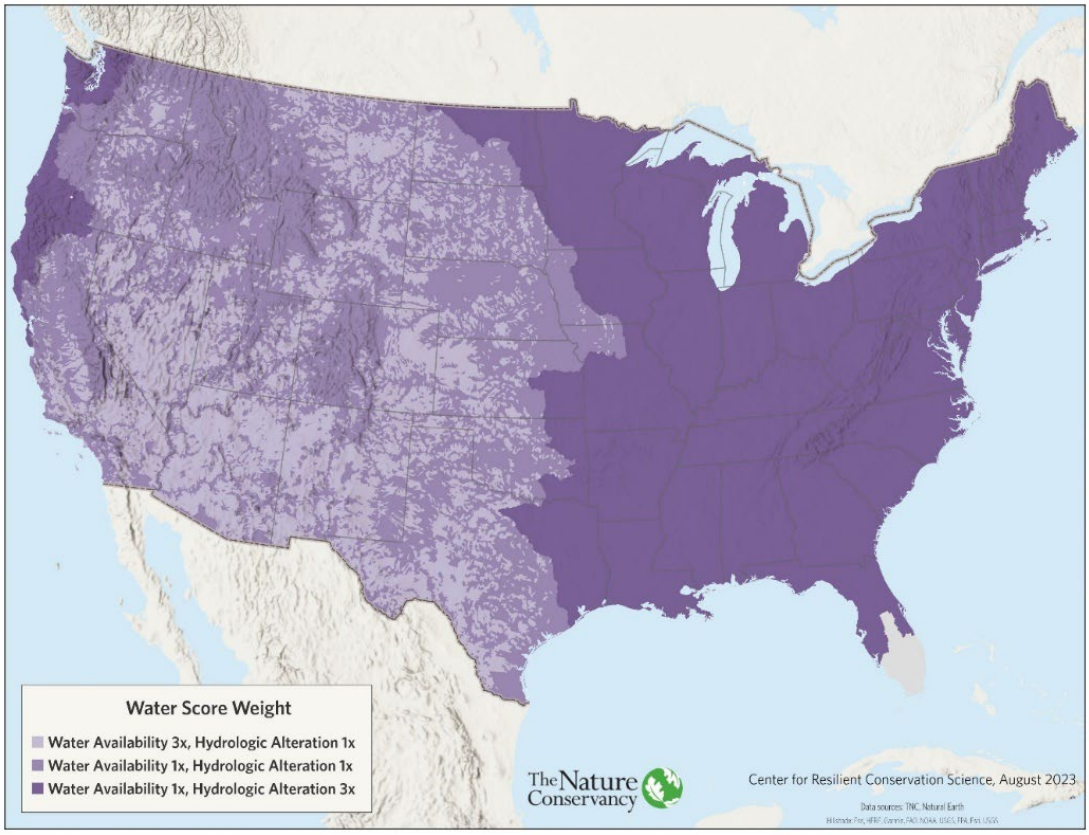

Figure 3.43. Water score. This map shows the final water score after combining potential water availability and hydrologic alteration with the weights and adjustments described in the text. This map is stratified by three climatic regions (humid, arid-perennial, and arid-intermittent) thus the results are relative to those regions.

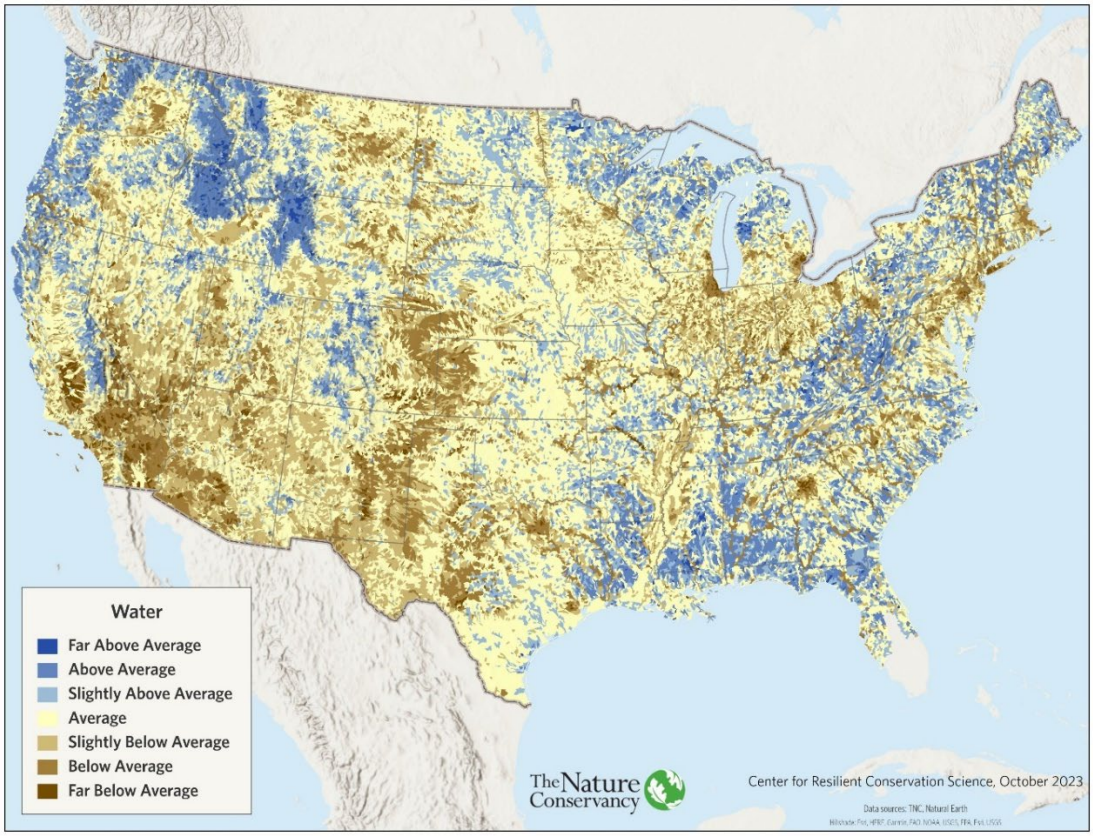

Integrated Freshwater Resilience Score

We determined a resilience score for each HUC-12 by calculating a weighted average of the physical score and the water score, with the relative weight of each component dependent on the climatic region (Figure 3.44, Table 3.9). In humid regions, more weight was given to the physical score, emphasizing the size and condition of the network. Less weight was given to the water score, which primarily reflects hydrologic alteration. Very little weight was given to water availability as water is generally not a limiting factor in this region. In the arid region, we gave equal weight to the physical and water score, reflecting the relative importance of both these factors. In xeric regions, more weight was given to the water score, with potential water availability being the largest contributor to the score. Arid non-xeric regions had intermediate weights (Table 3.9).

Table 3.9. Weights for combining the physical and water scores by climatic region.

Climatic Region	Physical Score Weight	Water Score Weight
Humid	2x	1x
Arid non-xeric	1x	1x
Arid xeric – more perennial	1x	2x
Arid xeric – more intermittent	1x	4x

Figure 3.44. Climatic regions and variable influence. These are the same climatic regions used throughout the analysis. Annotations describe the dominant factors in each of the regions.

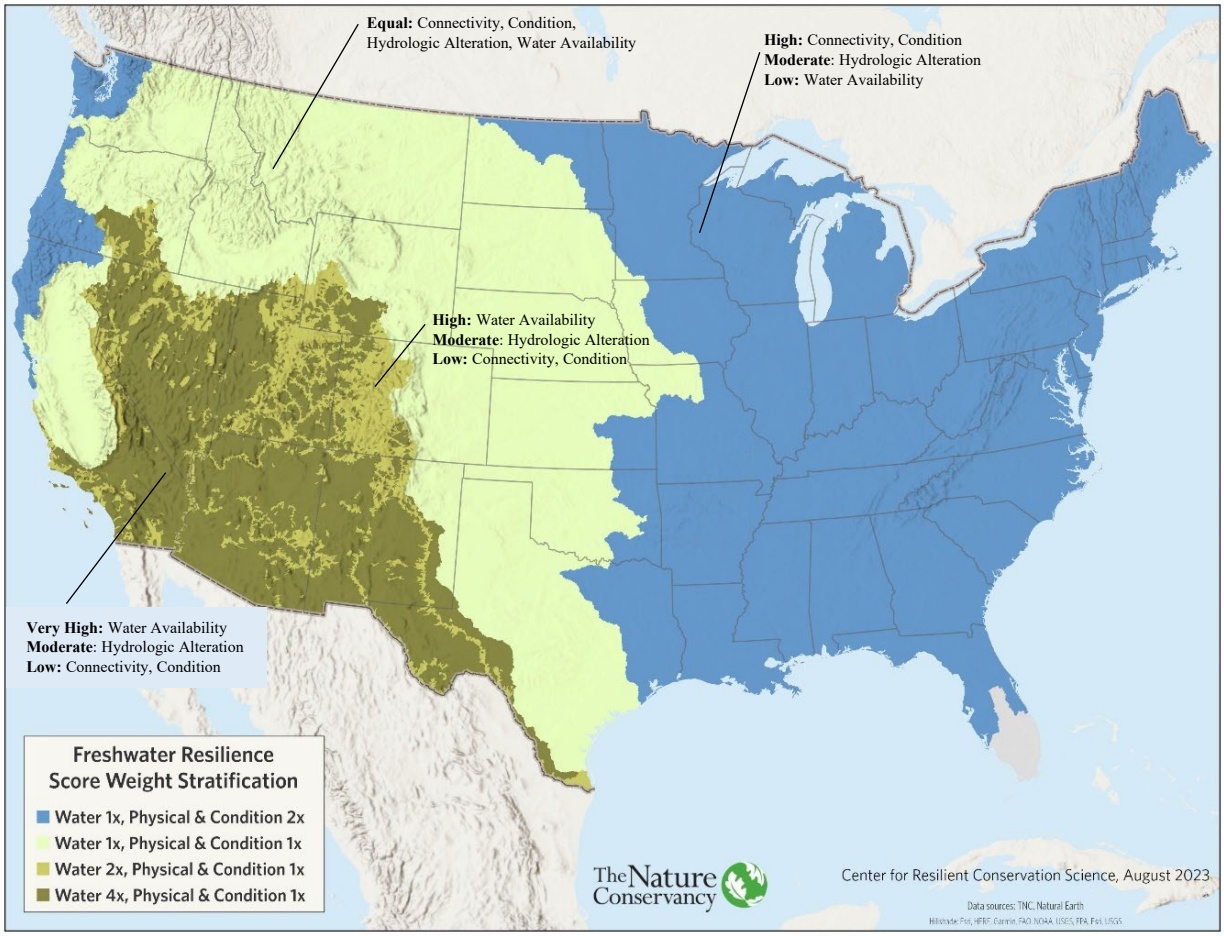

Best in Ecoregion

To ensure representation of all freshwater ecosystems, our final step was to include an ecoregional override. The override identified the highest scoring HUCs in each freshwater ecoregion (WWF & TNC 2019) and terrestrial ecoregion (TNC 2020b). If a HUC's ecoregional score was higher than the CONUS score and the CONUS score was not already greater than "Average" (> 0.5 SD), the HUC's resilience score was rescaled to be in the "Slightly Above Average" resilience class (> 0.5 to 1 SD). To prevent increasing the score of vulnerable watersheds, HUCs also had to meet the following criteria:

- "Average" for resilience, and
- "Average" or higher for all three major components: size-diversity, condition, water alteration, and
- Greater than "Average" for water availability if in the arid/xeric climatic zone

The ecoregional override raised the score of 3% of the HUCs (2,395 out of 95,973) to "Slightly Above Average," ensuring that the most resilient HUCs in each ecoregion were included as resilient if they met base criteria (Figure 3.45). The final freshwater resilience score incorporates this last adjustment and identifies 26% of CONUS as scoring greater than "Average" for resilience (Figure 3.46, Table 3.10).

Figure 3.45. Areas increased to "Slightly Above Average" resilience score based on an ecoregional override.

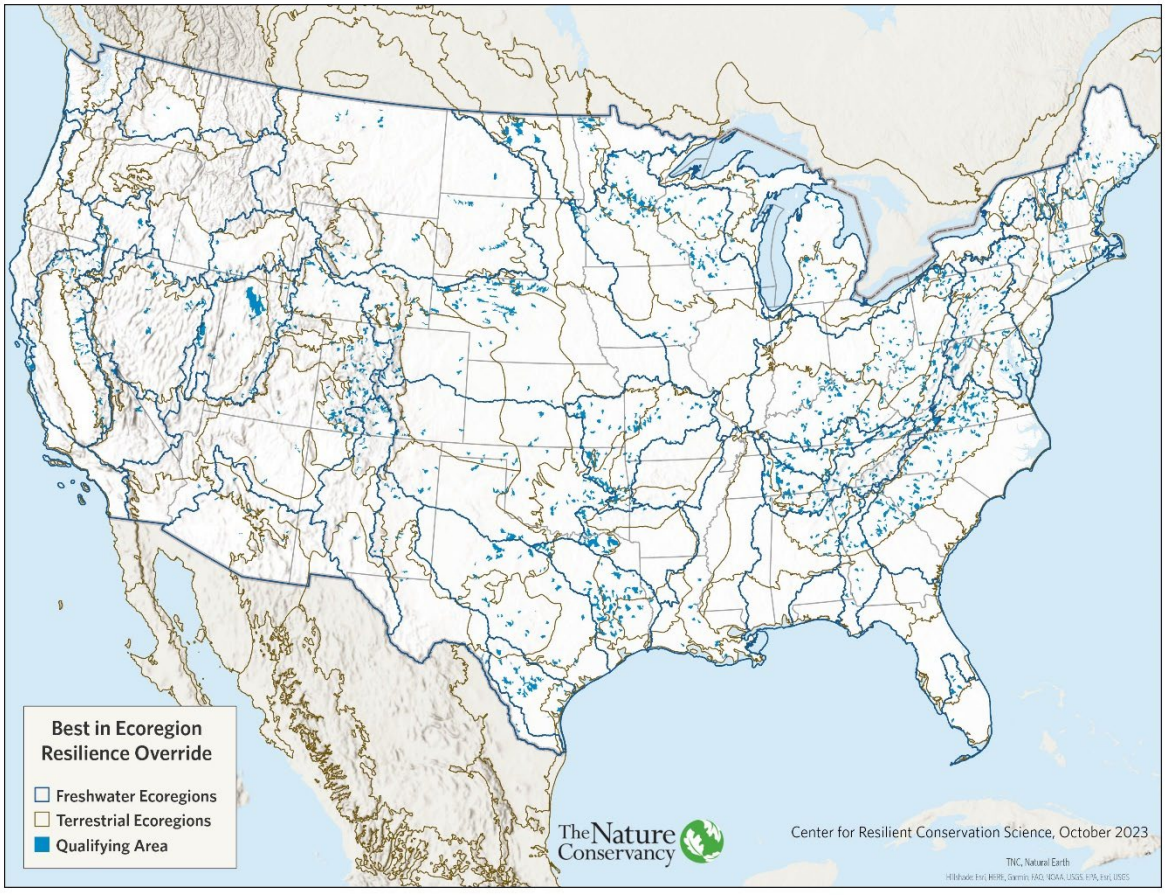

Figure 3.46. Final freshwater resilience score. This integrated map is stratified by arid and humid climatic regions and incorporates all the appropriate scores and adjustments relative to each region.

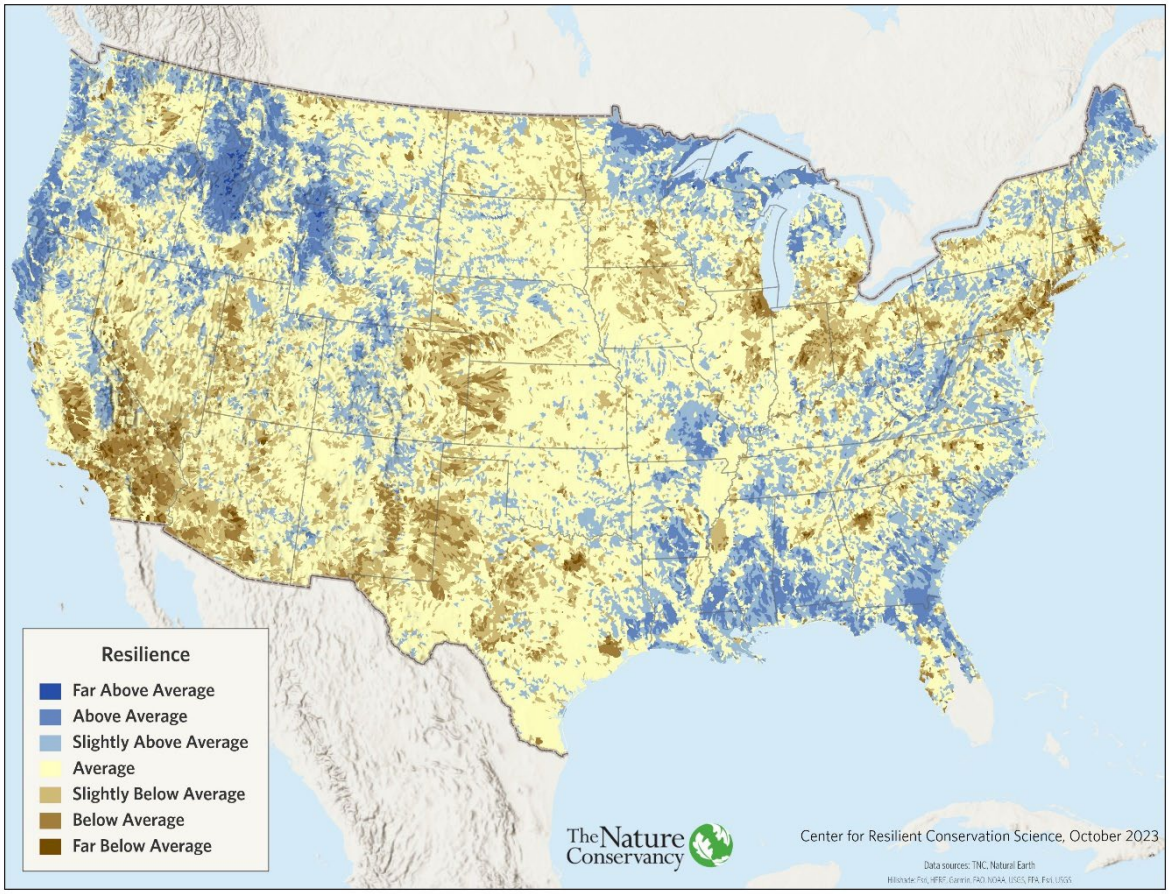

Table 3.10. Length and percentage of each resilience category.

	Freshwater Resilience Score							
Units	**Far Above Average**	**Above Average**	**Slightly Above Average**	**Average**	**Slightly Below Average**	**Below Average**	**Far Below Average**	**Total**
Kilometers	3,559	371,438	972,020	3,049,329	596,557	146,670	6,561	5,146,134
Miles	2,211	230,801	603,985	1,894,765	370,683	91,136	4,077	3,197,658
Percent	0%	7%	19%	59%	12%	3%	0%	100%
Cumulative Percent	0%	7%	26%	85%	97%	100%	100%	100%

CHAPTER

Freshwater Resilient & Connected Network 4

In this section we identify a representative, resilient, and locally connected network, the Freshwater Resilient and Connected Network (FRCN), that if conserved or restored could sustain freshwater biodiversity while facilitating the movement of species to adapt to a changing climate. Our approach was to identify a network of freshwater sites that have been recognized for their aquatic biodiversity value and then intersect the biodiversity network with the freshwater resilience map to identify a network of sites that are both resilient and biodiverse. We did not set a goal for spatial extent, but we were conscious of the United Nations Convention on Biological Diversity Kunming-Montreal Global Biodiversity Framework Target 3 (UNEP 2022) to "ensure and enable that by 2030 at least 30 per cent of terrestrial and inland water areas, and of marine and coastal areas, especially areas of particular importance for biodiversity." It became clear in our analysis that we could not represent all freshwater ecosystems, nor reach a 30% stream mile goal, without incorporating restoration areas into the results. Thus, identifying places for key restoration strategies became an essential part of the network design.

Recognized Biodiversity Value

We compiled many different spatial datasets to develop a map of recognized biodiversity value (RBV) areas currently supporting freshwater species and habitats that collectively represent the aquatic biodiversity of CONUS. These areas were derived from multiple-sources including national, state, and ecoregional assessments as well as individual species studies. The most comprehensive national source was TNC's freshwater ecoregional portfolio of sites identified through intensive, expert-driven planning efforts from 1998-2013. These 57 plans can be accessed here. We supplemented this national layer with areas of high range-size rarity for aquatic species from NatureServe's Map of Biodiversity Importance (MoBI, Hamilton et al. 2022). These areas have a concentration of aquatic species with restricted ranges. State-based assessments included State Wildlife Action Plans for 31 states (Appendix 5, Table A5-1), Crucial Habitat Assessment Tool (CHAT) designations for Oklahoma and Texas, and a freshwater biodiversity blueprint completed for California (Howard et al. 2018).

We used additional species data to confirm, or in some cases, supplement the national and state assessments. A full list of species sources can be found in Table A5-2 in Appendix 5. These included anadromous species critical habitat for the coasts from the National Oceanic and Atmospheric Administration (NOAA), critical habitat for aquatic or aquatic dependent inland species from the U.S. Fish and Wildlife Service (USFWS), strongholds for Brook Trout in the eastern U.S. (Fesenmyer et al. 2017), and Bull Trout and Cutthroat Trout refugia in the west from the U.S. Forest Service Climate Shield project (Isaak et al. 2017, 2022). All delineations of habitat were attributed to reach catchments from their original source data, which included flowlines, hexagons, watersheds, and free-form polygons.

The compiled map shows streams and rivers that have been recognized for their biodiversity value by any one of the above sources (Figure 4.1). The map identifies 1,513,827 miles of streams and rivers with recognized biodiversity value, 47% of all stream miles (3,191,174). It does not imply a ranking or

relative importance of any site or species, rather we were striving for full representation of all freshwater species. We combined the areas of recognized biodiversity value with the map of freshwater resilience to identify places with recognized biodiversity but only "Average" resilience (Figure 4.2). We considered it important to restore the resilience of these areas and an analysis of the challenges and restoration potential of each became the bases of the Freshwater Resilient and Connected Network described in the next section.

Figure 4.1. Areas of recognized biodiversity value. The map shows the 47% of all streams and rivers recognized for their biodiversity value in any of the almost 100 source datasets.

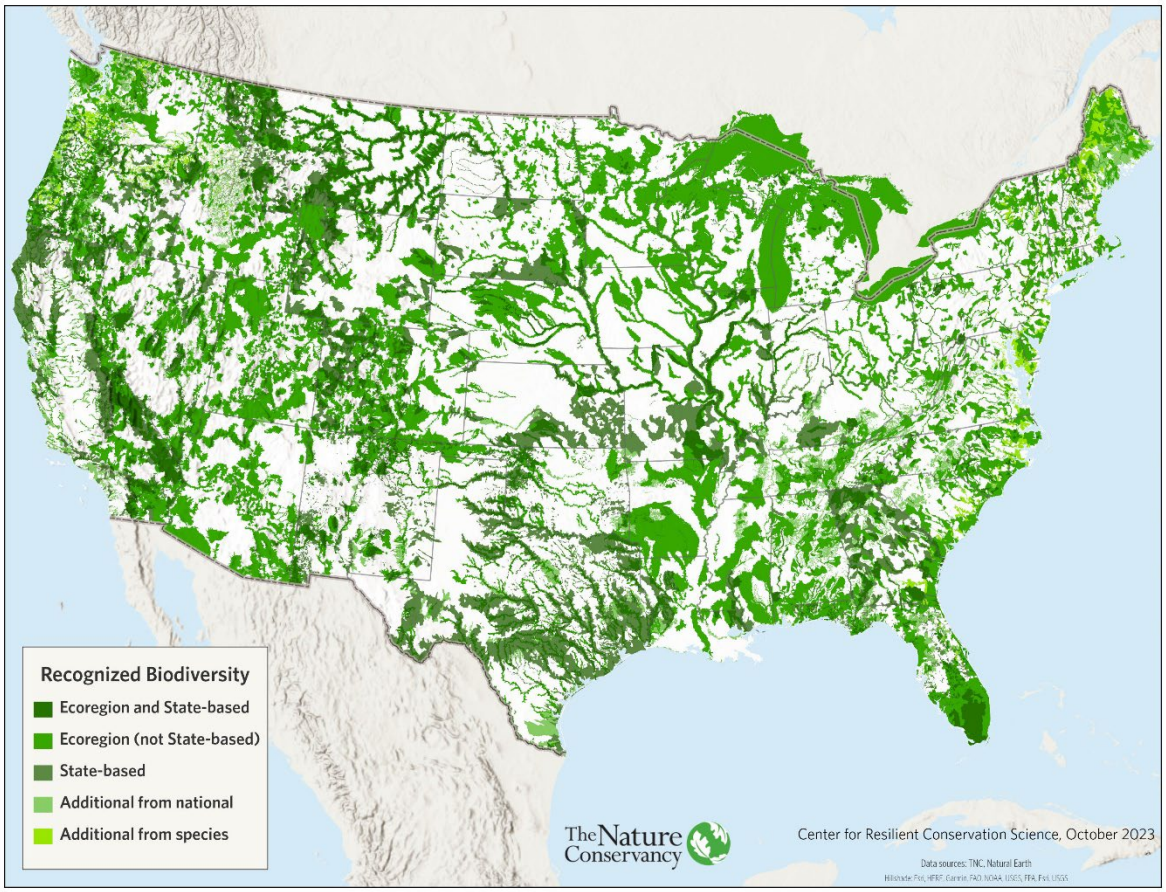

Figure 4.2. Freshwater resilience and biodiversity value. This map subdivides the areas of "Average" resilience into those with or without recognized biodiversity value.

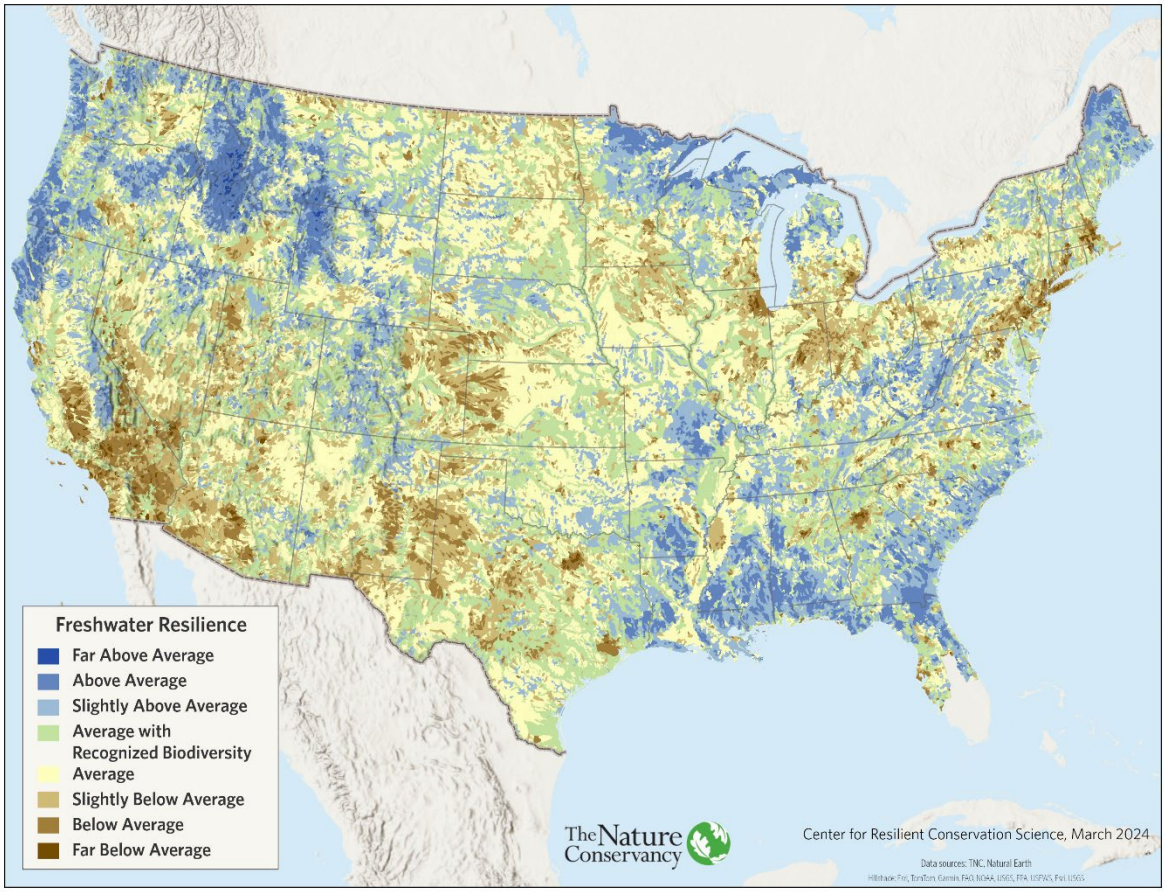

Mapping a Resilient and Connected Network

To create a representative and resilient freshwater network, we spatially combined the freshwater resilience scores and their components with the areas of recognized biodiversity value. We then used a series of queries (shown in italics below) to identify river reach catchments that met various criteria for both resilience and biodiversity. Initially, we planned to restrict the network to areas with greater than "Average" resilience scores, but we soon realized that to represent all the freshwater species and ecosystems across CONUS, we would need to include restorable sites with "Average" resilience. We defined restoration sites as locally connected river networks that had recognized biodiversity value and "Average" resilience scores with only one component scoring less than "Average" in their integrated score. Restoring the low scoring component, be it size, condition, flow alteration or water availability, would make the site resilient (i.e., increase its score to greater than "Average"). For example, a small biodiverse network that scored higher than "Average" for condition, flow, and water availability, but was below "Average" for size (and thus scored "Average" for resilience), could theoretically be restored to resilient by removing the impeding dam and increasing the size of the network. We identified the places where intervention would make the system resilient, but we did not measure the feasibility of restoration actions. In the case of water availability in arid regions, we categorized sites

as "verify water" if they were "Average" or lower. Below are the criteria we used to identify the network, and the percent of all stream miles in CONUS affected by the decision.

Resilient Sites

Resilient freshwater sites are long, diverse, locally connected stream networks in good condition, with adequate unaltered water. These sites have greater than "Average" freshwater resilience scores (>0.5 SD) and cover 26% of CONUS (Table 4.1). Sixty-eight percent of them also had recognized biodiversity value (17.9% of CONUS) and were selected for inclusion in the network. We also included sites that scored "Above Average" for resilience even if they had no recognized biodiversity (2.3% of CONUS) as these represent places where biodiversity could potentially thrive in the future. Together these two queries sum to 20% of all stream miles and encompass all areas in the network with greater than "Average" resilience and recognized biodiversity.

Resilient and Biodiverse (17.9%)

This category includes resilient areas that also have recognized biodiversity value.

Resilience score >0.5 SD and RBV = yes

Highest Resilience and Future Biodiversity (2.3%)

This category includes areas of "Above Average" resilience that currently are not recognized for biodiversity value.

Resilience score >1.0 SD and RBV = no

Restoration Sites

The next set of sites have recognized biodiversity values and are close to being resilient but need restoration of one critical factor to be fully resilient. Our starting criteria were that all these areas had to score "Average" for resilience and intersect RBV areas. From there, we selected those sites with one factor that scored less than "Average" (condition, flow, or connectivity) and which if restored, would likely raise the score to "Slightly Above Average" resilience. Collectively, this set adds another 14.6% of stream and river miles to the FRCN, bringing its total to 35%. In a few cases, we included segments of rivers altered for both flow and condition in the restore flow category if they had high connectivity and including those segments would make the FRCN more continuous.

Restore Condition (3.8%)

Areas of recognized biodiversity value with "Average" resilience. All resilience components are "Average" or above except the condition score, which was less than "Average." In the xeric region, we applied an additional water availability criterion to ensure that the system had water.

Humid Region: Resilience score average, RBV = yes, Size-diversity score ≥ avg, Water alteration ≥ avg, Condition score between >-2 SD & -0.5 SD.

Arid Region: Resilience score average, RBV = yes, Size-diversity score ≥ avg, Water alteration ≥ avg, Water Availability ≥ avg, Condition score between >-2 SD & -0.5 SD.

Xeric Region: Resilience score average, RBV = yes, Size-diversity score ≥ avg, Water alteration ≥ avg, Water Availability ≤ slightly above avg, Condition score between >-2 SD & -0.5 SD.

Restore Flow (4.6%)

Areas of recognized biodiversity value with "Average" resilience. All resilience components scored "Average" or above except the hydrologic alteration score which was less than "Average." Sites also had to contain some portion of a river with at least a 100 km^2 catchment (size 2).

Resilience score average, RBV = yes, Size-diversity score ≥ avg, Condition ≥ avg, Hydrologic alteration score ≤ -0.5 SD.

Restore Flow and Condition (3.1%)

Areas of recognized biodiversity value with "Average" resilience and all resilience components equal to "Average" or higher, except hydrologic alteration and condition which both score less than "Average." While this category includes two components that scored less than "Average," after studying the results we found that it was important to include this category to maintain connectivity of hydrologically altered rivers that had fragmenting gaps of low condition. This category recognizes that there are sites, where despite having both flow and condition challenges, they are still "Average" due to their high functional connectivity. Sites also had to contain some portion of a river with at least a 100 km^2 catchment (size 2).

Resilience score average, RBV = yes, Size-diversity score ≥ avg, Condition and Hydrologic alteration score ≤ -0.5 SD.

Reconnect (3.1%)

Areas of recognized biodiversity value with "Average" resilience. All resilience components scored "Average" or higher except for size which was "Slightly Below Average" or "Below Average." To ensure that a unit would benefit from dam removal, we limited the selected units to those where size was limited by a dam and the network was 60% or less of its original size. Because size is an FCN attribute, this query included a set of criteria to first identify higher scoring FCNs with certain enabling conditions, and then a set of finer scale HUC criteria. Only areas meeting both the FCN and HUC-12 criteria were included.

Step 1. FCN criteria: Area-weighted resilience score of average or better. Area-weighted flow alteration and condition score average or better. In arid ecoregions, area-weighted water availability average or better. Size "Slightly Below Average" or "Below Average" (-0.5 - -2 SD). FCNs bounded by dams and current network 60% or less of its natural size.

Step 2. HUC criteria: Resilience score average or better. Flow alteration and condition average or better. In arid ecoregions, water availability average or better.

Verify Water (1.8%)

Areas that scored greater than "Average" for resilience with respect to their freshwater or terrestrial ecoregion but had potential water availability scores that were "Average." These areas are shown in the Freshwater Resilient and Connected Network map, but the presence and availability of water should be verified by ground surveys. These represent another 1.8% of stream miles.

Arid or xeric ecoregions. Resilience score average and higher in ecoregion, RBV = yes, size-diversity, condition, and flow alteration scores ≥ avg, water availability score avg.

Freshwater Resilient and Connected Network

Cumulatively, the queries identified 36.6% of all stream/river miles in the conterminous U.S. for a total of approximately 1,110,000 miles. Of those streams and rivers, 20.2% fall in the resilient category, 14.6% are in the restoration category, and 1.8% need water verification (Table 4.1, Figure 4.3). Note that these numbers do not include the South Florida freshwater ecoregion where the resilience analysis was infeasible due to data limitations.

Table 4.1. Categories of streams and rivers included in the Freshwater Resilient and Connected Network (FRCN) by length and percentage.

Freshwater Resilient and Connected Network *All categories have **Recognized Biodiversity Value** except where indicated.	**Miles**	**Km**	**Percent**	**Cumulative Percent**
Resilient: Above Average	160,059	257,591	5.0	5.0
Resilient: Slightly Above Average	411,267	661,871	12.9	17.9
Resilient: Far Above Average, **No RBV***	73,913	118,952	2.3	20.2
Restore Condition	120,578	194,051	3.8	24.0
Restore Flow and Condition	98,332	158,250	3.1	27.1
Restore Flow	148,153	238,430	4.6	31.7
Reconnect	97,700	157,233	3.1	34.8
Possible Addition: Verify Water	58,447	94,061	1.8	36.6
Cumulative	1,168,449	1,880,439	36.6	36.6
Total	**3,191,174**	**5,135,698**	**100**	**100**

Figure 4.3. The Freshwater Resilient and Connected Network (FRCN). The networks shown in the map cover 36.6% of all stream miles, including 20% that are resilient, 15% that could be resilient with restoration, and 1.8% that might be resilient if sufficient water is verified.

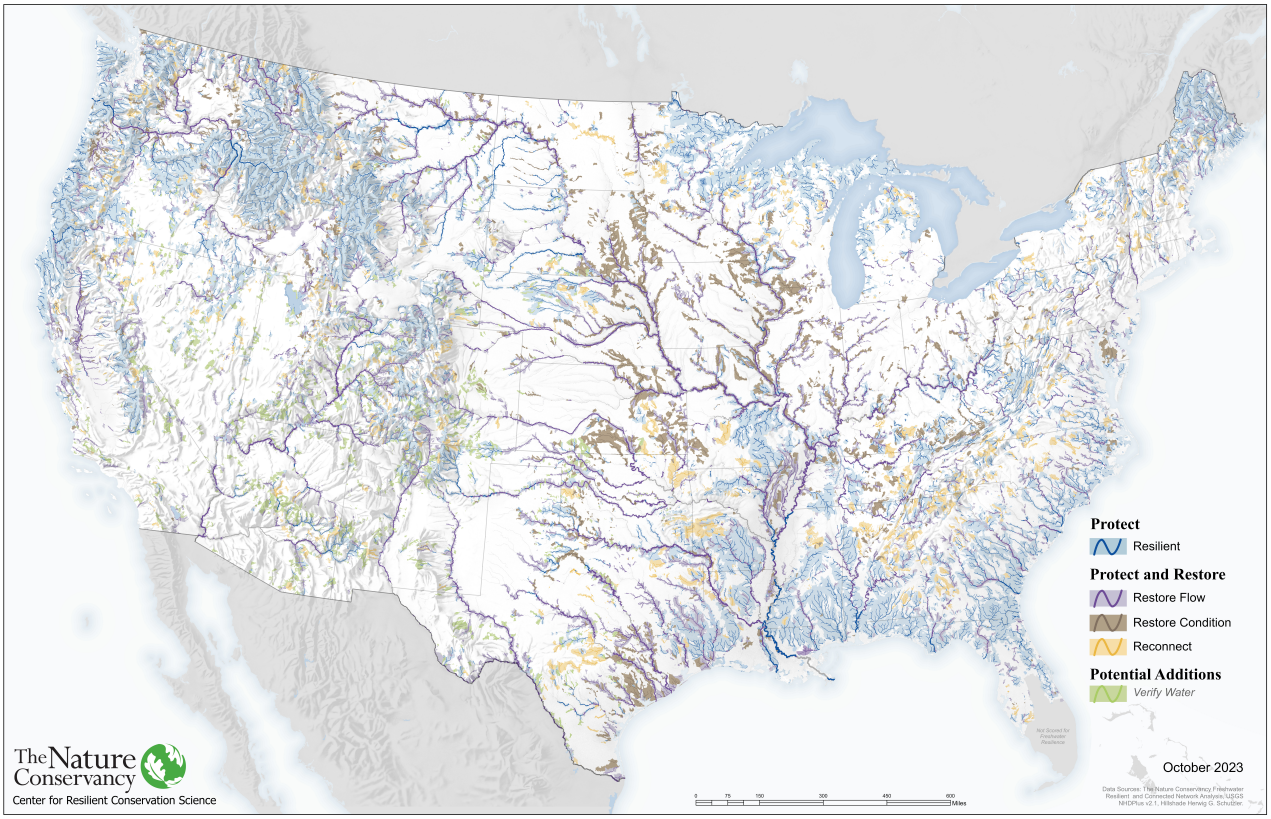

Results and Representation

Representation of Freshwater Features

To measure how well the Freshwater Resilient and Connected Network (FRCN) represents the full diversity of freshwater species and ecosystems, we overlaid a series of individual datasets on the FRCN and assessed how well the features represented were captured by the FRCN. These included:

- Stream sizes and river networks open to the ocean or Great Lakes,
- Wetlands, lakes, and ponds,
- Springs and groundwater dependent ecosystems,
- Freshwater and terrestrial ecoregions,
- Aquatic biodiversity

Stream Size and Unimpeded Rivers

An overlay of all stream miles revealed that the FRCN contains 35% (1.2 million miles) of streams and rivers in roughly the same size class proportion that they occur on the landscape (Table 4.2). The largest discrepancies were in the medium and large rivers, which together represent 5% of the nation's rivers, but 8% of the FRCN.

Table 4.2. Stream size classes by the FRCN.

Stream Size Class	% FRCN	FRCN Miles	% CONUS	CONUS Miles
Headwater & Creeks	81	949,890	86	4,416,700
Small Rivers	11	124,013	10	513,570
Medium-Mainstem Rivers	6	73,622	4	205,428
Large to Great Rivers	2	20,920	1	51,357
Total	100	1,168,445	100	5,135,698

Rivers that were open to the ocean or Great Lakes as well as those with long unimpeded stretches to the river mouth were well represented in the FRCN. These river networks come in many sizes and configurations, including small river networks open to the Great Lakes or the ocean and huge complex networks of the Mississippi for which the mainstem is unimpeded but many of the tributaries are dammed (Figure 4.4, Figure 4.5).

We identified 679 river networks (FCNs) that opened directly into the Great Lakes or ocean, with 199 having an open terminus into the Great Lakes and 480 having an open terminus into an ocean. These networks are particularly important due to their accessibility for anadromous fish and for Great Lakes migratory species. To measure how well these networks were captured by the FRCN, we calculated a weighted average percent FRCN overlap for each FCN. Specifically, we weighted the percent overlap of each size class of rivers in the FRCN by the proportion of that size class in the FCN. We considered a network "completely" covered if its FCN had more than 75% weighted average percent overlap. We considered networks with over 100 km of river length to be "large' and those with less than 100 km of river length to be "small." Most of the river FCNs open to an ocean or to the Great Lakes were small (81%), but some (19%) were large or very large (> 1,000 km). Examples of large networks included the Mississippi, Sacramento, Pascagoula, Neuse, Klamath, Rouge, Columbia, Suwannee, Altamaha, Pee Dee, and Delaware (Figure 4.4).

Among the networks open to the Great Lakes or an ocean, 99% of the large and 82% of the small networks had some overlap with the FRCN and 57% were completely within it. Among the 130 large river networks, 65% were considered completely covered in the FRCN (Table 4.3). Small networks had less complete overlap with the FRCN (55%), particularly in the ocean-connected set (49% completely overlapping) reflecting, in part, the fact that many of the small FCNs had lower resilience scores due to condition and hydrology challenges as well as small size and low diversity, even with a size bump for ocean connectivity.

Table 4.3. River networks open to an ocean or the Great Lakes, and unimpeded river stretches by percent in the FRCN.

Free-Flowing Rivers/ Stretches	Freshwater Resilient and Connected Network				
Connected to Coast	**Count**	**In**	**Partial**	**Sum**	**Out**
Large: Great Lakes	21	62%	33%	95%	5%
Small: Great Lakes	178	66%	16%	82%	19%
Very Large: Ocean	20	70%	30%	100%	0%
Large: Ocean	89	64%	33%	97%	1%
Small: Ocean	371	49%	21%	70%	29%
Total	679	57%	22%	79%	22%
Inland Unimpeded (Large Tributaries)	**Count**	**In**	**Partial**	**Sum**	**Out**
Large Inland Networks	22	77%	13%	90%	10%

Figure 4.4. River networks open to an ocean or the Great Lakes, shown by percent in the FRCN.

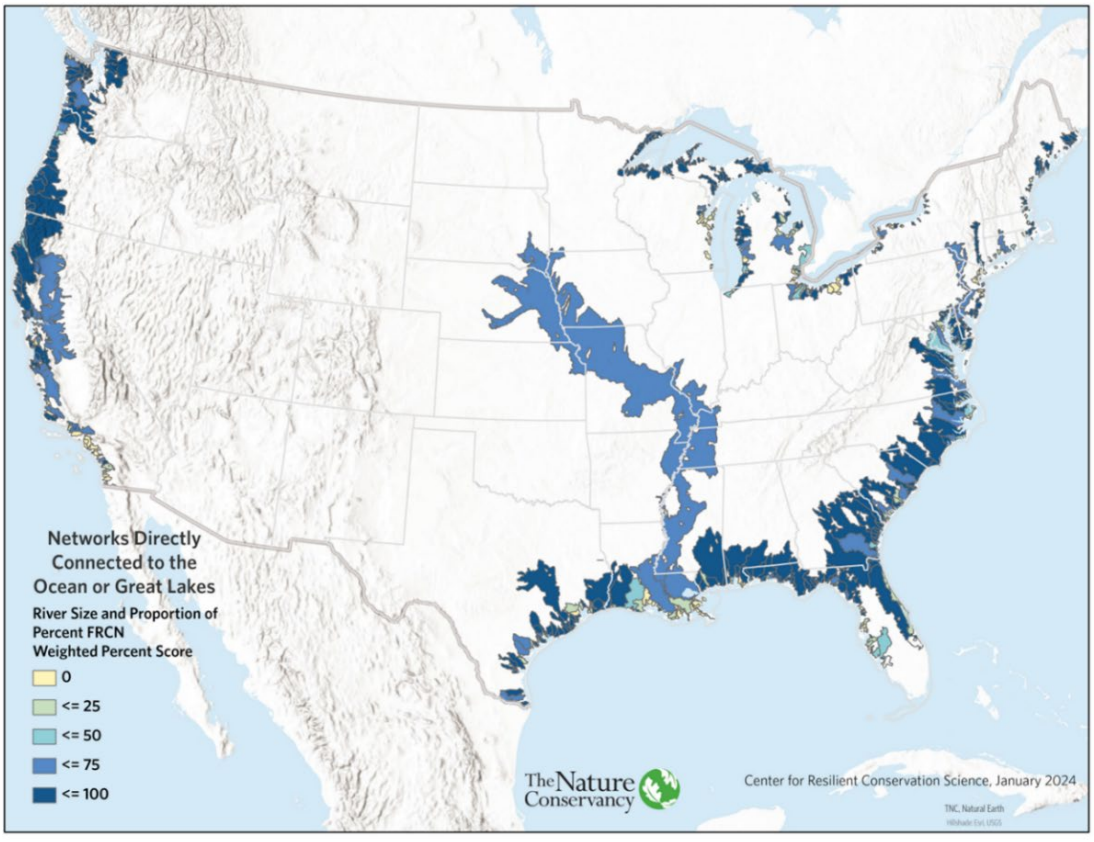

Figure 4.5. Large mainstem unimpeded inland and coastal river stretches (n=32).

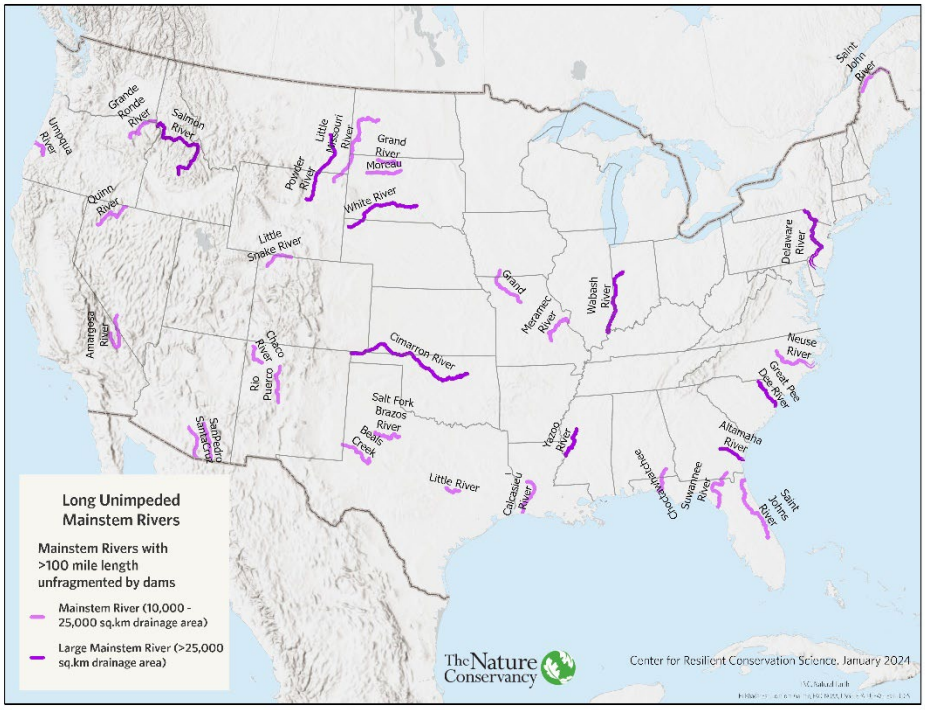

To limit our assessment to large rivers, we ran queries to identify unfragmented mainstem sections greater than 100 miles long that included some length of the very large river size class (> 10,000 km^2 drainage area). We identified 22 unimpeded inland mainstem rivers and of these, 90% had some overlap with the FRCN and 77% were completely within the FRCN (Table 4.3). This set included many well-known rivers such as the Salmon, Grande Ronde, Powder, Little Missouri, Moreau, White, Little Snake, Quinn, Amargosa, San Pedro, Santa Crux, Cimarron, Salt Fork Brazos, Beals Creek, Yazoo, Meramec, Grand, Wabash, and St. John. The few free-flowing rivers in the western U.S. that were not in the FRCN, such as the Chaco River in New Mexico, were ranked as vulnerable due to water availability issues, while the one eastern river, the Yazoo, was not in the FRCN because it had not been recognized for its biodiversity value in any of the assessments we compiled.

Wetlands, Floodplains, Lakes, and Ponds

To evaluate the representation of wetlands, we overlaid the 2019 NLCD wetlands (Dewitz & USGS 2019) and 100-yr. floodplain and riparian areas from Fathom 2.0 (Bates et al. 2021; First Street Foundation 2020) on the FRCN. Additionally, we overlaid TNC's Terrestrial Resilient and Connected Network (TRCN) dataset, which assessed millions of acres of wetlands for their terrestrial resilience factors (Anderson et al. 2023). Non-wetland floodplains are areas mapped as floodplain in the Fathom 2.0 dataset, but that do not maintain permanent water or wetlands. Many floodplains have both wet and dry regions.

Results indicate that 51% of all mapped wetlands and 35% of all non-wetland floodplains are in the FRCN. Together, the results show that 40% of the entire wetland and floodplain-riparian extent is in the FRCN. The number increases to 73% of all wetlands, 56% of all non-wetland floodplains, and

62% of the wetland and floodplain area when combined with the TRCN (Table 4.4). Visual comparison highlights how the TRCN captures isolated basin wetlands, prairie potholes, and large peatlands or swamps while the FRCN is focused on riverine and floodplain wetlands (Figure 4.6).

Table 4.4. Overlay of wetlands and floodplains on the freshwater and terrestrial RCNs. Floodplain refers to floodplain and riparian areas as mapped by the pluvial and fluvial portions of the Fathom 2.0 dataset.

Wetland and Floodplains	FRCN	Both RCNs	TRCN	SUM RCN	Not in RCN
Wetland: Basin	21%	28%	21%	71%	29%
Wetland: Floodplain/Fluvial	19%	34%	22%	75%	25%
TOTAL WETLAND	**20%**	**31%**	**22%**	73%	**27%**
Non-Wetland: Floodplain/Fluvial	18%	16%	21%	56%	44%
GRAND TOTAL	**19%**	**21%**	**22%**	62%	**38%**
Total Acres	67,362,831	76,593,669	77,214,801	136,834,999	358,006,301

Figure 4.6. Overlay of wetlands and floodplains on the freshwater and terrestrial RCNs.

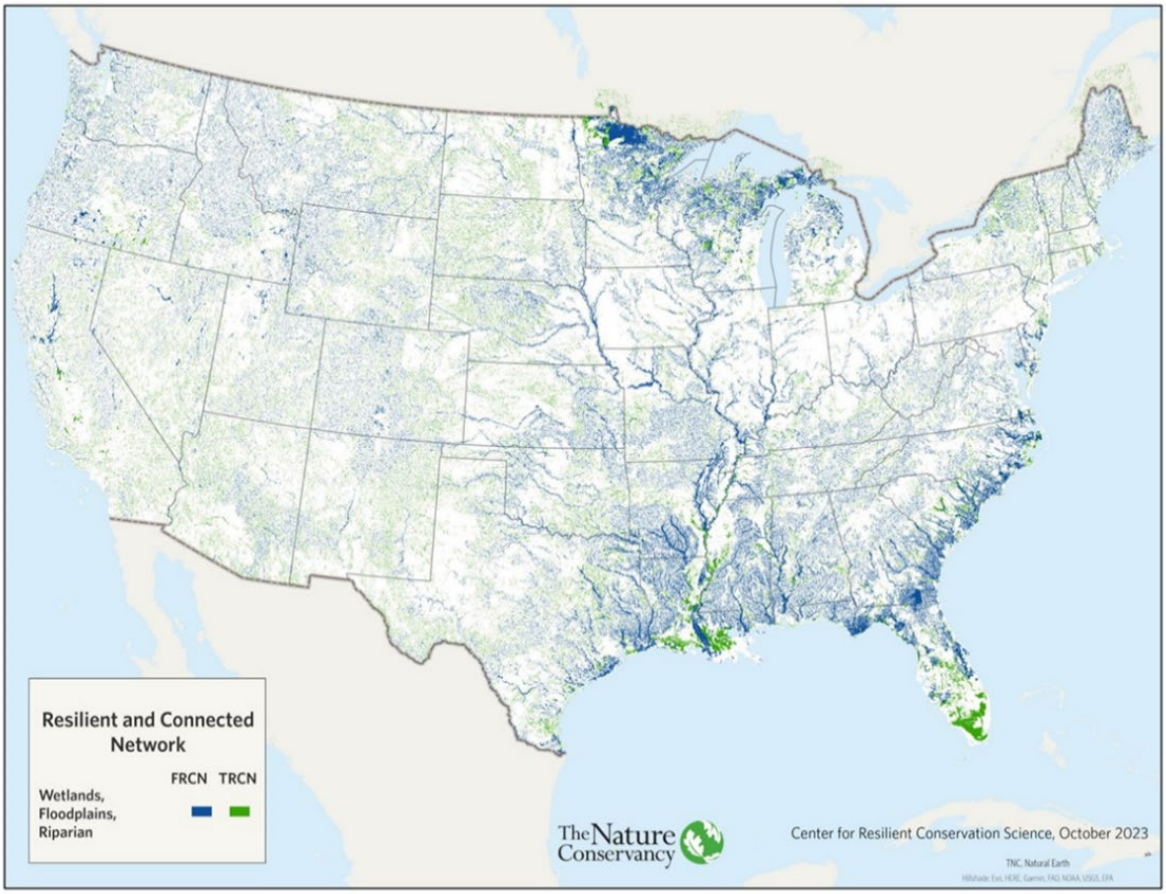

To assess the representation of lakes and ponds within the FRCN and TRCN, we overlaid NHDPlus lakes and ponds on the two networks. We separated the lakes and ponds into three groups:

1) Natural: all lakes in freshwater ecoregions where natural lakes are common
2) Mostly Natural: all lakes in freshwater ecoregions where natural lakes are uncommon but that were not tagged as a reservoir, and appeared from shape, size, and configuration to be natural. Some members of this group are likely to be small reservoirs.
3) Mostly Reservoirs: large waterbodies coded as a reservoir or likely to be a reservoir based on size, shape, configuration and/or name.

Results indicate that 47% of all lakes and ponds in CONUS are in the FRCN, including 50% of natural, 34% of mostly natural, and 55% of all reservoirs (Table 4.5). A high percentage of the reservoirs are in the FRCN as they are at the terminus of many of the larger networks. The TRCN does not add significantly more waterbodies except for the 16% in the mostly natural category, which includes isolated ponds such as those in North Dakota's prairie pothole region (Figure 4.7).

Table 4.5. Lakes and ponds in the freshwater and terrestrial RCNs.

Lakes and Ponds	FRCN	Both RCNs	TRCN	Total % (FRCN or TRCN)	None
Natural	44%	6%	6%	56%	44%
Mostly Natural	26%	8%	16%	50%	50%
Mostly Reservoirs	49%	6%	8%	63%	37%
Percent of Total	41%	6%	9%	56%	44%

Figure 4.7. Lakes, ponds, and reservoirs in the freshwater and terrestrial RCNs.

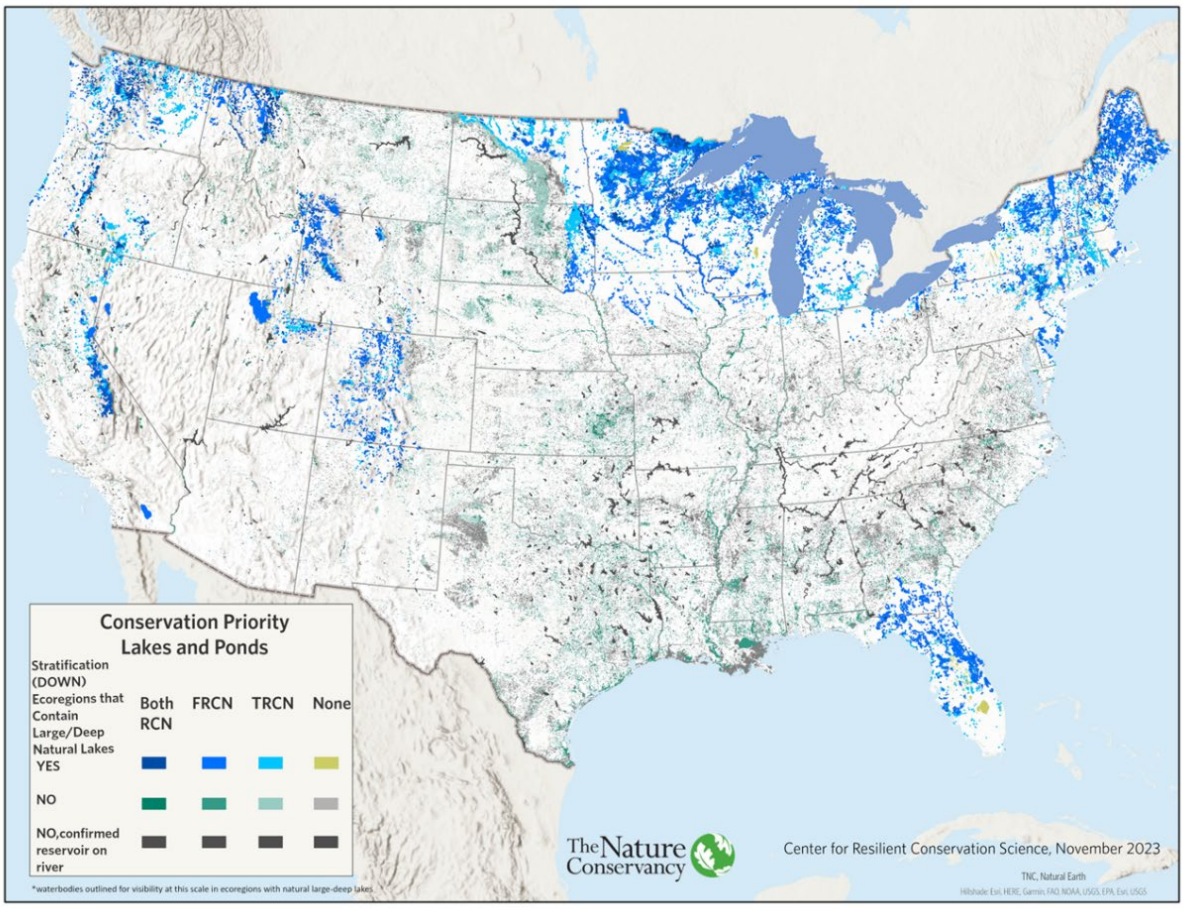

Groundwater Dependent Ecosystems

To assess the representation of groundwater features, we overlaid two separate datasets. The first was a seeps/spring dataset from the NHDPlus (USGS 2016) containing 149,263 individual points indicating a spring or seep. This dataset does not distinguish springs from seeps, nor does it provide a flow volume for each point, but it was the best available national compilation. This dataset was not independent of the resilience analysis because we used it in the groundwater section to confirm areas of suspected groundwater expression near the surface. The second dataset was a global map of groundwater dependent ecosystems (GDE) that was completed for the western U.S. (The Nature Conservancy & Desert Research Institute 2023).

Overlays indicated that the coverage of seeps and groundwater is fairly comprehensive and equally split between the FRCN and TRCN. Among the spring and seep points, 84% were covered by the two RCNs with the FRCN accounting for 44% and the TRCN overlapping considerably and adding another 40% (Figure 4.8, Table 4.6). Unexpectedly, a large portion of the points overlapped the FRCN category “verify water” and could perhaps be used as a form of verification themselves.

Figure 4.8. Seep and spring points overlaid on the freshwater and terrestrial RCNs.

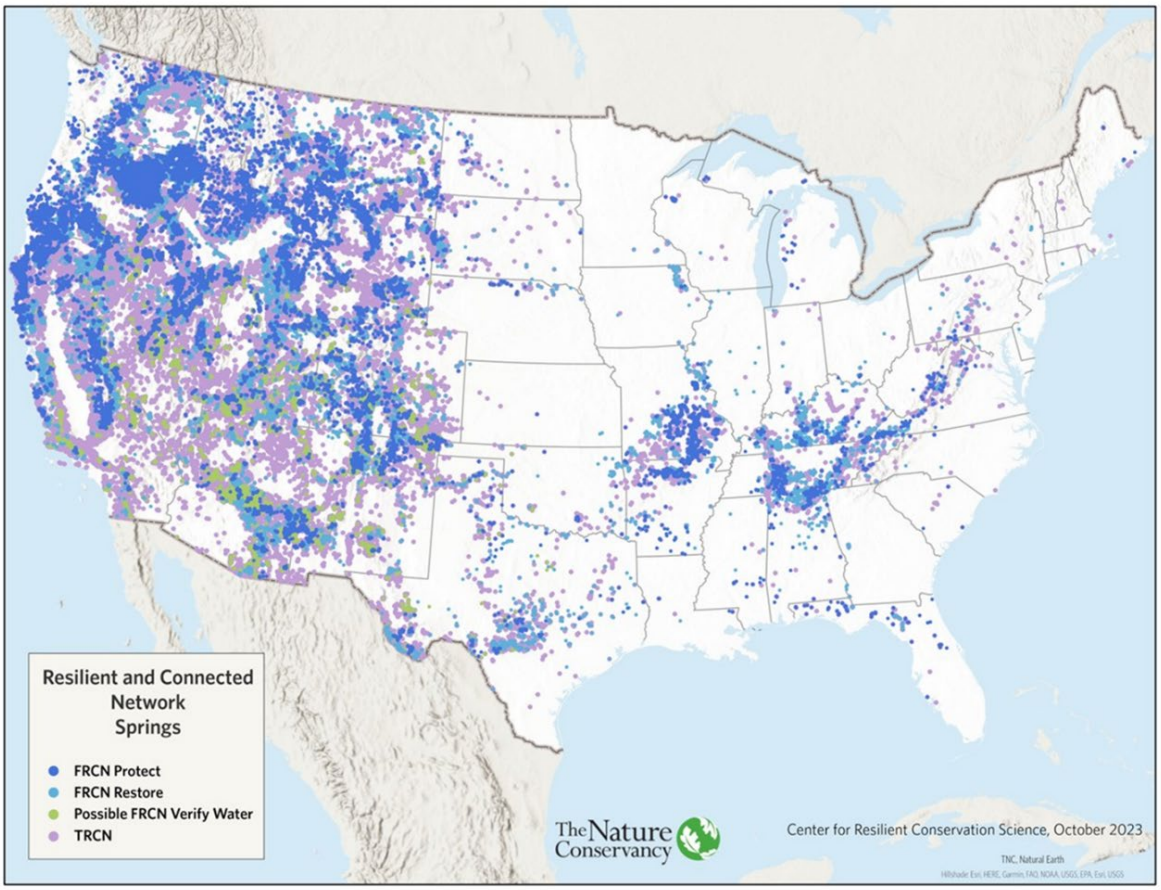

Table 4.6. Groundwater dependent ecosystems and seep/spring locations in the freshwater and terrestrial RCNs.

Groundwater Dependent Ecosystems	%FRCN	%Both	%TRCN	% Total RCN	None
Wetlands	21%	37%	25%	83%	17%
Floodplain/Riparian	14%	14%	25%	52%	48%
Total Wetland Setting	16%	20%	25%	60%	40%
Non-wetland Setting	15%	11%	22%	48%	52%
Total Any Setting	15%	13%	23%	51%	49%
Seeps and Springs	**%FRCN**	**%Both**	**%TRCN**	**% Total RCN**	**% Total RCN**
Mapped Points	12%	32%	40%	84%	16%

Results were similar for the GDEs with 83% of the wetland GDEs, 52% of the floodplain/riparian GDEs, and 48% of the non-wetland and non-floodplain/riparian GDEs being encompassed by one of the two RCNs. For GDE wetlands, 58% were in the FRCN, with the TRCN adding another 25% and overlapping on 37%. For floodplain/riparian GDE settings, the TRCN had the highest capture at 39%, with the FRCN having 28%, and 11% of that shared among both (for a total of 52%). The other non-wetland and non-floodplain GDEs are well represented with 48% in one of the RCNs; 22% in the

terrestrial, 15% in the freshwater, and 11% in both (Table 4.6). Overall, this suggests that GDE wetlands are well represented in both RCNs and that the terrestrial RCN captures the bulk of the non-wetland GDEs.

Ecoregions

To assess how well the FRCN is distributed across all types of freshwater ecosystems, we overlaid it on freshwater and terrestrial ecoregions and calculated the percentage of the river miles represented by the FRCN in each ecoregion. We calculated this measure for all flowlines and for perennial reaches only, as much of the western U.S. has ephemeral and intermittent river systems.

Results for the freshwater ecoregions (WWF & TNC 2019) indicated that of the 38 ecoregions, 58% (22) had over 30% of their stream miles represented. This increased to 97% (37) when we included only perennial streams (Figure 4.9). Representation was lowest in the deserts with the Mojave having less than 20% of its total stream and river miles, but over 50% of its perennial miles in the FRCN. As water availability and unaltered hydrology were key resilience characteristics, it is not surprising that our representation was more complete for perennial streams. Unexpectedly, the Chesapeake watershed also had less than 30% of its perennial stream miles in the FRCN. This appears to be due to multiple issues of condition and flow alteration around Baltimore and Washington D.C.

Figure 4.9. Distribution of the FRCN by freshwater ecoregion. The left map is for all streams and rivers, while the right is for perennial streams and rivers only.

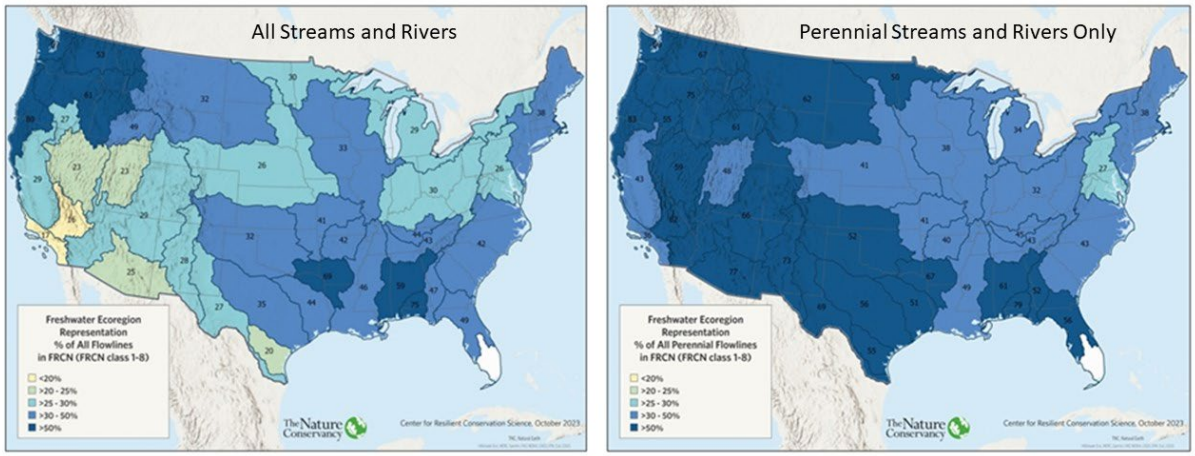

We found similar results for the 64 terrestrial ecoregions that occur mostly within the U.S (Figure 4.10). Sixty-three percent (40) had over 30% of all streamlines in the FRCN and 91% (58) had over 30% of their perennial stream and river miles in the FRCN. Again, the dry Sonoran, Mojave, and Great Basin ecoregions had representation under 20% for all reaches, but over 50% for perennial, reflecting the vulnerability of intermittent streams to climate change. Two eastern ecoregions also emerge as underrepresented: the North Central Tillplain and Lower New England. This pattern appears to reflect high levels of fragmentation from dams and highly altered hydrology in Lower New England and heavy agricultural impacts in the Tillplain.

Figure 4.10. Distribution of the FRCN by terrestrial ecoregion. The left figure is for streams and rivers, while the right figure is for perennial streams and rivers only.

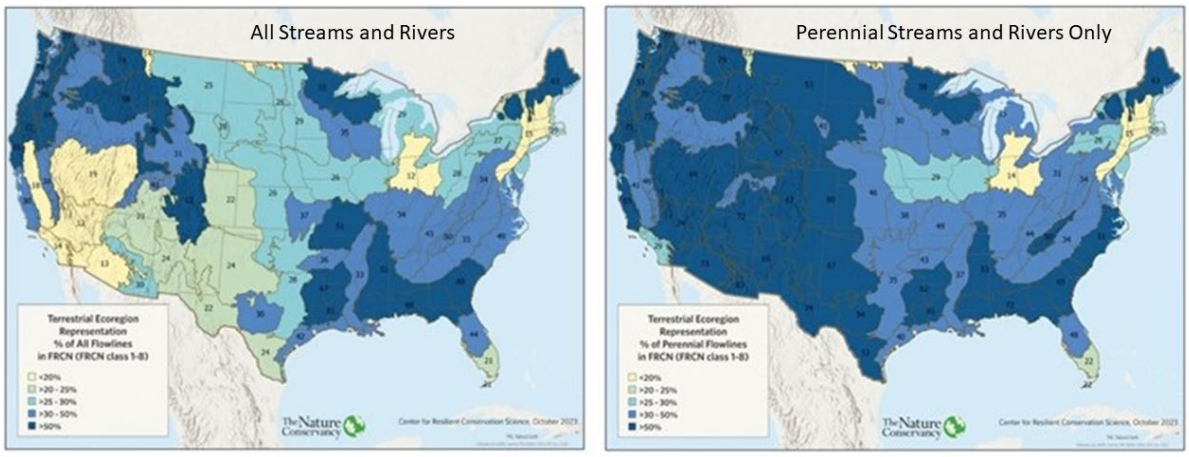

Aquatic Biodiversity

To estimate how well the FRCN represents the full spectrum of CONUS aquatic biodiversity, we overlaid several datasets depicting different aspects of freshwater biodiversity, beginning with the individual components of our recognized biodiversity value. Although the recognized biodiversity dataset was used to build the FRCN, we wanted to examine the correspondence of the FRCN with the specific biodiversity elements, but recognize they are not independent of the FRCN. Currently, 67% of the integrated recognized biodiversity data layer is in the FRCN (Figure 4.11), including:

- 91% of Atlantic Sturgeon
- 90% of Bull Trout area
- 89% of Pacific Northwest Critical Habitat
- 86% of Eastern Brook Trout Secure Stronghold areas
- 85% of Maine Atlantic Salmon areas
- 81% of Atlantic Alosine Priority areas
- 79% of U.S. Fish and Wildlife Service Freshwater Species Critical Habitat
- 77% of Northeast Lake Trout Resilient Lake area
- 72% of State Wildlife Action Plan (SWAP) Freshwater areas
- 72% of Chesapeake Bay Alosine area
- 69% of California FW blueprint
- 68% of TNC Freshwater portfolio area
- 67% of Range Size Rarity area (NatureServe MOBI)

The underrepresented areas largely correspond with regions of the country where freshwater systems are more vulnerable due to drought (Southwest), have impaired condition (upper Midwest agricultural region), or are highly fragmented by dams and barriers (Southern New England).

Figure 4.11. Correspondence of the FRCN with recognized aquatic biodiversity.

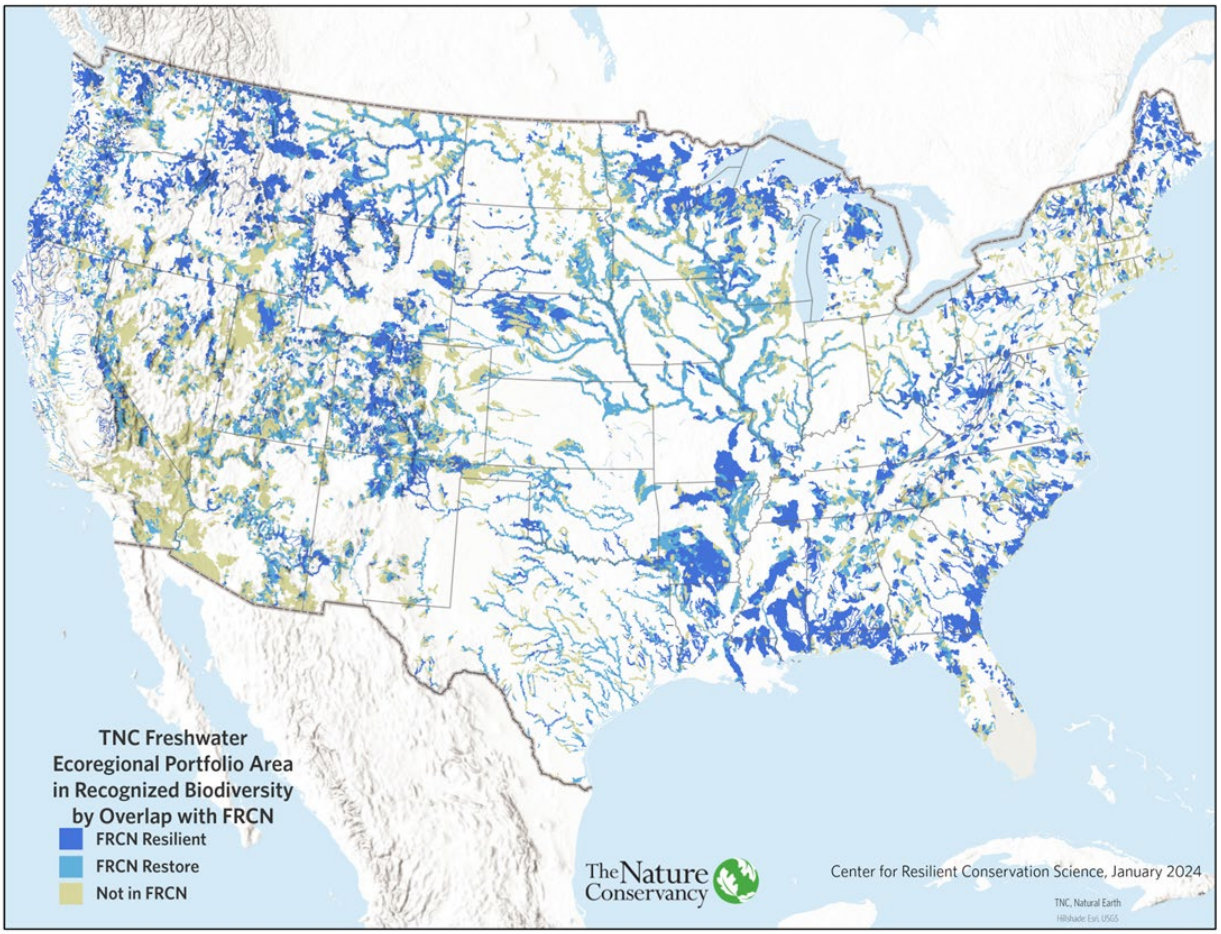

To investigate how well the FRCN captures rare native aquatic species, we calculated the total number of rare fish, mussel, and crayfish species for each HUC-8 watershed and compared that to the percent of the FRCN that covers the HUC-8 (Figure 4.12). The species distribution data was limited to globally rare native species (G1, G2, G3) of fish, mussels, and crayfish (NatureServe 2008 a,b,c).

We found that 99% of small watersheds containing a rare species overlapped with the FRCN and that in general, the greater the number of rare species, the higher the spatial overlap with the FRCN. Most HUC-8s with over ten rare species were completely within the FRCN while most HUCs with one to nine rare species were partially within the FRCN (Figure 4.12). However, we found a few HUCs with rare species that were not in the FRCN, and we are exploring the possibility of adding them as restoration sites.

Figure 4.12. Rare fish, mussels, and crayfish versus percent FRCN.

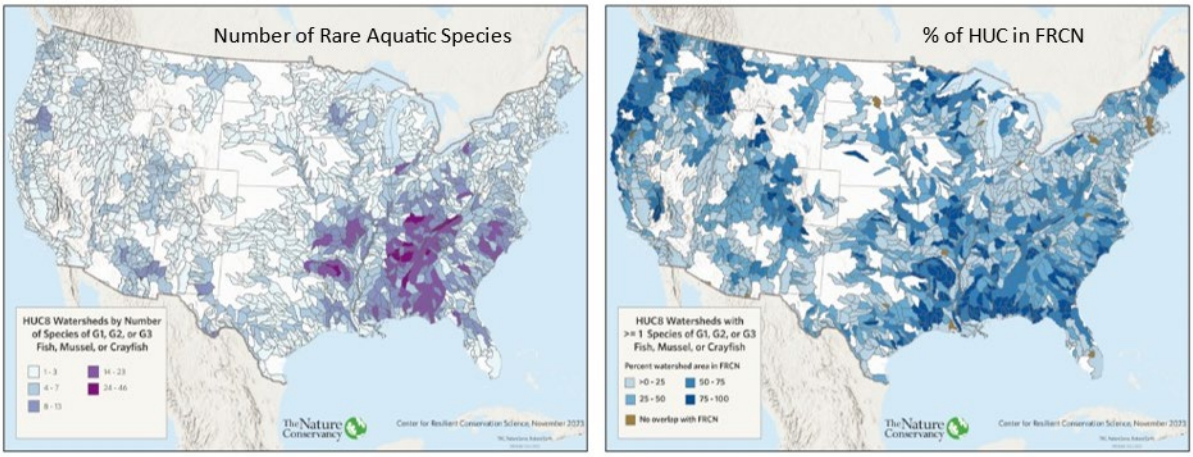

To measure how well the FRCN captures common and endemic species, we calculated the number of total fish species, strict endemics, and partial endemics for each freshwater ecoregion and compared that to the percentage of FRCN in the ecoregion. Results indicated that, in general, the FRCN captured a higher proportion of the ecoregion relative to the total number of fish species present (Figure 4.13, $R^2 = 0.067$). The three regions with the highest species richness and more than 20 endemics each – Lower Mississippi (256 species), Tennessee (242 species), and Mobile Bay (237 species) – all had 40-60% FRCN. In contrast, the three ecoregions with the lowest species richness and only five to seven endemics – Bonneville (21 species), Death Valley (15 species), and Sonora (12 species) all had 15-25% FRCN. However, there were notable outliers to this trend. The highest proportion of FRCN was found in the Washington, Oregon, and Northern California Coast ecoregions (78-88%). These ecoregions had high resilience but only moderate species richness and few endemics, although they are well known for their populations of anadromous species, including five species of Northwest salmon, steelhead, and bull trout. Notably, two ecoregions with high species richness, Teays-Old Ohio and Upper Mississippi, had relatively low representation by the FRCN, which appears to reflect the condition and flow challenges in these highly agricultural ecoregions.

Figure 4.13. Fish species richness and endemism versus percent FRCN by freshwater ecoregion. Note that only two ecoregions had partial endemics.

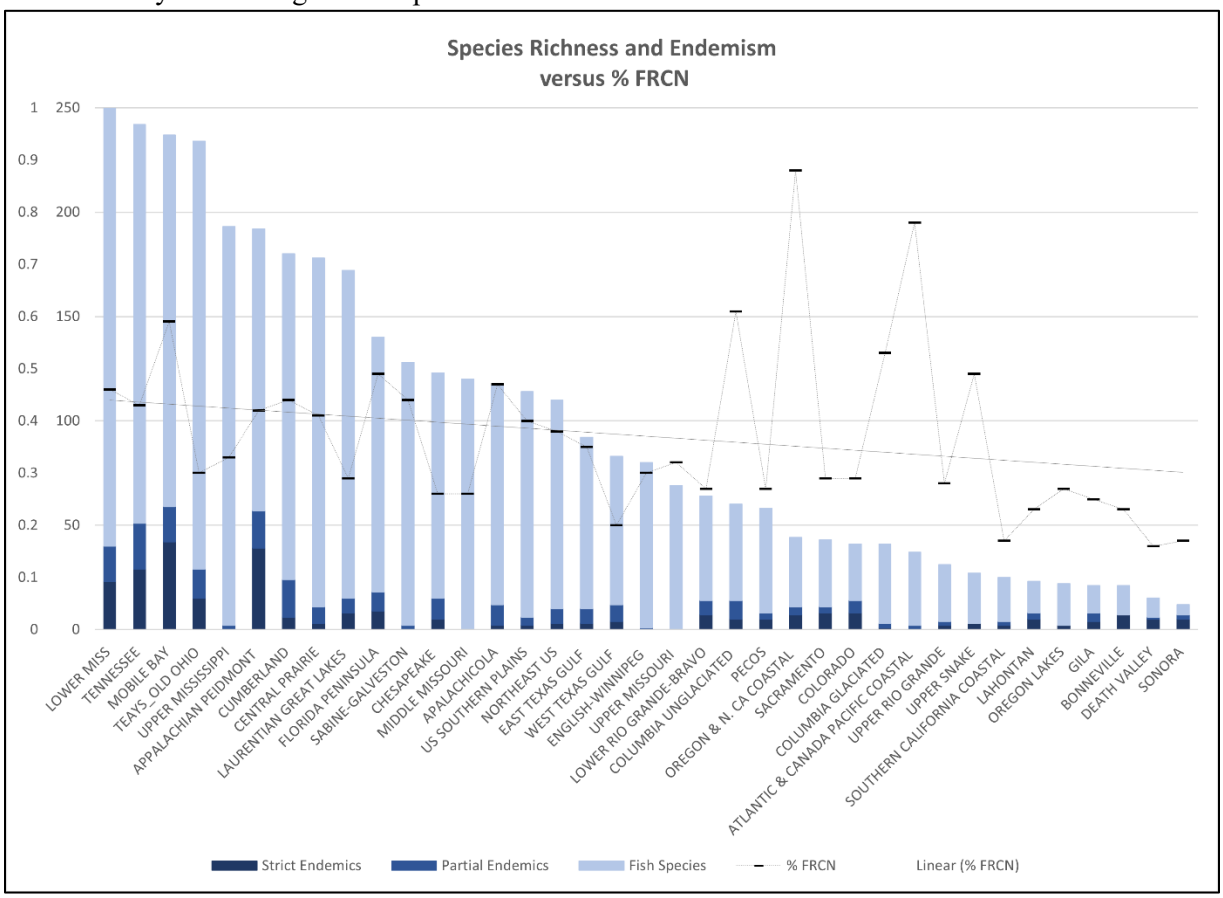

The Nature Conservancy Project Areas

In this section, we compared the networks identified by the FRCN with the places where TNC is already invested and working on freshwater strategies. As there is no spatial map of TNC project areas, we collected names of rivers in CONUS that TNC is currently working to protect and/or restore. We derived a draft list from reviewing all river records in TNC's Hub, an organization-wide project tracking database, then requested review from a representative of every state office in CONUS and received input from all but two states (MS, WV) and part of one (VA). We selected the rivers by name from the 20+ dendrite NHD. Based on information in the Hub and other knowledge of projects, we categorized each river as follows: R = restoration, P = protection, B = both. We added attribute fields to capture all the associated Hub records, and in many cases, single rivers are associated with more than one project or strategy record.

The precision of the spatial data varies state to state, with whole mainstems selected in some, and sections and/or tributaries in others. Additionally, we could not locate every stream name, 42 were not on the hydrography or in the NHDPlus GNIS field. We kept track of these issues and could supplement the line work with arcs from the high resolution NHD if desired. Finally, we dissolved the layer on the unique GNIS ID (not name because there are repeated river names) creating 576 records.

Results show that 94% of TNC projects overlapped with the FRCN. We grouped them into the following three categories based on their approximate boundaries (Figure 4.14).

• In	(50-100%)	56% of sites	68% of miles
• Partially In	(>0-50%)	23% of sites	26% of miles
• Out		21% of sites	6% of miles

Figure 4.14. The Nature Conservancy river projects by percent FRCN.

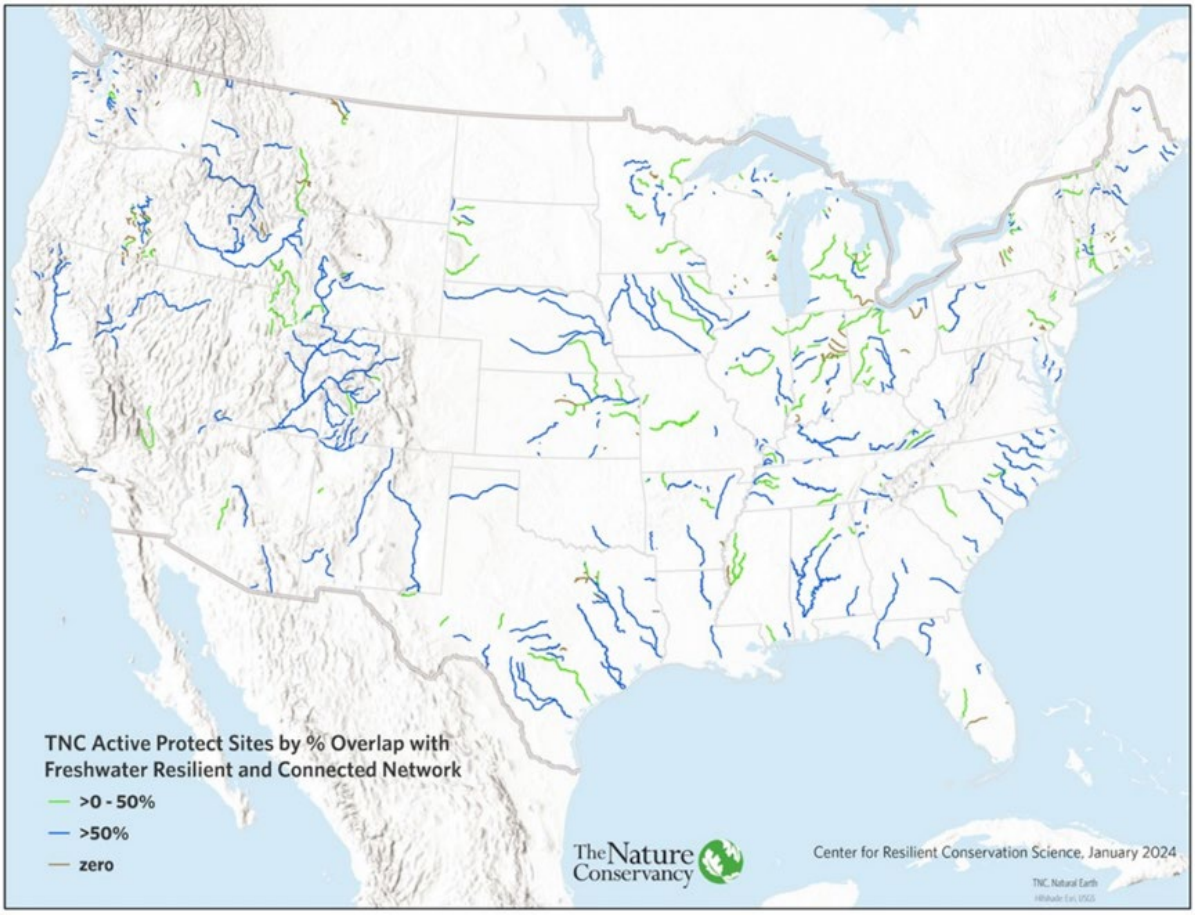

Summary of Representation in the FRCN

VERY GOOD (over 66% representation)

- **Stream Size Classes:** Representation in natural proportion with slight bias towards large rivers
- **Free-Flowing Rivers:** Over 80% of all large free-flowing rivers. Small coastal rivers are partially represented.
- **Recognized Biodiversity Value:** 67% of reaches recognized for their biodiversity value are in the FRCN. Sturgeon, Bull Trout, Salmon, and Eastern Brook trout have over 80%
- **Ecoregions:** 97% of freshwater ecoregions have over 30% of their perennial streams, and 58% of terrestrial ecoregions have over 30% of ALL streams including temporary and intermittent stream in the FRCN
- **TNC Project Areas:** By estimated river miles: 68% overlap strongly, 26% overlap partially, and 6% don't overlap the FRCN

GOOD (33%-66% representation)

- **Wetlands:** 51% of all wetlands. Additional isolated wetlands (22%) are in terrestrial RCN.
- **Groundwater Ecosystems:** 58% of all groundwater wetlands and 44% of all springs/seeps. Additional groundwater wetlands (25%) and springs and seeps (40%) in terrestrial RCN
- **Lakes and Ponds:** 50% of all natural lakes and 55% of reservoirs
- **Rare Species:** 99% of HUCs with rare species overlap with the FRCN. HUCS with over ten rare species have their majority in the FRCN.

CHAPTER

Discussion 5

Summary

The diverse freshwater biota of the U.S. evolved in free-flowing river networks now fragmented by thousands of dams that hinder the ability of freshwater species to move and adapt to a changing climate. Water withdrawal, ground water depletion, and water quality degradation have further altered the condition of the remaining habitat, such that fish, crayfish, and mussels are now the nation's most endangered species groups.

To help inform action to address the crises of freshwater biodiversity loss and climate change, we completed this three-year study involving over 60 freshwater conservationists to identify and map the characteristics that impart climate resilience to freshwater systems and assess the resilience of streams and rivers in CONUS. Physical factors included the size and diversity of each functionally connected network (FCN, stream network bounded on all sides by dams, mouth, or source), and condition indicators such as floodplain conversion, impervious surface, presence of mining, and elevated levels of nitrogen, phosphorus, and sediment. Water factors included access to surface water, degree of shallow groundwater depletion, and altered hydrology. We compiled or developed CONUS-wide maps for each factor at the HUC-12 scale, and then combined them into an integrated score using statistical transformations that equalized the mean and variance of each variable relative to one of three climatic regions: humid, arid-perennial, or arid-intermittent. A resilience score was calculated for each HUC-12 by combining the physical and water scores with ecologically appropriate weighting factors (i.e., increasing weight to water factors in the arid regions). Results identified 26% of CONUS as greater than "Average" (> 0.5 SD) for resilience.

A second goal of this study was to identify a set of resilient freshwater ecosystems that, if conserved, could potentially sustain the spectrum of aquatic biodiversity into the future. We identified this Freshwater Resilient and Connected Network (FRCN) by combining the continuous map of resilience with a map of freshwater sites recognized for their biodiversity per a compilation of 91 state, ecoregional, regional, or species-specific sources. Using a definition of "restorable" for HUC-12s with "Average" resilience and a single factor less than "Average," we distinguished a network of freshwater ecosystems encompassing 35% of CONUS stream miles that were either biodiverse and resilient (18%), biodiverse and restorable (16%), or highly resilient (1%).

While this is a riverine focused analysis, the small watersheds identified include a wide array of essential freshwater features. Resilient networks comprise connected rivers with a diversity of temperature classes and macrohabitats, unfragmented headwaters, natural floodplains and/or riparian zones, surface and groundwater features as measured by wetlands, lakes, springs, and seeps, and connections to the ocean or Great Lakes. Accordingly, the FRCN does an excellent job (>66%) of representing stream size classes, unimpeded river stretches, recognized biodiversity areas, freshwater ecoregions, and TNC project areas. The network does a good or adequate job (>33%) of capturing wetlands, groundwater dependent ecosystems, lakes and ponds, and rare species areas. The latter features are also represented in the terrestrial RCN (Anderson et al. 2023), and we are exploring how to integrate the two networks. For example, the two RCNs collectively contain 84% of all springs and

seeps, 83% of all groundwater dependent wetlands, and 73% of all wetlands. Conservation (both restoration and protection) of these river networks depends on and will benefit associated freshwater ecosystems, but that will not replace conservation action to benefit other types of freshwater habitats. An overlay of current and planned TNC freshwater projects suggests that all but 6% of the estimated stream miles are mostly or partially in the FRCN.

Applying the Results

The intention of this analysis was to provide conservationists in the U.S. a means to evaluate the relative resilience of freshwater river networks for biodiversity in the face of a changing climate so action can be taken to maintain and improve resilience. The FRCN was intended to provide an initial filter to focus conservation efforts on the resilient and near-resilient rivers that have freshwater biodiversity significance and represent the diversity of river systems and aquatic species across CONUS. We consider the FRCN to be an asset map of what we seek to conserve, not an action map to limit conservation and restoration work to the exact river catchments depicted on the map. Conservation of the network will involve multiple strategies including protection of resilient systems (19%), restoration of flow and/or condition (12%), and reconnecting small networks through barrier remediation (3%), although these are initial filters that will require further study. The conservation actions that will make a difference to resilience are not prescriptive and we recommend a full assessment be made of ecological integrity and threats as outlined in Higgins et al. (2021).

To make the analysis and findings available to a broad range of audiences and support their interpretation and application by practitioners, we designed and launched the Resilient River Explorer web tool (RRE, https://maps.tnc.org/resilientrivers). Along the top banner of the tool are links to several resources including a brief user guide, feedback forms, data downloads, and map service links for GIS users. The tool is organized into five thematic sections, each corresponding to a different way to use the results and accessible via tabs at the top of the page.

- The **Elements** tab is the starting point for new users of the tool. It provides an overview of the core concepts and datasets used in the analysis and sets the stage for users to dive deeper into the data in the subsequent tabs.

- The **Explore** tab is designed to help users understand how the various components of resilience come together into the final resilience score for any given location. This tab is also the most open-ended section of the tool, with reference and source-data layers available to view and provide context for the resilience score.

- The **Assess A River** tab summarizes the resilience results for a named river based on the HUC-12 scores. In addition to summarizing the results for a river, the "opportunities" subsection of this tab highlights spatially explicit conservation actions that have the potential to maintain or restore the resilience of the selected river.

- The **Terrestrial** tab incorporates TNC's terrestrial resilience data (Anderson et al. 2023) into the map and summarizes it for each of the freshwater resilience units (HUC-12s, FCNs, and their floodplains). While short of a full integration of the terrestrial and freshwater resilience data, these summaries can help users evaluate potential synergies between freshwater and terrestrial resilience in any given location.

- The **Scenarios** tab allows users to dynamically assess potential improvements to resilience that could be realized by removing one or more dams. Selecting a dam for removal in this tab triggers the recalculation of the connectivity and resilience scores to show the approximate impact of dam removal(s) on overall resilience. Additional scenario testing capabilities may be added in the future to model and evaluate other conservation actions.

Data Limitations and Future Analysis

This analysis used current, comprehensive river and land data for CONUS that supported a robust analysis, and the results have been reviewed by our steering committee. That said, the scale of the analysis created limitations in what data could be used because we needed consistency across the study area to avoid spatial bias from data discrepancies. For example, given the lack of consistent inventories of small dams on streams and headwaters, we know there are most certainly additional dams beyond what we included in this analysis. The resolution of the other underlying datasets also varies. For example, we used the 30-m NLCD for landcover and 12.5-km grid cells for the GRACE shallow groundwater data. Despite the variation in the scales of the input data and metrics, we sought to use the appropriate summary scale for each metric and to combine variables in a logical multi-scale framework. The resilience value of each analysis unit thus integrated local condition information with the size of the larger connected network within which a unit occurred.

Our measure of freshwater resilience is relative. We defined resilience as the ability of freshwater ecosystems to adapt, adjust, and maintain biological diversity in a changing climate. Our hypothesis for mapping freshwater resilience was that the physical setting and its condition, together with water availability and its alteration, drive resilience in freshwater systems by providing habitat options and the integrity to maintain ecological function. Supported by evidence, our assumption was that networks with more of these characteristics will be relatively more resilient than ecologically similar networks with less of these characteristics. However, there is not a specific threshold that guarantees a river is resilient. Thus, a river that is in our top class of resilience may still have restoration needs.

The resilience analysis and the FRCN are intended to be used with local information or other spatial and descriptive data to inform conservation action. The type of additional information depends on the questions one wants to answer. As an example, TNC's Appalachian freshwater team, working with representatives from federal agencies, wanted to query a suite of ecological and socioeconomic data to identify watersheds in the Appalachians where restoration of freshwater connectivity (dam removal, culvert replacements, etc.) could benefit both nature and people. The resulting Reconnecting Appalachian Rivers tool (RAR, https://www.maps.tnc.org/rar/#/prioritize) incorporates the freshwater resilience results with data on biodiversity, barriers, and disadvantaged communities at risk from future flooding.

A challenge in this study was to create fair comparisons across rivers in arid and humid zones as they differ in dominant processes and face different challenges. We considered climatic zones throughout the analysis, both in how individual component scores were calculated and in how we weighted model components to calculate resilience scores. In arid regions, we created a "verify water" category in the FRCN to identify HUCs that may be resilient, but the presence of sufficient water could not be verified from national datasets. To address this uncertainty, practitioners could access local and regional

hydrologic data, ground-check the identified networks, and consult climate models. A next step for this study would be to combine the resilience analysis with climate trends and projections.

A Final Note

The purpose of this report was to provide transparency into our methods such that natural resource managers, conservation planners, and practitioners can confidently integrate the results we have offered with other important values, such as human climate resilience, to achieve lasting conservation impact. The results and much of the underlying data are accessible and available for download through the Resilient River Explorer. We acknowledge that equity for people is not represented in this analysis as we were focused on the other species with which we share the planet, and who also need abundant clean freshwater. We recognize, however, that maps give values to lands and waters and are not neutral about human equity – both in what is interpreted to be important for conservation action, the sourcing of the data used, and who participated in the analysis. Reference layers representing human dimensions could be added in the future as we have explored with the Reconnecting Appalachian Rivers tool described above. Freshwater biodiversity resilience to climate change is essential to people, and while not the only measure of meaningful conservation, it is an essential ingredient to our conservation success.

References

Abramovitz, J.N, A. Ancharya. 1996. Imperiled Waters, Impoverished Future: The Decline of Freshwater Ecosystems. Worldwatch Paper, 128. J.A. Peterson, editor. Worldwatch Institute. 80 p.

Abood, S.A., Spencer, L., Wieczorek, M. 2022. U.S. Forest Service national riparian areas base map for the conterminous United States in 2019. Fort Collins, CO: Forest Service Research Data Archive. https://doi.org/10.2737/RDS-2019-0030

Alexander, L.C., Fritz, K.M., Schofield, K.A., Autrey, B.C., DeMeester, J.E., Golden, H.E., Goodrich, D.C., Kepner, W.G., Kiperwas, H.R., Lane, C.R., LeDuc, S.D., Leibowitz, S.G., McManus, M.G., Pollard, A.I., Ridley, C.E., Vanderhoof, M.K., and Wigington, P.J. 2018. Featured Collection Introduction: Connectivity of Streams and Wetlands to Downstream Waters. *Journal of the American Water Resources Association*, 54(2), 287–297. https://doi.org/10.1111/1752-1688.12630.

Allan, J. D. 1995. Stream Ecology: Structure and function of running waters. Kluwer Academic Publishers. Dordrecht, The Netherlands.

Alofs, K.M., Jackson, D.A., & Lester, N.P. 2014. Ontario freshwater fishes demonstrate differing range-boundary shifts in a warming climate. *Diversity and Distributions*, 20, 123–136. https://doi.org/10.1111/ddi.12130

American Rivers. 2022. Dam Removal List, Raw Dataset— ARDamRemovalList_figshare_Feb2022. Figshare. Available: https://doi.org/10.6084/m9.figshare.5234068. Retrieved: 4/9/2022.

Anderson, M.G., Clark, M., & Sheldon, A.O. 2014. Estimating Climate Resilience for Conservation across Geophysical Settings. *Conservation Biology*, 28(4), 959–970. https://doi.org/10.1111/cobi.12272

Anderson, M.G., M. Clark, A. Olivero, and J. Prince. 2019. Resilient Sites and Connected Landscapes for Terrestrial Conservation in the Rocky Mountain and Southwest Desert Region. The Nature Conservancy, Eastern Conservation Science.

Anderson M.G, Clark M., Olivero A.P., Barnett A.R., Hall K.R., Cornett M.W., Ahlering M., Schindel M., Unnasch B., Schloss C., Cameron D.R. 2023. A resilient and connected network of sites to sustain biodiversity under a changing climate. *Proc Natl Acad Sci,* 120(7):e2204434119. doi: 10.1073/pnas.2204434119.

Ator, S.W. 2020. SPARROW model inputs and simulated streamflow, nutrient and suspended-sediment loads in streams of the Northeastern United States, 2012 Base Year: U.S. Geological Survey data release, https://doi.org/10.5066/P9NKNVQO.

Barnhart, T.B., Molotch, N.P., Livneh, B., Harpold, A.A., Knowles, J.F. and Schneider, D. 2016. Snowmelt rate dictates streamflow. *Geophysical Research Letters*, *43*(15), pp.8006-8016.

Bates, P. D., Quinn, N., Sampson, C., Smith, A., Wing, O., Sosa, J., et al. 2021. Combined modeling of US fluvial, pluvial, and coastal flood hazard under current and future climates. *Water Resources Research*, 57, e2020WR028673. https://doi.org/10.1029/2020WR028673

Beier, P., & Brost, B. 2010. Use of land facets to plan for climate change: conserving the arenas, not the actors. *Conservation Biology*, 24(3), 701–710. https://doi.org/10.1111/j.1523-1739.2009.01422.x

Bowler, D. E., Mant, R., Orr, H., Hannah, D. M., and Pullin, A. S. 2012. What are the effects of wooded riparian zones on stream temperature*? Environmental Evidence*, 1(1), 1–9. https://doi.org/10.1186/2047-2382-1-3.

Burkhead, N. M. 2012. Extinction Rates in North American Freshwater Fishes, 1900 – 2010. BioScience, 62(9), 798–808. https://doi.org/10.1525/bio.2012.62.9.5

California Department of Fish and Wildlife. 2019. Passage Assessment Database, September 2019 version. (Available from: https://nrm.dfg.ca.gov/PAD/, Accessed 01 March 2020).

Canning, A.D. and Death, R.G. 2020. The influence of nutrient enrichment on riverine food web function and stability. *Ecol Evol.* 11(2):942-954. doi: 10.1002/ece3.7107. PMID: 33520177; PMCID: PMC7820149.

Center for Watershed Protection (CWP). 2003. Impacts of Impervious Cover on Aquatic Systems. Watershed Protection Research monograph No. 1.

Chithra, S.V., Harindranathan Nair, M.V., Amarnath, A., and Anjana, N.S. 2015. Impacts of Impervious Surfaces on the Environment. *International Journal of Engineering Science Invention*, 4(5), 27–31.

Comer, Patrick. 2022. Crosswalk of Landfire biophysical systems to Upper Montane, Subalpine, and Alpine Ecosystems. Personal Communication from Senior Ecologist, NatureServe.

Comte, L., and Grenouillet, G. 2013. Do stream fish track climate change? Assessing distribution shifts in recent decades. *Ecography*, 36(11), 1236–1246. https://doi.org/10.1111/j.1600-0587.2013.00282.x

Comte, L., Murienne, J., and Grenouillet, G. 2014. Species traits and phylogenetic conservatism of climate-induced range shifts in stream fishes. *Nature Communications*, 5, 5053. https://doi.org/10.1038/ncomms6053

Cooper, A.R., Infante, D.M., Daniel, W.M., Wehrly, K.E., Wang, L., and Brenden, T.O. 2017. Assessment of dam effects on streams and fish assemblages of the conterminous USA. *Science of the Total Environment*, 586, 879–889. https://doi.org/10.1016/j.scitotenv.2017.02.067

de Mello K., Valente R.A, Randhir T.O., Alves dos Santos A.C., and Vettorazzi C.A. 2018. Effects of land use and land cover on water quality of low-order streams in southeastern Brazil: watershed versus riparian zone. *Catena* 167: 130-138. https://doi.org/10.1016/j.catena.2018.04.027.

Dewitz, J., and U.S. Geological Survey, 2021, National Land Cover Database (NLCD) 2019 Products (ver. 2.0, June 2021): U.S. Geological Survey data release, https://doi.org/10.5066/P9KZCM54.

Doctor, D.H., Jones, J., Wood, N, Falgout, J., and Rapstine, N. 2020. Progress toward a Preliminary Karst Depression Density Map for the Conterminous United States. NCKRI Symposium 8: Proceedings of the 16th Multidisciplinary Conference on Sinkholes and the Engineering and Environmental Impacts of Karst. 315-326

Dodds, W., Gido, K., Whiles, M.R., Fritz, K.M., and Matthews, W.J. 2004. Life on the edge: the ecology of Great Plains prairie streams. *BioScience,* 54(3), 205–216. https://academic.oup.com/bioscience/article/54/3/205/22306

Eby, L.A., Helmy, O., Holsinger, L.M., & Young, M.K. 2014. Evidence of Climate-Induced Range Contractions in Bull Trout Salvelinus confluentus in a Rocky Mountain. *PLOSone*, 9(6), 1–8. https://doi.org/10.1371/journal.pone.0098812

Esselman, P., Infante, D., Wang, L., Cooper, A., Wieferich, D., Tsang, Y., Thornbrugh, D., and Taylor, W. 2013. Regional fish community indicators of landscape disturbance to catchments of the conterminous United States. *Ecological Indicators*. 26. 163–173. 10.1016/j.ecolind.2012.10.028.

Falcone, J.A., Murphy, J.C., and Sprague, L.A. 2018. Regional patterns of anthropogenic influences on streams and rivers in the conterminous United States, from the early 1970s to 2012. *Journal of Land Use Science*. 13:6, 585-614, doi: 10.1080/1747423X.2019.1590473

Federal Interagency Stream Restoration Working Group (FISRWG). 1998. Stream Corridor Restoration: Principles, Processes, and Practices. GPO Item No. 0120-A; SuDocs No. A 57.6/2:EN3/PT.653. ISBN-0-934213-59-3.

Fesenmyer, K.A., A.L. Haak, S.M. Rummel, M. Mayfield, S.L. McFall, and J.E. Williams. 2017. Eastern Brook Trout Conservation Portfolio, Range-wide Habitat Integrity and Future Security Assessment, and Focal Area Risk and Opportunity Analysis. Final report to National Fish and Wildlife Foundation. Trout Unlimited, Arlington, Virginia

First Street Foundation. 2020. First Street Foundation Flood Model Technical Methodology Document. Zenoda. https://zenodo.org/record/4740762CDFW.

Florida Department of Environmental Protection (FDEP), Division of Water Resource Management. 2021. Mandatory Phosphate Reclamation Units 2019 vector digital data. https://publicfiles.dep.state.fl.us/OTIS/GIS/data/MMP_MANPHO_REC_UNITS_2019.zip

Frei, R.J., Lawson, G.M., Norris, A.J., Cano, G., Vargas, M. C., Kujanpää, E., Hopkins, A., Brown, B., Sabo, R., Brahney, J., & Abbott, B.W. 2021. Limited progress in nutrient pollution in the U. S. caused by spatially persistent nutrient sources. *PLoS ONE*, 16(11 November), 1–26. https://doi.org/10.1371/journal.pone.0258952.

Getirana, A., Rodell, M., Kumar, S., Beaudoing, H.K., Arsenault, K., Zaitchik, B., Save, H., & Bettadpur, S. 2020. GRACE improves seasonal groundwater forecast initialization over the United States. *Journal of Hydrometeorology*, 21(1), 59–71. https://doi.org/10.1175/JHM-D-19-0096.1

Gido, K.B., Dodds, W.K., and Eberle, M.E. 2010. Retrospective analysis of fish community change during a half-century of landuse and streamflow changes. *Journal of the North American Benthological Society*, 29(3), 970–987. https://doi.org/10.1899/09-116.1

Gressler, B.P., Haro, A.J., and Young, J.A. 2022. Fishway Structure Data in the Eastern United States: U.S. Geological Survey data release, https://doi.org/10.5066/P9IB1GWS.

Hamilton, H., Smyth, R.L., Young, B.E., Howard, T.G., Tracey, C., Breyer, S., Cameron, D.R, Chazal, A., Conley, A.K., Frye, C., and C. Schloss. 2022. Increasing taxonomic diversity and spatial resolution clarifies opportunities for protecting US imperiled species. *Ecological Applications* 32 e2534.

Hare, D. K., Helton, A. M., Johnson, Z. C., Lane, J. W., & Briggs, M. A. 2021. Continental-scale analysis of shallow and deep groundwater contributions to streams. *Nature Communications*, 12(1), 1–10. https://doi.org/10.1038/s41467-021-21651-0

Heiner, M., Higgins, J., Li, X., & Baker, B. 2011. Identifying freshwater conservation priorities in the Upper Yangtze River Basin. *Freshwater Biology*, 56(1), 89–105. https://doi.org/10.1111/j.1365-2427.2010.02466.x

Higgins, J.V., Bryer, M.T., Khoury, M.L. and Fitzhugh, T.W. 2005. A Freshwater Classification Approach for Biodiversity Conservation Planning. *Conservation Biology*, 19, 432-445. https://doi.org/10.1111/j.1523-1739.2005.00504.x

Higgins, J., Zablocki, J., Newsock, A., Krolopp, A., Tabas, P., & Salama, M. (2021). Durable freshwater protection: A framework for establishing and maintaining long-term protection for freshwater ecosystems and the values they sustain. *Sustainability (Switzerland)*, *13*(4), 1–17. https://doi.org/10.3390/su13041950

Hill, R.A., Weber, M.H., Leibowitz, S.G., Olsen, A.R. & Thornbrugh, D.J. 2016. The Stream-Catchment (StreamCat) Dataset: A database of watershed metrics for the conterminous United States. *J Am Water Resour Assoc* 52, 120–128.

Hill, R.A., Hawkins, C.P., & Carlisle, D.M. 2013. Predicting thermal reference conditions for USA streams and rivers. *Freshwater Science*, *32*(1), 39-55. https://www.journals.uchicago.edu/doi/full/10.1899/12-009.1

Hill, R.A., Hawkins, C.P., and Jin, J. 2014. Predicting thermal vulnerability of stream and river ecosystems to climate change. *Climatic Change* 125(3): 399-412

Hollister, J.W., Milstead W.B., Urrutia M.A. 2011. Predicting Maximum Lake Depth from Surrounding Topography. *PLoS ONE* 6(9): e25764. doi:10.1371/journal.pone.0025764

Horton, J.D. 2017. The state geologic map compilation (SGMC) geodatabase of the conterminous United States. https://doi.org/10.3133/ds1052 http://pubs.usgs.gov/ds/425</onlink> https://www.safewater.org/fact-sheets-1/2017/1/23/miningandwaterpollution. Accessed October 5, 2023.

Houborg, R., Rodell, M., Li, B., Reichle, R., & Zaitchik, B. F. 2012. Drought indicators based on model-assimilated Gravity Recovery and Climate Experiment (GRACE) terrestrial water storage observations. *Water Resources Research*, 48(7). https://doi.org/10.1029/2011WR01129

Howard, J.K., Fesenmyer, K.A., Grantham, T.E., Viers, J.H., Ode, P.R., Moyle, P.B., Kupferburg, S. J., Furnish, J.L., Rehn, A., Slusark, J., Mazor, R.D., Santos, N.R., Peek, R.A., & Wright, A.N. 2018. A freshwater conservation blueprint for California: Prioritizing watersheds for freshwater biodiversity. *Freshwater Science*, 37(2), 417–431. https://doi.org/10.1086/697996

IUCN. 2023a. Freshwater fish highlight escalating climate impacts on species - IUCN Red List. https://www.iucn.org/press-release/202312/freshwater-fish-highlight-escalating-climate-impacts-species-iucn-red-list. Accessed on February 20, 2014.

IUCN. 2023b. The IUCN Red List of Threatened Species. Version 2023-1. https://www.iucnredlist.org. Accessed on February 16, 2024.

Isaak, D., M. Young, D. Nagel, D. Horan, M. Groce, and S. Parkes. 2017. Climate Shield bull trout and cutthroat trout population occurrence scenarios for the western U.S. Rocky Mountain Research Station, U.S. Forest Service Data Archive, Fort Collins, CO.

Isaak, D.J., Young, M.K., Horan, D.L., Nagel, D., Schwartz, M.K., & McKelvey, K.S. 2022. Do metapopulations and management matter for relict headwater bull trout populations in a warming climate? *Ecological Applications*, 32(5), 1–26. https://doi.org/10.1002/eap.2594

Johnson, T.B., and D.O. Evans. 1990. Size-dependent winter mortality of young-of-the-year white perch: climate warming and invasion of the Laurentian Great Lakes. *Transactions of the American Fisheries Society*, 119(2):301–313

Jones Jr, C.E., Leibowitz, S.G., Sawicz, K.A., Comeleo, R.L., Stratton, L. E., Morefield, P.E., & Weaver, C.P. 2021. Using hydrologic landscape classification and climatic time series to assess hydrologic vulnerability of the western US to climate. *Hydrology and earth system sciences*, *25*(6), 3179-3206.

Juracek, K. E. 2015. The aging of America's reservoirs: in-reservoir and downstream physical changes and habitat implications. *Journal of the American Water Resources Association*, 51(1), 168–184. https://doi.org/10.1111/jawr.12238

Karp, M.A., Peterson, J.O., Lynch, P.D., Griffis, R.B., Adams, C.F., Arnold, W.S., Barnett, L.A. K., Dicosimo, J., Fenske, K.H., Gaichas, S.K., Hollowed, A., Holsman, K., Karnauskas, M., Kobayashi, D., Leising, A., Manderson, J.P., Mcclure, M., Morrison, W.E., Schnettler, E., Link, J.S. 2019. Food for thought: accounting for shifting distributions and changing productivity in the development of scientific advice for fishery management. *ICES Journal of Marine Science*, 76(March), 1305–1315. https://doi.org/10.1093/icesjms/fsz048

Kaufmann, P.R., Hughes, R.M., Paulsen, S.G., Peck, D.V., Seeliger, C.W., Weber, M.H., & Mitchell, R.M. 2022a. Physical habitat in conterminous US streams and rivers, Part 1: Geoclimatic controls and anthropogenic alteration. *Ecological Indicators*, 141(January), 109046. https://doi.org/10.1016/j.ecolind.2022.109046

King, R.S. and M.W. Baker. 2010. Considerations for analyzing ecological community thresholds in response to anthropogenic environmental gradients. *Journal of the North American Benthological Society*. 29(4)**:** 998-1008.

LANDFIRE, Biophysical Setting Layer (LC16_BpS_200). LANDFIRE 2016 REMAP LF 2.0.0 (U.S. Department of the Interior, Geological Survey, and U.S. Department of Agriculture, Washington, DC, 2016). https://www.landfire.gov/viewer/. Accessed 11 May 2022.

LANDFIRE. 2020. Existing Vegetation Type Layer (EVT), LANDFIRE 2.2.0, U.S. Department of the Interior, Geological Survey, and U.S. Department of Agriculture. Accessed at http://www.landfire/viewer.

Lyons, J., Zorn, T., Stewart, J., Seelbach, P., Wehrly, K., and Wang, L. 2009. Defining and Characterizing coolwater streams and their fish assemblages in Michigan and Wisconsin, USA. *North American Journal of Fisheries Management*, 29(4), 1130–1151. https://doi.org/10.1577/M08-118.1

Lynch, A. J., Cooke, S. J., Arthington, A. H., Baigun, C., Bossenbroek, L., Dickens, C., Harrison, I., Kimirei, I., Langhans, S. D., Murchie, K. J., Olden, J. D., Ormerod, S. J., Owuor, M., Raghavan, R., Samways, M. J., Schinegger, R., Sharma, S., Tachamo-Shah, R. D., Tickner, D., … Jähnig, S. C. 2023. People need freshwater biodiversity. Wiley Interdisciplinary Reviews: Water, 10(3), 1–31. https://doi.org/10.1002/wat2.1633

Lynch, A.J., Myers, B. J.E., Chu, C., Eby, L.A., Falke, J.A., Kovach, R.P., Krabbenhoft, T.J., Kwak, T.J., Lyons, J., Paukert, C.P., & Whitney, J.E. 2016. Climate Change Effects on North American Inland Fish Populations and Assemblages. *Fisheries*, 41(7), 346–361. https://doi.org/10.1080/03632415.2016.1186016

Mid-America Regional Council (MARC). What is Sediment Pollution? https://cfpub.epa.gov/npstbx/files/ksmo_sediment.pdf Accessed September 15, 2023.

Martin, E. 2019. Atlantic Coast Whole System Diadromous Fish Prioritization. https://www.atlanticfishhabitat.org/wpcontent/uploads/2019/12/TNC_AtlanticCoast_AlosinePrioritization.pdf

Martin, E. H. and J. Levine. 2017. Northeast Aquatic Connectivity Assessment Project - Version 2.0: Assessing the ecological impact of barriers on Northeastern rivers. The Nature Conservancy, Brunswick, Maine. http://maps.freshwaternetwork.org/northeast/

Maus, V., Giljum, S., Gutschlhofer, J. *et al.* 2020. A global-scale data set of mining areas. *Sci Data* **7**, 289. https://doi.org/10.1038/s41597-020-00624-w

Maus, V., Giljum, S., da Silva, D.M. *et al.* 2022. An update on global mining land use. *Sci Data* **9**, 433. https://doi.org/10.1038/s41597-022-01547-4

Mayer, T. D., & Naman, S. W. 2011. Streamflow response to climate as influenced by geology and elevation. *Journal of the American Water Resources Association*, 47(4), 724–738. https://doi.org/10.1111/j.1752-1688.2011.00537.x

McCabe, Gregory J., and David M. Wolock. 2021. Water balance of the turn-of-the-century drought in the Southwestern United States. *Environmental Research Letters*, 16(4): 044015.

McManamay R.A., Troia M.J., DeRolph C.R., Olivero Sheldon A, Barnett, Kao S-C, et al. 2018. A stream classification system to explore the physical habitat diversity and anthropogenic impacts in riverscapes of the eastern United States. *PLoS ONE,* 13(6): e0198439. https://doi.org/10.1371/journal.pone.0198439

McManamay, R.A. and DeRolph, C.R. 2019. A stream classification system for the conterminous United States. *Scientific Data*, 6(1), pp.1-18.

McManamay, R. A., George, R., Morrison, R. R., & Ruddell, B. L. 2022. Mapping hydrologic alteration and ecological consequences in stream reaches of the conterminous United States. *Sci Data* 9, 1–14. https://doi.org/10.1038/s41597-022-01566-1

Miller, M. P., S. G. Buto, D. D. Susong, and C. A. Rumsey. 2016. The importance of base flow in sustaining surface water flow in the Upper Colorado River Basin, *Water Resources Research*, 52:3547–3562.

Miller, O.L., Wise, D.R., and Anning, D.W. 2020. SPARROW model inputs and simulated streamflow, nutrient and suspended-sediment loads in streams of the Southwestern United States, 2012 Base Year: U.S. Geological Survey data release, https://doi.org/10.5066/P9GFLBG8.

Muhlfeld, C.C., Kovach, R.P., Jones, L.A., Al-Chokhachy, R., Boyer, M.C., Leary, R.F., Lowe, W. H., Luikart, G., & Allendorf, F.W. 2014. Invasive hybridization in a threatened species is accelerated by climate change. *Nature Climate Change*, 4:7, 4(7), 620–624. https://doi.org/10.1038/nclimate2252

Murphy, J. 2020. Changing suspended sediment in United States rivers and streams: linking sediment trends to changes in land use/cover, hydrology, and climate. *Hydrol. Earth Syst. Sci.*, 24, 991–1010, 2020. https://doi.org/10.5194/hess-24-991-2020

National Oceanic and Atmospheric Agency, U.S. Department of Commerce. NOAA. "Critical Habitat - Maps and GIS Data (West Coast Region)". Accessed March 2023. https://www.fisheries.noaa.gov/resource/map/critical-habitat-maps-and-gis-data-west-coast-region.

NatureServe. 2008a. Watershed Distribution Maps of Freshwater Fishes in the Conterminous United States. Version 2. Arlington, VA. U.S.A.

NatureServe. 2008b. Preliminary Draft Watershed Distribution Maps of Rare (G1-G3) Crayfishes in the Conterminous United States. Arlington, VA. U.S.A.

NatureServe. 2008c. Watershed Distribution Maps of Freshwater Mussels of the United States and Canada. Version 2. Arlington, VA. U.S.A.

ODFW (Oregon Department of Fish and Wildlife). 2019. Oregon Fish Passage Barriers. (Available from: https://nrimp.dfw.state.or.us/nrimp/default.aspx?pn=fishbarrierdata, Accessed 01 March 2020)

Olivero-Sheldon, A. and M.G. Anderson. 2016. Northeast Lake and Pond Classification System. The Nature Conservancy, Eastern Conservation Science, Eastern Regional Office. Boston, MA.

Olivero Sheldon, A., Barnett, A. & Anderson, M. G. 2015. A stream classification for the Appalachian Region. The Nature Conservancy, Eastern Conservation Science, Eastern Regional Office: Boston, MA https://www.conservationgateway.org/ConservationByGeography/NorthAmerica/United States /edc/reportsdata/freshwater/habitat/Pages/Appalachian-Stream-Classification.aspx 2015.

Paukert, C., Olden, J.D., Lynch, A.J., Breshears, D.D., Christopher Chambers, R., Chu, C., Daly, M., Dibble, K.L., Falke, J., Issak, D., Jacobson, P., Jensen, O. P., & Munroe, D. 2021. Climate change effects on North American fish and fisheries to inform adaptation strategies. *Fisheries*, 46(9), 449–464. https://doi.org/10.1002/fsh.10668

Pelletier, M. C., Ebersole, J., Mulvaney, K., Rashleigh, B., Gutierrez, M. N., Chintala, M., Kuhn, A., Molina, M., Bagley, M., & Lane, C. 2020. Resilience of aquatic systems: Review and management implications. *Aquatic Sciences*, 82(2), 1–44. https://doi.org/10.1007/s00027-020-00717-z.

Pengra, B.W., Stehman, S.V., Horton, J.A., Auch, R.F., Dockter, D.J., Kambly, S., and Taylor, J.L. 2021. LCMAP CONUS Intensification Reference Data Product 1984-2019 land cover, land use and change process attributes: U.S. Geological Survey data release, https://doi.org/10.5066/P9QA5Q25.

Pennock, C.A., Budy, P., Macfarlane, W.W., Breen, M.J., Jimenez, J., & Schmidt, J.C. 2022. Native fish need a natural flow regime. *Fisheries*, 47(3), 118–123. https://doi.org/10.1002/fsh.10703.

Pericak A.A., Thomas, C.J., Kroodsma, D.A., Wasson, M.F., Ross, M.R.V., Clinton, N.E., et al. 2018. Mapping the yearly extent of surface coal mining in Central Appalachia using Landsat and Google Earth Engine. *PLoS ONE,* 13(7): e0197758. https://doi.org/10.1371/journal.pone.0197758.

Peterson, R.A. 2021. Finding Optimal Normalizing Transformations via bestNormalize. The R Journal, 13:1, 310-329, DOI:10.32614/RJ-2021-041

Piggott, J.J., Townsend, C.R., & Matthaei, C.D. 2015. Climate warming and agricultural stressors interact to determine stream macroinvertebrate community dynamics. *Global Change Biology*, 21(5), 1887–1906. https://doi.org/10.1111/gcb.12861.

Pringle, C.M. 2001. Hydrologic connectivity and the management of biological reserves: a global perspective. *Ecological Applications*, 11(4), 981–998.

Pringle, C. 2003. What is hydrologic connectivity and why is it ecologically important? *Hydrological Processes*, 17(13), 2685–2689. https://doi.org/10.1002/hyp.5145.

PRISM (https://prism.oregonstate.edu/normals/) 30-year normals monthly air temp (800m USA grid of 30yr normals 1981-2010.

Provencher, L., Blankenship, K., and Byer, S. Handbook for Mapping High-Elevation Forest Thinning Opportunities to Increase Runoff in the Colorado River Basin Above Lake Mead: A Report to the Colorado River Program's Forest and Snow Management Team. 2021. The Nature Conservancy, Reno NV. 31p.

R Core Team. 2022. R: A language and environment for statistical computing. R Foundation for Statistical Computing, Vienna, Austria. URL https://www.R-project.org/.

Rieman, B. E., & Isaak, D. J. 2010. Climate change, aquatic ecosystems, and fishes in the rocky mountain west: Implications and alternatives for management. USDA Forest Service - General Technical Report RMRS-GTR, 250, 1–53. https://doi.org/10.2737/RMRS-GTR-250

Robertson, D.M., and Saad, D.A. 2019. Spatially referenced models of streamflow and nitrogen, phosphorus, and suspended-sediment loads in streams of the Midwestern United States: U.S. Geological Survey Scientific Investigations Report 2019–5114, 74 p. including 5 appendixes, https://doi.org/10.3133/sir20195114.

Roland, V.L., II, and Hoos, A.B. 2020. SPARROW model inputs and simulated streamflow, nutrient and suspended-sediment loads in streams of the Southeastern United States, 2012 Base Year: U.S. Geological Survey data release, https://doi.org/10.5066/P9A682GW.

Rosgen, D. L. 1994. A classification of natural rivers. *Catena* 22, 169–199.

Rosgen, D.L. 1996. Applied River Morphology. Wildland Hydrology, Pagosa Springs, CO

Russi D., ten Brink P., Farmer A., Badura T., Coates D., Förster J., Kumar R. and Davidson N. (2012) The Economics of Ecosystems and Biodiversity for Water and Wetlands. Final Consultation Draft. https://www.ramsar.org/sites/default/files/migration_files/documents/pdf/TEEB/TEEB_Water-Wetlands_Final-Consultation-Draft.pdf

Saad, D.A., and Robertson, D.M. 2020. SPARROW model inputs and simulated streamflow, nutrient and suspended-sediment loads in streams of the Midwestern United States, 2012 Base Year: U.S. Geological Survey data release, https://doi.org/10.5066/P93QMXC9.

Santhi, C.P., Allen, P., Muttiah, R., Arnold, J. & Tuppad, P. 2008. Regional estimation of base flow for the conterminous United States by hydrologic landscape regions. *Journal of Hydrology*, 351:139-153. 10.1016/j.jhydrol.2007.12.018.

Safe Drinking Water Foundation (SDWF). 2017. Mining and Water Pollution Fact Sheet. Available from: https://www.safewater.org/fact-sheets-1/2017/1/23/miningandwaterpollution. Accessed September 2023.

Seaber, P.R., Kapinos, F.P., and Knapp, G.L. 1987. Hydrologic Unit Maps: U.S. Geological Survey Water-Supply Paper 2294, 63 p.

Soller, D.R. 2009. Map database for surficial materials in the Conterminous United States (Geologic units, 1:5,000,000). Vector digital data.

Soller, D.R., Packard, P.H., and Garrity, C.P. 2012. Database for USGS Map I-1970 — Map showing the thickness and character of Quaternary sediments in the glaciated United States east of the Rocky Mountains: U.S. Geological Survey Data Series 656, available at https://pubs.usgs.gov/ds/656/.

Soulard, C.E., Acevedo, W., Stehman, S.V., and Parker, O.P. 2016. Mapping extent and change in surface mines within the United States for 2001 to 2006. *Land Degradation and Development,* 27 (2): 248-257.

Southeast Aquatic Resource Partnership (SARP). 2022. SARP Comprehensive Southeast Aquatic Barrier Inventory – Dams sarp_all_dams_feb2022_fixed.csv.7z.

Starnes, L.B. and Gasper, D.C. 1995. Effects of Surface Mining on Aquatic Resources in North America (Revised, Full Text). American Fisheries Society (AFS) Policy Statement #13. https://fisheries.org/policy-media/policy-statements/afs-policy-statement-13/

Stein, B.A., and S.R. Flack. 1997. 1997 Species Report Card: The State of U.S. Plants and Animals. The Nature Conservancy, Arlington, Virginia. 26pp.

Stets, E.G., Sprague, L.A., Oelsner, G.P., Johnson, H.M, Murphy, J.C., Ryberg, K., Vecchia, A.V., Zuellig, R.E., Falcone, J.A., and Riskin, M.L. 2020. Landscape drivers of dynamic change in water quality of U.S. rivers. *Environmental Science and Technology,* 54 (7), 4336-4343. DOI: 10.1021/acs.est.9b05344

Tarboton, D.G. 2003. A workbook to accompany the Rainfall-Runoff Processes Web module. Utah State University, Hydrology Research Group . https://uwrl.usu.edu/hydrology/files/rrp/rainfall-runoff-processes.pdf

The Nature Conservancy and Desert Research Institute 2023. Global Groundwater Dependent Ecosystem Map, Version 1.2.0. June 2023. https://kklausmeyer.users.earthengine.app/view/global-gde)

The Nature Conservancy. 2020a. CONUS Landforms, based on terrestrial resilience plans 2016-2019. The Nature Conservancy, Center for Resilient Conservation Science. Newburyport, MA. Data download: https://tnc.app.box.com/file/959024468113?s=7dgi8gbc6w7e39qu14yjgwdix96aqoro; AGOL Map Service: https://tiles.arcgis.com/tiles/F7DSX1DSNSiWmOqh/arcgis/rest/services/Landforms/MapServer

The Nature Conservancy. 2020b. TNC Terrestrial Ecoregion Boundaries. The Nature Conservancy, Center for Resilient Conservation Science. Newburyport, MA. Data download: https://tnc.app.box.com/s/nkph9u19ucy11uzuo961x9qjynbbdtcb; AGOL Map Service: https://tnc.maps.arcgis.com/home/item.html?id=0316dce180e14f339181ac8d4986b4d5

The Nature Conservancy. 2020c. CONUS Geophysical Settings based on terrestrial resilience plans 2016-2019. The Nature Conservancy, Center for Resilient Conservation Science. Newburyport, MA. Data download: https://tnc.app.box.com/file/959021593944?s=voj4tfz0dyokpvwrldji9b3nbrsi36xl;AGOL Map Service: https://tiles.arcgis.com/tiles/F7DSX1DSNSiWmOqh/arcgis/rest/services/Geophysical_Settings/MapServer

Theobald D.M., Harrison-Atlas D., Monahan W.B., Albano C.M. 2015. Ecologically-Relevant Maps of Landforms and Physiographic Diversity for Climate Adaptation Planning. *PLoS ONE*, 10(12): e0143619. doi:10.1371/journal.pone.0143619

Theobald, D. 2022. SRTM CHILI CONUS. 30-m grid dataset. Google Earth Engine Extract 5/18/2022.

Tickner, D., Opperman, J.J., Abell, R., Acreman, M., Arthington, A.H., Bunn, S.E., Cooke, S.J., Dalton, J., Darwall, W., Edwards, G., Harrison, I.A.N., Hughes, K., Jones, T.I.M., Leclère, D., Lynch, A.J., Leonard, P., Mcclain, M.E., Muruven, D., Olden, J.D., and Young, L. 2020. Bending the curve of global freshwater biodiversity loss: an emergency recovery plan. *BioScience,* 70(4):330–342. https://doi.org/10.1093/biosci/biaa002

Timpane-Padgham, B. L., Beechie, T., & Klinger, T. 2017. A systematic review of ecological attributes that confer resilience to climate change in environmental restoration. *PLoS ONE*, 12(3), e0173812. https://doi.org/10.1371/journal.pone.0173812

Townsend PA, Helmers DP, Kingdon CC, McNeil BE, de Beurs KM, Eshleman KN. 2009. Changes in the extent of surface mining and reclamation in the Central Appalachians detected using a 1976–2006 Landsat time series. *Remote Sensing of Environment*, 113(1):62–72.

Trabucco, A., and Zomer, R.J. 2018. Global Aridity Index and Potential Evapo-Transpiration (ET0) Climate Database v2. CGIAR Consortium for Spatial Information (CGIAR-CSI). Published online, available from the CGIAR-CSI GeoPortal at https://cgiarcsi.community

United Nations Environmental Programme (UNEP). 2022. Convention on Biodiversity, Kunming-Montreal Global Biodiversity Framework. https://www.cbd.int/doc/decisions/cop-15/cop-15-dec-04-en.pdf.

U.S. Army Corps of Engineers (USACE). 2021. National Inventory of Dams (NID). Accessed Jan 6, 2021. https://nid.sec.usace.army.mil/

U.S. Department of Agriculture (USDA). 2006. Digital General Soil Map of U.S. STATSGO2. Tabular digital data and vector digital data. http://websoilsurvey.nrcs.usda.gov

U.S. Energy Information Administration (EIA) and U.S. Department of Labor, Mine Safety and Health Administration. 2020. Coal Mines digital vector data. https://atlas.eia.gov/datasets/eia::coal-mines-1/about

U.S. Environmental Protection Agency (USEPA). 2012. National Aquatic Resource Surveys. National Lakes Assessment 2012. Available from http://www.epa.gov/national-aquatic-resource-surveys/data-national-aquatic-resource-surveys.

U.S. Environmental Protection Agency (USEPA). 2020. National Rivers and Streams Assessment 2013–2014: A Collaborative Survey. EPA 841-R-19-001. Washington, DC. https://www.epa.gov/national-aquatic-resource-surveys/nrsa

U.S. Fish and Wildlife Service (USFWS). Lahontan Cutthroat Trout 5-Year Review: Summary and Evaluation, U.S. Fish and Wildlife Service, Nevada Fish and Wildlife Office. Reno, Nevada, March 30, 2009.

U.S. Fish and Wildlife Service (USFWS), U.S. Department of the Interior. FWS HQ ES Critical Habitat. Accessed March 2023. https://gis-fws.opendata.arcgis.com/maps/794de45b9d774d21aed3bf9b5313ee24/about

U.S. Geological Survey (USGS). 2003. Principal Aquifers of the 48 Conterminous United States, Hawaii, Puerto Rico, and the U.S. Virgin Islands. 1:2,500,000. http://nationalatlas.gov/atlasftp.html.

U.S. Geological Survey (USGS). 2005. Active Mines and Mineral Processing Plants in the United States in 2003: U.S. Geological Survey, Reston, Virginia. https://mrdata.usgs.gov/mineplant/

U.S. Geological Survey (USGS). 2016. USGS National Hydrography Dataset (NHD)V21 Downloadable Data Collection - National Geospatial Data Asset (NGDA) National Hydrography Dataset (NHD): USGS - National Geospatial Technical Operations Center (NGTOC): Rolla, MO and Denver, CO, http://nhd.usgs.gov, http://viewer.nationalmap.gov/. https://www.sciencebase.gov/catalog/item/4f5545cce4b018de15819ca9

U.S. Geological Survey (USGS). 2020. National Anthropogenic Barrier Dataset (NABD) Version 2 Beta. Updated as of 6/23/2020 NABDV2 (USGS, A. Cooper personal communication).

Valayamkunnath, P., Barlage, M., Chen, F., Gochis, D.J., and Franz, K. J. 2020. Mapping of 30-meter resolution tile-drained croplands using a geospatial modeling approach. *Scientific Data*, 7:257. https://doi.org/10.1038/s41597-020-00596-x.

Vannote, RL,G. W. Minshall, K. W. Cummins, J.R. Sedell, and E. Cushing. 1980. The river continuum concept. *Canadian Journal of Fisheries and Aquatic Sciences,* 37:130-137.

Wang, L. 2009. Defining and characterizing coolwater streams and their fish assemblages in Michigan and Wisconsin, USA. *North American Journal of Fisheries Management*, 29:1130-1151. 10.1577/M08-118.1.

Wang, L., Infante, D., Esselman, P., Cooper, A., Wu, D., Taylor, W., Beard, D., Whelan, G. and Ostroff, A. 2011. A hierarchical spatial framework and database for the National River Fish Habitat Condition Assessment. *Fisheries*, 36(9):436-449, DOI: 10.1080/03632415.2011.607075.

Weary, D.J., and Doctor, D.H., 2014. Karst in the United States of America: a digital map compilation and database. U.S. Geological Survey Open-file Report 2014-1156. https://pubs.usgs.gov/of/2014/1156/

Whitney, J. E., Al-Chokhachy, R., Bunnell, D. B., Caldwell, C. A., Cooke, S. J., Eliason, E. J., Rogers, M., Lynch, A. J., & Paukert, C. P. 2016. Physiological Basis of Climate Change Impacts on North American Inland Fishes. *Fisheries*, 41(7), 332–345. https://doi.org/10.1080/03632415.2016.1186656

Wise, D.R. 2020. SPARROW model inputs and simulated streamflow, nutrient and suspended-sediment loads in streams of the Pacific Region of the United States, 2012 Base Year (ver 1.1, June 2020): U.S. Geological Survey data release, https://doi.org/10.5066/P9AXLOSM.

Woodward, G., Perkins, D. M., & Brown, L. E. 2010. Climate change and freshwater ecosystems: Impacts across multiple levels of organization. *Philosophical Transactions of the Royal Society B: Biological Sciences*, 365(1549):2093–2106. https://doi.org/10.1098/rstb.2010.0055

Wolock, D. M. 2003. Base-flow index grid for the conterminous United States. U.S. Geological Survey Open-File Report 03-263. U.S. Geological Survey. Reston, Virginia. https://onlinelibrary.wiley.com/r/eap1of19https://doi.org/10.1002/eap.2534

Wolock, D. M., Winter, T. C. and McMahon, G. 2004. Delineation and evaluation of hydrologic landscape regions in the United States using geographic information system tools and multivariate statistical analyses. *Environmental Management*, 34:S71-S88.

Wolock, D.M. and McCabe, G.J. 2017. USGS Water Balance Tabular Dataset. https://data.usgs.gov/datacatalog/search?otherKeyword=%5B%22water+balance+model%22%5D

World Wildlife Fund (WWF) and The Nature Conservancy (TNC). 2019. Freshwater Ecoregions of the World. feow.org

Zomer, R.J., Trabucco, A., Bossio, D.A., & Verchot, L.V. 2008. Climate change mitigation: A spatial analysis of global land suitability for clean development mechanism afforestation and reforestation. Agriculture, *Ecosystems and Environment*, 126(1–2):67–80. https://doi.org/10.1016/j.agee.2008.01.014

APPENDIX

Model Diagrams 1

Appendix 1 contains full-page figures that detail the model components for each climatic region used in the freshwater resilience analysis. Diagrams are available for the following five regions:

- Humid ecoregions
- Arid, non-xeric, perennial-dominated systems
- Arid, non-xeric, intermittent-dominated systems.
- Arid, xeric, perennial-dominated systems.
- Arid, xeric, intermittent-dominated systems.

Figure A1-1. Freshwater resilience model for the humid region.

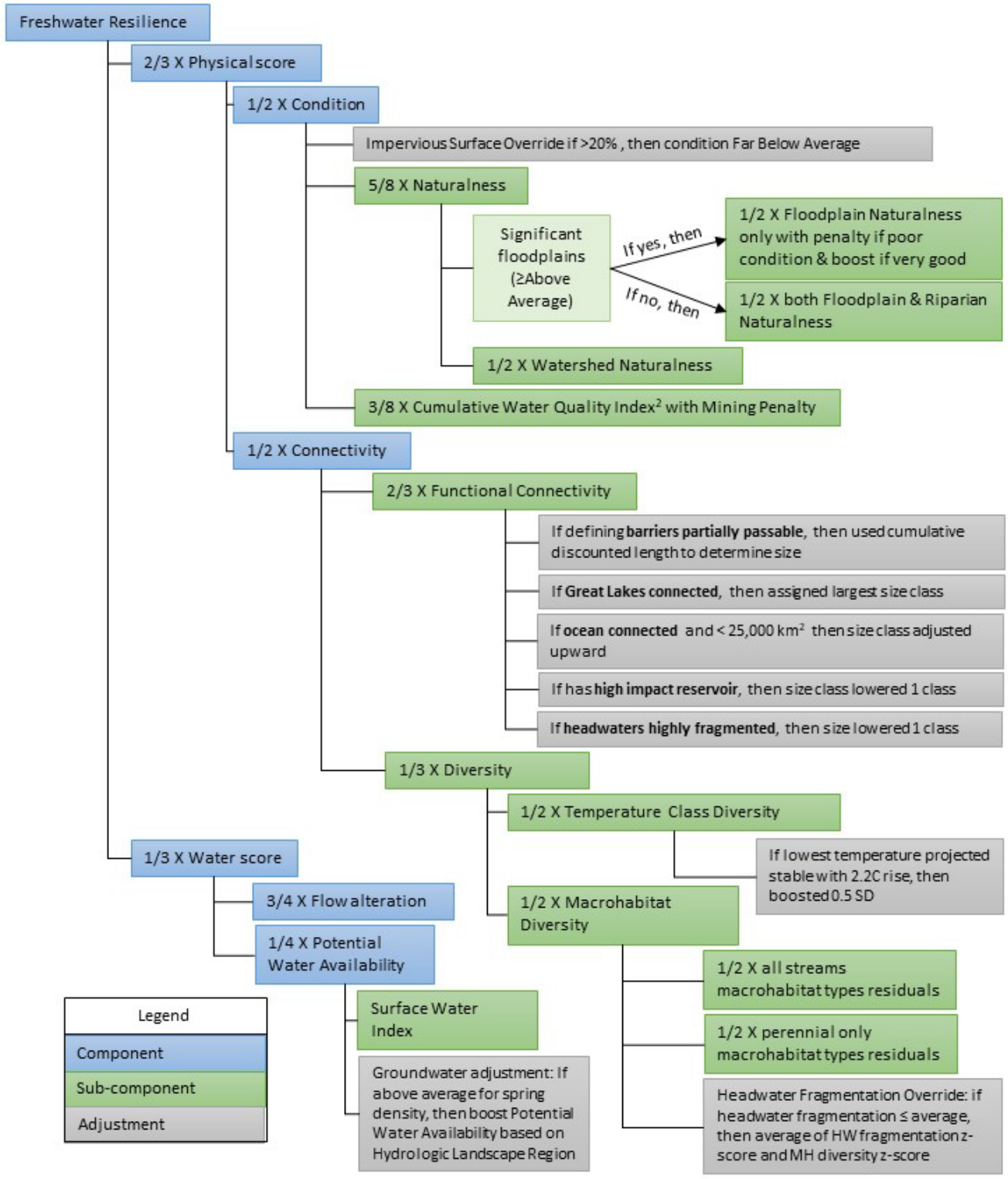

Figure A1-2. Freshwater resilience model for arid, non-xeric, and perennial-dominated systems.

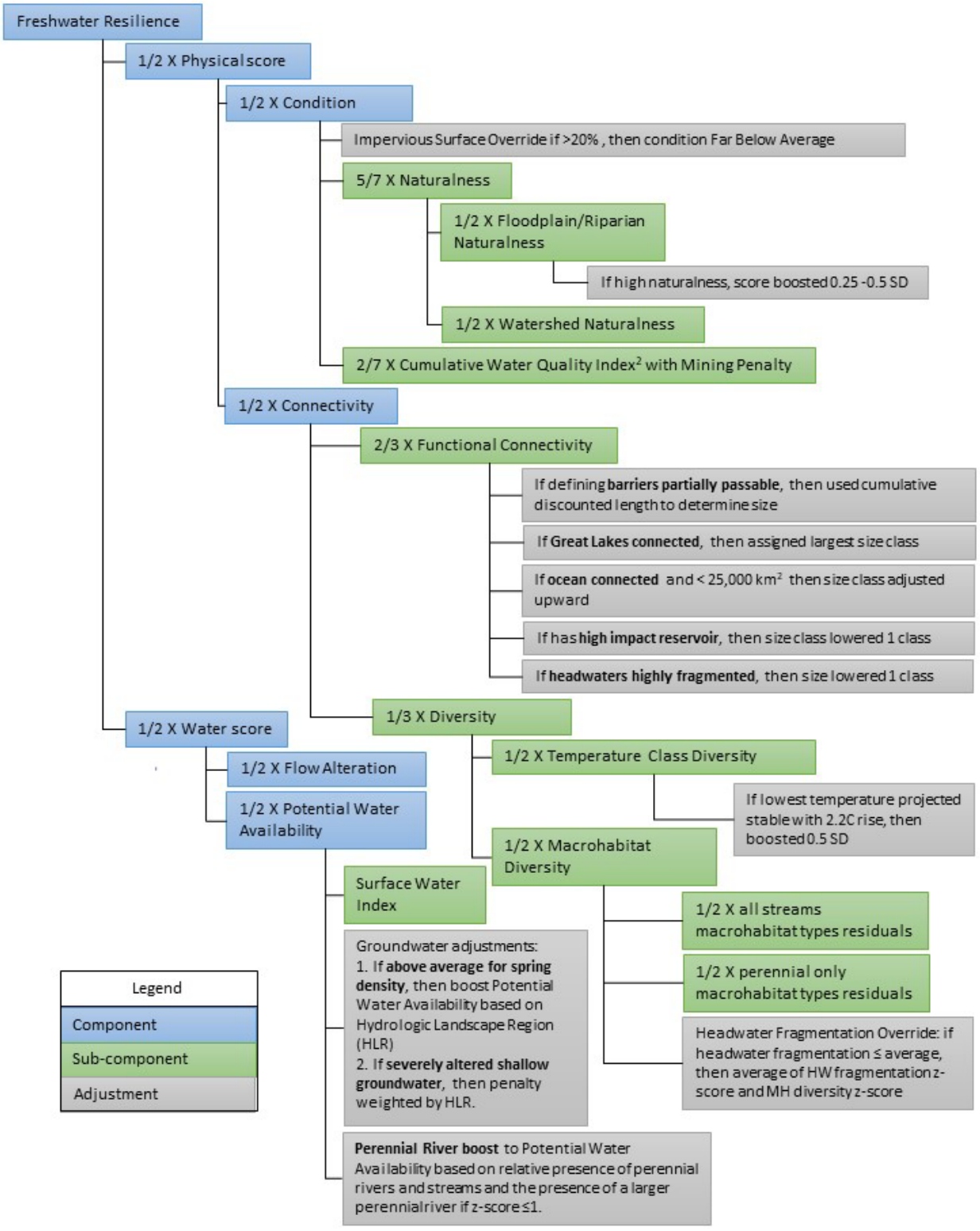

Figure A1-3. Freshwater resilience model for arid, non-xeric, and intermittent-dominated systems.

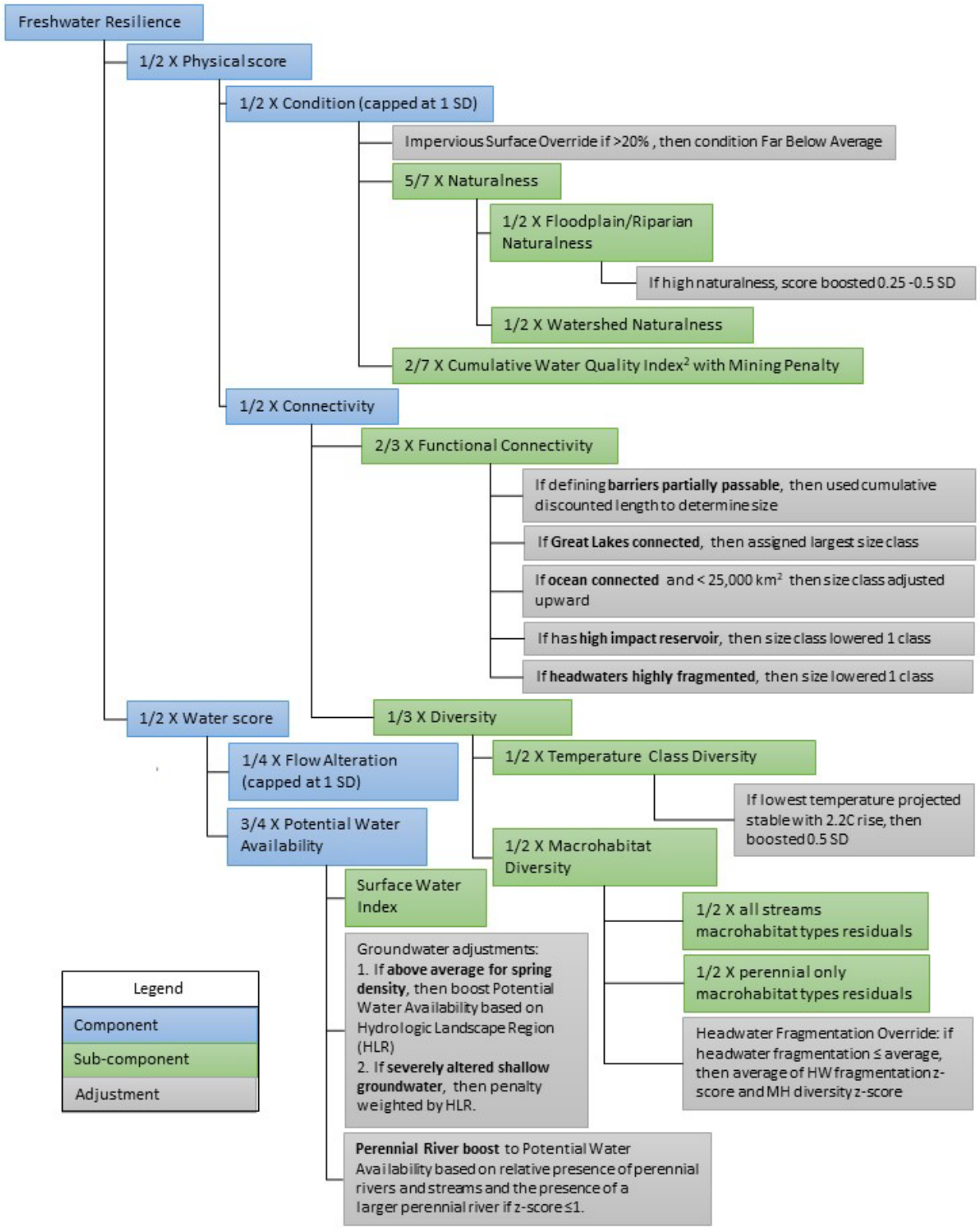

Figure A1-4. Freshwater resilience model for arid, xeric, and perennial-dominated systems.

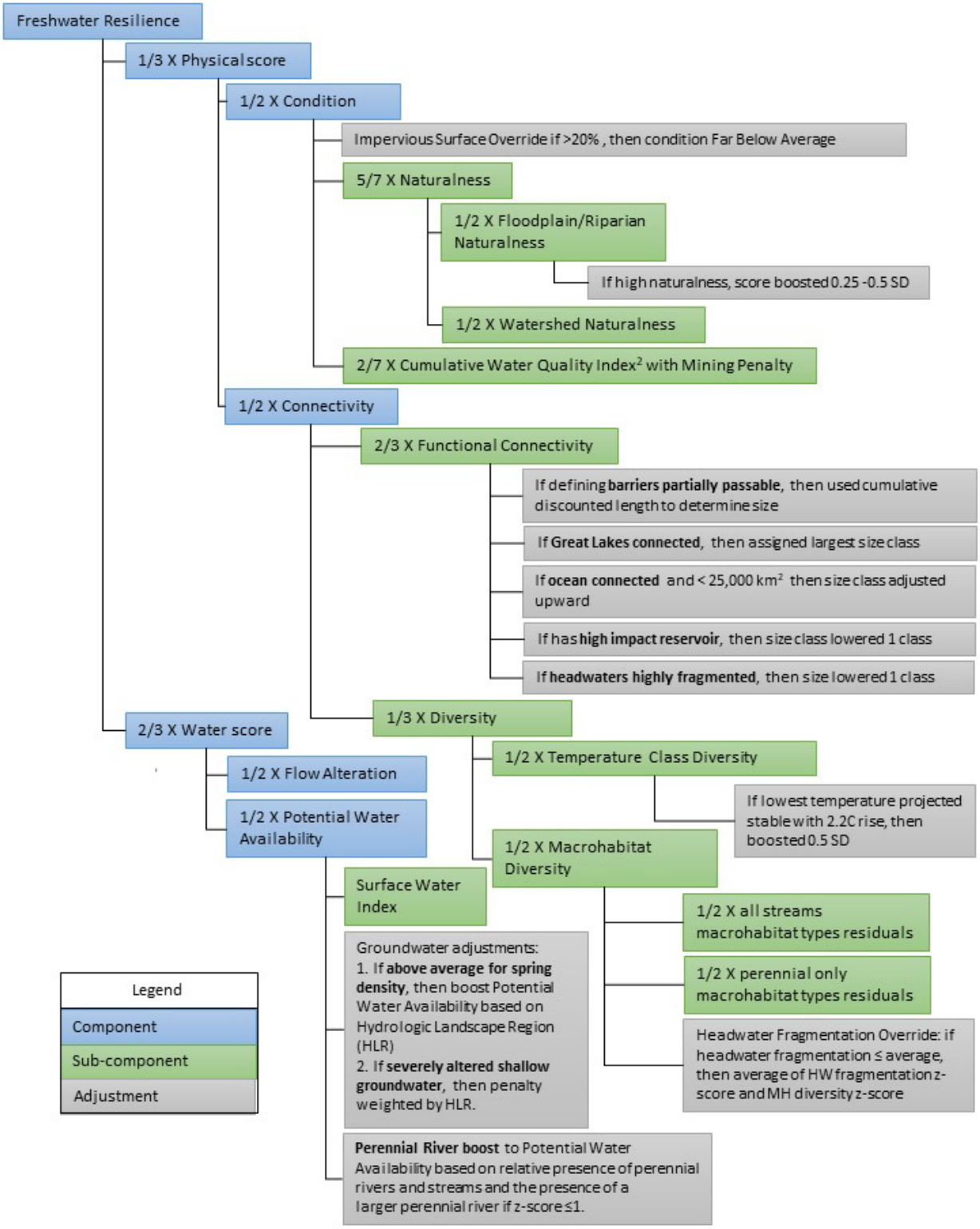

Figure A1-5. Freshwater resilience model for arid, xeric, and intermittent-dominated systems.

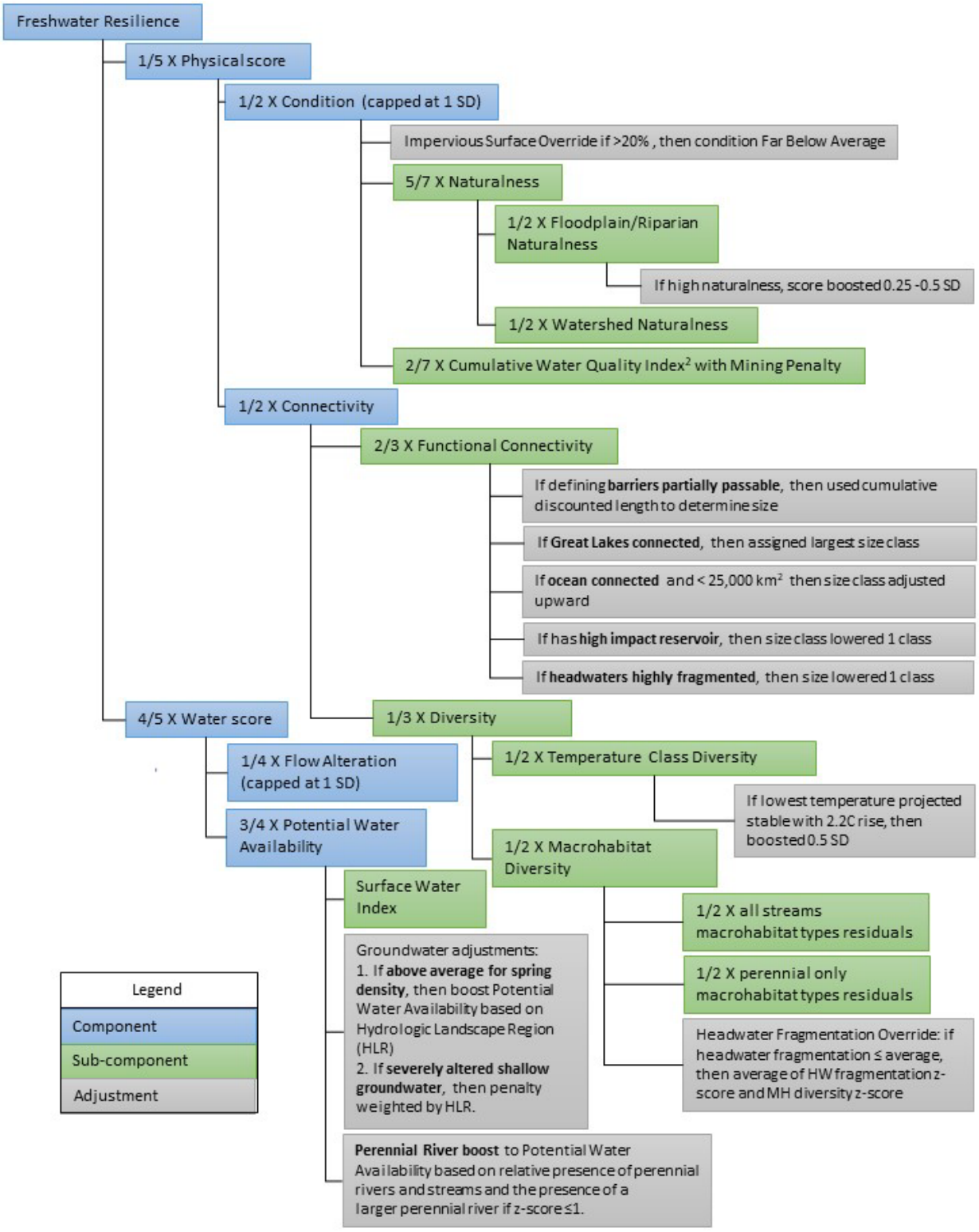

Source Data & Analysis Scales 2

The following table details the datasets and their scale for each of the freshwater resilience model components.

Table A2-1. Freshwater resilience model components: data sources and scale of assessment.

Freshwater Resilience Components					Assessment Unit	
Score	**Component**	**Sub-Component**	**Detail**	**Data Sources**	**FCN**	**HUC - 12**
Physical	Connectivity & Diversity	Functional Connectivity	Size adjusted by passability of dams, location of reservoirs, connectivity to the great lakes and ocean, and headwater fragmentation	NHDPlusV21 (USGS 2016) Dams on Rivers reviewed by team from source National Anthropogenic Barrier Database (NABD) (updated V2 Beta 6/2020), Northeast Connectivity Project (12/2/2020), Southern Aquatic Resource Partnership (2/2022), and CA State Dams. (10/2022) EPA (Hollister et al. 2011) Size classes: (Wang et al. 2011)	X	
			Headwater Connectivity	Same as above (stream dams only)	X	X
		Diversity	Temperature Class Diversity	EPA Stream Cat: Reference Summer Stream Temperature Model 2014 (Hill et al. 2016); Future Scenario 2.2C rise.	X	
			Macrohabitat Diversity	McManamay & DeRolph 2019; Higgins et al. 2005		X
	Condition	Floodplain, Riparian, and Watershed Naturalness	Floodplain and Riparian Naturalness	NLCD 2019 with mining footprint FATHOM v2 100-yr pluvial and fluvial (Bates et al. 2021; First Street Foundation 2020)		X
			Watershed Naturalness	NLCD 2019 with mining footprint		X

Table A2-1. continued

Freshwater Resilience Components					Assessment Unit	
Score	**Component**	**Sub-Component**	**Detail**	**Data Sources**	**FCN**	**HUC - 12**
Physical	Condition	Water Quality	Cumulative N, P, and Sediment Index	USGS SPARROW 2012 NHDPlusV21 (USGS 2016)		X
			Percent Mining	Appalachian LCC Mining Disturbed Area (Braven Beaty, TNC) A global-scale data set of mining areas (Maus et al. 2020) LCMAP Barrens change analysis; EIA coal mines; USGS NCRDS FLDEP Mandatory Phosphate Mined Units & Reclaimed Units Landfire EVT; USGS Surface Mines 2001-2006 NLCD 2019		X
Water	Potential Water Availability		Surface Water Topographic Storage Index	Water and waterbodies: NHDPlusv21 Pluvial areas: Landforms (TNC 2020a) Tiling: AgTile 2020 Land cover: NLCD 2019 Snowpack: CHILI Heat Load Index, Theobald; Elevation ≥ Upper Montane from LANDFIRE Biophysical Settings and TNC Western Resilience Settings		X

Table A2-1. continued

Freshwater Resilience Components					Assessment Unit	
Score	**Component**	**Sub-Component**	**Detail**	**Data Sources**	**FCN**	**HUC - 12**
Water	Potential Water Availability	Groundwater adjustments	Springs	NHDPlusv2.1		X
			Perennial high density (arid region only)	NHDPlusv2.1		X
			Groundwater Depletion	NASA's GRACE "Shallow Groundwater Drought Indicator: Wetness Percentile relative to 1948-2012" for Feb. & March 2002 - 2022 Wolock et al. (2004), with hydrologic landscape region edits based on TNC CRCS bedrock and soils CONUS data (TNC 2022)		X
	Flow Alteration			NHDPlusV21 catchments (USGS 2016) McManamay et al. (2022) Hydrologic Alteration Index		X

APPENDIX 3

Macrohabitat Components

For the connectivity component of the physical score, we calculated a diversity score that measures the physical habitat variation in a Functionally Connected Network (FCN) and was calculated as follows:

Diversity Score = (Temperature score + Macrohabitat Diversity score) / 2

Macrohabitats are the finest scale unit of hierarchical aquatic classification types defined in TNC's freshwater classification approach (Higgins et al. 2005). They define stream reach types or lake types and are based on key abiotic variables known to structure aquatic communities at the reach or lake scale. For this analysis, we created simplified macrohabitat types to represent variation in major aquatic physical habitats at the stream reach or individual lake scale using variables possible to model in GIS. Our hypothesis was that HUC-12 units with more macrohabitats would provide more options for species to adapt to change and thus support resilience. Here, we provide details on how we created the simplified macrohabitat types.

Size

Stream size is indicative of major ecosystem changes along the stream-river continuum, such as transitions in the state and source of energy and ecosystem metabolism. Stream size has been given the highest classification importance in many reach scale stream classification systems because of its strong effect on determining aquatic biological assemblages at the reach scale (Vannote et al. 1980; Higgins et al. 2005). The well-known "river continuum concept," depicted in Figure A3-1, illustrates how the physical size of a stream relates to major ecosystem changes from small headwater streams dominated by coarse organic matter to autochthonous production by plankton in large river mouths (Vannote et al. 1980; FISRWG 1998).

Figure A3-1. The River Continuum Concept from Vannote et al. 1980 (FISRWG 1998).

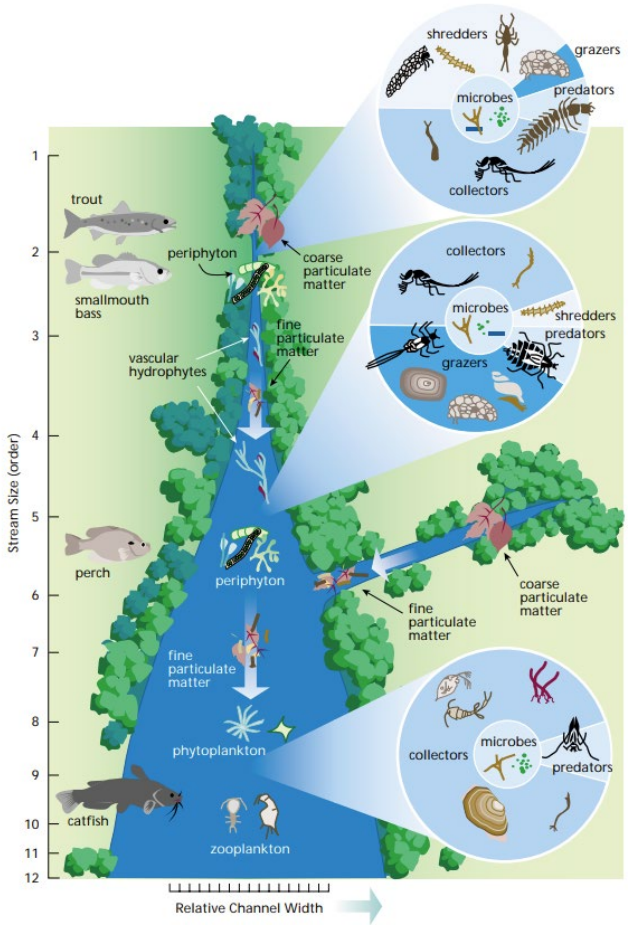

Size classes were defined based on total upstream drainage which is the most stable and geomorphologically comparable measure of size across the country. Size class breaks were based on the National River Fish Habitat Condition Assessment (Wang et al. 2011) which was designed to provide a coarse-level understanding of diversity at a national scale. We made two small modifications, adding two very large river classes and combining the two smallest classes (Table A3-1).

Table A3-1. River reach size classes.

Size Class Number	Size Class Name	Catchment Area (km^2)
10,11	Headwaters, Creek	≤ 100
20	Small Rivers	≤ 1000
30	Medium Rivers	≤ 10,000
40	Mainstem Rivers	≤ 25,000
50	Large Rivers	≤ 100,000
60	Great Rivers	≤ 1,000,000
70	Mega Rivers	> 1,000,000

Gradient

Stream gradient also highly influences aquatic communities at the reach scale due to its influence on stream bed morphology, flow velocity, sediment transport/deposition, substrate, and grain size (Rosgen 1994). As shown in Figure A3-2, high gradient streams are dominated by step-pools to plane-bed systems with substrates of cobble and boulders, and colluvial sediment transport. Low gradient systems are dominated by riffle-pool systems, with substrates of sand, gravel, and cobble, alluvial storage, and depositional sediment regimes. Very low gradient streams are dominated by ripple-dune streams with very high sinuosity. These rivers have sand, gravel and finer sediment substrates, alluvial storage and depositional sediment regimes, and slight entrenchment with critical adjacent floodplain systems (Rosgen 1996; Allan 1995).

Figure A3-2. Illustration of how gradient shapes riverine habitats (FISRWG 1998).

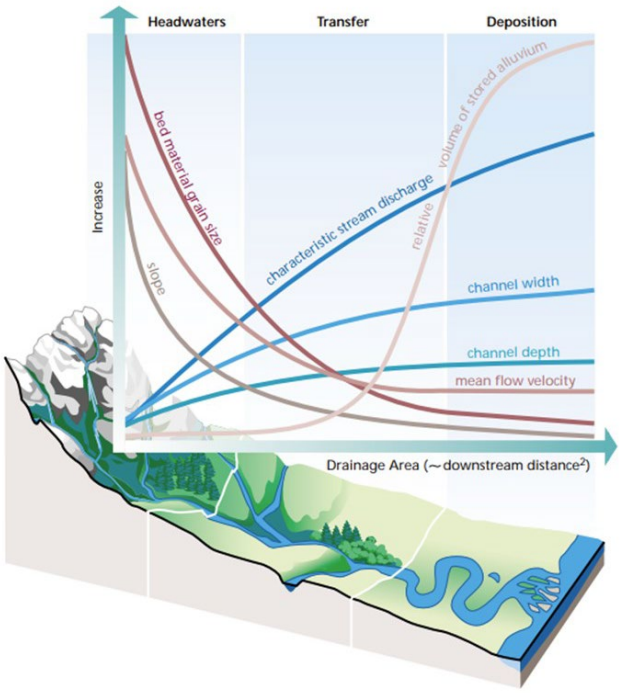

Gradient classes were based on McManamay et al. (2019), except that we combined the two highest classes, which were inextricably correlated (Table A3-2). Gradient in the source NHDPlus reaches represents the average gradient over the length of an entire arc based on the length and elevational change from node to node.

Table A3-2. Gradient classes.

Gradient Class Name	Slope
Very Low	<0.001
Low	0.001-0.005
Moderate	0.005-0.02
Moderate - High	0.02-0.04
High and Steep	>0.04

Local Temperature

Stream temperature is fundamental to freshwater resilience because it sets the physiological limits of persistence for many organisms and temperature extremes may directly preclude certain taxa from inhabiting a water body. Seasonal changes in water temperature often cue development or migration, and temperature can influence growth rates and fecundity. Ideally, a resilient stream network would span a range of current temperatures offering options for both coldwater and warmwater species and provide connected habitats for species to stay within their thermal preferences in the future (Woodward et al. 2010).

Mean summer stream water temperature modeled data was available for most reaches from the EPA Stream-Catchment (StreamCat) dataset (Hill et al. 2016), a national source widely used to study reference temperatures. We extracted the variable Mean Summer Stream Temperature (MSST 2014) to represent the predicted reference-condition mean summer stream temperatures. The missing data for streams in Northern Michigan was filled in using Lyons et al. (2009). Temperature predictions were not available for all very large rivers because the source EPA MSST data constrained their predictions to stream segments that were within the range of predictor values used to develop the model and the largest rivers (>100,000 km^2) were not represented in the gage dataset.

The continuous predictions were placed into five summer temperature classes following McManamay et al. (2019), except that we lumped the two coldest classes for which there were few reaches (Table A3-3). The temperature class breaks closely matched other stream and river classifications developed in Michigan (Lyons et al. 2009), the Appalachians (Olivero-Sheldon et al. 2015), and Eastern U.S (McManamay et al. 2018).

Table A3-3. Temperature classes in Celsius and Fahrenheit.

Temperature Class	Celsius	Fahrenheit
Very Cold	<15	<59
Cold	>15-18	59-64.4
Cool	>18-21	64.4-69.8
Cool-Warm	>21-24	69.8-75.2
Warm	>24C	>75/.2

Tidal

Streams and rivers that connect directly to the ocean or to large tidal river estuaries are influenced by ocean tides. Their water flow and level fluctuate with the tides and salinity can range from fresh to brackish to saline. They often represent a unique diversity of habitat for anadromous, diadromous, and euryhaline species. We had two classes, tidal and non-tidal, as defined by the "Tidal" attribute in the source NHDPlus data (USGS 2016).

Lakes

We included lakes in the HUC-12 macrohabitat diversity to represent distinct lentic ecosystem types. Depth is a critical variable related to summer lake stratification and the presence of permanent coldwater habitat for species like lake trout, rainbow smelt, burbot, and landlocked salmon. For the macrohabitat analysis, we defined lakes as any waterbody over ten acres in surface area and we classified them into two types: 1) deep, > 30 ft., and 2) shallow, < 30 ft. We assumed that waterbodies without depth records were shallow.

A summary of the five components and their classes is provided in Table A3-4 and Figure A3-3.

Table A3-4. Macrohabitat component class summary.

Size Class (cumulative drainage area in km^2)	Gradient	Temperature	Tidal	Lakes
Headwaters-Creek (≤ 100)	Very low (<0.001)	Very Cold (<15C; < 59F)	Tidal	Deep
Small River (>100 & ≤ 1,000)	Low (0.001 – 0.005)	Cold (>15-18C; 59-64.4F)	Non-tidal	Shallow
Medium Rivers (>1,000 & ≤ 10,000)	Moderate (0.005 – 0.02)	Cool (>18-21C; 64.4-69.8F)		
Mainstem Rivers (>10,000 & ≤ 25,000)	Moderate-High (0.02 – 0.04)	Cool-Warm (>21-24C; 69.8-75.2F)		
Large Rivers (> 25,000 & ≤ 100,000)	High & Steep (>0.04)	Warm (>24C; >75.2)		
Great Rivers (> 100,000 & ≤ 1,000,000)				
Mega Rivers (> 1,000,000)				

Figure A3-3. Macrohabitat components. Clockwise from top: size classes, gradient classes, temperature classes, tidal classes, and lake depth classes.

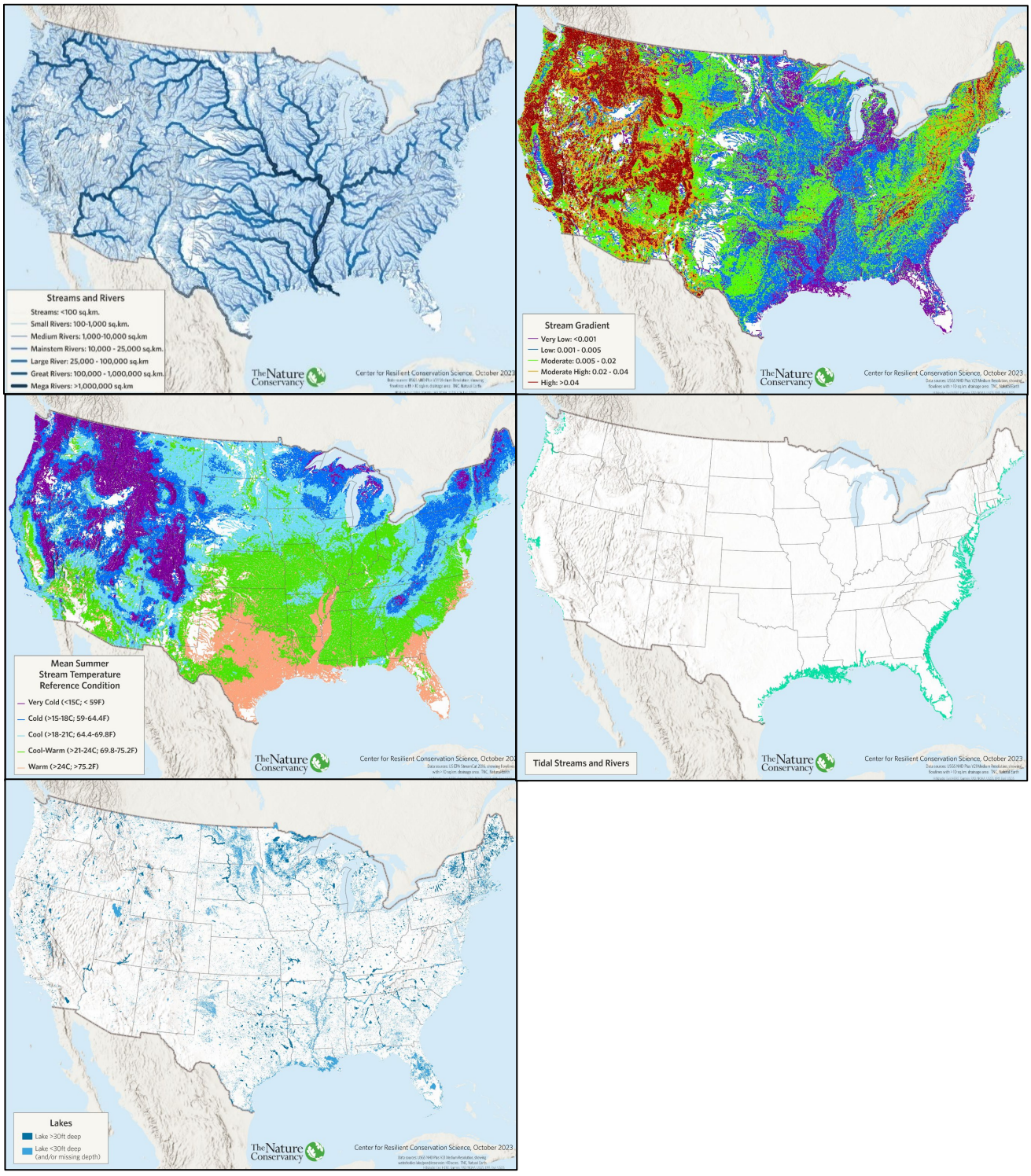

Calculating Macrohabitat Diversity

The macrohabitat components were combined at the reach flowline scale to code each NHDPlus flowline with its size class, temperature class, gradient class, and tidal class. Each unique combination of these classes was considered a "macrohabitat." All macrohabitat types longer than one km in a HUC-12 were extracted and counted toward a total diversity count of types present in the HUC. The total length (km) of all perennial and intermittent/ephemeral stream-river macrohabitat types was summarized. Additionally, the length (km) of only perennial stream-river macrohabitat types was summarized for each HUC-12 to explore the difference in diversity when ephemeral and intermittent streams were included versus when they were excluded. The presence of a deep lake or shallow lake was then added to the total stream-river macrohabitat counts to increase the total by one or two if deep, shallow, or both types of lakes were present in a HUC-12. The final macrohabitat diversity score for each HUC-12 unit was calculated based on the number of macrohabitat types relative to the average number of macrohabitats expected for the size of the HUC. Because the count of macrohabitats was correlated with the size of the HUC, we used a Poisson regression to establish a relationship between the size of the HUC and the count of macrohabitats, and then calculated the standardized residuals to identify HUCs that had more or less macrohabitat diversity than expected for their size. The standardized residuals were used as the z-score. See details of the statistical models below.

Perennial Reaches Only Model

```
m1 <- vglm(formula = CLPm19S755e ~ logSqKM , family = poissonff(), data = tab)
summary(m1)
Call:
vglm(formula = CLPm19S755e ~ logSqKM, family = poissonff(), data = tab)
Coefficients:
             Estimate Std. Error z value            Pr(>|z|)
(Intercept) -0.225599   0.021434  -10.53 <0.0000000000000002 ***
logSqKM      0.287002   0.004723   60.77 <0.0000000000000002 ***
Signif. codes:  0 '***' 0.001 '**' 0.01 '*' 0.05 '.' 0.1 ' ' 1
Name of linear predictor: loglink(lambda)
Residual deviance: 168330.6 on 82670 degrees of freedom
Log-likelihood: -185421 on 82670 degrees of freedom
Number of Fisher scoring iterations: 5
No Hauck-Donner effect found in any of the estimates
```

All Reaches Model, Perennial + Intermittent/Ephemeral (Using R Statistical Package)

```
m2 <- vglm(formula = CLAm19S755e ~ logSqKM , family = poissonff(), data = tab)
summary(m2)
Call:
vglm(formula = CLAm19S755e ~ logSqKM, family = poissonff(), data = tab)

Coefficients:
             Estimate Std. Error z value            Pr(>|z|)
(Intercept) -0.191308   0.017137  -11.16 <0.0000000000000002 ***
logSqKM      0.376811   0.003762  100.17 <0.0000000000000002 ***
Signif. codes:  0 '***' 0.001 '**' 0.01 '*' 0.05 '.' 0.1 ' ' 1
Name of linear predictor: loglink(lambda)
```

Residual deviance: 73712.31 on 82670 degrees of freedom
Log-likelihood: -170717.5 on 82670 degrees of freedom
Number of Fisher scoring iterations: 5
No Hauck-Donner effect found in any of the estimates

Maps of the residual scores (Figure A3-4) of the two models highlighted mountainous HUC-12s with higher diversity than expected by area alone. When non-perennial reaches were excluded, the arid west had a significant reduction in diversity scores over much of the arid region. We combined the two scores together giving equal weight to each in the final diversity score, and thus more weight was given to perennial streams which were included in both models.

Macrohabitat Diversity = (standard residual all streams + standard residual perennial only)/2

Small dams on headwaters and creeks make the accessibility of all types of macrohabitats within a HUC-12 more difficult. In HUCs with "Average" or worse headwater fragmentation, we adjusted the macrohabitat diversity score by taking the average of the combined macrohabitat diversity z-score and the headwater fragmentation z-score. If headwater fragmentation was low, we kept the diversity score as it was, assuming that some portion of the macrohabitat types present in the HUC would probably be accessible, at least at some part of the year. Finally, we integrated all the components and penalties into a single weighted map of macrohabitat diversity for CONUS (Figure 3.14).

Figure A3-4. Weighting factors for macrohabitat diversity score. Clockwise from upper left: residual z-score for all streams, residual z-score for perennial streams only, and habitat fragmentation penalty.

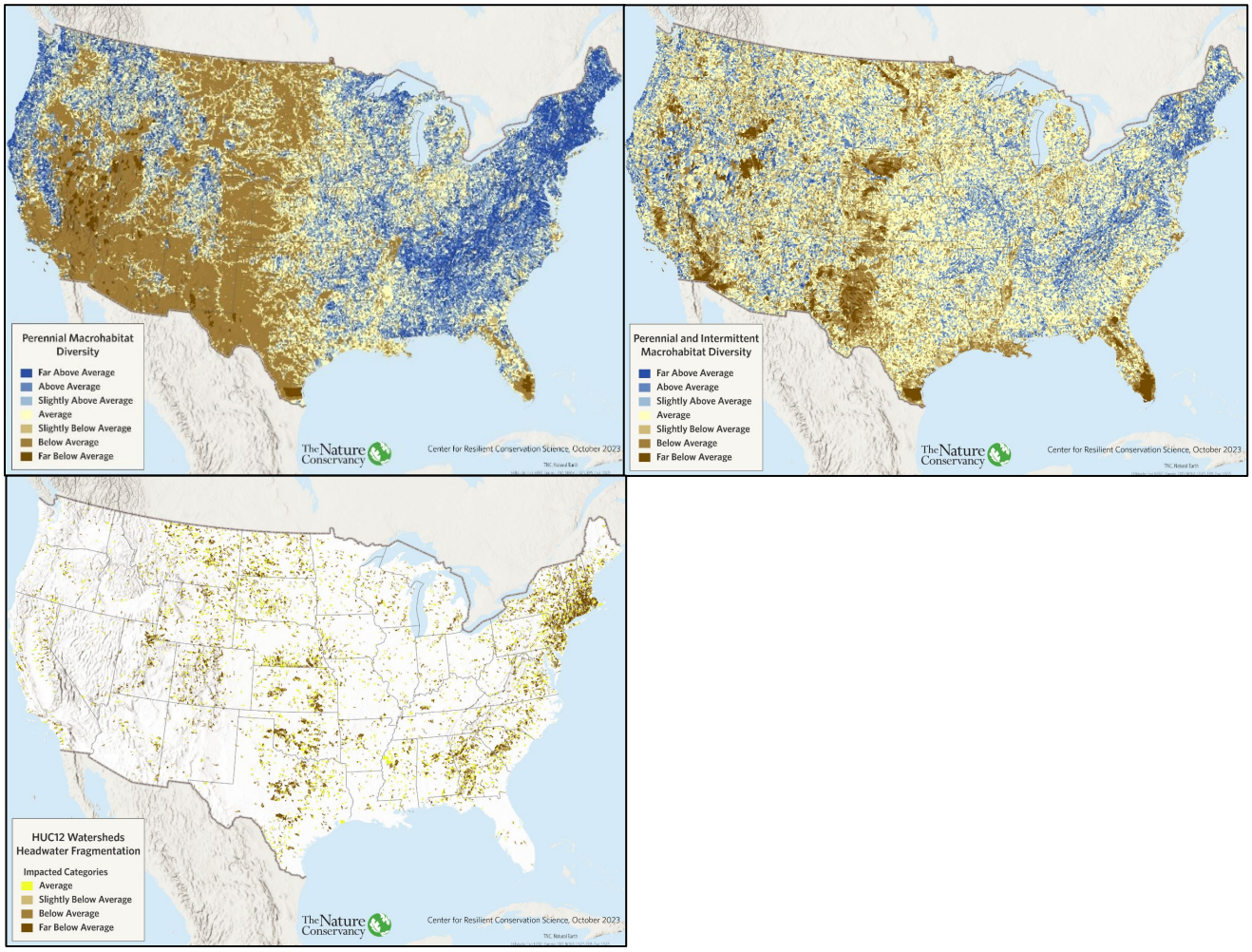

Mapping Groundwater Potential 4

Our goal was to assign each HUC-12 watershed in CONUS to a groundwater potential class based on the hydrologic flow paths corresponding to the soil and geologic setting type as identified in the USGS hydrologic landscape regions (HLRs, Wolock et al. 2004). According to the hypotheses of the HLRs framework, areas with permeable bedrock would have "deep groundwater hydrologic flow paths" and areas with permeable soils would have "shallow groundwater flow paths," while those with impermeable bedrock and impermeable soils would have overland hydrologic flow paths not driven by groundwater.

The original HLRs dataset used surface sandy soil texture and bedrock and deep aquifer types to estimate the effect of underlying geologic settings on surface runoff, infiltration, and groundwater flow. The underlying geologic setting was summarized for small watersheds (~200 km^2) which had been generated form a coarse 1-km resolution digital elevation model (DEM) in this original 2004 HLR dataset. The input geology in the original HLRs was based on a very coarse aquifer dataset mapped at a scale of 1:2.5M (USGS 2003). Given the availability of newer and higher resolution bedrock geology and soils datasets, we used the methods in Wolock et al. (2004) to create updated HLRs subsurface and surface permeability datasets.

Subsurface Permeability

We adopted the permeability classes of general lithologic groups as described in the original HLRs. These classes ranged from the highest permeability rank of seven to the lowest permeability rank of one as follows:

Subsurface Permeability Rank: (1= low permeability, 7 = high permeability)
1: Not a principal aquifer
2: Sandstone aquifers
3: Semiconsolidated sand aquifers
4: Igneous basalt and metamorphic volcanic rock aquifers
5: Sandstone and carbonate rock aquifers
6: Unconsolidated sand and gravel aquifers
7: Carbonate rock aquifers

To assign a subsurface permeability class to each HUC-12 watershed, we initially evaluated the subsurface geologic source used by Wolock et al. (2004) and the USGS map of Principal Aquifers of the 48 Conterminous United States 1:2.5M scale (USGS 2003). The bedrock aquifer types in the USGS (2003) product had been much more finely mapped in recent USGS state bedrock geology maps (Horton 2017) and in other sources such as the USGS National Karst map (Weary & Doctor 2014). Previously, we had used the USGS state geology polygons to develop a terrestrial settings dataset

(TNC 2020c) and already classified the formations into a very similar grouping as that used in the HLRs subsurface permeability classes. The recent USGS karst map (Doctor et al. 2020) also provided new finely mapped karst formations. Using these updated geologic sources, we extracted four of the six HLRs subsurface permeability classes from our terrestrial settings (TNC 2020c), the USGS state bedrock data (Horton et al. 2017), and/or the recent karst mapping (Doctor et al. 2022). The updated geologic data were placed into the following HLRs subsurface permeability rank classes (Figure A4-1):

- Class 2: Sandstone (and non-calcareous shale) aquifers: (sandstones, arenite, arkose, conglomerate, or sandstone mixed with mudstone, claystone, bentonite, politic schist, argillite, phyllite (slightly metamorphosed shale), black shale or oil shale)

- Class 4: Igneous basalt and metamorphic volcanic rock aquifers. Includes basalt, andesite, mafic volcanic, alkali volcanic rock. Mafic and felsic volcanic such as rhyolite, trachyte, basanite in major or minor rock types, USGS Karst dataset: Volcanic rocks with potential for pseudokarst feature. Also mafic/intermediate rock such as: quartz-poor alkaline to slightly acidic igneous and meta-igneous rock. Syenite, diorite, gabbro, anorthosite, migmatite, syenite, tectonite, hornfels, amphibolite, monzonite , amphibole schist, dioritic, and monzodiorite. Ultramafic rocks that were extremely rare in this region, such as magnesium-rich alkaline igneous and meta-igneous rock, serpentine, and peridotites.

- Class 5: Sandstone and carbonate rock aquifers. Mixed sedimentary/limestone formations. Moderately alkaline sedimentary or meta-sedimentary rock with some calcium but less than rocks in the purely calcareous rock aquifer class. Calcareous shales, mixed sedimentary rocks with calcareous components, calcium-silicate, and calcium-silicate schist rocks, usually in the minor components of the rock. Note, in the data set any mixed bedrock with one of the three major components in the dataset listed as limestone or dolostone was assigned here.

- Class 7: Carbonate rock aquifers. Alkaline sedimentary or metasedimentary rock with high calcium content such as limestone, dolostone, marlstone, calcarenite, carbonite, chalk, coquina, marble, and marl; USGS Karst “carbonate rocks at or near the surface.”

As we were unable to extract the remaining two types of deep, non-bedrock aquifers from existing state bedrock geology sources, we used the following two types from the original map of Principal Aquifers of the United States (USGS 2003):

- Class 3: Semiconsolidated sand aquifers

- Class 6: Unconsolidated sand and gravel aquifers

Areas not covered by the above classes were divided into two final classes:

- Class 1: Not a Principal Aquifer, Granite. Included quartz-rich: resistant igneous and meta-igneous or meta-sedimentary rock such as granite, granodiorite, gneiss, tonalite, migmatite, quartzite, mylonite, latite, dacite. Mapped using TNC terrestrial settings (TNC 2020c) and the USGS state bedrock data (Horton et al. 2017).

- Class 1.75: Not a Principal Aquifer, Deep Surficial Sediment Setting. Areas of deep surficial soil where bedrock was deeply buried, and the areas was not identified in the source bedrock or deep semi or unconsolidated sand/gravel aquifer datasets.

Figure A4-1. Subsurface permeability: bedrock and deep surficial aquifer type

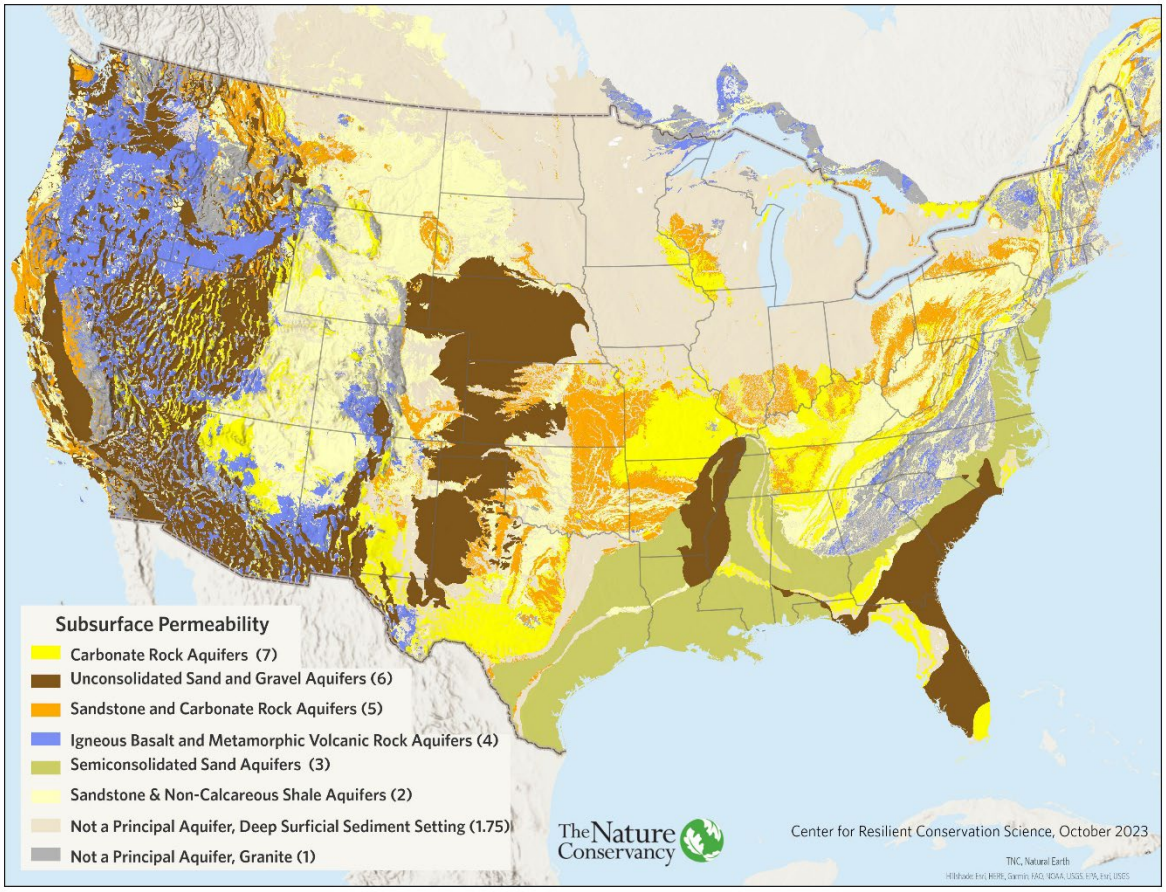

Similar to Wolock et al. (2004), we used small watersheds to summarize the underlying permeability patterns. Each input geologic class was assigned a permeability rank from one to seven. We then calculated the mean subsurface permeability value for each HUC-12 to place the watersheds in one of three summary groups representing high, moderate, and low subsurface permeability as follows (Figure A4-2):

- Low: 0-1.5
- Moderate >1.5 – 3.25
- High >3.25

Figure A4-2. Subsurface permeability summary classes.

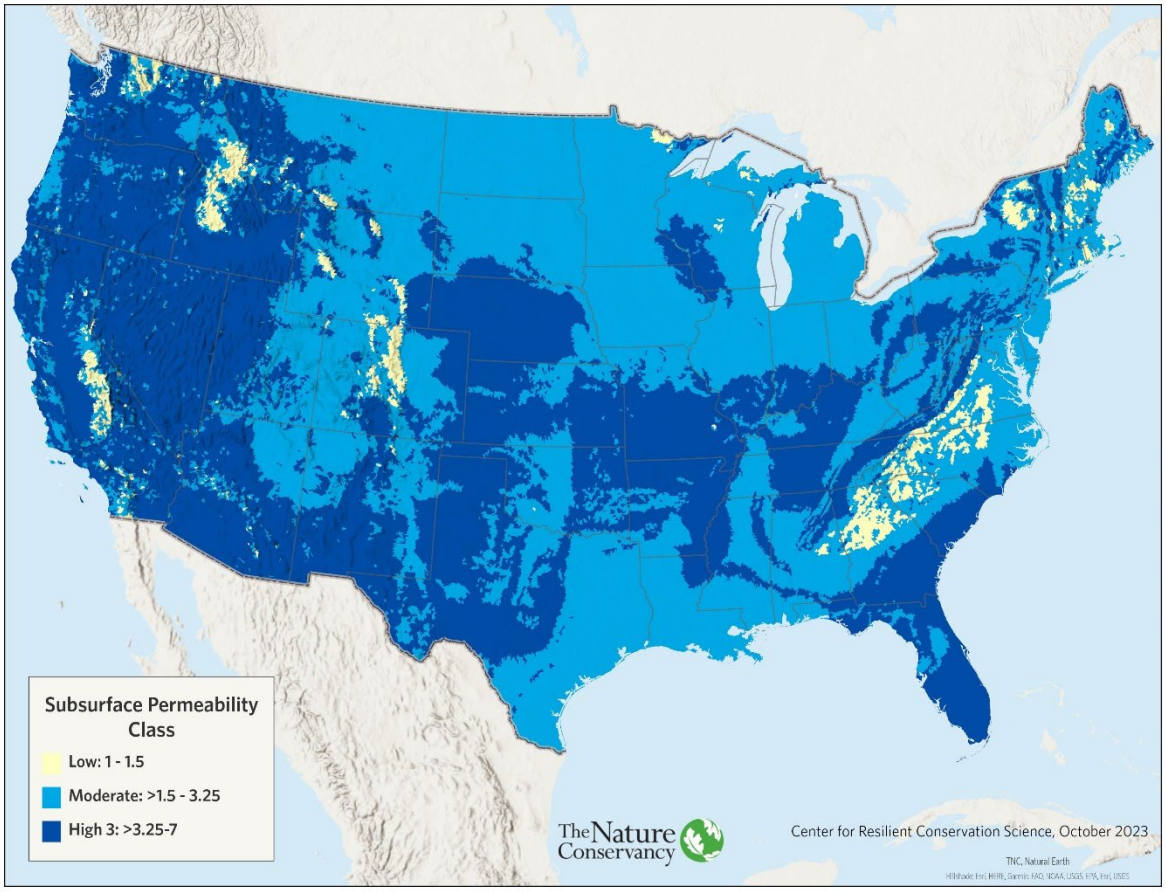

Surface Permeability: Deep Sandy Soils

Surface permeability classes were mapped using the approach in Wolock et al. (2004), which focused on identifying areas of surficial sand. The percentage of sand in the soil is directly related to its permeability, with permeability increasing as the percentage of sand in the soil increases (Wolock et al. 2004). Sandy areas were mapped using TNC's terrestrial settings geology and soils dataset (TNC 2020c) which placed areas of deeper surficial deposits into soil texture categories. In TNC's terrestrial settings, soil texture was mapped where deeper soils occurred within ecoregions, while bedrock types were mapped elsewhere (and had been used in the previous HLRs subsurface permeability classification). In most ecoregions, the category "discontinuous or patchy surficial material" from the national USGS Surficial Materials in the Conterminous United States (Soller 2009) defined the extent of where bedrock was mapped, and soil texture was mapped in all the remaining areas where deeper soils occurred and bedrock was completely buried. The soil texture in TNC's terrestrial settings was derived from sources such as SSURGO, STATSGO, POLARIS, and Soller (2012) which represented the best available and appropriate data source in each ecoregion (TNC 2020c).

The categories of sand, acidic loam, and calcareous loam were extracted from TNC's terrestrial settings geology and soils layer and used to map two categories, loam and sand (Figure A4-3). In a small portion of the Pacific NW and California where soil texture categories had not been used in the

TNC settings, STATSGO2 was used to map sand and sandy loam/loamy sand in areas where deeper soils occurred and were not classified as “discontinuous or patchy bedrock” in Soller et al. (2009).

Figure A4-3. Deep surficial sandy sediment texture type.

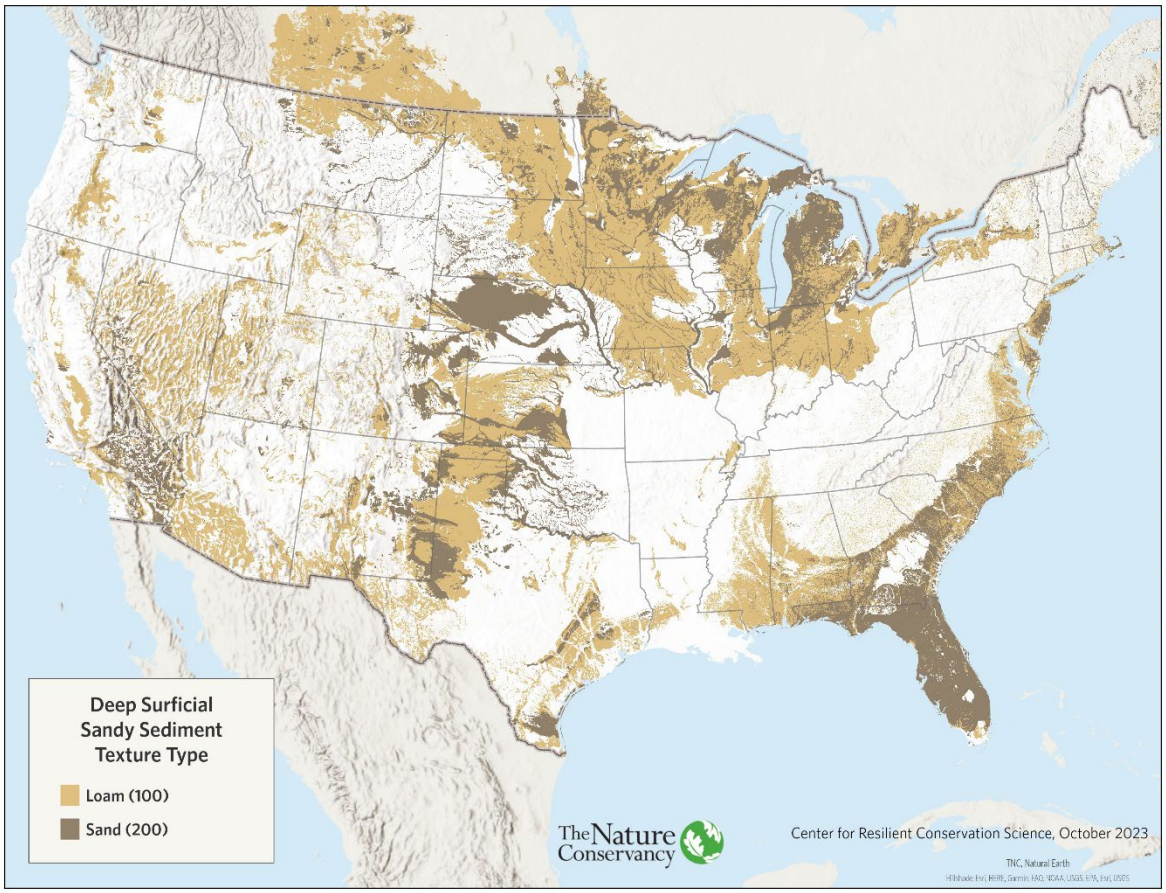

We assigned sand areas a permeability of 200 and loam areas a permeability of 100, half the permeability of sand. We sampled the mean surface permeability value for each HUC-12 and placed the watersheds into three summary groups representing high, moderate, and low surface permeability as follows (Figure A4-4):

- Low: 0-50
- Moderate: >50-100
- High: >200

Figure A4-4. Surface permeability summary classes.

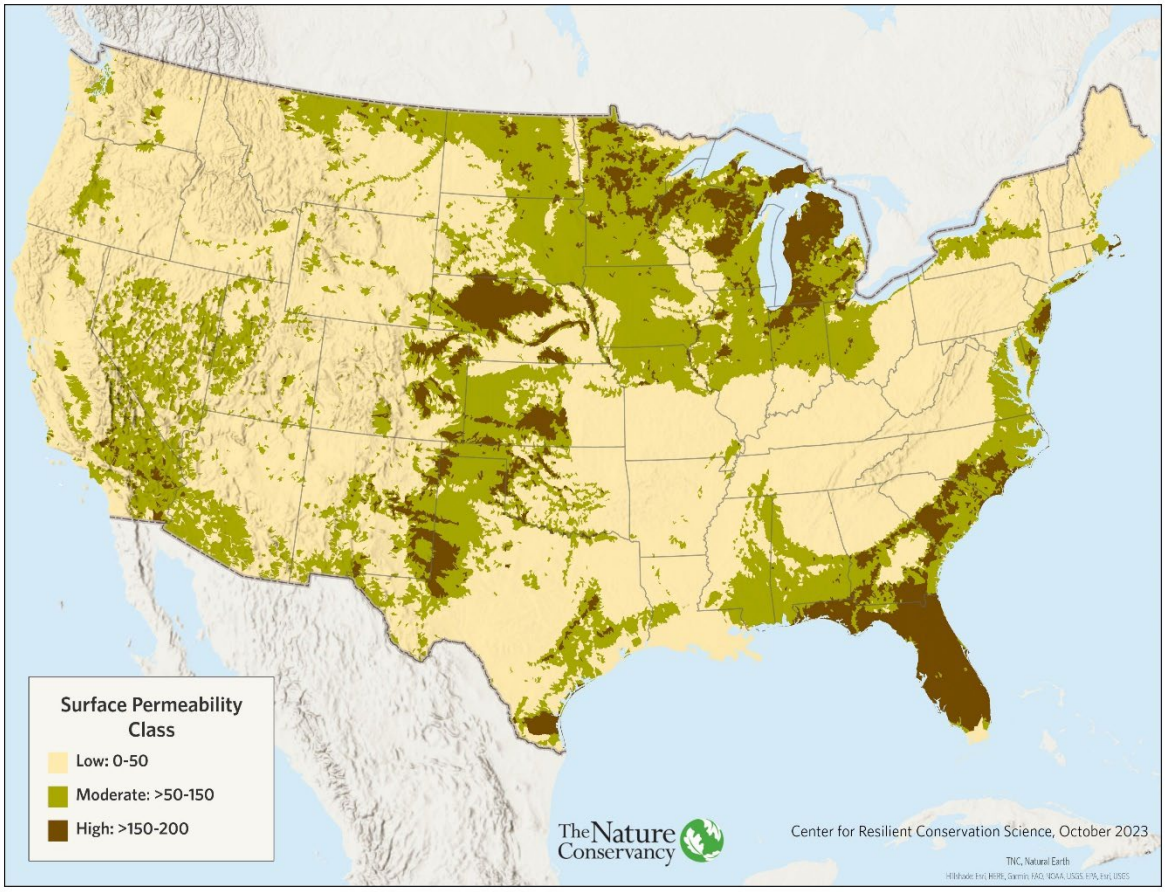

Deriving Groundwater Potential Classes

We combined the summary surface and subsurface bedrock permeability classes to identify areas with low, moderate, or high overall potential groundwater based on enduring geologic and soil settings (Table A4-1). If an area was high in "either" deep groundwater or shallow groundwater, it was identified as having high overall groundwater availability. If an area was moderate in both, or moderate in either deep groundwater or shallow groundwater, it was placed into the moderate groundwater class. If an area was low in both deep groundwater and shallow groundwater, it received a low overall groundwater potential assignment.

Table A4-1. Resultant groundwater potential class from the combination of surface and subsurface permeability class.

DOWN: Subsurface Permeability, Deep Groundwater	ACROSS: Surface Permeability, Shallow Groundwater		
	Low	Moderate	High
Low	Low	Moderate	High
Moderate	Moderate	Moderate	High
High	High	High	High

Lastly, we augmented the groundwater potential assignment after review of the NHDPlus springs dataset (USGS 2016). We noticed some areas where springs were present and expressing groundwater at the surface, but that had been misclassified as low groundwater areas by the coarse geologic mapping of subsurface and surface material permeability. Although many of these springs reflected key groundwater expressions at the surface, we did not want to automatically increase the HLRs groundwater potential class of all HUC-12 watersheds that contained any spring/seep point because a single spring point could be an error and/or very rare small insignificant groundwater feature. We also did not want to increase the groundwater potential HLRs class of any HUC-12 that was in an area of high snowpack as those spring/seeps are often more surface water driven as snowmelt collects above impermeable bedrock in very shallow mountain soils, which didn't match the other deeper permeable soil and deep bedrock permeability concepts currently the driver of moderate or high HLRs groundwater potential. Consequently, we decided to move a HUC-12 to a higher groundwater potential class if most of it was not located in areas with 25% or more snow water balance, using the following rules:

- Move HUC-12s with six or more springs to the high groundwater potential class, if not already in the high category (six represents the 1st natural break of a seven-class break distribution on all HUC-12s with a spring)

- Move HUC-12 watersheds with two to five springs and less than 25% snow that are in the low class to the moderate class, or if in the moderate class, move to the high class.

The final groundwater potential classes are shown in Figure A4-5.

Figure A4-5. Groundwater potential class from hydrologic landscape regions (HLRs) soil and geologic setting.

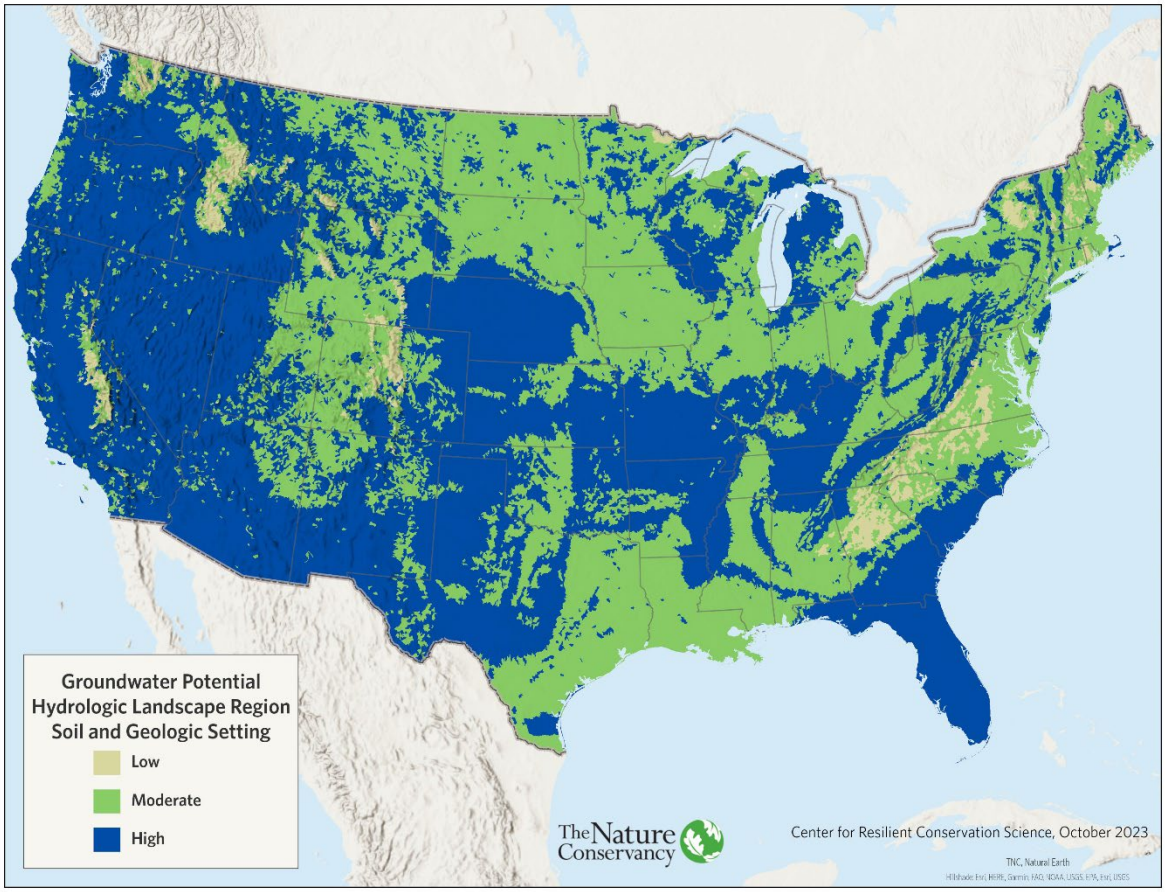

APPENDIX 5

Recognized Biodiversity Data Sources

Table A5-1. State plans and analyses of freshwater biodiversity.

State	Plan Title & Date	Link to Source
AR	Ecologically Sensitive Waters	https://gis.arkansas.gov/product/ecologically-sensitive-streams-line/
CA	Howard et al. (2018) A Freshwater Conservation Blueprint for California	https://www.journals.uchicago.edu/doi/full/10.1086/697996 https://databasin.org/datasets/b03819ca45bc46aa912966bb062763ee/
CO	Colorado (2015): Crucial Habitat for Tier 1 Terrestrial Animal and Plant SGCN (Figure 21).	http://cpw.state.co.us/aboutus/Pages/StateWildlifeActionPlan.aspx
FL	Florida (2016) Priority 1 and 2 CLIP V.4 Significant Surface Waters	https://www.fnai.org/services/clip https://www.fnai.org/pdf/CLIP_v4_technical_report.pdf
GA	Georgie (2015). SWAP High Priority Watersheds Priority Conservation Areas.	https://georgiawildlife.com/sites/default/files/wrd/pdf/swap/appendix-f-aquatic-habitat-technical-team-report-high-priority-watersheds.pdf
IL	Illinois (2016): COAs currently recognized through the Illinois Wildlife Action Plan (Figure 1).	https://www.dnr.illinois.gov/conservation/iwap/pages/default.aspx
IN	Indiana (2015): Indiana conservation opportunity areas	https://www.in.gov/dnr/fishwild/7580.htm

Table A5-1. continued

State	Plan Title & Date	Link to Source
KS	Kansas (2016): Aquatic Ecological Focal Areas	https://www.sciencebase.gov/catalog/item/58498170e4b06d80b7b094c7https://ksoutdoors.com/Services/Kansas-SWAP
KY	Kentucky (2013) State Wildlife Action Plan	https://fw.ky.gov/WAP/Pages/default.aspx ; map downloaded from ftp://ftp.kymartian.ky.gov/kdfwr/swap/huc8_fish_bivalve_overlap.zip
LA	Louisiana (2015) Conservation Opportunity Areas.	https://www.wlf.louisiana.gov/assets/Conservation/SWG/Files/17_WAP_2017_Ch_8.pdf
MA	Massachusetts (2022) BioMap3	https://biomap-mass-eoeea.hub.arcgis.com/
MI	Cohen (2011) Michigan: Biodiversity Stewardship Areas	https://mnfi.anr.msu.edu/reports/MNFI-Report-2011-08.pdf
MN	Minnesota (2015): The Wildlife Action Network map,	PrioritizedNetwork_Aquatic_20150914.SHP - file from MN DNR Nongame Wildlife Program; Priority Rank (gridcode=4) https://www.dnr.state.mn.us/mnwap/index.html
MS	Mississippi (2015) Mississippi Conservation Opportunity Areas	Mississippi Conservation Opportunity Areas: Geospatial Data Presentation Form: vector digital data https://www.sciencebase.gov/catalog/item/5849874be4b06d80b7b094fa
MO	Missouri (2015): 2015 Conservation Opportunity Areas	https://mdc.mo.gov/sites/default/files/downloads/SWAPopt.pdf
MT	Montana (2015): Aquatic Focal Areas	http://fwp.mt.gov/fishAndWildlife/conservationInAction/actionPlan.html
NE	Nebraska (2015): Nebraska Natural Legacy Project: Biologically Unique Landscapes and Demonstration Sites	http://outdoornebraska.gov/naturallegacyproject/
NV	Nevada (2017) Wildlife Action Plan.	https://www.ndow.org/wp-content/uploads/2022/01/2013-NV-WAP-Complete-NOT-ADA.pdf
NH	New Hampshire (2015): WAP	https://www.wildlife.state.nh.us/wildlife/wap.html
NM	New Mexico (2016): Conservation Opportunity Areas (Fig. 11)	https://nmswap.org

Table A5-1. continued

State	Plan Title & Date	Link to Source
NC	North Carolina (2015) State Wildlife Action Plan	https://www.ncwildlife.org/plan
ND	North Dakota (2015): North Dakota State Wildlife Plan focal areas	https://gf.nd.gov/wildlife/swap
OH	Ohio (2015): State Wildlife Action Plan	Ohio COAs aquatic subset - https://www.sciencebase.gov/catalog/item/58499154e4b06d80b7b09547; http://wildlife.ohiodnr.gov/ohioswap
OK	WAFWA (2013): Critical Habitat Assessment Tool - Oklahoma	https://www.wafwachat.org/ ; see also: https://www.wildlifedepartment.com/sites/default/files/2021-11/Oklahoma%20Comprehensive%20Wildlife%20Conservation%20Strategy.pdf
OR	Oregon (2016): Oregon Conservation Strategy	https://oregonconservationstrategy.org/
PA	Pennsylvania (2011). Conservation Opportunity Areas.	Pennsylvania Conservation Opportunity Areas from https://www.sciencebase.gov/catalog/item/584991a4e4b06d80b7b0954b
SD	South Dakota (2015): Wildlife Action Plan	https://gfp.sd.gov/UserDocs/WAPCh4_AquaticSystems.pdf https://gfp.sd.gov/wildlife-action-plan/
TN	Tennessee (2015) SWAP	https://www.tn.gov/content/tn/twra/wildlife/action-plan/tennessee-wildlife-action-plan.html
TX	WAFWA (2018): Critical Habitat Assessment Tool - Texas	from WAFWACHAT.org
VT	Vermont (2018) Vermont Conservation Design	https://vtfishandwildlife.com/sites/fishandwildlife/files/documents/Conserve/VT%20Conservation%20Landscape-level%20Design/Vermont-Conservation-Design-Summary-Report-February-2018.pdf This feature layer is displayed on the Biofinder website at https://anrmaps.vermont.gov/websites/BioFinder/ under Species Components, Aquatic Habitats – Highest Priority.
WI	Wisconsin 2015: Wisconsin Conservation Opportunity Areas	https://dnr.wi.gov/topic/wildlifehabitat/actionplan.html A compiled statewide map is here: https://dnr.wi.gov/topic/WildlifeHabitat/documents/MapCOA_statewide.pdf
WY	Wyoming (2010): Conservation Opportunity Areas	wgfd.maps.arcgis.com Links to the 2017 and the 2010 plan: https://wgfd.wyo.gov/Habitat/Habitat-Plans/Wyoming-State-Wildlife-Action-Plan

Table A5-2. Sources for species data in Recognized Biodiversity Value.

Data Layer	Origin	Link to Source
Critical Habitat for Salmon, Steelhead, Green Sturgeon	NOAA Fisheries - Critical Habitat - Maps and GIS Data (West Coast Region)	https://www.fisheries.noaa.gov/resource/map/critical-habitat-maps-and-gis-data-west-coast-region
Bull Trout strongholds	Climate Shield (Isaaks et al. 2017, 2022)	https://www.fs.usda.gov/rm/boise/AWAE/projects/ClimateShield/maps.html
Atlantic Salmon Critical Habitat in Maine	NOAA 2023	https://www.fisheries.noaa.gov/resource/map/atlantic-salmon-gulf-maine-dps-critical-habitat-map-and-gis-data
Atlantic Subspecies Atlantic Sturgeon	NOAA 2023	https://www.fisheries.noaa.gov/resource/map/atlantic-sturgeon-critical-habitat-map-and-gis-data
Eastern Brook Trout Secure strongholds	Trout Unlimited (Fesenmyer et al. 2017)	https://www.tu.org/science/conservation-planning-and-assessment/conservation-portfolio/eastern-brook-trout-conservation-portfolio/
TNC Atlantic Coast Alosine Prioritization (top 5%)	Martin (2019) Atlantic Coast Whole System Diadromous Fish Prioritization	https://www.atlanticfishhabitat.org/wp-content/uploads/2019/12/TNC_AtlanticCoast_AlosinePrioritization.pdf
Chesapeake Alosine occurrences	Martin, E. H. 2019. Chesapeake Fish Passage Prioritization: An Assessment of Dams in the Chesapeake Bay Watershed. The Nature Conservancy. Data is based on the professional opinion of the Chesapeake workgroup (which includes the fish passage coordinators in MD, VA & PA, USFWS & NOAA staff).	https://maps.freshwaternetwork.org/chesapeake/
Critical Habitat for inland aquatic species	USFWS 2023	https://gis-fws.opendata.arcgis.com/maps/794de45b9d774d21aed3bf9b5313ee24/about

APPENDIX

Estimated Mining Areas 6

For the water quality component of the condition score, we wanted to include a measure for mine lands in HUC-12 watersheds. While there are a range of both national and regional spatial datasets that identify mine footprints in the U.S., many are outdated, inconsistent, and/or have incomplete geographic coverage. To estimate the potential impact of surface mining activities (e.g., mountaintop removal, quarries, strip mines, open pit mines, dredging) on watersheds, we developed a new dataset of mining footprints in CONUS using current land cover with global, national, regional, and state mining datasets. Each data source is described and then we summarize our approach to identify surface mining areas.

Mining Point Locations

- *U.S. Active Mines and Mineral Processing Plants* (USGS 2005). This is a USGS point dataset of active mines and mineral processing plants in the U.S that we downloaded from https://mrdata.usgs.gov/mineplant/. The dataset includes mineral and metal operations considered active in 2003. For our analysis, we removed peat mines and processing plant locations, unless they included the site mines.

- *U.S. Coal Mines* (US EIA 2020). This is a U.S. Energy Information Administration (EIA) dataset. We downloaded a point dataset representing operating surface and underground coal mines in the U.S. in 2020 from the EIA U.S. Energy Atlas at https://atlas.eia.gov/maps/coal-mines-1.

Spatial Extents

- *Appalachian Mining Disturbed Areas.* TNC staff developed this layer, which reflects landscape conditions up to and around 2015, by merging several datasets for the Appalachian mining region encompassing the states of Pennsylvania, West Virginia, Ohio, Virginia, Kentucky, Tennessee, and Alabama. Mining disturbance areas were initially compiled using a combination of state mining agency permit data and aerial photo interpretation. Three additional datasets based on regional aerial photo assessment projects were used to improve the accuracy of the mining disturbance areas (Townsend et al. 2009; and Pericak et al. 2018). There were no distinctions made between surface disturbances due to surface mines, valley fills, mining roads, preparation plants, underground mines, or reclaimed mined lands. In Eastern Kentucky, mining areas were based on an aerial photo digitization project completed by TNC in 2006 and updated with data from Pericak et al. (2018) and a Downstream Strategies mining analysis. Western Kentucky mining areas are based solely on agency permit data.

- *Florida Phosphate Mining Areas* (FDEP 2021). Central Florida (Polk, Hillsborough, Manatee, and Hardee counties) has an extensive phosphate mining region that encompasses about 1.3 million acres of land often referred to as the “Bone Valley.” There is an additional mine in

Hamilton county located in North Florida. Since 1975, land mined for phosphate in Florida is required to be reclaimed through contouring and revegetation. Florida's Department of Environmental Protection maintains spatial data on phosphate mine boundaries and reclamation units. We downloaded the 2019 Mandatory Phosphate Reclamation Units that identifies reclamation units of all active mandatory phosphate mines in Florida in 2019 at https://geodata.dep.state.fl.us/explore?query=phosphate.

- *Global Mining Areas Dataset* (Maus et al. 2020). Recently published and publicly accessible global dataset of above-ground mining areas derived from analysis of satellite imagery (https://doi.org/10.1594/PANGAEA.910894). The dataset includes open cuts, tailings dams, waste rock dumps, water ponds, and processing infrastructure. Note that after completion of the freshwater resilience analysis in June 2023, Maus et al. (2022) published an updated version of the global mining dataset in July 2023 that significantly increased the initial 2020 mining area.

- *LANDFIRE EVT Quarries-Strip Mines-Gravel Pits-Well and Wind Pads* (LANDFIRE 2020). Grid value 7295 from the 2020 LANDFIRE (LF) 2.2.0 30-m Existing Vegetation Type (EVT) raster. We aggregated the selected pixels using the eight nearest neighbors, and then converted to polygon.

- *LCMAP Barren Lands* (Pengra et al. 2021). USGS Land Change Monitoring, Assessment, and Projection (LCMAP) v1.2 30-m raster grids for 1990, 2000, 2010, and 2020 (https://www.usgs.gov/special-topics/lcmap/collection-12-conus-science-products). Using the four decadal time periods, we identified cells that transitioned to barren land cover (grid value 8). We aggregated the resultant LCMAP barren pixels using an 8-neighbor region group rule in ArcGIS and converted the grouped cells into a polygon. In examining the LCMAP barren areas, we found they did a good job of expanding existing surface mine areas from other datasets (e.g., USGS surface mines, global mining dataset) but also identified areas where it was difficult to determine if mining was occurring.

- *USGS Surface Mining Areas* (Soulard et al. 2016). USGS produced 30-m raster of moderate to large surface mining areas in CONUS using a semi-automated procedure with mine point locations from https://onlinelibrary.wiley.com/action/downloadSupplement?doi=10.1002%2Fldr.2412&file=ldr2412-sup-0001-mines.zip and https://onlinelibrary.wiley.com/action/downloadSupplement?doi=10.1002%2Fldr.2412&file=ldr2412-sup-0002-gains.zip).

Identifying and Refining Surface Mining Areas

After exploring the above data sources, we used several different approaches, trial and error, and substantial manual review to refine and expand existing mining areas as well as identify new ones.

To refine the spatial extent of mapped mining areas using current land cover, we created a layer of land uses that could be associated with mining operations. We extracted the following 2019 NLCD land cover classes: open water (class 11), development (classes 21-24), barrens (31), shrub/scrub (52), grassland (71), pasture/hay (81), and row crops (82). We removed roads using the 2019 NLCD

Impervious Surface source grid, aggregated the remaining cells using a four-neighbor rule, and converted the aggregated raster cells to polygons.

To update and check the USGS surface mine areas, we first merged the USGS 2001 and 2006 surface mine grids, selected mine cells (grid value 1), aggregated the mining pixels using four nearest neighbors, and converted to polygon. We reviewed the resultant polygons with coal and mineral mine point locations and discovered that many of the small sites were not near coal or other mines and appeared to simply be barren areas. We used several rules to address this issue with search distances and the large size threshold from Soulard et al. (2016). First, we retained surface mine polygons that intersected mining polygons from the other mining areas datasets or that were within 500 meters of USGS mineral mine points (excluding processing plants) or within 2,000 meters of coal mine points. We manually reviewed polygons that were greater than 500 m and less than or equal to 1,000 m from USGS mine locations. We grouped the remaining polygons (>250K) into size classes. Polygons less than 10,000 m^2 did not appear to be surface mines and were removed. Most polygons greater than 10,000 m^2 and less than 50,000 m^2 were not mines with a few exceptions that we retained. We manually reviewed all large polygons greater than 100,000 m^2 and those between 50,000 and 100,000 m^2. The size thresholds intentionally removed western US oil fields. We retained smaller polygons that intersected larger surface mining polygons that we positively identified as mines. Because the USGS surface mining areas were based on 2006 data, we selected LCMAP barren polygons that intersected the USGS surface mining polygons and found the barren polygons did a great job of capturing new mining areas and helped fill in holes. We converted the selected LCMAP polygons to a raster and merged those with the USGS surface mining grid using Cell Statistics in ArcGIS to retain the data source. Lastly, we intersected the reviewed surface mines with the global mining areas, Appalachian mining footprint, LCMAP barrens, and LANDFIRE EVT mine class to add a field identifying polygons that overlapped with the USGS dataset.

To refine and check the footprints in the 2020 global mines dataset, we clipped the 2019 NLCD land cover mine layer and the LCMAP barrens by the global mining polygons, merged the two and assigned unique values to retain the land cover source. We identified one polygon from the global mining dataset that didn't intersect these two datasets or the USGS surface mining dataset. The polygon was in Arkansas and review suggested it was not a mine. In the Appalachian region, we manually investigated the global mining footprints that did not intersect TNC's Appalachian mining footprint and retained those that appeared be mining areas based on imagery and mine point data.

To identify potential new coal mining areas not in the other datasets, we selected LANDFIRE polygons greater than or equal to 250,000 m^2 that were within 2,000 m of coal mines. After removing the resultant polygons that intersected global mines, USGS surface mines, and Appalachian mines, no new coal areas were identified. We repeated this process for the LCMAP barrens polygons and identified four new potential areas. After examination, one area was retained and all nearby LCMAP barren polygons were selected to represent the full mining footprint based on satellite imagery.

To identify potential new non-coal mining areas, we selected LANDFIRE polygons 100,000 m^2 or larger within 500 m of mines. A total of 104 polygons remained after removing those that intersected existing mining areas in the other datasets. These were manually reviewed using imagery and the LCMAP barren polygons. Most were retained and the footprint of many was refined by incorporating intersecting LCMAP barren polygons. While manually reviewing the polygons, we identified additional smaller LANDFIRE polygons that improved the mine footprint. We used the same process

for the LCMAP barren polygons. There were more than 200 polygons that did not spatially intersect mining polygons in the other datasets, and most were retained after manual review. In some cases, the footprint was improved by incorporating nearby LCMAP polygons or LANDFIRE polygons. After identifying the LANDFIRE and LCMAP surface mines, we ran a spatial intersection between reviewed surface mines and the LCMAP and LANDFIRE smaller polygons to further fill out mining areas where there were intersections. Lastly, we examined mining points that did not have nearby mining area polygons and examined those with the LCMAP barrens, NLCD layer, and the LANDFIRE EVT polygons to identify potential new mining areas.

In addition, there were geographies that required detailed manual review and additional datasets; of note are portions of Florida and Louisiana. While the existing mining datasets identified some of the phosphate mining areas in Central Florida, we wanted to remove reclaimed sites and identify new ones to ensure that only active mines were represented. Using the Florida phosphate mining data, we excluded the reclamation units where work had been completed or there was no disturbance, and selected the units with a future work, work scheduled, or work in progress status. We clipped the global mining, LCMAP barrens, LANDFIRE, and USGS surface mine polygons by the selected reclamation units and retained those polygons to represent the active phosphate mining areas. In Louisiana, there is extensive sand and gravel mining along the Amite River and Bogue Chitto River. The USGS surface mine and other datasets picked up some of these locations, but we ended up manually adding new ones based on imagery examination and using the LCMAP barrens, LANDFIRE, and NLCD datasets.

Finally, we did some additional clean up, error checking, and data source coding for all the selected mining areas. We converted the selected mining polygons to a 30-m raster and merged all the grids using Cell Statistics in ArcGIS to retain the source datasets for all mapped mining areas. We created a mining area raster where all mining areas were coded as 10 and then we merged this on top of the 2019 NLCD land cover for use in the water quality mining metric and the floodplain, riparian, and watershed land cover naturalness metrics.